UNIVERSITY OF TECHNOLOGY SYDNEY

Deciphering the molecular mechanisms of helminth-host interactions

by Sumaiya Chowdhury

Thesis submitted in fulfilment of the requirements for the degree of

Doctor of Philosophy

under the supervision of
A/Prof Sheila Donnelly
A/Prof Nham Tran
Dr Dayna Sais

University of Technology Sydney
Faculty of Science

September 2025

Certificate of original authorship

I, Sumaiya Chowdhury, declare that this thesis is submitted in fulfilment of the requirements for the award of Doctor of Philosophy, in the School of Life Sciences, Faculty of Science at the University of Technology Sydney.

This thesis is wholly my own work unless otherwise referenced or acknowledged. In addition, I certify that all information sources and literature used are indicated in the thesis.

This document has not been submitted for qualifications at any other academic institution.

This research was supported by the Australian Government Research Training Program (RTP) Scholarship doi.org/10.82133/C42F-K220.

Signature: Production Note:
Signature removed prior to publication.

Date: 10th September 2025

Acknowledgments

The completion of this thesis represents the culmination of years of hard work, exploration, and growth, and it would not have been possible without the help, guidance, and support of numerous individuals. I am deeply grateful to those who have contributed to this journey.

First and foremost, I extend my heartfelt gratitude to my supervisors, **A/Prof. Sheila Donnelly** from the School of Life Sciences, UTS, and **A/Prof. Nham Tran**, and **Dr. Dayna Sais** from the School of Biomedical Engineering, UTS. Their unique combination of expertise has been invaluable to this project.

I would like to express my heartfelt gratitude to **Sheila** for introducing me to the captivating world of helminths. Exploring their ingenious strategies for host invasion has been an intellectually enriching experience, one that I will always treasure. Although you supervised me from far away, all the way from Ireland, your guidance never felt distant. I have greatly admired and aspired to learn from your critical thinking, insightful approach to scientific challenges, and exceptional writing and communication skills. Your dedication, discipline, and unwavering commitment to high standards have continually inspired me to refine my own abilities. Your influence has played a crucial role in shaping the quality of this dissertation, for which I am incredibly grateful.

To **Nham**, thank you for your approachable and encouraging mentorship throughout my research journey. I have thoroughly enjoyed exploring the fascinating world of miRNAs, non-coding RNAs, and their role in cross-kingdom gene regulation under your guidance. My time in your lab has provided me with a strong foundation in advanced molecular biology techniques, for which I am immensely grateful. Your mentorship extended well beyond the research project itself, offering me valuable insights into the broader aspects of scientific research and providing career advice that will guide me in the future.

To **Dayna**, thank you for introducing me to bioinformatics and guiding me through advanced lab techniques. Your willingness to help with technical queries, troubleshooting, and your thoughtful feedback have been crucial to my experiments. I have learned so much from our conversations, even in passing moments. Your meticulous attention to details, and perseverance have been an inspiration.

I am also deeply grateful to the former members of the **Donnelly lab**. **Alison**, your work provided the groundwork for this research project, **Mayra**, thank you for handing down essential lab techniques and for your support and warm friendship, and **Joyce** for all your help and always offering to help.

To the **Tran lab members**, including **Sarah**, **Ha**, and **Thao**, thank you for your invaluable help and support and your camaraderie, which has made working in the lab an enjoyable and enriching experience.

I sincerely thank **Prof. John Dalton** for generously providing precious *Fasciola hepatica*-infected sheep sera samples from longitudinal field trials, as well as *F. hepatica* samples from various life stages of the parasite. Although I have not had the opportunity to meet him in person, his insightful feedback, enthusiasm, and collaboration have significantly contributed to this dissertation.

To the Scientific support team at UTS, especially, **Sarah**, and **Luke**, and **Fiona** from the Ernst Facility, I am deeply grateful for your technical assistance and willingness to help at every step throughout my research.

To my fellow PhD office mates, **Jos**, **Andy**, **Andie**, **Rashad**, **Hao**, **Lisa**, **Giang**, **Riley**, **Senani** and **Tayyeba**, our time together has been one of the highlights of this journey. Each of you, at different stages of your own PhD, brought unique energy, wisdom, and kindness into the office. Our space was not just a workplace but a sanctuary of laughter, encouragement, and shared experiences. Whether we were celebrating milestones or navigating challenges, your friendship made the journey so much more enjoyable. I will forever cherish the memories we created, the bonds we formed, and the inspiration I drew from each of you.

I extend my deep gratitude to my ex-supervisor and mentor, **Prof. Mark Gorrell**, who encouraged me to pursue a PhD. The foundational training I received in your lab, along with your advice and encouragement, gave me the confidence to embark on this journey. I am forever indebted to you and look forward to continuing to seek your guidance throughout my research career.

To my dear husband **Ayman**, words cannot fully express my gratitude. You have been my unwavering rock throughout this journey. Your constant support and love have been the

foundation of my PhD experience. From the very beginning, you believed in my dreams, encouraging me to take the leap and pursue my passion for research. Through every challenge, you offered strength, patience, and reassurance when I needed it most. Your sacrifices and dedication made this dissertation possible. You inspired me to stay resilient and committed to my work. Your selflessness in managing the household and caring for our children allowed me to fully immerse myself in this endeavour.

To my children, **Nawaaf** and **Zainab**, thank you for your patience and understanding during my long hours of work. Your encouragement reminding me that "science is important" and has motivated me to persevere. Thank you for being my practice audience for my presentations and even offering feedback! Your smiles and hugs have been my greatest source of comfort and strength.

To my mother, thank you for instilling in me the values of perseverance and purpose. To my sister **Munira**, your offer to fly from Melbourne whenever I needed support has been a tremendous source of reassurance.

Finally, I dedicate this thesis to my late father. I know he would have been incredibly proud of this accomplishment. His insatiable curiosity and inquisitiveness continue to inspire me in all aspects of my life.

List of publications and presentations

This thesis originates from collected works featured in,

Hypothesis and theory article:

Chowdhury, S., Sais, D., Donnelly, S., & Tran, N. (2024). The knowns and unknowns of helminth-host miRNA cross-kingdom communication. *Trends in Parasitology*. https://doi.org/10.1016/j.pt.2023.12.003

Research articles:

Chowdhury, S., Ricafrente, A., Cwiklinski, K., Sais, D., Dalton, J. P., Tran, N., & Donnelly, S. (2024). Exploring the utility of circulating miRNAs as diagnostic biomarkers of fasciolosis. *Sci Rep*, *14*(1), 7431. https://doi.org/10.1038/s41598-024-57704-9

Sais, D., Chowdhury, S., Dalton, J. P., Tran, N., & Donnelly, S. (2024). Both host and parasite non-coding RNAs co-ordinate the regulation of macrophage gene expression to reduce pro-inflammatory immune responses and promote tissue repair pathways during infection with *Fasciola hepatica*. *RNA Biol*, *21*(1), 62-77. https://doi.org/10.1080/15476286.2024.2408706

Sais, D., Chowdhury, S., Nguyen, P. T., Cwiklinski, K., Nguyen, T. D., Nguyen, T. A., Dalton, J., Donnelly, S., & Tran, N. (2025). Dynamic shifts in isomiR profiles during parasite maturation of *Fasciola hepatica*. *RNA biology*, *22*(1), 1-22. https://doi.org/10.1080/15476286.2025.2538271

Chowdhury, S., Sais, D., Tran, N., Donnelly, S. *Fasciola hepatica* selects a sequence variant of miR-125b-5p to communicate with host immune cells, due to its enhanced efficacy as compared to the canonical miRNA. *Manuscript in preparation.*

Conferences:

Chowdhury, S., Sais, D., Tran, N., Donnelly, S. . (2024). *Characterising the influence of parasite-derived 3' isomiRs on the biological activity of host macrophages.* Oral presentation. RNA biology in host-pathogen interactions, Porto, Portugal.

Chowdhury, S., Ricafrente, A., Sais, D., Cwiklinski, K., Dalton, J., Tran, N., Donnelly, S. (2024). *Circulating miRNAs as promising biomarkers for early diagnosis of Fasciola hepatica infection.* Oral presentation. Sydney RNA Symposium 2024, Sydney, Australia.

Chowdhury, S., Ricafrente, A., Sais, D., Cwiklinski, K., Dalton, J., Tran, N., Donnelly, S. (2023). *Assessing helminth microRNAs as potential biomarkers for the diagnosis of acute fasciolosis.* Oral presentation. The Australian Society for Parasitology Annual Conference 2023, Darwin, Australia.

Chowdhury, S., Sais, D., Tran, N., Donnelly, S. (2023). *Discovery of parasite-derived isomiRs in mammalian host macrophages during infection.* Poster presentation. 50 Years of Shine-Dalgarno Symposium 2023, Canberra, Australia.

Chowdhury, S., Ricafrente, A., Sais, D., Cwiklinski, K., Dalton, J., Tran, N., Donnelly, S. (2023). *miRNAs as potential diagnostic biomarkers of Fasciola hepatica infection.* Oral presentation. EMBL Australia Postgraduate Symposium 2023, Sydney, Australia.

Table of Contents

Certificate of original authorship i

Acknowledgments ii

List of publications and presentations v

Supplementary material xii

List of Appendices xii

List of figures xiii

List of tables xvi

Abbreviations xvii

Abstract 1

Chapter 1: Introduction 3

1.1. Helminth infections are a major health and economic burden 5

1.2. Controlling helminth infections is challenging 9

1.3. Exploring helminth-derived miRNAs as a new frontier for diagnostic and therapeutic advances 10

1.4. The knowns and unknowns of helminth-host miRNA cross-kingdom communication 13

1.4.1. The theory of cross-kingdom miRNA communication 13

1.4.2. Helminth-derived miRNAs alter the host immune response to establish chronic infection 13

1.4.3. Delivery of helminth miRNAs to host cells 18

1.4.3.1. miRNAs are released by helminths in extracellular vesicles and non-vesicular forms 18

1.4.3.2. Helminth-derived extracellular vesicles are taken up by host immune cells 19

1.4.3.3. Selective sorting of parasite-derived miRNAs into EVs 19

1.4.4. miRNA-mediated regulation of gene expression 21

1.4.4.1. The miRNA biogenesis pathway 21

1.4.4.2. Processing of helminth miRNAs in mammalian cells 24

1.4.4.3. Mechanisms of helminth miRNA-mediated regulation of host gene expression 26

1.5. Finding the knowns to the unknowns 29

1.6. Using *Fasciola hepatica* as a model organism to explore helminth-host miRNA-mediated cross communication 30
1.7. Thesis hypothesis and aims 38

Chapter 2: Assessing the viability of using the differential expression of circulating miRNAs as a biomarker for the diagnosis of *F. hepatica* infection. 39
2.1. Introduction 41
2.2. Methods 43
2.2.1. Sheep sera samples from experimental *Fasciola hepatica* infections 43
2.2.2. Ethics statement 45
2.2.3. RNA isolation from sheep sera, lamb tissue, and newly excysted juveniles 45
2.2.4. Sequencing and bioinformatics 46
2.2.5. Characterisation of the Differential Expression of miRNAs in sheep sera 47
2.2.6. RT-qPCR 47
2.2.7. Statistical analysis 48
2.3. Results 49
2.3.1. Differential abundance of host circulating miRNAs during *Fasciola hepatica* infection 49
2.3.2. Small RNA sequencing revealed the presence of *Fasciola hepatica*-derived miRNAs in the serum of infected sheep 53
2.3.3. Selection of sheep and *Fasciola hepatica*-derived miRNAs as potential biomarkers of fasciolosis 54
2.3.4. Circulating oar-miR-133-5p and oar-miR-3957-5p can diagnose fasciolosis from as early as seven days post-infection 63
2.4. Discussion 67

Chapter 3: **Comparing the functional activity of *F. hepatica*-derived canonical and isomiR miRNAs in the regulation of macrophage inflammatory responses** 71
Publication statement 72
3.1. Introduction 73
3.2. Methods: 75
3.2.1. Sequencing Data and Bioinformatic Analysis 75
3.2.1.1. Peritoneal macrophages 75
3.2.1.2. Fasciola hepatica intra-mammalian life stages 75

3.2.1.3. Fasciola hepatica isomiR profiling 75
3.2.1.4. Target prediction and gene enrichment analysis 76
3.2.2. Isolation of bone marrow derived macrophages (BMDM) 76
3.2.3. *In vitro* macrophage transfection and LPS stimulation 76
3.2.4. Cytotoxicity assay 77
3.2.5. Cytokine assay 77
3.2.6. RNA extraction 77
3.2.7. Detection of fhe-miR-125b mimic in transfected cells 78
3.2.8. Quantification of expression level of macrophage endogenous genes 78
3.2.9. Luciferase Assay 79
3.2.10. Ago2 pulldown assay 82
3.2.10.1. Ago2 immunoprecipitation 82
3.2.10.2. Quantification of Ago-bound miRNAs 82
3.2.10.2. Western blot confirmation of Ago2 in immunoprecipitated fractions 82
3.2.11. Statistical analysis 83

3.3. Results 84
3.3.1. Peritoneal macrophages of *Fasciola hepatica* infected mice are enriched with parasite-derived miRNAs with peak abundance at 18 hours post infection 84
3.3.2. Worm-derived miRNAs in the peritoneal macrophages of *Fasciola hepatica* infected mice are predominantly isomiRs 87
3.3.3. *Fasciola hepatica* selectively exports isomiRs into host peritoneal macrophages 90
3.3.4. The 3' trimmed fhe-miR-125b-5p isomiR is predicted to have a reduced binding affinity for host gene targets as compared to the canonical miRNA 93
3.3.5. The fhe-miR-125b-5p canonical and isomiR sequences regulated the LPS-stimulated pro-inflammatory response in macrophages with equal efficacy 96
3.3.6. The fhe-miR-125b-5p isomiR directly regulated the expression of host genes more efficiently than its canonical counterpart 106
3.3.7. The 3' trimmed isomiR fhe-miR-125b displayed enhanced interaction with host Ago2 as compared to the canonical miRNA. 111

3.4. Discussion 113

Chapter 4: **Deciphering the mechanisms by which parasite-derived miRNAs exploit the host RNA interference (RNAi) machinery to regulate host gene expression** 117
4.1. Introduction 118

4.2. Methods....120
4.2.1. Generation of Ago2 and Dicer gene knockout (KO) macrophage cells. 120
4.2.2. Cell culture....120
4.2.3. Assessment of cell confluency....122
4.2.4. CFSE cell proliferation assay....122
4.2.5. Cytotoxicity Assay....122
4.2.6. Scratch Wound Assay....123
4.2.7. Phagocytosis Assay....123
4.2.8. Assessment of the inflammatory response of WT and KO clones 124
4.2.9. Quantification of cell number using CyQUANT Assay....124
4.2.10. Transfection of *Fasciola hepatica* miRNA mimics....125
4.2.11. Statistical analysis....125
4.3. Results....126
4.3.1. Generation of Ago2 and Dicer gene knockout RAW264.7 murine macrophage cells 126
4.3.2 Growth dynamics of the Ago2 and Dicer gene knockout (KO) RAW264.7 macrophage subclones....129
4.3.3. Ago2 and Dicer KOs differentially influence macrophage migration while preserving phagocytic function....129
4.3.4. Loss of Ago2 dampens, while loss of Dicer exaggerates, proinflammatory responses to LPS....134
4.3.5. Selection of subclones A3 and D3 as representative Ago2 and Dicer KOs 135
4.3.6. Functional activity of fhe-miR-125b-5p was preserved in Ago2- and Dicer-deficient macrophages 139
4.4. Discussion....145
Chapter 5: **General Discussion**....150
5.1. Host and parasite miRNA signatures: toward sensitive and stage-specific helminth diagnostics....152
5.1.1. Limitations and future directions....154
5.2. IsomiRs: expanding the paradigm of miRNA-mediated parasite-host interaction....155
5.2.1. Limitations and future directions....156
5.3. Ago2 and Dicer KO macrophages: a valuable platform for understanding miRNA-mediated parasite-host interaction 157

5.3.1. Limitations and future directions 159
5.4. Evolutionary implications: hypotheses and emerging concepts 160
5.5. Therapeutic and translational implications 161
5.6. Conclusion 162
References: 164

Supplementary material

Supplementary tables listed below can be accessed at: https://doi.org/10.26195/pysj-f855

Supplementary Table 1.1

Supplementary Table 2.1

Supplementary Table 2.2

Supplementary Table 2.3

Supplementary Table 3.1

Supplementary Table 3.2

List of Appendices

Appendix A: Published review article: The knowns and unknowns of helminth-host miRNA cross-kingdom communication. *Trends in Parasitology*. 2024;40(2). doi:10.1016/j.pt.2023.12.003 185

Appendix B: Published original article: "Exploring the utility of circulating miRNAs as diagnostic biomarkers of fasciolosis" *Scientific reports* (2024) 14:7431; doi: 10.1038/s41598-024-57704-9 202

Appendix C: Monash Genome Modification Platform Final Report: Generation of Ago2 Knockout RAW264.7 Cells 218

Appendix D: Monash Genome Modification Platform Final Report: Generation of Dicer Knockout RAW264.7 Cells 245

List of figures

Figure 1.1. Prevalence of helminth infections in human. 6

Figure 1.2. Helminth miRNAs are predicted to regulate the immune response during infection. 15

Figure 1.3. Mammalian miRNA biogenesis pathways. 23

Figure 1.4. Proposed mechanism of helminth-miRNA mediated cross-kingdom regulation of host immune response. 28

Figure 1.5. *Fasciola hepatica* life cycle in its definitive host involves their residence in multiple tissue niches while manipulating the host innate immune responses. 32

Figure 1.6. Host immune response to *F. hepatica* infection. 35

Figure 2.1. Differential abundance of sheep miRNAs in sera during *Fasciola hepatica* infection. 50

Figure 2.2. Circulating host-miRNA profiles are distinct during early and late *F. hepatica* infection compared to non-infected animals. 52

Figure 2.3. Selection of host and *F. hepatica* miRNAs as potential biomarkers for pre-hepatic and hepatic stages of fasciolosis. 54

Figure 2.4. Validation of sequencing data using PCR and primers designed to detect the expression of sheep miRNAs. 56

Figure 2.5. Detection of fhe-miR-124-3p. 58

Figure 2.6. Detection of fhe-Novel-11-5p. 59

Figure 2.7. *F. hepatica* miR-124-3p was present as several sequence variants (isomiR) in sera of infected sheep. 61

Figure 2.8. Discovery of the presence of oar-miR-124-3p. 62

Figure 2.9. RT-qPCR assessment of sera samples invalidates the diagnostic potential of oar-miR-323a-3p and fhe-miR-124-3p. 64

Figure 2.10. RT-qPCR demonstrates the differential expression of oar-miR-133-5p and oar-miR-3957-5p in sera from infected sheep as compared to uninfected animals. 66

Figure 3.1. Worm-derived miRNAs detected in the peritoneal macrophages of mice infected with *F. hepatica* were predominantly isomiRs. 88

Figure 3.2. The most abundant worm-derived miRNAs in macrophages had increased 3' trimmed isomiRs expression in the NEJs, as compared to juvenile (JUV) or adult (AD) worm. 92

Figure 3.3. Application of the −20 kcal/mol free energy cut-off on the miRanda predicted target sites indicated that the 3′-trimmed fhe-miR-125b isomiR has reduced binding capacity for host targets compared to the canonical sequence. 94

Figure 3.4. The gene targets of fhe-miR-125b-5p isomiR that were excluded after applying the FE cutoff (< −20 kcal/mol) were enriched in pathways related to host responses, including cell communication, behaviour, localisation, and response to stimulus. 95

Figure 3.5. The canonical and isomiR fhe-miR-125b-5p regulated the inflammatory response to bacterial LPS in macrophages to the same extent. 100

Figure 3.6. Except for the reduced expression of *P2rx7,* the fhe-miR-125b canonical and isomiR mimics had no effect on the expression of predicted gene targets in unstimulated BMDMs. 101

Figure 3.7. Both isomiR and canonical fhe-miR-125b-5p significantly suppressed the expression of host genes that had been increased in response to LPS stimulation of macrophages. 102

Figure 3.8. Neither the isomiR nor canonical fhe-miR-125b-5p impacted the expression of genes downregulated by LPS stimulation of macrophages. 103

Figure 3.9. Transfected macrophages displayed the same levels of expression of fhe-miR-125b canonical (Can) and isomiR (Iso) sequences. 104

Figure 3.10. Transfection of macrophages with canonical and isomiR fhe-miR-125b mimics did not significantly impact cell viability. 105

Figure 3.11. Validation of the luciferase reporter assay using hsa-miR-21 and its endogenous target *Pdcd4* to assess miRNA-target direct interactions. 108

Figure 3.12. Luciferase reporter assay demonstrated that the fhe-miR-125b-5p isomiR repressed host target genes more effectively than the canonical form. 109

Figure 3.13. The cloned *Stat3* sequence in the psiCHECK-2 vector contains multiple potential binding sites for mmu-miR-23a-3p. 110

Figure 3.14. fhe-miR-125b isomiR is loaded more efficiently onto host Ago2 than the canonical form. 112

Figure 4.1. LPS induced proinflammatory cytokines were downregulated by fhe-miR-125b-5p in RAW264.7 murine macrophage cell line. 127

Figure 4.2. Characterization of Ago2 KO cell growth dynamics. 130

Figure 4.3. Characterization of Dicer KO cell growth dynamics. 131

Figure 4.4. Functional characterization of Ago2 KO macrophage clones. 132

Figure 4.5. Functional characterization of Dicer KO macrophage clones. 133

Figure 4.6. Proinflammatory cytokine production by Ago2 KO and Dicer KO clones. 136

Figure 4.7. Assessment of M1 polarization and proinflammatory gene expression in Ago2 KO macrophages in response to LPS. 137

Figure 4.8. Dicer KO macrophages had elevated proinflammatory gene expression in response to LPS compared to WT. 138

Figure 4.9. fhe-miR-125b-5p repressed LPS-induced TNF secretion in Ago2 and Dicer KO cells. 141

Figure 4.10. fhe-miR-125b-5p repressed LPS-induced IL6 secretion in Ago2 KO cells. 142

Figure 4.11. Assessment of fhe-miR-125b-5p mediated suppression of endogenous target genes in Ago2 and Dicer KO macrophages. 144

Figure 5.1. Proposed novel targeting strategies for advancing diagnostics and therapeutic intervention in *Fasciola hepatica* infection. 163

List of tables

Table 1.1. Prevalence of human helminth infection worldwide 7

Table 1.2. Functional studies demonstrating cross-kingdom immunomodulatory role of helminth miRNAs in mammalian cells 16

Table 2.1. Details of the experimental *F. hepatica* infections in sheep. 44

Table 2.2. Mature miRNA sequences used to design Custom TaqMan primers 48

Table 2.3. Total read counts of *Fasciola hepatica* miRNAs detected within sheep sera samples 53

Table 2.4. Assessment of primer sensitivity and specificity using lamb tissue and sheep sera. 56

Table 3.1. Sequences of mature fhe-miR-125b-5p canonical and isomiR mimics 77

Table 3.2. Gene names and corresponding TaqMan gene expression assay IDs for qPCR 79

Table 3.3. Cloned 3′ UTR regions of predicted fhe-miR-125b-5p target genes in psi-Check-2 vector for luciferase reporter assays. 81

Table 3.4. *F. hepatica* derived miRNAs were enriched in the peritoneal macrophages of infected mice. 86

Table 3.5. The *Fasciola hepatica*-derived miRNAs in mouse macrophages during infection displayed length heterogeneity. 89

Table 3.6. Reported abundance of the four selected *F. hepatica* miRNA isomiRs across different worm life stages. Sequence abundance is visualized as a heat map using a red colour scale for each sample. 91

Table 3.7. Selection of predicted host target genes of fhe-miR-125b associated with macrophage M1 polarization and proinflammatory signalling. 97

Table 4.1. CRISPR-Cas9 sgRNAs used for the generation of Ago2 and Dicer1 gene knockouts in RAW264.7 cells. 121

Table 4.2. Ago2 and Dicer1 gene knockout subclones in RAW264.7 cells received from the Monash Genome Modification Platform (Monash University, Australia) 128

Abbreviations

Abbreviation	Definition
AD	Adult *Fasciola hepatica*
Ago	Argonaute (family of RNA-binding proteins, Ago1-Ago4 in mammals)
ALYREF	Aly/REF export factor (RNA-binding protein)
BMDM	Bone marrow–derived macrophage
bp	Base pair
Can	Canonical form of miRNA mimic
Cas9	CRISPR-associated protein 9
CCBY	Creative Commons Attribution License
CFSE	Carboxyfluorescein succinimidyl ester
cDNA	Complementary DNA
C. elegans	*Caenorhabditis elegans*
CO_2	Carbon dioxide
CRISPR	Clustered regularly interspaced short palindromic repeats
DGCR8	DiGeorge critical region 8 (partner protein of Drosha)
Dicer	Endoribonuclease in miRNA biogenesis
DMEM	Dulbecco's Modified Eagle Medium
DNA	Deoxyribonucleic acid
dpi	Days post infection
Drosha	RNase III enzyme for pri-miRNA cleavage
dsRNA	Double-stranded RNA
E. coli	*Escherichia coli*
ELISA	Enzyme-linked immunosorbent assay
ENS	Ensembl gene/transcript identifier
EV	Extracellular vesicle
F. hepatica (fhe)	*Fasciola hepatica*
FBS	Foetal bovine serum
FE	Free energy (kcal/mol, miRNA–mRNA binding strength)
fhe-miR	*Fasciola hepatica* microRNA
gDNA	Genomic DNA
GO	Gene Ontology

h	Hour(s)
Hif1a	Hypoxia-inducible factor 1 alpha
IL6	Interleukin 6
Il17rd	Interleukin 17 receptor D
Iso	IsomiR form of miRNA mimic
JUV	Juvenile Fasciola hepatica
KO	Knockout
LDH	Lactate dehydrogenase
lncRNA	Long non-coding RNA
LPS	Lipopolysaccharide
M-CSF	Macrophage colony-stimulating factor
min	Minute
miRNA (miR)	MicroRNA
miRanda	MicroRNA target prediction algorithm
mRNA	Messenger RNA
mtDNA	Mitochondrial DNA
MVP	Major vault protein (RNA-binding protein)
NEJ	Newly excysted juvenile Fasciola hepatica
Nod1	Nucleotide-binding oligomerisation domain-containing protein 1
nt	Nucleotide
NTC	No-template control
P2rx7	P2X purinoceptor 7
PAMP	Pathogen-associated molecular pattern
PBS	Phosphate-buffered saline
PCR	Polymerase chain reaction
Pin1	Peptidyl-prolyl cis-trans isomerase NIMA-interacting 1
PKR	Protein kinase R
POC	Point-of-care
pre-miRNA	Precursor microRNA
pri-miRNA	Primary microRNA transcript
qPCR	Quantitative polymerase chain reaction (real-time PCR)
RBP	RNA-binding protein
Revigo	Gene ontology semantic clustering tool

RISC	RNA-induced silencing complex
RNA	Ribonucleic acid
RNAi	RNA interference
RNA Seq	RNA sequencing
ROS	Reactive oxygen species
RPMI	Roswell Park Memorial Institute medium
rpm	Revolutions per minute
RT	Reverse transcription
RT-qPCR	Reverse transcription quantitative polymerase chain reaction
Runx1	Runt-related transcription factor 1
S. haematobium	*Schistosoma haematobium*
S. japonicum	*Schistosoma japonicum*
S. mansoni	*Schistosoma mansoni*
SNP	Single nucleotide polymorphism
siRNA	Small interfering RNA
SEM	Standard error of the mean
Stat3	Signal transducer and activator of transcription 3
SYNCRIP	Synaptotagmin-binding cytoplasmic RNA-interacting protein (RBP)
tRNA	Transfer RNA
TNF	Tumour necrosis factor
UTR	Untranslated region
w	Weeks
wpi	Weeks post infection
WT	Wild type
XPO5	Exportin-5
YBX1	Y-box binding protein 1

Abstract

Parasitic worms (helminths) infect over 1.5 billion people worldwide and cause tens of billions of dollars in annual losses to global livestock productivity, including more than $450 million each year in Australia alone. Their success as pathogens lies in their ability to manipulate host protective immune responses and establish chronic infections. Current control strategies rely heavily on mass drug administration in humans and routine anthelmintic drenching in livestock; however, these measures are increasingly undermined by the rapid emergence of drug resistance, the absence of effective vaccines, and the poor sensitivity of existing diagnostics for detecting early or low-intensity infections. Together, these challenges highlight the urgent need for innovative strategies to detect, control, and ultimately reduce the burden of helminth infections.

Against this backdrop, parasite-derived microRNAs (miRNAs) have emerged as promising mediators of host-parasite interactions. Yet their mechanisms, functions, and integration into host RNA interference (RNAi) pathways remain poorly understood. Using *Fasciola hepatica* as a model organism, this PhD project investigated the roles of helminth miRNAs in parasite-host communication, with a focus on their potential as diagnostic biomarkers, their mechanisms in regulating host innate immune responses, and their exploitation of mammalian RNAi machinery.

Chapter 1 explored the contribution of helminth-derived miRNAs to cross-kingdom communication by reviewing reported evidence of their selective release, uptake, processing, and downstream effects during infection. This revealed that many parasite miRNAs are conserved with mammalian sequences and therefore predicted to target host immune-regulatory genes. Packaged within extracellular vesicles (EVs) or bound to protein carriers, they can be delivered into host cells where they alter gene expression to consequently regulate host immune responses, thus facilitating parasite persistence. Based on this review, the thesis proposed that helminth-derived miRNAs and their molecular functionality present promising avenues for the development of new diagnostic tools and therapeutic interventions.

Building on this foundation, Chapter 2 investigated the potential application of circulating miRNA profiling as a biomarker of fasciolosis. Using serum samples from a longitudinal sheep infection model, small RNA sequencing revealed dynamic shifts in host miRNA expression as early as two days post-infection. Distinct host- and parasite-derived signatures distinguished

the pre-hepatic and hepatic phases of infection, while qPCR validation identified oar-miR-133 and oar-miR-3957 as robust early biomarkers. These findings present the translational promise of miRNAs as specific, sensitive, and stage-resolved indicators of infection.

Chapter 3 advanced the understanding of helminth-derived miRNAs functionality by showing for the first time, that parasite-derived miRNAs are predominantly present as diverse isoforms (isomiRs) in macrophages of *F. hepatica*-infected mice. Comparative sequencing across parasite life stages, EVs, and host cells suggested selective deployment of isomiRs into host immune cells. While functional assays revealed that a 3′-trimmed isomiR of fhe-miR-125b-5p suppressed LPS induced inflammatory responses to similar levels as the canonical counterpart, dual luciferase reporter assays suggested the isomiR had stronger regulatory effect for select innate immune genes. Furthermore, Argonaute2 (Ago2) pulldowns from transfected macrophages, showed a preferential loading of the isomiR onto host Ago2. These findings established isomiRs as biologically functional molecules actively exploited by *F. hepatica* to fine-tune host immunity.

Chapter 4 further dissected the mechanistic requirements of parasite miRNAs and isomiRs in host cells using CRISPR-Cas9-engineered Ago2 and Dicer knockout (KO) RAW264.7 macrophages. While Chapter 3 showed preferential loading of fhe-miR-125b onto Ago2, the parasite miRNAs retained activity in Ago2-deficient cells, implicating redundancy in their interaction with mammalian Ago proteins. Remarkably, parasite miRNAs also remained functional in Dicer KO cells, indicating that mature worm-derived miRNAs bypass canonical biogenesis and directly associate with host Ago proteins to exert RNAi activity. Together, these results reveal the evolutionary flexibility of parasite miRNAs in co-opting mammalian RNAi machinery to sustain immunomodulatory control.

Collectively, this research using *F. hepatica* as a model organism provides new insights into helminth biology. It demonstrates that host- and parasite-derived miRNAs hold promise as stage-specific biomarkers for early detection of infection, shows that *F. hepatica* selectively deploys isomiRs to modulate host immunity, and uncovers the flexible mechanisms by which parasite miRNAs engage mammalian RNAi pathways to maintain regulatory control. These discoveries redefine current paradigms of cross-kingdom communication and lay the groundwork for innovative diagnostic and therapeutic strategies to combat helminthiases.

Chapter 1:

Introduction

Publication Statement

An edited version of Section 1.4 of this chapter has been published as a Review article in *Trends in Parasitology*: Chowdhury S, Sais D, Donnelly S, Tran N. The knowns and unknowns of helminth-host miRNA cross-kingdom communication. Trends Parasitol. 2024 Feb;40(2):176-191. doi: 10.1016/j.pt.2023.12.003. (Appendix A)

The text presented here has been edited for insertion into the general introduction and to support continuity. The numbering of sections, style of referencing, the numbering of tables and figures have also been altered to align with the formatting of the thesis.

Copyright Declaration: Under the Elsevier Terms and Conditions, authors retain the copyright to their work. Furthermore, all Elsevier articles are Open Access and distributed under the terms of the Creative Commons Attribution License (CC-BY 3,0), which permits the use, distribution, and reproduction of material from published articles, provided the original authors and source are credited and subject to any copyright notices concerning any third-party content.

Author Contribution: Sumaiya Chowdhury (graduate student) is the first author of this article. In consultation with her supervisors, she conceived and planned the review, conducted the literature search, designed, and wrote the first draft of the manuscript. Her supervisors, Sheila Donnelly, Nham Tran and Dayna Sais guided the conception and contributed to the writing and editing of the final manuscript.

Signatures:

Sumaiya Chowdhury (graduate student) Production Note: Signature removed prior to publication.

Dayna Sais (PhD supervisor) Production Note: Signature removed prior to publication.

Sheila Donnelly (PhD supervisor) Production Note: Signature removed prior to publication.

Nham Tran (PhD supervisor) Production Note: Signature removed prior to publication.

1.1. Helminth infections are a major health and economic burden

Parasitic worms (helminths) are a polyphyletic group of extracellular macro-parasites comprising of nematodes (roundworms), cestodes (tapeworms), and trematodes (flatworms). They are considered highly adept pathogens due to their ability to establish chronic infection in their mammalian hosts that can last for decades. Although these parasites differ significantly in their host preferences, life cycle, routes of infection and tissue tropism (Figure 1.1), a universal feature of all helminths is their ability to manipulate the host's immune responses during both the acute and chronic phases of infection, allowing them to evade protective mechanisms and promote regulatory pathways that enable their long-term survival [1]. During this time, while feeding on tissues and blood to sustain their own survival and reproduction, helminths inflict tissue damage and impair the host's ability to absorb essential nutrients, contributing to malnutrition and pathology [2].

Almost 300 different species of helminths have been identified with the capacity to infect humans [3]. Accordingly, helminth infections are a major global public health problem with recent estimates suggesting that 1.5 billion people harbour one or more of the most common worms: *Schistosoma spp., Fasciola hepatica, Ascaris lumbricoides, Necator americanus, Ancylostoma duodenale, Trichuris trichiura, and Strongyloides stercorali* (Table 1.1; Figure 1.1) [4, 5]. These worms are particularly widespread in low- and middle-income regions, where sanitation is poor and healthcare infrastructure is limited [6]. In endemic areas, chronic helminth infections impair physical and cognitive development, reduce work productivity, and exacerbate poverty [6]. Moreover, exposure to helminths is difficult to avoid for ruminants grazing on pastures and as such, infections place a significant economic burden on the livestock productivity, affecting growth rates, fertility, meat quality, wool and milk production [7]. Helminthiasis is responsible for tens of billions of dollars of loss to the global livestock industry annually [7]. In Australia, these parasitic infections in livestock are conservatively estimated to cost > $450 million per year [8]. Despite this widespread impact on human health and economic productivity, helminth infections remain categorized as neglected tropical diseases, receiving limited attention and resources in global health initiatives [9].

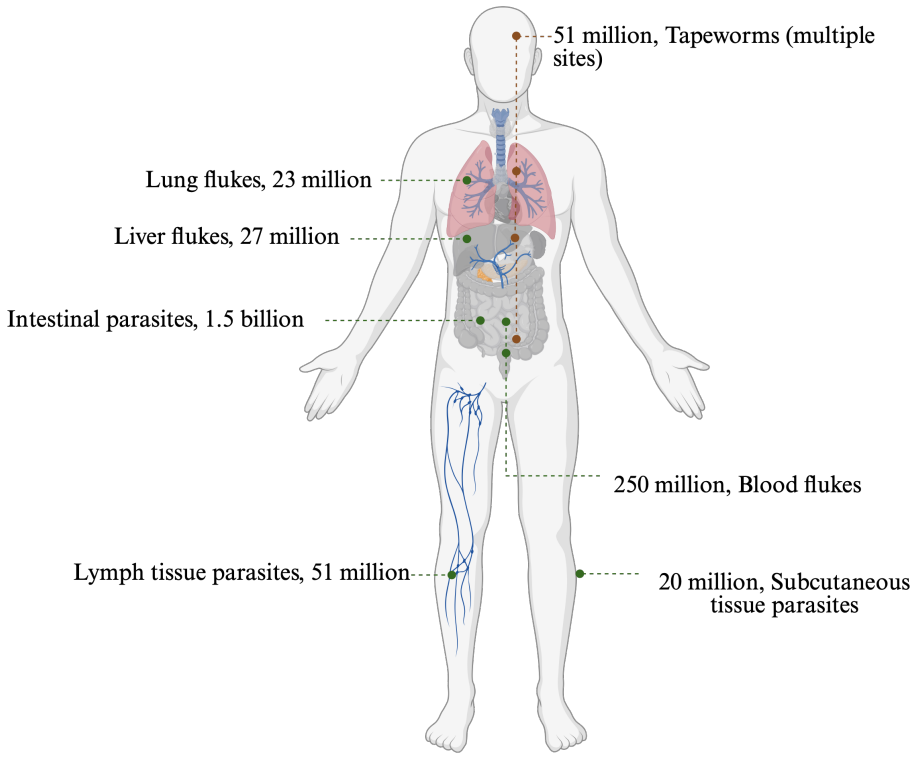


Figure 1.1. Prevalence of helminth infections in human. *Helminths comprise of a diverse group of parasitic worms that can infect various tissues and organs in humans and other animals, leading to diverse health complications. Globally, helminth infections are estimated to affect around 1.5 billion people, posing a major public health challenge. This Figure was created using Biorender.com*

Table 1.1. Prevalence of human helminth infection worldwide

Parasite type	Helminth species	Pathology	Geographical distribution	Estimated prevalence	Refs
Lung flukes	*Paragonimus spp.*	An acute syndrome with cough, abdominal pain, discomfort, and low-grade	South America; Eastern Asia; Africa	23 million	[10]
Liver flukes	*Fasciola hepatica*	Toxaemia, cholangitis, eosinophilia	81 countries globally	2.5 million	[11]
	Clonorchis sinensis	Cholangitis, abscesses, biliary carcinoma	South Korea, China, northern Vietnam, and far-eastern Russia	15 million	[12]
	Opisthorchis spp.	Cholangitis, abscesses, biliary carcinoma	Southeast Asia	10 million	[13]
Intestinal parasites	*Ascaris lumbricoides*	Moderate infections can lead to undernutrition in children	Predominantly in Central and South America, Africa and Asia	732 million	[14]
	Necator americanus	None; development of abdominal pain and anemia depends on worm burden	Especially common in southern China, Southeast Asia, the Americas and most of Africa	500 million	[15]
	Ancylostoma duodenale	None; development of abdominal pain and anemia depends on worm burden	Mediterranean region and northern India and China		
	Strongyloides stercoralis	None; development of abdominal pain and anemia depends on worm burden	Predominantly found in South-East Asia, Africa, and Western Pacific	613 million	[16]
	Trichinella spiralis	Typically asymptomatic; can be associated with abdominal and muscle pain	Global distribution	11 million	[17]
	Trichuris trichiura	Typically asymptomatic; heavy worm burdens associated with anemia and painful stool passage	Prevalent worldwide, and is most common in warm, moist, tropical and subtropical regions	290 million	[18]
	Enterobius vermicularis	Typically asymptomatic; but can be associated with nocturnal perianal pruritus	Worldwide; highest prevalence in children	> 200 million	[5]
Lymph tissue parasites	*Wuchereria bancrofti*	Typically asymptomatic; but can be associated with enlarged lymph nodes leading to lymphedema	Africa and Asia	51 million	[19]
	Brugia malayi	Typically asymptomatic; but can be associated with enlarged lymph nodes leading to lymphedema			

	Brugia timori	Typically asymptomatic; but can be associated with enlarged lymph nodes leading to lymphedema			
Blood flukes	*Schistosoma mansoni*	Can be associated with cercarial dermatitis, Katayama fever; abdominal pain, liver fibrosis	Central and West Africa, Egypt, Brazil, the Arabian Peninsula, Surinam, Venezuela, Madagascar and the West Indies	250 million	[20]
	Schistosoma japonicum	Can be associated with cercarial dermatitis, Katayama fever; abdominal pain, liver fibrosis	China, Japan, Indonesia and the Philippines		
	Schistosoma haematobium	Can be associated with hematuria, scarring, calcification, squamous cell carcinoma, and egg granulomas in brain or spinal cord.	Africa, Middle East and India		
Subcutaneous tissue parasites	*Onchocerca volvulus*	Dermatitis, subcutaneous nodules, sclerosing lymphadenitis, and eye disease.	Predominantly in sub-Saharan Africa	20 million	[21]
Tape worms	*Echinococcus spp*	Typically, asymptomatic for years; cyst rupture is associated with secondary pathologies	Globally distributed. Alveolar echinococcosis is confined to the northern hemisphere, in particular regions of China, the Russian Federation and continental Europe and North America	1 million	[22]
	Tania solium	Most intestinal infections are asymptomatic; Neurocysticercosis is associated with seizures, intracranial hypertension and psychiatric disturbances	Globally distributed	50 million	[23]

1.2. Controlling helminth infections is challenging

Several persistent challenges prevent the effective control of helminth infections. One of the most significant barriers is the lack of tools for early diagnosis. Many helminth infections, especially in animals, are clinically asymptomatic until substantial pathology has occurred [1] and current diagnostic tools lack the sensitivity and specificity required for effective surveillance and timely intervention.

For over a century, the gold standard for diagnosing helminths has been coprological examination, detecting eggs (or L1 larvae in the case of lungworms) in faecal samples. Despite being cost-effective and relatively straightforward, this method has several limitations. These include intermittent egg shedding, low infection intensities that fall below detection thresholds, and degradation of samples due to improper handling or storage [24]. To improve accuracy, at least three fresh faecal samples should be examined over a 10-day period using concentration techniques. Even then, this method requires a skilled parasitologist, offers limited sensitivity in endemic regions where infections are typically low-grade, demands immediate analysis post-collection, and often fails to differentiate between different worm species [24]. Some serological ELISAs against anti-helminth antibodies have shown superior sensitivity compared to coprological tests. However, these methods also lack specificity, as antibodies can persist long after the infection has resolved, leading to false-positive results. Additionally, cross-reactivity with antibodies from other parasitic infections or unrelated pathogens can further compromise diagnostic accuracy [24].

Due to the lack of reliable diagnostics, helminth control programs have heavily relied on mass drug administration (MDA) in humans and routine blanket treatments in animals using broad-spectrum anthelmintics, such as ivermectin, diethylcarbamazine, albendazoles and praziquantel [25, 26]. While these methods are widely implemented, they are not without problems. They are costly, do not provide protection against reinfection, and the reliance on the limited arsenal of anthelminthics are driving the emergence of drug-resistant helminth strains [9, 27]. Furthermore, repeated use of chemical treatments has adverse environmental consequences and raises concerns about residues entering the food chain, posing risks to both ecosystem and human health.

There are currently no preventative vaccines against helminths. Anti-helminthic vaccine development remains an active but challenging field. Unlike vaccines for bacterial or viral infections, helminth vaccines face unique challenges due to the parasites' sophisticated

mechanisms for immune evasion and their complex life cycles, which span multiple developmental stages and tissue-specific niches, each expressing different antigens [28]. The earliest anthelmintic vaccine efforts used attenuated or irradiated worm homogenates. While these crude mixtures of disrupted whole worms demonstrated moderate to substantial protective effects in livestock [7, 29], such approaches present significant challenges in achieving standardization, reproducibility, and consistent efficacy [28, 30]. The composition of these homogenates varies depending on the worms' developmental stage and condition, and many of the included antigens are weakly immunogenic or even immunosuppressive, ultimately limiting their protective potential.

Together, these challenges highlight the urgent need for improved diagnostic tools, sustainable treatment approaches, and innovative vaccine strategies to achieve effective and long-lasting control of helminth infections. A deeper understanding of helminth-host interactions will be instrumental in developing novel and sustainable strategies for helminth control. Parasite-derived excretory and secretory (ES) molecules are particularly promising targets, as they are positioned at the host–parasite interface and play crucial roles in modulating host immune responses.

1.3. Exploring helminth-derived miRNAs as a new frontier for diagnostic and therapeutic advances

MicroRNAs (miRNAs) are small non-coding RNAs ~18-24 nucleotides (nt) in length that act as key post-transcriptional regulators of gene expression [31]. They function by binding to complementary sequences within the 3′ untranslated regions (3′ UTRs) of target messenger RNAs (mRNAs), leading to mRNA degradation or translational repression [31]. Through this mechanism, miRNAs play crucial roles in virtually all biological processes, including development, metabolism, immune regulation, and disease pathogenesis.

In helminths, growing research has highlighted the presence and importance of miRNAs in regulating parasite biology. To date, miRNAs have been identified in a wide range of parasitic species, and the core components of the miRNA biogenesis and silencing pathway, including Dicer, Argonaute (Ago) proteins, and other associated factors are evolutionarily conserved in helminths, underscoring the functional significance of miRNA-mediated gene regulation in these organisms [32, 33]. Helminths exhibit complex life cycles, transitioning through morphologically and physiologically distinct stages across various host environments. These

developmental transitions are orchestrated by tightly regulated gene expression programs, in which miRNAs are believed to serve as key molecular switches [34]. By controlling cell fate and phenotype, miRNAs are most likely essential regulators for growth and development of worms and their rapid adaptation to environmental cues.

Our understanding of miRNA biology in helminths is largely built upon foundational research in the free-living nematode *Caenorhabditis elegans*, a model organism that has been extensively used to decipher miRNA function. The landmark discovery of the first miRNAs, lin-4 and let-7 in *C. elegans*, and their central role in regulating developmental timing by regulating heterochronic genes, controlling larval stage transitions provided the preliminary understanding of miRNA-mediated post-transcriptional regulation [35, 36]. Orthologs of lin-4 have been identified in other nematodes, and let-7 has been found across a range of helminth species, where it plays a key role in developmental transitions [37-40]. Moreover, across various helminth species, distinct stage-specific miRNA expression profiles have been documented, underscoring the dynamic regulatory roles of miRNAs throughout the parasite life cycle [40-42]. Supporting this, a functional study has revealed that knockdown of *miR-71* in a model cestode disrupts normal development and promotes premature strobilation [43]. Furthermore, several *Schistosoma japonicum* miRNAs have been functionally characterized to be involved in female reproductive development and ovary maturation by targeting genes associated with egg production and reproductive tissue maintenance [44-47]. These findings highlight the essential roles of miRNAs in governing temporal developmental processes in helminths.

In *C. elegans*, oxidative stress induces changes in miRNA expression that promote the expression of enzymes involved in antioxidant defence mechanisms. Additionally, knockout of ALG-1, an Ago2 ortholog in *C. elegans* compromises resistance to oxidative stress and shortens lifespan [48]. miRNA pathways are also essential in heat shock recovery in *C. elegans* [49]. During host invasion and immune confrontation, parasitic worms encounter high levels of reactive oxygen species (ROS) [50]. Therefore, based on the observations for *C. elegans,* it is feasible that miRNA-mediated mechanisms may also help parasitic helminths regulate their responses to fluctuating microenvironments as they traverse between different host tissues and undergo physiological transitions during their development. This hypothesis has been supported by the evidence that stage-specific miRNAs of *Fasciola hepatica* regulate glycolysis and anaerobic metabolic genes coinciding with the metabolic shift from aerobic to anaerobic

conditions during migration from the peritoneum to the liver [41]. Furthermore, Schistosoma miRNAs modulate expression of tegument-associated genes, contributing to tegument transformation that is essential for immune evasion in host [51].

The compilation of this emerging evidence supports a fundamental role for miRNAs in helminth development, maturation and adaptation to the host environment which opens potential new targets for infection control. However, it is important to recognize the limitations of extrapolating findings from *C. elegans* to parasitic species, given their divergent lifestyles and the requirement of a definitive host. Parasitic helminths are thought to have evolved from free living ancestors, thereby retaining ancestral genomic components while also acquiring new ones to support their parasitic lifestyle [52, 53]. The divergence in miRNAs and their targets from *C. elegans* to parasitic nematodes [54] further emphasise the need for functional studies directly in parasitic species, in order to uncover species-specific roles and advance our understanding of miRNA-mediated regulation in these parasites.

An intriguing facet specific to parasitic helminth miRNAs is their role in the host-parasite relationship. Helminths secrete miRNAs, often encapsulated in extracellular vesicles (EVs) into host tissues and fluids. These parasite-secreted miRNAs are detectable in blood, urine, and other biofluids, making them promising biomarkers for diagnostic applications that could be specific to the individual parasite [55]. Moreover, helminth infections dysregulates host miRNA expression profiles from the early onset of infection, offering additional avenues for sensitive biomarker discovery [56, 57]. Combining both parasite-derived and host-dysregulated miRNAs may provide a more robust and sensitive approach for the diagnosis of helminth infections, reflecting both the direct secretions from the parasite and the associated responses within the host.

Beyond their diagnostic utility, helminth extracellular miRNAs are increasingly recognized as agents of cross-kingdom communication, modulating host immune signalling pathways in ways that favour parasite persistence and immune modulation.

1.4. The knowns and unknowns of helminth-host miRNA cross-kingdom communication

1.4.1. The theory of cross-kingdom miRNA communication

"Cross-kingdom communication" refers to the transmission of extracellular chemicals and bioactive molecules resulting in the regulation of biological signals between genetically diverse species. This term was first coined in the 1980's following the realisation that distinct cells can communicate with each other through secreted hormones [58]. Subsequently, the concept expanded with the discovery that bacteria had the capacity to manipulate the signal transduction of plant and mammalian cells, while host hormones cross-signalled with quorum sensing molecules to regulate bacterial gene expression [59].

Most recently, miRNAs have emerged as important mediators of inter-kingdom communication. It is thought that in metazoans, miRNAs originated as a defence mechanism against pathogens with predominantly antiviral functions, but over time, have evolved to target intrinsic genes. As a result, endogenous miRNAs have developed as a highly conserved mechanism of gene regulation that controls a multitude of biological functions, such as developmental processes, cell cycle processes, intracellular signalling, and homeostasis [60].

miRNAs possess the ability to move between cells, acting as intermediates in cellular communication. Several studies conducted in animals and plants have provided increasing evidence that pathogens, including bacteria, viruses, fungi, and protozoa, utilise these mobile miRNAs as a mechanism to manipulate host gene expression [61]. Most recently, we, and others, have demonstrated that larger, multicellular helminths also deploy miRNAs to specifically divert and manipulate their host's immune responses, to prevent their expulsion and tolerate their presence which permits the establishment of chronic infections [34, 41, 62-65]. However, while there has been extensive characterisation of the helminth miRNomes and their corresponding host target genes, very little is known about how these miRNAs are selected by the parasite for transfer to host cells and, once there, how they integrate into the host cell miRNA biogenesis pathway.

1.4.2. Helminth-derived miRNAs alter the host immune response to establish chronic infection

Unlike bacteria or viral pathogens, helminths do not replicate in their hosts. Instead, they require time to grow to maturity, reproduce and release their offspring in the form of eggs. To accomplish this cycle, helminths have evolved mechanisms to regulate the host immune cell

signalling pathways to prevent their expulsion while also safeguarding the fitness of the host [66]. During helminth infection, the typical innate detection systems of the host are not activated as expected and the adaptive immune response is directed towards a tolerant or hyporesponsive state [67, 68]. As a result, parasitic worms establish chronic infections to complete their life cycle, while the tissue damage caused by their feeding and migration is readily repaired, and excessive inflammation is controlled [69, 70]. Understanding the communication pathways between helminths and their hosts during this process will inform the development of new anthelminthic therapeutics.

Historically, the focus for this research has been on the identification and characterisation of parasite secreted proteins as it was assumed these were the most likely molecules to be in contact with host immune cells and operate as immune modulators [71-73]. However, more recently helminth-derived miRNAs are emerging as key manipulators of host immune cells [34, 41, 54, 62, 74-84]. The miRNA profile of helminths has been characterised in over 35 species of trematodes, nematodes and cestodes [84]. Comparative analysis of miRNA sequences has revealed that helminth miRNAs are well conserved, with many parasite miRNAs sharing sequence identity with mammalian miRNAs and thus predicted to have the same regulatory functions as their host miRNAs, many of which target immune-modulating genes (Supplementary Table 1.1; Figure 1.2 A). *In silico* analysis has also predicted that several non-conserved, novel parasite miRNA sequences could target host genes involved in immune pathways, thus suggesting immune modulatory functionality (Supplementary Table 1.1; Figure 1.2 B) [34, 75]

The breadth of miRNAs and corresponding mammalian targets suggests a high degree of redundancy, with multiple helminth miRNAs (conserved and novel) predicted to act on single host gene targets within multiple immune cells (Supplementary Table 1.1; Figure 1.2 C). Such findings support the hypothesis that by hijacking the host endogenous miRNA system of gene regulation, helminths can alter host gene expression and hence modulate the host immune response to a phenotype that favours parasite survival and reproduction. There is now supporting experimental evidence for this possibility from both *in vivo* mouse infection models and *in vitro* transfections of mammalian cells (Table 1.2), which collectively and convincingly support that helminth-derived miRNAs can be taken up by mammalian cells and once internalised, operate to regulate gene expression, to alter key immune pathways and cellular processes.

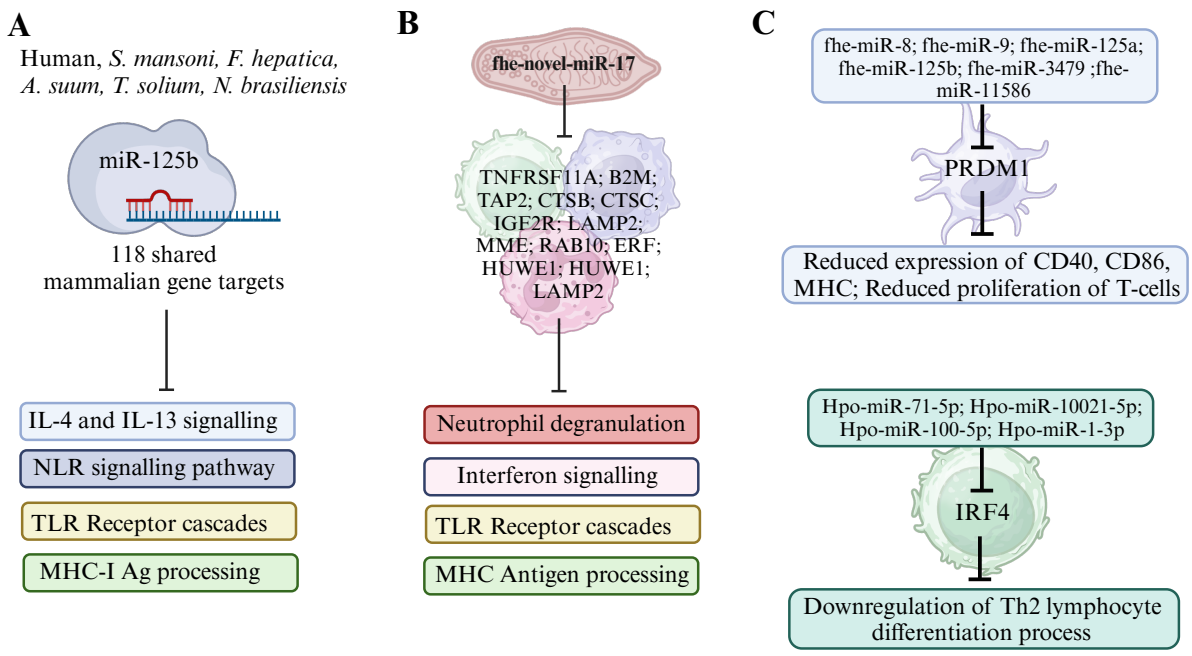


Figure 1.2. Helminth miRNAs are predicted to regulate the immune response during infection. *(A) Several parasites express miR-125b, a highly conserved miRNA also expressed in mammalian cells, with roles in the activation of multiple immune processes. miRbase (https://mirdb.org) predicts that human miR-125b has 925 gene targets. Of these, the parasite miR-125bs have been predicted to target 118 genes. Pathway analysis of these targets using Reactome suggests that parasite miRNAs would impact the processing and presentation of antigen by Major Histocompatibility Complex I (MHC) and cell signalling pathways activated by IL-4, IL-13, NOD-like Receptors (NLR), and Toll Like Receptors (TLR); (B) The prediction of gene targets for novel, non-conserved, parasite miRNAs suggests that they also have the capacity to regulate mammalian gene targets. For example, miRanda, PITA, and RNAhybrid predicted thirteen mammalian gene targets for Fasciola hepatica novel miR-17. Reactome analysis attributed these genes to immune pathways associated to neutrophil degranulation, Interferon signalling, TLR receptor signalling, and MHC I and II mediated antigen processing; (C) Multiple parasite miRNAs are predicted to target the same mammalian gene suggesting a level of redundancy. As an example, six different miRNAs expressed by Fasciola hepatica have been predicted to target Positive Regulatory Domain I-Binding Factor 1 (PRDM1), a protein that promotes the expression of costimulatory molecules on dendritic cells that are necessary for efficient T-cell activation, and the development of an effector adaptive immune response. Similarly, four different miRNAs produced by the nematode Heligmosomoides polygyrus are predicted to target Interferon Regulatory Factor (IRF)-4, a key regulatory transcription factor in the development of immune cells. This Figure was created using Biorender.*

Table 1.2. Functional studies demonstrating cross-kingdom immunomodulatory role of helminth miRNAs in mammalian cells

Parasite	Parasite-derived miRNA(s)	Host gene target(s)	Host target cell	Model used for study	Immune response	Refs
Fasciola hepatica	fhe-miR-125b-5p	*Traf6*	Peritoneal macrophages	*In vitro* murine bone marrow derived macrophages	Suppression of M1 macrophage phenotype	[63]
Clonorchis sinensis	csi-let-7a-5p	*Clec7a, Socs1*	Hepatic macrophages	*In vitro* RAW264.7 murine macrophage cell line	Promotion of M1 phenotype by upregulation of NF-kB signalling and induction of proinflammatory cytokines TNF, Interleukin(IL)-6 and IL-1b.	[85]
Schistosoma mansoni	sma-miR-10	*Map3k7*	T cells	*In vitro* human HEK-293 human embryonic kidney cell line	Suppression of host Th2 cell differentiation by regulating the Th2 transcriptional pathway	[86]
Schistosoma japonicum	sja-miR-71a	*Sema4D*	Hepatic stellate cells	*In vivo* murine model of *S. japonicum* infection; targets validated *in vitro* using 293T human embryonic kidney cell line	Inhibition of hepatic stellate cell activation by downregulation of the TGF-β1/SMAD and IL-13/ Signal Transducer And Activator Of Transcription (STAT)6 pathways and regulation of the Th1/Th2/Th17 and regulatory T cell balance	[87]
Schistosoma japonicum	sja-miR-2162	*Tgfbr3*	Hepatic stellate cells	*In vivo* murine model of *S. japonicum* infection and *in vitro* rat HSC-T6, human LX-2 cell line, mouse primary hepatic stellate cells	Activation of hepatic stellate cells via activation of TGF-b signalling pathway, and activation of hepatic fibrosis	[88]
Schistosoma japonicum	sja-miR-71a	*Fzd4*	HepG2 and SMMC-7721 hepatoma cell line	*In vivo* murine model and *in vitro* HepG2 human hepatoma cells	Anti-tumour activity: inhibit tumour proliferation by cell cycle arrest at G_0/G_1 phase	[89]
Schistosoma japonicum	sja-miR-125b, sja-bantam	*Pros1, Fam212b*	Circulating monocytes	*In vitro* RAW264.7 murine macrophage cell line	Increased monocyte proliferation and TNF production	[79]
Heligmosomoides polygyrus	hpo-let-7, hpo-miR-200, hpo-miR-435	*Dusp1*	Epithelial MODE-K cell line	*In vitro* MODE-K murine enterocyte cell line	Increased anti-inflammatory responses by repression of mitogen activated protein kinase (MAPK) signalling	[62]

Heligmosomoides polygyrus	hpo-miR-71-5p	*Irf4*	T cells	*In vitro* murine primary CD4+ T cells	Downregulation of genes and pathways of the Th2 lymphocyte differentiation process: interferon (IFN)γ signalling, the IL-2/STAT5 signalling, and the mTOR signalling pathways.	[90]
Ascaris suum	asu-miR-791-3p	*Mtor*	T cells	*In vitro* murine primary CD4+ T cells	Downregulation of genes and pathways of the Th2 lymphocyte differentiation process: interferon gamma signalling, the IL-2/STAT5 signalling, and the mTOR signalling pathways.	[90]
Taenia pisiformis	tpi-miR-let-7-5p	*Cebpd*	Macrophages	*In vitro* RAW264.7 murine macrophage cell line	Suppression the host Th2 immune response by repression of M1 phenotype markers and promotion of M2 phenotype markers.	[91]
Taenia solium and Taenia crassiceps	miR-10-5p, let-7-5p	Not validated	Peritoneal macrophages	*In vitro* murine primary peritoneal macrophages	Downregulation of proinflammatory cytokines in IFN-γ treated M1 macrophages, and downregulation of anti-inflammatory cytokines in IL-4 treated M2 macrophages.	[92]
Echinococcus multilocularis	emu-miR-4989-3p	Not validated	Macrophages	*In vitro* RAW264.7 murine macrophage cell line	Inhibition of macrophage nitric oxide (NO) production and increased TNF production	[77]
E Echinococcus multilocularis	emu-miR-71	Not validated	Macrophages	*In vitro* RAW264.7 murine macrophage cell line	Inhibition of macrophage NO production and altered inflammatory response	[93]

1.4.3. Delivery of helminth miRNAs to host cells

1.4.3.1. miRNAs are released by helminths in extracellular vesicles and non-vesicular forms

The most widely characterised mechanism of intracellular (and cross-kingdom) communication is via the secretion and uptake of EVs [94]. Encapsulation of miRNAs in EVs protects them from degradation by RNases in the harsh extracellular environment of the bloodstream or the digestive system [62]. Furthermore, intercellular delivery of miRNA via EVs can circumvent the recipient cell's transcriptional regulations, offering a comparatively straightforward mechanism of gene regulation.

While only characterised in a few studies, the presence of non-vesicular extracellular (ex)-miRNA has also been described in all three classes of helminths [75, 82, 95]. Although it is possible that these ex-miRNAs have been accidently released by damaged cells or dying parasites, in humans it has been shown that miRNAs are also actively transported in highly stable complexes with proteins [96]. It has been reported that more than half of the miRNAs found in human serum is bound to ribonucleoproteins, including Ago2 [97, 98], although other proteins such as high-density lipoprotein (HDL), and Ago1, 3 and 4 have also been implicated in ex-miRNA binding, transport, and delivery to cells [99, 100]. However, there is still no direct evidence that these miRNA-protein complexes operate in a functional way to alter recipient cell gene expression. Nonetheless, the observation that the profile of miRNAs bound to HDL is distinct from that found in EVs, suggests a complementary and independent mechanism of miRNA transport and gene regulation [101].

For helminths, the current data indicates that the choice to secrete miRNAs packaged in EVs or in vesicle free form may be influenced by the requirements for different stages of their life cycle. For example, during the L4 larval stage of the *H. contortus* life cycle, ex-miRNAs are more abundant in the vesicle free fraction of the parasite secretions as compared to the adult stage, in which miRNAs are found primarily in the vesicle enriched fraction [82]. Similarly, the miRNAs secreted by adult *T. spiralis*, which inhabit intestinal mucosa, are primarily packaged in vesicles, whereas, the muscle stage larvae, which live intracellularly, secrete unencapsulated miRNAs [95]. While a similar stage-specific differential abundance of free versus vesicular miRNAs has not been described for any cestodes or trematodes, analysis of the excretory/secretory products of the schistosomula of *Schistosoma mansoni* identified the presence of both forms of miRNAs [65], suggesting that this process of miRNA transfer is common to all helminths. However, it is important to note that vesicle free extracellular miRNA-protein complexes may originate from EVs that lyse during isolation and preparation. Although this could be determined by the analysis of multiple biological replicates and independent preparations of parasites and their secretory products, it is technically challenging given the paucity of material that is often obtained from these parasites. Despite this caveat, the fact that

several miRNA sequences that were identified in the EV-depleted library of *H. contorus* L4 larvae, were not found within the EV-enriched library [82], suggests the vesicle free miRNAs are released independently of the EV packaged sequences.

1.4.3.2. Helminth-derived extracellular vesicles are taken up by host immune cells

Examination of the cargo of helminth-derived EVs revealed that miRNAs are highly represented, [62, 102, 103] and it has now been shown for several species of helminths that EV encapsulated miRNAs are internalised by mammalian host cells, particularly by immune cells such as, macrophages, monocytes, and dendritic cells [104]. The specificity of this cellular interaction is determined by the size of the vesicles as illustrated with EVs derived from *E. granulosus,* with smaller EVs (10K and 2K) taken up by host hepatic cells more efficiently than larger EVs (110K) [105]. The intracellular location in host cells after uptake is influenced by the surface proteins on the parasite-derived EVs. This was shown by the addition of antibodies specific to the surface proteins of *H. polygyrus* EVs, which resulted in the enhanced uptake of the EVs but redirected them to lysosomes for degradation in the recipient cell [106]. Blocking worm EV release is detrimental to parasite survival in their hosts [107] likely because this also blocks the delivery of parasite-derived immunomodulatory miRNAs to host cells, which, in turn, would allow the development of host protective immune responses to mediate parasite expulsion.

1.4.3.3. Selective sorting of parasite-derived miRNAs into EVs

There are several pieces of evidence that suggest the selection and incorporation of miRNAs into parasite-derived EVs is an active controlled process rather than an arbitrary occurrence. Firstly, the abundance of miRNAs within helminth EVs does not reflect the profile of intracellular expression, with miRNAs that are relatively highly expressed intracellularly not found in the secreted EVs, suggesting preferential selection of miRNA for cargo [77]. Furthermore, while the proteins involved in EV biogenesis pathways have been shown to be constitutively expressed, the EV miRNA cargo is developmentally regulated [78, 108]. This life stage-specific miRNA packaging in the EVs is likely necessary to cater for the differential requirements of host gene regulation during the various life stages of the helminths. Secondly, several miRNAs are consistently found in EVs of different species of helminths, suggesting an evolutionarily conserved mechanism for the packaging and release of specific miRNAs [54, 81, 82]. Notably, the miRNAs within the helminth EVs contain more conserved miRNAs with higher seed sequence identity to mammalian host miRNA compared to helminth intracellular miRNAs, which may simply correspond to the conservation of ancient miRNAs across metazoans or might reflect an active selection for compatibility with host miRNA machinery.

Furthermore, the most abundant EV encapsulated miRNAs are predicted to primarily target mammalian genes involved in the immune and inflammatory pathways (Supplementary Table 1.1).

According to the available data, most common EV miRNAs with immune-modulatory functions are let-7, miR-125, miR-71, miR-2, miR-9, miR-10, miR-31, and miR-87 (Supplementary Table 1.1), and the most predominant predicted pathways targeted are MAPK, TGF-beta, TNF, Wnt signalling, IGF signalling pathway (Supplementary Table 1.1). The profile of EV miRNAs and their host targets is remarkably similar between the trematodes (flukes) and nematodes (round worms), with cestodes (tapeworms) displaying a more distinct profile of miRNA abundance and gene targets (Supplementary Table 1.1). This is somewhat surprising as trematodes and cestodes belong to the same phyla (platyhelminth), so these differing profiles may, in fact, reflect the relative lack of characterisation of cestode miRNomes compared to the more advanced characterisation of trematodes and nematodes.

Although these observations present convincing evidence that helminth miRNAs are selectively sorted for delivery to their host cells, the mechanism by which this occurs is unknown. Research on mammalian cells has highlighted a prominent role for the Ago2 protein in sorting miRNA via the KRAS-MEK-ERK signalling pathway [109]. While the presence of Ago2 orthologues in the genome of most trematodes and cestodes, would suggest that a similar process may be utilised by these worms, there is no evidence of this protein interacting with any miRNAs within parasite EVs [32]. However, nematodes also express a lineage-specific expansion of Ago proteins (WAGO), one of which reportedly mediates the exports of small interfering RNAs into the EVs of *H. bakeri* [110]. The conservation of WAGO in Clade V nematodes suggests the existence of a specialised RNA secretion pathway for these helminths.

Several RNA binding proteins (RBPs) are also known to be involved in selective sorting of miRNA into EVs in mammalian systems [111]. Comparing the sequences of EV packaged miRNAs to the miRNAs that are retained in mammalian cells, revealed the presence of specific sequence motifs within miRNAs which determined whether they were exported or retained by cells. Specifically, miRNA sequences that were enriched in EVs had one to four motifs of 4-7 nucleotides with high G+C content and lower Gibbs free energy than the miRNAs that were retained in cells [112]. Pulling down interacting proteins from cell lysates with EV enriched miRNAs displaying these motifs identified SYNCRIP, ALYREF, RBMX, and FUS as RBPs with central roles in the selective sorting of miRNAs. Other RBPs identified through their interactions with specific miRNAs include HNRNPA2B1, YBX-1, and MVP [111]. However, although transcripts for these proteins can be

found in helminth genomes, only MVP is reported in platyhelminth EV proteomic data, suggesting that either these RBPs are present at undetectable level, or they are present in helminth EVs only at certain timepoints during infection. Alternatively, other proteins may be utilised in helminth EV miRNA sorting [32].

One such candidate is calpain, a calcium dependent cysteine protease that is detectable in several species of trematode and cestode [113]. Inhibition of calpain expression reduces the quantity of several miRNAs in *S. japonicum* EVs [114], supporting a function in miRNA shuttling into EVs. In addition, orthologues of ADP-ribosylation factor 6 and Exportin-5, proteins which interact to shuttle a precursor-miRNA complex into EVs in mammalian cells, have been reported in several species of platyhelminths and cestode EVs [76, 115, 116], suggesting that this mechanism of precursor-miRNA packaging may be operational in helminth species. However, most studies examining helminth-derived EVs have primarily focused on the detection of mature miRNA sequences. Consequently, it is not known whether helminth-derived miRNAs are also delivered to host cells as primary, or precursor, miRNA sequences. Future studies to ascertain the precise form of miRNAs within EVs will be critical to better understand their mechanisms of transcriptional regulation, and thus functional implications, in recipient cells.

1.4.4. miRNA-mediated regulation of gene expression

1.4.4.1. The miRNA biogenesis pathway

The miRNA biogenesis pathway is well conserved in eukaryotes and is a tightly regulated process that involves a cascade of molecular processing by enzymes and protein interactions. First, the miRNA genes are transcribed by RNA polymerase II into nascent primary (pri)-miRNA transcript [117]. Then, in the canonical miRNA biogenesis pathway, the pri-miRNA transcript is processed in the nucleus by the microprocessor complex of Drosha and DGCR8 to generate an intermediary stem-loop structure called precursor (pre)-miRNA (Figure 1.3) [118]. This pre-miRNA is exported to the cytoplasm by an exportin-5 (XPO5)/RanGTP complex [119]. In the cytoplasm the stem-loop structure of the pre-miRNA is processed/ diced by an RNase III endonuclease Dicer to form ~22bp mature miRNA duplex (Figure 1.3) [120]. One strand of the duplex miRNA loads onto Ago proteins and is termed the guide strand [121]. The unloaded strand, called the passenger strand, unwinds from the guide strand, and is degraded by the cellular machinery. Whether the 5p or 3p strand is loaded on Ago varies greatly depending on the thermodynamic features of the miRNA strands, cell type or cellular environment [122]. The Ago-loaded mature miRNA along with other proteins forms the RNA- induced silencing complex (RISC) [123]. Finally, the RISC complex guided by the miRNA strand can then bind to complementary mRNA sequence to induce mRNA degradation or translational

repression. While the conventional model dictates that high sequence complementarity leads to sequence degradation, whereas low sequence complementarity leads to reversible post-transcriptional suppression, recent evidence of deviations from this model suggests a more nuanced and complex balance between degradation and repression. It is suggested that the mode of miRNA gene silencing is influenced by factors, such as developmental stage and environmental conditions [124]. However, the mechanistic details, particularly the criteria that determine whether a target mRNA is degraded or translationally repressed by a cognate miRNA remains to be elucidated.

Besides the canonical pathway, several non-canonical miRNA biogenesis pathways are responsible for the production of mature miRNAs from structurally diverse small RNAs. The most common non-canonical pathways are Drosha/DGCR8-independent and Dicer-independent pathways [125]. Mirtrons are small RNA hairpin structure that arise from introns during mRNA splicing events, as such they resemble Dicer substrate and do not require Drosha/ DGCR8 processing (Figure 1.3) [126]. Mirtrons contribute to ~15% of total mature miRNA population in human and are prevalent in *C. elegans* [127]. Another unique class of miRNAs that bypass the microprocessor cleavage step are 5' 7-methylguanosine (m^7G) capped pre-miRNAs, derived directly from RNA polymerase II transcript. Unlike the canonical miRNAs, the capped pre-miRNAs are transported to the cytoplasm via Exportin-1 for Dicer processing (Figure 1.3) [125]. The observation that 5' m^7G pre-miRNAs identified in *C. elegans* are lineage specific miRNAs, suggested that these miRNA genes are newly acquired, and that this pathway of biogenesis may have emerged later in evolution [128]. On the other hand, Dicer-independent miRNAs are processed by Drosha from endogenous short hairpin RNA (shRNA) transcripts (Figure 1.3). These pre-miRNAs require Ago2 to complete their maturation within the cytoplasm because they are of insufficient length to be Dicer-substrates [129]. This, in turn, promotes loading of the entire pre-miRNA into Ago2 and Ago2-dependent slicing of the 3p strand [130]. The 3′-5′ trimming of the 5p strand completes their maturation [131]. However, Dicer processed small interfering (si)-RNAs are more efficient at gene silencing than the dicer independent siRNAs [132].

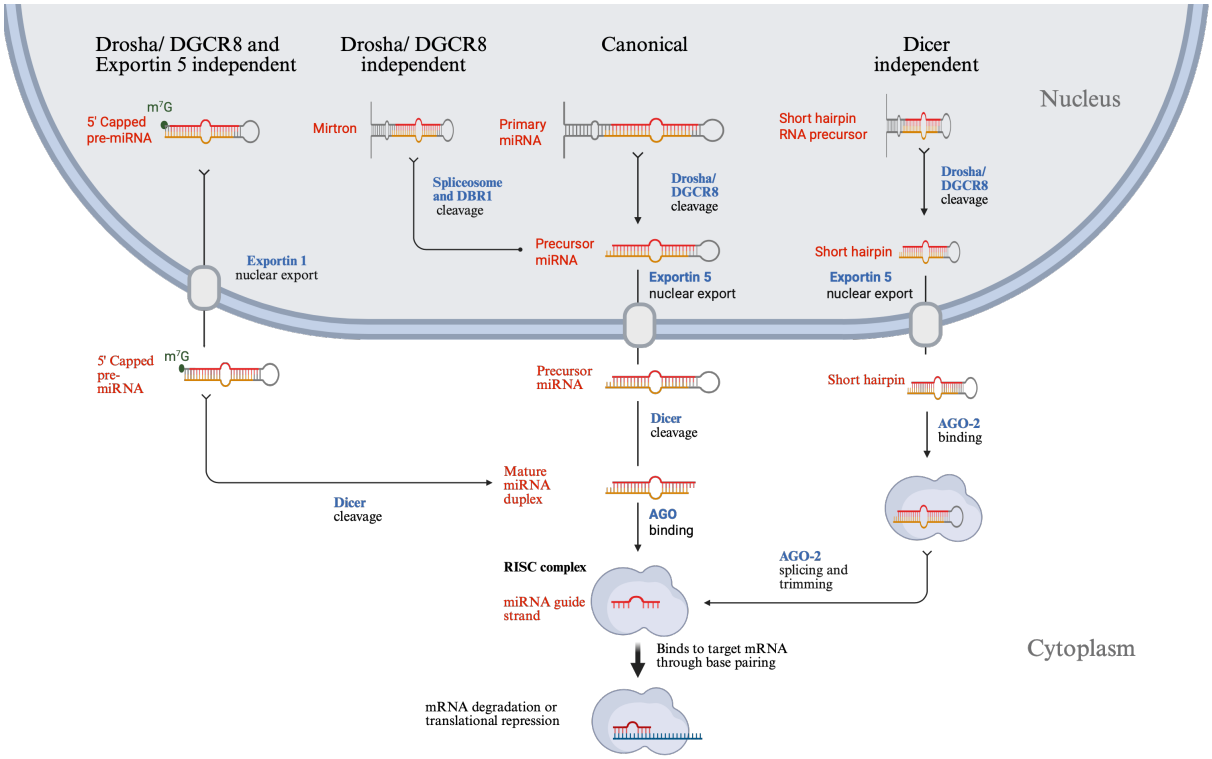


Figure 1.3. Mammalian miRNA biogenesis pathways. *In the canonical miRNA biogenesis pathway, the pri-miRNA transcript is processed in the nucleus by Drosha and DGCR8 to generate an intermediary stem-loop structure called precursor (pre)-miRNA. This pre-miRNA is exported to the cytoplasm by Exportin-5. In the cytoplasm, the stem-loop structure of the pre-miRNA is cleaved off by Dicer to form a mature miRNA duplex. One strand of the duplex miRNA loads onto Ago and is termed the guide strand. The Ago loaded miRNA along with other proteins form the RISC complex. Finally, the RISC complex guided by the miRNA strand binds to complementary mRNA sequence to induce mRNA degradation or translational repression. In the non-canonical miRNA biogenesis pathway, structurally diverse small RNAs can be processed into mature miRNAs by bypassing one or more of the key biogenesis enzymes, leading to alternative processing mechanisms. Mirtrons and 7-methylguanine capped (m7G)-pre-miRNAs bypass Drosha/ DGCR8 processing; while mirtrons are exported from the nucleus to the cytoplasm by canonical Exportin 5, m7G-pre-miRNAs are alternatively shuttled via Exportin 1. In the cytoplasm, both the precursors are processed by Dicer. On the other hand, small hairpin RNAs (shRNAs) are processed by Drosha/DGCR8 complex and exported via Exportin 5, but instead of Dicer, they are alternatively processed by Ago2. All pathways ultimately produce mature functional miRNAs that can load onto Ago and form miRISC complex. This Figure was created using Biorender.com*

1.4.4.2. Processing of helminth miRNAs in mammalian cells

The notion that the miRNA biogenesis pathway can be exploited by foreign miRNAs to mediate cross-kingdom communication was first demonstrated in plants whereby fungal miRNAs were found to load onto plant Ago proteins leading to silencing of mitogen-activated protein kinase genes and consequent suppression of protective immunity [133]. Subversion of host cell miRNA machinery by pathogen-derived miRNAs has now been identified in viral, bacterial and plasmodium infections [59, 61, 134]. The detection of fhe-miR-125b, a highly conserved parasite-derived miRNA, in Ago2-pull down products from macrophages of *F. hepatica*-infected mice [63] and the identification of sja-miR-125b from *S. japonicum* in Ago pulldown products from macrophages treated with parasite-derived EVs in vitro [79] now provide evidence that miRNAs from parasitic worms can also be incorporated into the miRISC machinery of mammalian cells.

The loading of miRNAs to Ago protein is a very precise process that involves thermodynamics and base-match composition and is partially dictated by the sequence and structure of the miRNA [135]. As the seed sequence of both Fasciola fhe-miR-125b and Schistosome sja-miR-125b is identical to mammalian miR-125 [63], and as conserved miRNA sequences are the most abundant in helminth EVs, it was initially proposed that only helminth miRNAs that are close homologs to mammalian sequences may be functional in their host cells. However, the recent detection of *H. polygyrus* miR-71 loaded onto Ago2 in transfected Th2 cells implies that this conservation may not be essential as this helminth miRNA is specifically expressed by nematodes and does not have a homolog in mammalian cells [90].

In addition to the influence of miRNA sequence and structure, loading onto Ago is also partly dictated by the functional requirements of the cell at any particular time. In this way, miRNA mechanisms of gene regulation can be spatially and temporally controlled as required. A cell-specific functionality for helminth miRNAs has not been explored, as most experimental studies of helminth miRNAs have focused on the modulation of the biological activity of a single cell type (Table 1.2). However, the biological outcome of *H. polygyrus* miR-71 transfection was examined in both Th2 cells and macrophages, although similar measures of functionality were not assessed in both cell types [90]. While transfection of Th2 cells resulted in a significant reduction in expression of the transcription factor *Irf4*, transfection of macrophages had no significant effect on the production of cytokines, although their expression would be expected to be altered because of changes in expression of *Irf4* [136]. Despite these caveats, the results provide a suggestion of varied efficacy for helminth miRNA that is dependent on the cell type, a notion that requires further consideration.

Loading onto Ago2 represents the final step in the canonical miRNA biogenesis pathway (Figure 1.3) and supports the presence of mature helminth miRNAs in mammalian cells and alludes to potential functionality within the mammalian miRNA machinery. However, it does not determine whether the worm miRNAs are delivered to their host cells as mature sequences that are directly loaded to Ago2 or as pri-miRNA transcripts or precursor miRNAs that are processed by Drosha and/or Dicer. While some sequence features for Drosha cleavage are common between *C. elegans* and human miRNAs, *C. elegans* lack other structures and sequence motifs that are critical for efficient cleavage by human Drosha [137]. Moreover, despite the high similarity in domain structures and polypeptide sequences of *C. elegans* and human Drosha, the *C. elegans* enzyme has different substrate recognition approaches and cleavage mechanisms compared to the human microprocessor [137]. In contrast, the observation that a Schistosome specific pri-miRNA mimic (pri-sja-miR-2162) was processed into a mature functional miRNA in hepatocytes suggests that unlike the miRNAs of the free living *C. elegans*, miRNAs secreted by parasitic worms can be fully embedded into the mammalian miRNA biogenesis pathway [88]. This may further indicate that the capacity to utilise host miRNA biogenesis pathways evolved as an adaptation to parasitism and builds on the proposal that this functionality is not solely dependent on conservation with specific mammalian miRNA sequences.

The pre-miRNAs released by Drosha typically comprise of a near perfect based-paired stem, a large terminal loop, and a 2nt overhang at the 3' end, which is essential for efficient Dicer cleavage, [138]. Given that the large majority of helminth miRNAs (conserved and novel) possess these precursor characteristics, processing by mammalian Dicer could be expected [64]. Moreover, a position dependent 3-bp motif in pre-miRNAs, termed the GYM motif, recently determined to influence the cleavage site and efficiency of human Dicer cleavage is positionally conserved in nematodes [139] which further validates the possibility that helminth-derived miRNAs can be efficiently processed by the human miRNA biogenesis pathway.

The possibility that parasite-derived miRNAs are also processed via non-canonical pathways in host cells cannot be excluded. Although knowledge of non-canonical miRNA processing of exogenous pathogen-derived miRNAs within host cells remains limited, evidence of non-canonical miRNA processing of viral miRNAs by host cells have been reported. For instance, mirtron like viral product from *Sindbis* virus is processed in a Dicer dependent and Drosha independent manner in infected murine fibroblast cells *in vitro* [140]. On the other hand, *SARS-CoV-2* small viral RNA biogenesis is not affected by Drosha and Dicer deficiency in infected host cells and it is suggested that viral factors or other cytoplasmic proteases during infection could be involved in the maturation of viral miRNAs [141].

In addition to the control of miRNA functionality by aspects of the biogenesis pathway such as enzyme cleavage, and selection for Ago loading, the stability of miRNAs also shapes the biological impact to cells by influencing the evolution of target sites in the 3'UTR of genes [142]. Since miRNAs target 3' UTRs of genes, target genes that are co-expressed with a miRNA evolve to selectively avoid complementary base pairing with miRNAs that are co-expressed with the gene [143]. *H. polygyrus* miRNA, hpo-miR-71-5p, was detected continuously for several days after transfection into recipient mouse cells, suggesting that the helminth miRNAs are highly stable in host cells. As such, it is plausible that the helminth miRNAs can influence the evolution of target sites of host genes. Of interest, the production of miRNA sequence variants (isomiRs**)** is emerging as a mechanism to regulate miRNA stability and degradation [144]. While some miRNA variants arise from different loci, other isomiRs are produced from the same loci as the canonical sequence and occur due to variabilities in miRNA biogenesis or by post-transcriptional modifications [144]. A lineage specific high sequence variation rate has been observed in platyhelminths; proposed to be a result of coevolution with their hosts [145], and uridylation (addition of a uridine at the 3' end) of certain miRNAs, a variation which determines miRNA stability, is conserved among cestode species [146]. Furthermore, trimmed 3' isomiRs have been found to be increased in response to immune activation, bacterial and viral infection and these 3' shorter isomiRs reportedly display greater stability than the canonical miRNAs [147]. Based on these observations, it is evident that further exploration is needed to determine the exact nature of the exogenous helminth miRNAs (mature, pri-, or pre-; canonical or isomiR) that is being delivered to the host cells. In addition, understanding the cellular location of these miRNAs (nucleus or cytoplasm) would help elucidate the point at which they are incorporated into the mammalian miRNA machinery.

1.4.4.3. Mechanisms of helminth miRNA-mediated regulation of host gene expression

As the expected correlation to an increased expression of a miRNA is the reduced expression of its target gene, to date, the functional validation of a helminth miRNA in host cells has been assessed by measuring the expression of its predicted host gene target(s) within transfected or infected cells. This has typically been supported by the demonstration of a specific interaction by the helminth miRNA with the host gene 3'-UTR using in vitro luciferase reporter systems.

While this is certainly an acceptable approach, it is only one possible outcome. An alternative mechanism could be that by sequestering the host cell components of the miRNA biogenesis pathway, worm miRNAs prevent their occupation by mammalian miRNAs, thus altering the concentration levels of functional endogenous host miRNAs. This effect has been observed following the

transfection of cells with siRNAs [148] which resulted in the rapid reduction of Ago2 associated endogenous miRNAs. This alteration in Ago loading appeared to impact most highly expressed miRNAs, with low abundant miRNAs unchanged, repressed or even increased. Due to this competition for Ago loading, the expression of many miRNA target genes is altered resulting in an effect on the biology of the cell.

Furthermore, some worm miRNAs have been shown to regulate the transcriptional levels of the miRNA biogenesis components either by direct binding or as downstream effect. Target prediction software predicts Ago1-4 and Dicer-1 are direct targets of several worm EV miRNAs, notably, miR-277, let-7, miR-10, and miR190, [81, 149-152]. Moreover, overexpression of *E. multilocularis* miR-71 mimic in mouse macrophages resulted in the enhanced expression of genes that encode the RISC components, Ago1 and Ago4, which in turn caused downregulation of several host miRNAs involved in the activation and regulation of inflammatory responses [93].

Finally, miRNAs indirectly alter the expression of gene targets by binding to other miRNAs by sequence complementarity thus preventing their interaction with the 3'-UTR of their gene targets [153]. There is growing evidence of viral miRNA:host miRNA direct interactions. For instance, in *SARS-CoV-2* infection, small viral RNAs have been predicted to form stable duplexes with host miRNAs, and concurrently, many of the predicted target host miRNAs are also found downregulated during *SARS-CoV-2* infection [154]. Similarly, a *Simian virus 40* encoded miRNA binds to host cell miRNAs and prevents their binding to target mRNAs, leading to increased telomerase activity and viral replication. There is also evidence that the miRNA:miRNA binding happens within Ago2 associated RISC [155]. In such a manner, parasite-derived miRNAs might bind host miRNAs to directly regulate the abundance and availability of the host miRNAs, and hence affect host gene expression.

Thus, the regulatory interplay between helminth miRNAs and host gene expression likely unfolds through multifaceted mechanisms (Figure 1.4). Even though helminth miRNA targeted host gene regulation is becoming more and more evident, further exploration into the miRNA pathway could unveil the full spectrum of intricate mechanisms by which parasitic miRNAs exert control over host gene expression.

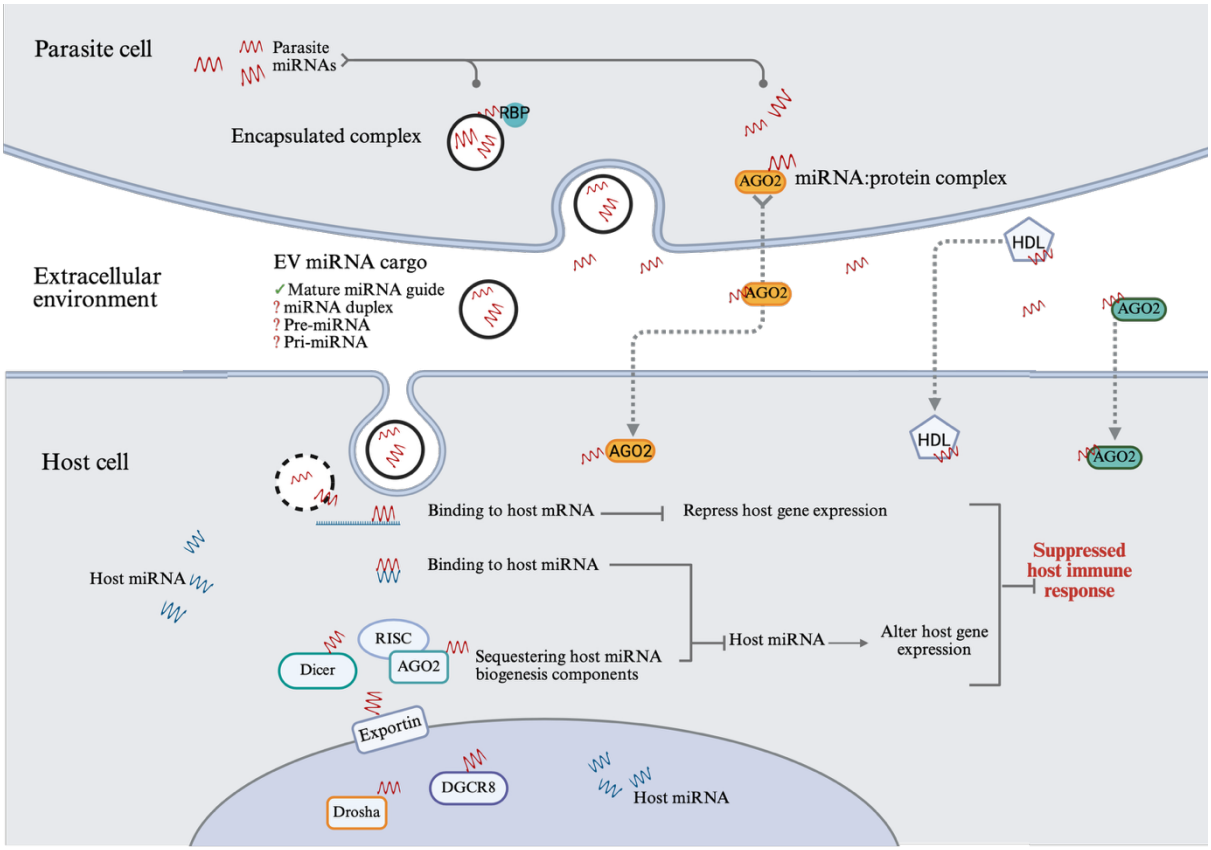


Figure 1.4. Proposed mechanism of helminth miRNA-mediated cross-kingdom regulation of host immune response. *Parasite-miRNAs are selectively sorted and transported to host cells via extracellular vesicles (EV) or by forming stable miRNA: protein (e.g. Ago2 and HDL) complexes with both parasite and host-derived proteins. Once internalised by the host cells, the helminth-derived miRNAs can mimic host miRNAs, and incorporate into the host cell miRNA biogenesis pathway to form functional miRISC complex and consequently repress host gene expression. Beyond their direct interaction with host genes, the exogenous helminth-miRNAs may exert their influence on host miRNAs in multiple ways. They can sequester host's miRNA biogenesis components, including Ago and Dicer. Alternatively, these parasitic miRNAs may directly bind host miRNAs by complementary base pairing. Through these mechanisms, the extracellular miRNAs from helminths may orchestrate manipulation of both host cell mRNAs and miRNAs. As such, this intricate process serves to finely regulate the host gene function to ultimately manipulate the host immune response, ensuring the parasite's prolonged survival and successful establishment of chronic infection. This Figure was created using Biorender.com.*

1.5. Finding the knowns to the unknowns

The expanding characterisation of helminth miRNomes and their corresponding predicted mammalian gene targets, combined with the increased detection of parasite-derived miRNA sequences within the cells of infected mammalian hosts, is providing growing validation to the hypothesis that parasitic worms can effectively modulate their host miRNA machinery to regulate the protective immune response to benefit their long-term survival. However, as described here, there is many unknowns regarding the mechanisms by which helminth miRNAs enter and function within their host cells.

Mechanistic approaches can be guided by models of miRNA biogenesis in mammalian cells and in the model worm *C. elegans*. However, it will be also important to consider the diversity between helminth species. As mentioned here, at the most fundamental level, understanding the impact of sequence, structure, and cellular localisation of helminth miRNAs on the interaction with host Ago, will be critical to fully elucidate the mechanism of loading and functionality. In addition, a deeper understanding of helminth miRNA sequences will provide more detailed information on the specific form (pri-, pre-, or mature; canonical or isomiR) that is packaged into EVs for transfer and will reveal potential cleavage sites for enzymes of the mammalian miRNA biogenesis pathway. These insights will predict the specific entry point for the helminth miRNA into the mammalian processing system, which can then be supported by *in vitro* assessment using cells deficient/overexpressing different components of the biogenesis pathway. Finally, the broad impact that helminth miRNAs have on their host cells should be fully assessed, beyond the simple characterisation of predicted gene targets and their level of expression. Consideration should also be given to a likely shift in the Ago loading of endogenous host miRNAs, and the possible regulation of host miRNAs activity by direct interaction. Once again, the determination of these outcomes can be achieved through the application of standard in vitro assays already established for mammalian miRNAs and a more comprehensive understanding of the sequences of parasite miRNAs.

While these studies will undoubtedly provide new insights into the functionality of helminth miRNAs, it is important to consider that these *in vitro/in silico* analyses may not reflect the complex dynamic microenvironment of an infection. Unlike free-living *C. elegans*, the model worm commonly used for the characterisation of miRNA biogenesis and function, parasitic worms require a mammalian host for survival, which challenges the ability to perform and assess the contribution that individual miRNAs make to the modulation of host immune cells *in vivo* and thus the parasite's survival. However, these studies will become more achievable in the future with the development of organoid culturing systems that better mimic the *in vivo* environment of the host, thus allowing for

extended in vitro survival and the support of developmental processes and interactions with immune cells [156-158].

Not discussed above, but of relevance to a holistic understanding of the host-parasite relationship is the observation that cross-kingdom communication of miRNAs is bidirectional [159]. Plant hosts use miRNAs as part of their defence systems, transporting miRNA into fungal pathogens to inhibit the expression of virulence genes [160]. Similarly, mammalian hosts have been shown to transfer miRNAs to malaria parasites, which consequently mediates resistance to infection [161]. While this pathway of communication has not been reported between host and helminths, it is plausible that mammalian miRNAs (extracellular or vesicular) could be taken up by helminths as they feed on host blood and tissue. However, given the success of helminth parasites in colonising their mammalian hosts and establishing chronic infections, it is equally likely that this mechanism of host defence is less effective against worms as compared to the microbial, and intracellular pathogens such as malaria. Indeed, it is more likely that helminth parasites are utilising host miRNAs as signals/cues for development and maturation.

Overcoming the technical challenges raised here and solving some of the unknowns highlighted will unravel this sophisticated mechanism of communication between helminths and their hosts. Addressing these considerations will also ascertain whether interfering with the functions of parasite miRNAs and/or manipulating the expression of their gene targets offers a new strategy to achieve therapeutic control of these pathogens and regulation of mammalian inflammatory responses.

1.6. Using *Fasciola hepatica* as a model organism to explore helminth-host miRNA-mediated cross communication

Fasciola hepatica (the liver fluke) is considered one of the most successful helminth due to its ability to infect the greatest variety of mammals, and the widest geographical spread compared to any other parasitic worm [162, 163]. This not only implies a superior adaptation to parasitism compared to most other helminths that generally only infect a single host but also suggests that they have evolved a minimal number of universal processes of virulence and immune modulation and hence serves as an ideal model to study the helminth-host relationship.

In addition, within its mammalian host, the liver fluke progresses through clearly defined developmental stages that correspond to specific host tissues (gut, liver, and bile duct) [164], providing accessibility, and a framework for dissecting the parasite's adaptive strategies and mechanisms of host manipulation. Moreover, studies of *F. hepatica* infection in its definitive hosts

(e.g. sheep and cattle) and in experimental models (rodents) report a consistent profile of the host immune response, making *F. hepatica* a tractable model for studying helminth-host interactions. Additionally, the availability of updated draft genomes, extensive stage-specific transcriptomics and proteomics provides a unique platform to elucidate the molecular mechanisms that govern these interactions [165-173].

Mammalian definitive hosts of *F. hepatica* become infected through the ingestion of vegetation contaminated with encysted dormant larvae, known as metacercariae [164, 174]. Upon reaching the host's intestine, the acidic environment triggers excystment, releasing newly excysted juveniles (NEJs) (Figure 1.5). These NEJs actively perforate the intestinal wall and migrate through the peritoneal cavity and penetrate the liver capsule [164]. As they develop, the juvenile flukes feed and tunnel through the liver parenchyma for weeks to grow and mature into adult worms [175]. Eventually, the adult flukes reach the bile duct, where they can reside for an average of 20 years. Once established, the adults produce thousands of eggs, which are excreted in the host's faeces, perpetuating the parasitic life cycle. During this process, the liver fluke inflicts insidious health consequences on the host, through extensive liver damage, anaemia and reduced life expectancy, collectively known as fasciolosis.

To date, intervention strategies against *F. hepatica* have had limited success [176]. Most approaches have focused on targeting adult parasites. However, by this stage of infection, the parasite is actively destroying the liver tissue as it feeds and migrates towards the bile duct [177]. A more effective preventative approach would be to target the NEJs, the early migratory stages of the parasite, before they enter the host liver (Figure 1.5). However, this strategy would require an ability to diagnose infection during the first few weeks after ingestion of the metacercariae, which is challenging because the early prepatent phase is largely clinically silent, with limited inflammatory responses that would otherwise signal infection.

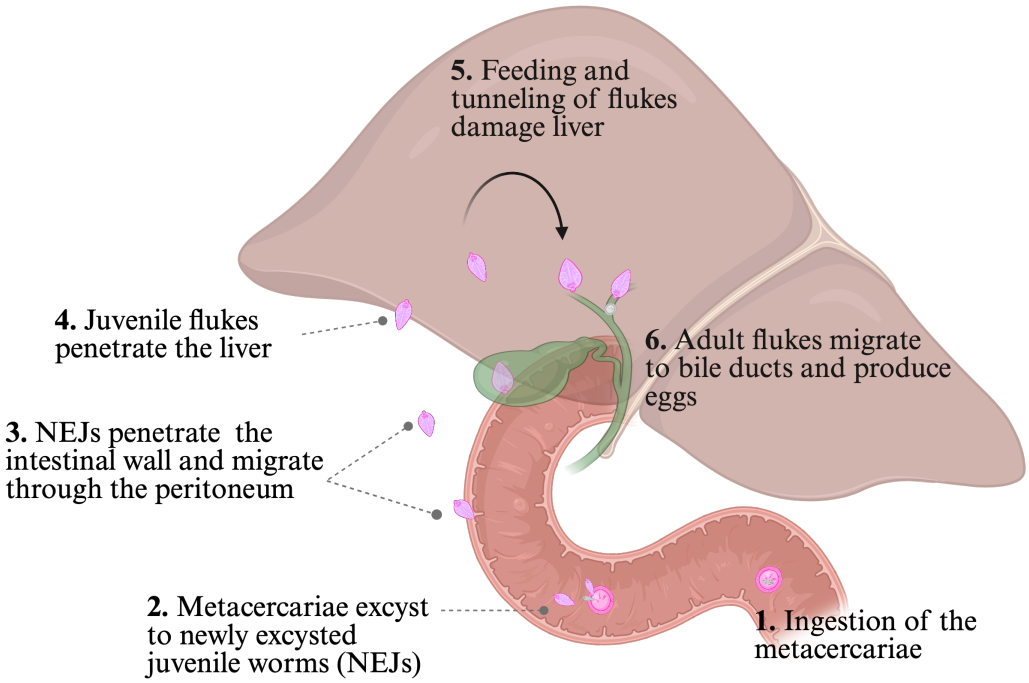


Figure 1.5. Fasciola hepatica life cycle in its definitive host involves their residence in multiple tissue niches while manipulating the host innate immune responses. *(1) Mammalian definitive hosts of F. hepatica become infected through the ingestion of vegetation contaminated with encysted dormant larvae, known as metacercariae. (2) Upon reaching the host's intestine, the acidic environment triggers excystment, releasing newly excysted juveniles (NEJs). (3) The NEJs perforate the intestinal wall and migrate through the peritoneal cavity. (4) The flukes penetrate the liver capsule. (5) The immature flukes feed and tunnel through the liver for weeks to grow and mature into adult worms. [178] (6) The adult flukes reach the bile ducts, where they produce eggs, which are excreted in the host's faeces, perpetuating the parasitic life cycle. This Figure was created using Biorender.com.*

1.6.1 Fasciola hepatica manipulates the host's immune responses to establish chronic infection

Like all helminth infections, macrophages are the predominant innate immune cell present during the early stages of infection with *F. hepatica* [175, 179]. Typically, in response to an invading pathogen, the mammalian innate response induces an M1 macrophage phenotype to mediate host protection from infection through the production of pro-inflammatory cytokines, cytotoxic nitric-oxide and other antibacterial effector molecules [180]. However, during the pre-hepatic stages of infection with *F. hepatica*, as the NEJs penetrate the intestinal wall and migrate through the peritoneal cavity, infected animals display no clinical signs or inflammatory changes in the intestine wall [181, 182]. Macrophages in the peritoneal cavity of infected mice or sheep do not exhibit a significant increase in the production of pro-inflammatory cytokines (e.g., TNF, IL-12, IFNγ) or anti-microbial effectors (such as, iNOS, nitric oxide (NO)). Evidence from clinical trials and experimental infections suggest that host M1 macrophages and their associated pro-inflammatory mediators are effective against the NEJs [183, 184]. Therefore, the absence of this phenotype of immune response during an infection suggests that immediately after infection, *F. hepatica* NEJs employ mechanisms to disarm the host's protective pro-inflammatory innate 'early-response' to prevent their detection at a vulnerable time in their invasion and ensure safe passage to the liver (Figure 1.6). Once in the liver, the flukes cause extensive tissue damage by feeding and migrating and at this point of infection, an anti-inflammatory M2 phenotype of immune response predominates (Figure 1.6), characterized by Arg1 and Ym1. This macrophage phenotype mediates the induction of the adaptive Th2 immune response, regulates the host protective M1/Th1 immune response and instead promotes tissue repair in the host [185]. The importance of this M2-driven host protective response is further supported by studies showing that *F. hepatica* infection in mice lacking programmed death ligand 2 (PD-L2), a molecule essential for M2 macrophage induction and Th2 polarization, results in exacerbated liver pathology and premature host mortality [186]. However, the number of worms recovered from these immunodeficient mice was similar to that in wild-type controls [186], supporting the idea that once the parasites reach the liver, the host immune response becomes primarily focused on limiting tissue damage rather than mounting effective anti-parasitic immunity.

Besides macrophages, other innate immune cells, eosinophils, dendritic cells, and neutrophils also display a modulated immune response during *F. hepatica* infection, despite of an influx of these cells into the peritoneum during infection [182, 187]. Although *ex vivo* studies show that eosinophils isolated from infected cattle can kill *F. hepatica* newly excysted juveniles (NEJs), *in vivo* these cells are largely ineffective against the parasites, and eosinophils recovered from the peritoneal fluid of infected sheep are not degranulated, suggesting that they are not activated [187]. Similarly, dendritic cells within the peritoneal cavity lose their antimicrobial properties and ability to prime naïve T cells

toward a protective Th1 profile [188, 189]. Neutrophils have also been shown to exhibit a reduced ability to produce reactive oxygen species or undergo NETosis when exposed to *F. hepatica in vitro* [190].

Consequently, in parallel with these innate responses, the adaptive immune response to *F. hepatica* initially comprises a mixture of Th1 and Th2 cells [191]. However, the parasite specific Th1 differentiation is soon suppressed and the Th2 profile becomes dominant as the parasites penetrate the liver [191]. Later, when the flukes reach the bile duct, the fluke-specific T cell population evolves into a combination of regulatory T cells and anergic effector T cells, promoting healing of the fluke damaged tissues, and ultimately mediating host tolerance of the growing parasites (Figure 1.6).

Understanding the mechanisms that *F. hepatica* uses to suppress the host's immune response during the early stages of infection will provide opportunities to counter these strategies to target the NEJs, preventing the flukes from penetrating the liver capsule and thus reduce disease pathology.

Helminths achieve their immunomodulatory effects primarily by releasing a broad range of ES products [1, 102, 178, 192-196]. As a prototypical helminth, *F. hepatica* secretes a range of molecules, either individually or packaged within EVs, as it migrates through host tissues. While these assist with parasitic activities, including tissue degradation, haemoglobin digestion, and egg production, the ES products also possess potent immunomodulatory properties. Research to date has largely focused on the characterisation of proteins within these ES products, leading to the identification of several of the *F. hepatica* proteins, such as, Cathepsin L1, FhHDM, and FH12, with immune modulating properties [185, 197-201]. However, as mentioned above, more recently, as it has become increasingly apparent that helminth-derived microRNAs (miRNAs) also contribute to the regulation of the host immune response.

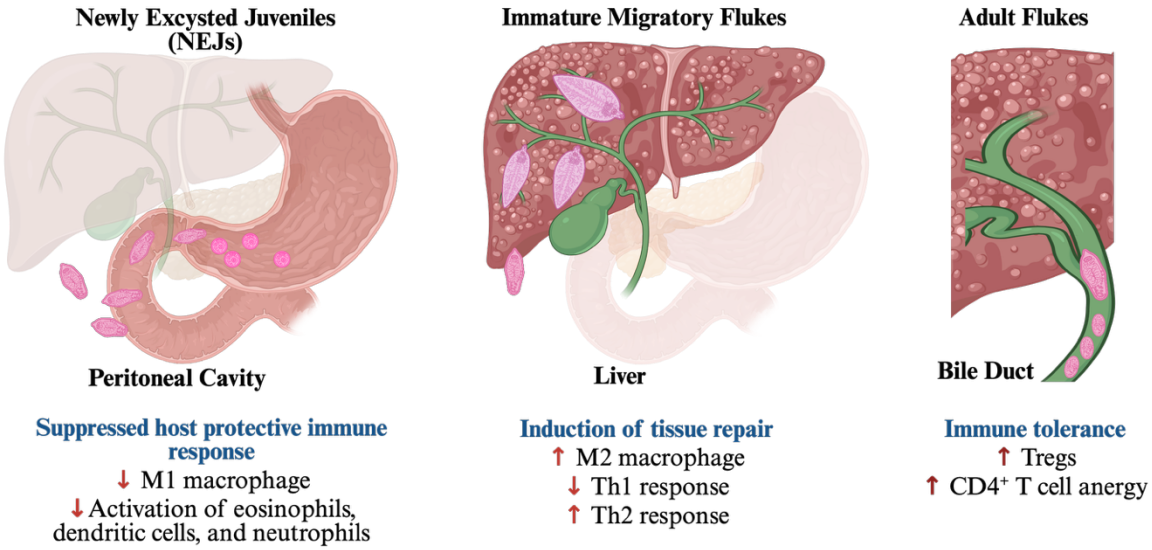


Figure 1.6. Host immune response to F. hepatica infection. *As the newly excysted juvenile worms penetrate the intestine and enter the peritoneum, the host's protective M1 macrophage response is actively suppressed. Although eosinophils, dendritic cells, and neutrophils are recruited to the site, these cells remain largely inactivated. Once in the hepatic tissue, the immune response shift towards M2 macrophage phenotype and a Th2-dominated environment which promotes tissue repair over parasite clearance. During chronic infection in the bile ducts, there is a predominance of regulatory T cells (Tregs) and immune hypo-responsiveness/anergy in effector T cells, which helps limit excessive immunopathology and facilitates parasite persistence. Figure adapted from Quinteros, O'Brien [175]. This Figure was created using Biorender.com.*

1.6.2. Fasciola hepatica subverts the mammalian miRNA machinery to suppress early innate immune responses

To explore the possibility that *F. hepatica* was utilising miRNAs to regulate the activity of host immune cells, my host research group firstly characterised the miRNA profile at the different life stages of *F. hepatica* [33, 41]. As expected, each intra-mammalian life stage of this parasite has a distinct miRNA profile. In particular, the NEJs have a miRNA profile that is quite distinct compared to the juvenile and adult flukes. While this likely reflects the large developmental changes that occur from the NEJ to juvenile life stage, it may also support the immune regulation of host cells that is required during migration through the host peritoneal cavity.

Supporting this notion, using a mouse model of *F. hepatica* infection 25 Fasciola-derived miRNAs were identified in the peritoneal macrophages of infected mice, with parasite miRNAs detected as early at 6h, and peaking at 18h post infection, a time that coincides with the migratory stage of the parasite through the peritoneum [63]. Most of these Fasciola miRNAs have been previously reported to be present in the worm EVs, suggesting that the worm miRNAs are exported to host cells primarily via this mechanism [63, 202]. In addition, all of these worm miRNAs are highly conserved and several of them were orthologues of mouse miRNAs with identical seed sequences, suggesting that the worm miRNAs can mimickthe host miRNA sequences to function in host cells [56, 63].

Consistent with a functional role, worm-derived miRNAs in the peritoneal macrophage were found to be loaded onto mammalian Ago2, the core protein of the RNA induced silencing complex (RISC) that binds to mRNA to exert transcriptional repression [63]. Therefore, finding a mature parasite miRNA interacting with mammalian Ago2 suggests that the worm miRNAs can engage the mammalian miRNA machinery to mediate cross-kingdom gene regulation.

Bioinformatic target prediction further supports this observation, indicating that several of the detected parasite miRNAs in macrophages have the potential to regulate mammalian genes involved in innate immune responses [41, 63, 202]. This has been further confirmed *in vitro*, with macrophages transfected with fhe-miR-125b, leads to the targeted suppression of host genes resulting in the regulation of proinflammatory responses [63].

Collectively, these findings support a pivotal role for *F. hepatica* miRNAs in shaping the host's early innate immune responses to prevent their expulsion. A deeper understanding of the fluke miRNAs and how they operate within host cells could unlock a powerful avenue for developing novel diagnostic biomarkers, vaccines, and non-chemotherapeutic interventions, thus offering promising strategies to control fasciolosis at its earliest and most vulnerable stage of infection. Furthermore, this

would also provide foundational knowledge of how worms may have adapted to utilise the miRNA biogenesis machinery to support a parasitic lifestyle.

1.7. Thesis hypothesis and aims

Building on knowledge to date and addressing fundamental gaps in understanding, this PhD dissertation has focused on elucidating the role of miRNAs in the parasite-host interaction during the pre-hepatic stage of infection with *F. hepatica* with the aim of providing foundational knowledge of parasite-host communication and to support the development of new strategies for diagnosis and infection control.

Accordingly, the hypothesis is that worm-derived miRNAs are released during infection and have adapted to exploit the host mammalian miRNA biogenesis pathway to subvert immune protection pathways and thus support virulence and long-term survival.

The following experimental aims were investigated:

Aim 1 Assessing the viability of using the differential expression of circulating miRNAs as biomarkers for the diagnosis of *F. hepatica* infection.

Aim 2 Comparing the functional activity of *F. hepatica*-derived canonical and isomiR miRNA sequences in the regulation of macrophage inflammatory responses.

Aim 3 Deciphering the mechanisms by which parasite-derived miRNAs exploit the host RNA interference (RNAi) machinery to regulate host gene expression.

Chapter 2:

Assessing the viability of using the differential expression of circulating miRNAs as a biomarker for the diagnosis of *F. hepatica* infection.

Publication Statement

The contents of this chapter have been published as a research paper in Scientific Reports: Chowdhury S, Ricafrente A, Cwiklinski K, Sais D, Dalton JP, Tran N, Donnelly S. Exploring the utility of circulating miRNAs as diagnostic biomarkers of fasciolosis. Sci Rep. 2024 Mar 28;14(1):7431. doi: 10.1038/s41598-024-57704-9. (Appendix B)

The text presented here has been edited for insertion into the thesis and to support continuity. The numbering of sections, style of referencing, the numbering of tables and figures have been altered to align with the formatting of the thesis.

Copyright Declaration: Under Springer Nature Terms and Conditions, Ownership of copyright in the Article will be vested in the name of the Author. When reproducing the Article or extracts from it, the Author will acknowledge and reference first publication in the Journal. The article is Open Access and distributed under the terms of the Creative Commons Attribution License (CC-BY 3,0), which This licence allows readers to copy, distribute and transmit the Article as long as it is attributed back to the author.

Author Contribution: Sumaiya Chowdhury (graduate student) designed the experiments, performed, analysed and interpreted the data, and wrote the manuscript. Co-authors Alison Ricafrente performed the initial design, data acquisition and interpretation; Krystyna Cwiklinski, and John Dalton provided the sera and parasite samples for analysis. Sheila Donnelly, Nham Tran and Dayna Sais guided the conception and experimental analysis and contributed to the writing and editing of the final manuscript.

Signatures:

Sumaiya Chowdhury (graduate student) Production Note: Signature removed prior to publication.

Alison Ricafrente Production Note: Signature removed prior to publication.

Krystyna Cwiklinski Production Note: Signature removed prior to publication.

John Dalton Production Note: Signature removed prior to publication.

Dayna Sais (PhD supervisor) Production Note: Signature removed prior to publication.

Sheila Donnelly (PhD supervisor) Production Note: Signature removed prior to publication.

Nham Tran (PhD supervisor) Production Note: Signature removed prior to publication.

2.1. Introduction

As mentioned in chapter 1, *Fasciola hepatica*, is a trematode that causes fasciolosis, a major public health issue and neglected tropical disease affecting 2.5 million people in 81 countries [11]. Prevalence of liver fluke infection is thought to be on the rise due to the spread of drug-resistant parasites and climate change [203, 204]. While *F. hepatica* has adapted to infect every mammalian host that it has encountered [163, 205], grazing ruminants are most susceptible to infection due to their ingestion of pasture and water contaminated with the infective metacercariae. As such, fasciolosis is a significant economic burden to the livestock industry, with global losses of over US $3 billion per annum [7, 206].

As there is currently no effective vaccine against *F. hepatica* [177], liver fluke control relies heavily on the available chemical drugs, such as triclabendazole (TCBZ), closantel, and clorsulon [207]. Due to the challenge of detecting pre-patent infection, farmers opt for preventative treatment measures involving blanket treatment of animals before release onto pasture and further treatment depending on factors such as housing time, local climate, fasciolosis prevalence, age of herd, and grazing period [208-210]. Apart from the financial burden of drenching an entire herd with flukicides, this practice is driving the emergence of drug resistance against these available chemical treatments. As such, 'test before you treat' strategies are now being advocated for sustainable parasite control [211-213]. If early diagnosis was possible, anthelmintics could be administered to infected animals only, which would prevent/minimise the parasites from breaching the liver capsule. This approach would reduce liver damage and avert the loss of animals. Additionally, it would decrease the number of eggs dispersed onto pasture and curtail the unwarranted use of flukicides.

While several methods currently employed to diagnose fasciolosis in ruminants are effective, they have notable limitations, especially for the detection of early infection [24, 210]. The gold standard for liver fluke detection is the faecal egg count (FEC), which is a preferred technique as the presence of liver fluke eggs represents a definitive diagnosis [214, 215]. It is inexpensive, and both the sample collection and protocol are uncomplicated [24]. However, this method only detects infection at 8-12 weeks [216]. In addition, due to the uneven distribution of eggs in the faeces when the worm burden is low this method lacks sensitivity [217]. Coproantigen ELISAs can detect liver flukes two to three weeks earlier than FEC [218] but this antigen-based assay lacks sensitivity due to the low and inconsistent abundance of the liver fluke antigens in the host samples [219, 220]. Higher sensitivity can be obtained using serological techniques [221]. Detection of anti-liver fluke antibodies in serum is a more sensitive alternative, and ELISAs for these have been proven to detect infection from three to four weeks post-infection. However, this method cannot distinguish between new and previous

infections [219]. Additionally, maternal antibodies can persist in lambs for up to 12 weeks post-birth, limiting the applicability of this assay during the first two months on pasture [222]. Another complication of antibody detection is the lack of specificity due to cross-reaction with antibodies raised in response to other infections [223]. Finally, although the presence of liver enzymes within sera samples, including glutamate dehydrogenase (GLDH), gamma-glutamyl transferase (GGT) and albumin, are a good indication of liver damage, these changes are transient, variable, and not specific for the liver fluke [224].

Micro(mi)RNAs are small non-coding RNAs that play a central role in all biological processes [225] and offer great promise as markers of disease. Importantly, changes in their expression profiles have been correlated to several pathologies, including infectious diseases [226]. In addition, circulating miRNAs are present and highly stable in most bodily fluids, including blood, saliva, urine, and milk, making them robust candidates for non-invasive diagnostic and prognostic biomarkers [227].

Several studies have reported alterations in the abundance of both host and parasite-derived miRNAs in circulation during helminth infections, suggesting their utility as biomarkers for detecting infection [55, 228-230]. While the diagnostic potential of circulating miRNAs during fasciolosis has not yet been explored, it has been previously shown that *F. hepatica* miRNAs are expressed in a life cycle stage-specific manner and that fluke-derived miRNAs can be detected in host cells during the pre-hepatic stage of infection [63, 231].

Therefore, the aim of this study was to determine whether a differential abundance of host and *F. hepatica* miRNAs in sera was evident in experimental infected sheep that could be used to diagnose *F. hepatica* infection, particularly from the early pre-hepatic stage of infection. Such an outcome would enable prompt and effective intervention before the parasite causes significant liver pathology.

2.2. Methods

2.2.1. Sheep sera samples from experimental *Fasciola hepatica* infections

Sheep sera samples were available through previous experimental infection studies, which were all performed according to standardised protocols to ensure consistency and reproducibility between studies. Male sheep were orally infected with *F. hepatica* metacercariae, and blood samples collected by jugular venepuncture at various time points (Table 2.1), using appropriate blood collection tubes for serum collection. The blood was allowed to clot at room temperature, followed by centrifugation at 1000 x g for 10 minutes in a refrigerated centrifuge. The serum was collected and aliquoted into 1mL aliquots that were frozen at -80 °C. Four sets of sheep sera samples were used in this study, with each set representing an independent infection cohort (Table 2.1). The samples from sets A, B and D, were processed in the Molecular Parasitology Laboratory, Ireland. The samples collected in Spain (Set C) were transported to the Molecular Parasitology Laboratory in Ireland frozen on dry ice. Upon delivery, they were placed at -80 °C. Samples used for this study were defrosted in the fridge the evening before RNA extraction; this process was the first time they had been thawed since collection. Samples from Set A and Set B were used to prepare the small RNA sequencing library. Set C (pre-hepatic time points) and Set D (hepatic time points) were used for RT-qPCR validation of the diagnostic potential of selected miRNAs. Sets C and D were obtained from longitudinal sheep *F. hepatica* infection studies that included non-infected age-matched animals as field controls.

Table 2.1. Details of the experimental *F. hepatica* infections in sheep.

Samples for Sequencing		
	Set A	**Set B**
Study type	Cross-sectional	Longitudinal
Cohort (infection type)	Pre-hepatic infection	Hepatic infection
Sheep breed	Dorset cross sheep	Dorset cross sheep
Sheep age (at day 0)	6 months	6 months
F. hepatica isolate	Italian isolate (Ridgeway Research, UK)	South Gloucester isolate (Ridgeway Research, UK)
Infection dose	150 metacercariae	150 metacercariae
Collection time points	0, 2, 9, 14, 18 dpi (n = 6/timepoint)	3, 7, 10, 14 wpi, Neg-14 wpi (n = 6/timepoint)
Study location	AFBI, UK	AFBI, UK
Study reference	[232]	[232]
Samples for qPCR validation		
	Set C	**Set D**
Study type	Longitudinal	Longitudinal
Cohort (infection type)	Pre-hepatic infection	Hepatic infection
Sheep breed	Merino-breed sheep	Dorset cross sheep
Sheep age (at day 0)	8 months	6 months
F. hepatica isolate	Italian isolate	Italian isolate
Infection dose	150 metacercariae	120 metacercariae
Collection time points	0 dpi (n = 3 non-infected; 9 pre-infection) 7, 14 dpi (n = 14 non-infected; 11 infected)	3, 15, 20, 23 wpi (n = 6 non-infected; 4-5 infected/timepoint)
Study location	Cordoba, Spain	AFBI, UK
Study reference	Not published	[232]

dpi: days post infection; wpi: weeks post infection

2.2.2. Ethics statement

Experimental procedures at Agri-Food and Biosciences Institute (AFBI; UK) were carried out under license from the Department of Health, Social Services and Public by the Animal (Scientific Procedures) Act 1986 (License No. PPL 2771; PPL 2801), after ethical review by the AFBI Animal Ethics Committee. Experimental procedures at the University of Cordoba, Spain were carried out under license from 22-12-2015-381 in accordance with EU Directive 2012/707/UE and RD 53/2013 following ethical approval from the University of Cordoba Bioethics Committee (code no, 2015-PI-038).

2.2.3. RNA isolation from sheep sera, lamb tissue, and newly excysted juveniles

Small RNA extraction was performed on sheep sera using Tri-Reagent as described previously [233]. Frozen serum samples were thawed and 400 µL aliquots were treated with proteinase K (1 mg/mL; Thermo Fisher Scientific) for 20 minutes at 37 °C to degrade proteins. Then, 750 µL Tri-Reagent RT LS (Molecular Research Centre, USA) and 100 µL 4-bromoanisole (Molecular Research Centre, USA) was added to each 400 µL of serum samples to solubilise the nucleic acids. The homogenate was gently mixed and centrifuged at 12,000 x *g* for 20 minutes. The nucleic acids were precipitated with 5 µL of glycogen (5 mg/µL; Thermo Fisher Scientific) and 500 µL of 100 % isopropanol (Sigma-Aldrich) at - 20 °C overnight. The RNA precipitate was pelleted by centrifugation at 12,000 x g, for 15 minutes, washed twice with 70% ethanol (Sigma-Aldrich) and reprecipitated by centrifugation at 12000 x g for 10 minutes, and finally re-suspended in RNase free H_2O (ThermoFisher Scientific). For each serum sample, the RNA extracted from a total of 800 µL starting volume of sera was combined for subsequent analysis. All samples were processed at the same time, and each 400 µL aliquot was processed in the same manner. This process on average yielded 50 ng/µL of RNA per individual serum sample. The quality and quantity of RNA was assessed by POLARstar® Omega Multimode Microplate Reader for small RNA sequencing library preparation (BMG Labtech) or NanoDrop reader for qPCR (Thermo Fisher Scientific).

RNA was extracted from a sample of lamb rump using RNAzol RT (Molecular Research Centre Inc, USA). Approximately 100 mg of tissue was snap-frozen with liquid nitrogen and homogenised in 1 mL of RNAzol RT with a mortar and pestle for RNA extraction, which was performed as described previously [63] and yielded 2 µg of RNA.

The NEJ RNA had been previously isolated, as described [231]. NEJs were excysted using our standardised protocols. The *Fasciola hepatica* metacercariae (Italian isolate), sourced from Ridgeway Research Ltd (UK) were used for excystment and 24 hours culture of NEJs. Specifically,

metacercariae were removed from the visking tubing and incubated for a maximum of 10 minutes in 2 % sodium hypochlorite with agitation at room temperature to remove the outer cyst wall. The parasites were then washed in distilled water by sedimentation to remove all traces of sodium hypochlorite. The washed parasites were re-suspended in excystment medium (1.2 % sodium bicarbonate, 0.9 % sodium chloride, 0.2 % sodium tauroglycocholate, 0.07 % concentrated hydrochloric acid, 0.006 % L-cysteine) and incubated for up to 3 hours at 37 °C in 5 % CO2. NEJs were recovered using a pipette and washed several times in PBS by sedimentation to remove all traces of the excystment media. The NEJs were then transferred to pre-warmed (37 °C) culture medium, RPMI 1640 (Thermo Fisher Scientific) containing 2 mM L-glutamine, 30 mM HEPES, 0.1 % (w/v) glucose, and 2.5 µg/mL gentamycin) and incubated for 24 hours at 37°C in 5 % CO2. Following the incubation, the NEJs were centrifuged at 400 x *g* for 5 minutes to pellet the NEJs and the media was removed. The NEJ pellet was washed three times with PBS and stored at -80 °C prior to RNA extraction. This process was carried out in triplicate using 1000 NEJs per replicate. No serum was used in the culture media as these samples were also used for proteomic analyses as described in another study [166]. RNA was extracted using the miRNeasy mini kit (Qiagen) according to the manufacturer's instructions. The QIAzol Lysis Reagent was added directly to the frozen NEJ pellet for lysis and homogenization, and the RNA eluted into a final volume of 50 µL RNase-free water. RNA integrity and concentration were verified using the 260/280 LVis plate functionality of the PolarStar Omega Spectrophotometer (BMG LabTech) and the Quant-iT RiboGreen RNA Assay Kit (Termo Fisher Scientific). The RNA was transported to University of Technology, Sydney frozen on dry ice and stored at -80 °C upon delivery.

2.2.4. Sequencing and bioinformatics

RNA extracted from each time point (representing six animals) was pooled into a single representative sample to provide sufficient yield of RNA for sequencing. RNA library preparation was performed by Macrogen Oceania (NSW, Australia) using 1 µg of total RNA with the TruSeq Small RNA library Prep Kit (Illumina) according to manufacturer's instruction (Part#15004197 Rev. G) and sequenced using Illumina NextSeq 500. The quality of the raw FASTq files was assessed using FastQC [234], and consequently the adaptor sequences were excised, and low-quality sequences were removed (< 20 phred score, and short read length < 18 nt) using the bioinformatic tool CutAdapt (v3.4) [235]. The cleaned sheep sera sequence reads were then aligned against known sheep mature miRNAs from miRBase: *Ovis aries* (Oar_V4.0) using Bowtie (v1) [236], allowing zero mismatches. The miRNA sequence reads that did not align against the sheep miRNAs were then aligned against *F. hepatica* mature miRNA sequences from miRBase (Fhepatica_v1) and other published sources [41, 78, 152, 231] (Supplementary Table 2.1) allowing zero mismatches. The

counts for the sheep and *F. hepatica* miRNAs were extracted from the resultant SAM files using SamTools [41].

2.2.5. Characterisation of the Differential Expression of miRNAs in sheep sera

DESeq2 [237] was performed on the sheep miRNA read counts to assess the differential expression of circulating host-miRNAs during infection in comparison to non-infected sheep. The sequencing data from Set A, infection cohort (2, 9, 14, and 18 days post infection; dpi) were grouped as "pre-hepatic infection", and samples in the Set B cohort (3, 7, 10, 14 weeks post infection; wpi) were grouped as "hepatic infection", while the sequencing data from 0 dpi (pre-infection) and 14 days non-infected animals were grouped to provide a duplicate set of "non-infected" samples. Only miRNAs with a sum of >10 counts across all samples and with an adjusted p value < 0.05 as determined by the DESeq2 analysis comparing each infection group to non-infected controls, were included in the subsequent analyses. Log2Fold change of 2 (Log2FC2) or 4-fold cut-off was applied to identify the most differentially expressed miRNAs.

2.2.6. RT-qPCR

Custom TaqMan small RNA primers were designed for sheep and *F. hepatica* miRNAs, as listed in Table 2.2. The custom TaqMan RT primers and TaqMan™ MicroRNA Reverse Transcription Kit (Applied Biosystems) were used for the synthesis of cDNA from 150 ng of RNA extracted from each sample (Set A and B were pooled RNA samples from 6 individual sheep at each time point; Set C and D were individual samples), as per manufacturer's instructions. Then 4.5 µl of cDNA was used for qPCR, with undiluted cDNA used for *F. hepatica* miRNAs, while for the sheep miRNAs the cDNA was diluted 1:2 in dH_2O. The qPCR was performed using the custom TaqMan primer and TaqMan™ Fast Advanced Master Mix. Samples were prepared on a MicroAmp optical 96-well reaction plate as technical triplicates (Life Technologies) and analysed using the QuantStudio 6 Flex real-time PCR system (Life Technologies). Default settings on the instrument software for TaqMan® reagent Fast was used for qPCR reaction, initial denaturation at 95 °C for 20 seconds, followed by 40 cycles of 1 second denaturation at 95 °C and a 20 second annealing/extension at 60 °C. The starting concentration of the samples, presented as N0 value, was calculated from the qPCR amplification raw data using LinRegPCR software v11 [238].

Table 2.2. Mature miRNA sequences used to design Custom TaqMan primers

Species	miRNA	Canonical/ isomiR	Sequence
Ovis aries	oar-miR-133-5p	Canonical	UUGGUCCCCUUCAACCAGCUGU
	oar-miR-323a-3p	Canonical	CACAUUACACGGUCGACCUCU
	oar-miR-3957-5p	Canonical	CUCGGAGAGUGGAGCUGUGGGUGU
	oar-miR-1197-3p	Canonical	CCCUUCCUGGUAUUUGAAGACG
F. hepatica	fhe-Novel-11-5p	Canonical	AAGCUCGUAGUUGGAUCUGGGU
	fhe-miR-124-3p	Canonical	UUAAGGCACGCGGUGAAUGUCA
	fhe-miR-124-3p	IsomiR	UUAAGGCACGCGGUGAAU

2.2.7. Statistical analysis

Statistical analysis of RT-qPCR data was performed with GraphPad Prism (v 10). Non-parametric Welch's two tailed t-test was performed to compare infected versus non-infected samples at each timepoint. *P* value < 0.05 was considered as statistically significant.

2.3. Results

2.3.1. Differential abundance of host circulating miRNAs during *Fasciola hepatica* infection

To identify the presence of circulating miRNAs that are associated with developing fasciolosis, that may be considered as candidate diagnostic biomarkers, small RNA sequencing was performed on RNA extracted from sera of experimentally infected sheep. Sera collected from two distinct *F. hepatica* infection studies (Set A and B; Table 2.1) was used for this analysis; Sera in the Set A samples were collected at 2, 9, 14, 18 dpi, and Set B comprised of sera taken at 3, 7, 10, 14 wpi [232]. Sera was also collected from uninfected animals in each study, harvested at time points coincident with a pre-infection (0 dpi; Set A) and 14 weeks (Set B) timepoint.

As the initial RNA sequencing analysis of these individual samples was unsuccessful due to low RNA yield, RNA from six sera samples at each time point was pooled for preparation of the small RNASeq library. The resulting sequencing data was screened against the 153 mature miRNA sheep sequences registered in miRBase (Oar_V4.0). On average, 104 and 108 out of 153 sheep miRNAs were detected in the uninfected and infected sheep samples, respectively (Supplementary Table 2.2). Hierarchal clustering of the sequencing data from the different time points revealed a distinct separation in the miRNA expression between early and late infection (Figure 2.1A). To measure differential expression (DE) during disease progression, the sequencing reads were grouped as pre-hepatic (2, 9, 14 and 18 dpi; thus n = 4) and hepatic (3, 7, 10 and 14 wpi; n = 4) samples. Comparative analysis was then conducted using the expression profile from the sera from non-infected sheep (pre-infection 0 dpi and 14 wpi; n = 2). Principal component analysis (PCA) verified that samples produced distinct clusters, correctly grouping the pre-hepatic and hepatic samples (Figure 2.1B).

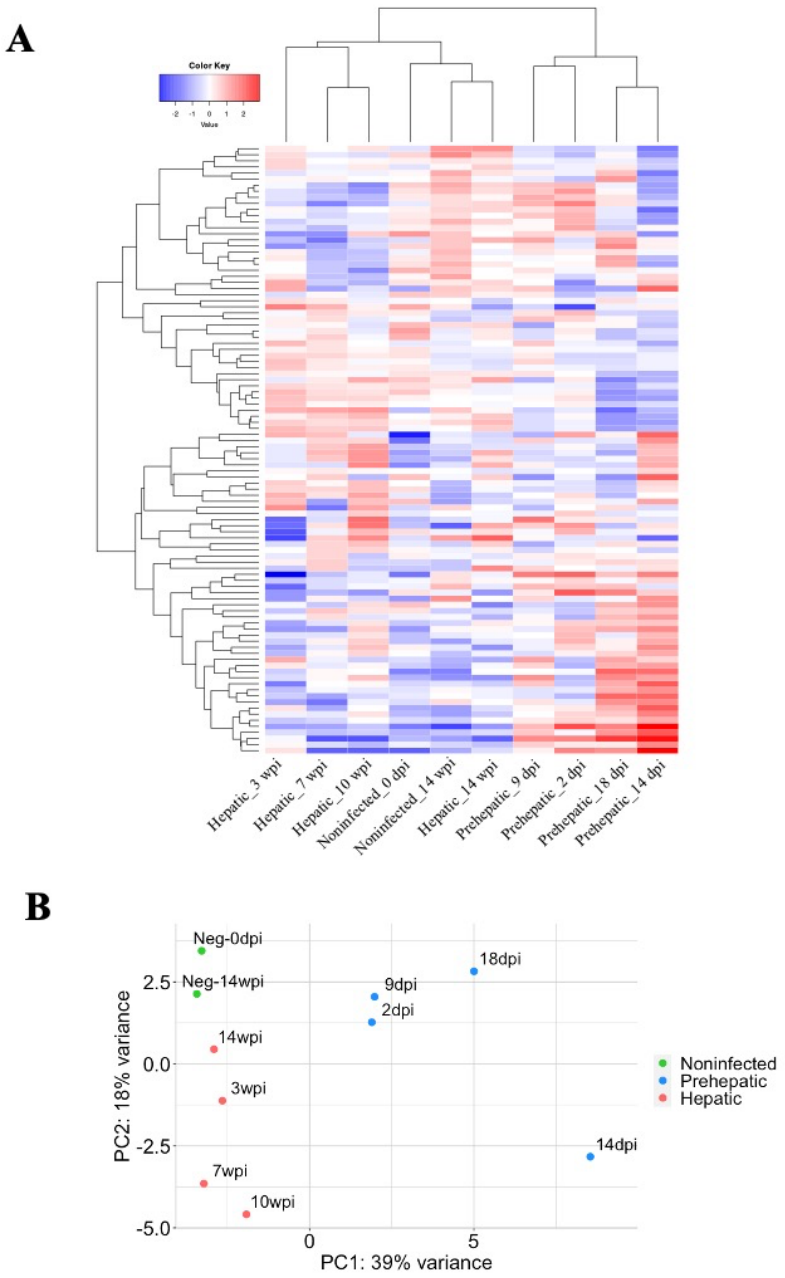


Figure 2.1. Differential abundance of sheep miRNAs in sera during Fasciola hepatica infection. *(A) Heatmap of relative abundance of sheep miRNAs (CPM) in non-infected sheep (0 day-Neg, 14 week-Neg), early/pre-hepatic infection (2 days post infection (dpi), 9 dpi, 14 dpi, 18 dpi), and late/hepatic infection (3 weeks post infection (wpi), 7 wpi, 10 wpi, 14 wpi). The heatmap was created using idep.96 [239], miRNAs were ranked by their standard deviation across all samples and hierarchical clustering carried out for the top 100 miRNAs . Expression of miRNAs represented as high (red) or low (blue) relative to total expression of miRNA across infection groups. (B) Principal component analysis (PCA) plot of total sheep miRNA abundance in non-infected sheep (green), pre-hepatic infection (2-18 days post infection) (blue), and hepatic infection (3-14 weeks post infection) (red).*

Comparing the sheep miRNAs between the non-infected, pre-hepatic, and hepatic stages of infection revealed several distinct miRNAs that were significantly increased or decreased in their abundance during the progression of infection. A four-fold cut-off (Log2FC2) was applied to these miRNA profiles to distinguish the subset of miRNAs that were most highly altered in expression and, therefore, most likely to be above a threshold of differential abundance to support the diagnosis of infection and potentially differentiate between the pre-hepatic and hepatic stages of disease.

This revealed the presence of six miRNAs that significantly increased during the pre-hepatic stage of the infection phase when compared to non-infected animals (Figure 2.2A; Supplementary Table 2.3A). Of these, the change in expression ranged from 2 to 6-fold, but the differential expression of oar-miR-323a-3p, oar-miR-133-5p, and oar-miR-3957-5p were the most significantly increased in the infected animals. The increased expression of oar-miR-3957-5p and oar-miR-541-3p, seen in the pre-hepatic samples, was also evident during the hepatic stage in infected sheep as compared to non-infected sheep, albeit at a reduced level (Figure 2.2B; Supplementary Table 2.3B). In contrast, the presence of oar-miR-133-5p, and oar-miR-323a-3p were significantly downregulated during the hepatic stage of infection, as compared to the pre-hepatic timepoints (Figure 2.2C; Supplementary Table 2.3C). Additionally, oar-miR-1197-3p was identified as the only miRNA significantly reduced during the hepatic stage of infection compared to uninfected animals and pre-hepatic infection (Figure 2.2B, C; Supplementary Table 2.3B, 3C).

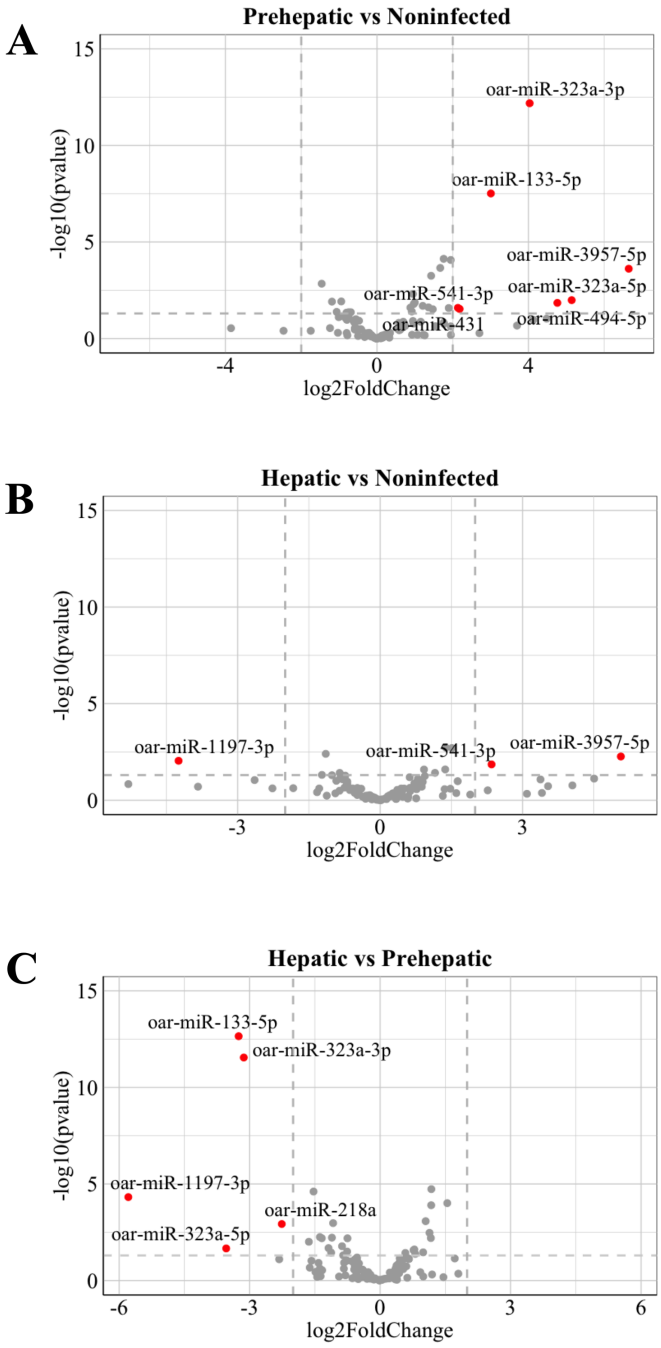


Figure 2.2. Circulating host-miRNA profiles are distinct during early and late F. hepatica infection compared to non-infected animals. *Volcano plots show differential expression of sheep miRNAs using DESeq2 in (A) pre-hepatic infection compared to non-infected sera samples, (B) hepatic infection vs non-infected sera samples, and (C) hepatic infection vs pre-hepatic infection. Genes that are more than ± log2 fold change 2 (FC) with significant p value (<0.05) are denoted in red.*

2.3.2. Small RNA sequencing revealed the presence of *Fasciola hepatica*-derived miRNAs in the serum of infected sheep

To determine if miRNAs derived from *F. hepatica* were present in the sera from infected sheep, sequencing reads that did not align to sheep mature miRNAs were screened against known *F. hepatica* miRNAs (Supplementary Table 2.1). Critically, no parasite-derived miRNA sequences were identified within the sera samples collected from non-infected sheep and, thus, validated this approach. In contrast, six liver fluke miRNAs were found within the sera from infected sheep (Table 2.3). These miRNAs displayed a distinct pattern of expression correlating to the division of samples into pre-hepatic and hepatic phases of infection. Specifically, two miRNAs were detected only at the pre-hepatic stage of infection: fhe-miR-124-3p and fhe-miR-71a-5p; however, fhe-miR-124-3p had higher read counts and was observed at all the timepoints, suggesting it may be a more robust infection marker than fhe-miR-71a-5p. While three microRNAs (fhe-Novel-102-3p, fhe-miR-277a-3p, and fhe-miR-750-3p) were linked to the hepatic phase of the infection, their counts per million (CPM) were all below 13, suggesting a low abundance. Only fhe-Novel-11-5p, was found throughout the entire infection, detected in all serum samples from both the pre-hepatic and hepatic stages.

Table 2.3. Total read counts of *Fasciola hepatica* miRNAs detected within sheep sera samples

	Non-infected		Pre-hepatic				Hepatic			
miRNA	**Neg-0 dpi**	**Neg-14 wpi**	**2 dpi**	**9 dpi**	**14 dpi**	**18 dpi**	**3 wpi**	**7 wpi**	**10 wpi**	**14 wpi**
fhe-miR-124-3p	0	0	59	32	44	28	0	0	0	0
fhe-Novel-11-5p	0	0	7	0	0	3	13	12	6	0
fhe-Novel-102-3p	0	0	0	0	0	0	0	13	9	0
fhe-miR-277a-3p	0	0	0	0	0	0	0	8	5	7
fhe-miR-750-3p	0	0	0	0	0	0	0	5	0	4
fhe-miR-71a-5p	0	0	0	8	0	0	0	0	0	0

(n = 6 sheep sera pooled/ time point); dpi: days post-infection; wpi: weeks post-infection. Neg-0 dpi: pre-infection timepoint, Neg-14 wpi: 14 weeks age-matched non-infected control.

2.3.3. Selection of sheep and *Fasciola hepatica*-derived miRNAs as potential biomarkers of fasciolosis

Based on this sequence analysis, a panel of sheep and parasite-derived miRNAs were curated as potential biomarkers of *F. hepatica* infection due to their differential abundance in infected compared to non-infected sheep and their presence across the different stages of infection (Figure 2.3). This panel comprised four sheep miRNAs and two *F. hepatica* miRNAs. The sheep miRNAs included oar-miR-133-5p and oar-miR-323a-3p, which were the most significantly upregulated miRNAs in pre-hepatic infection vs non-infected animals; oar-miR-3957-5p which was consistently elevated (log2FC4) in pre-hepatic and hepatic infection; and oar-miR-1197-3p which was downregulated in hepatic infection compared to both non-infected and pre-hepatic infection. The parasite miRNAs for the selected candidate diagnostic biomarker panel included fhe-miR-124-3p and fhe-novel-11-5p, which had the highest read numbers in sheep sera.

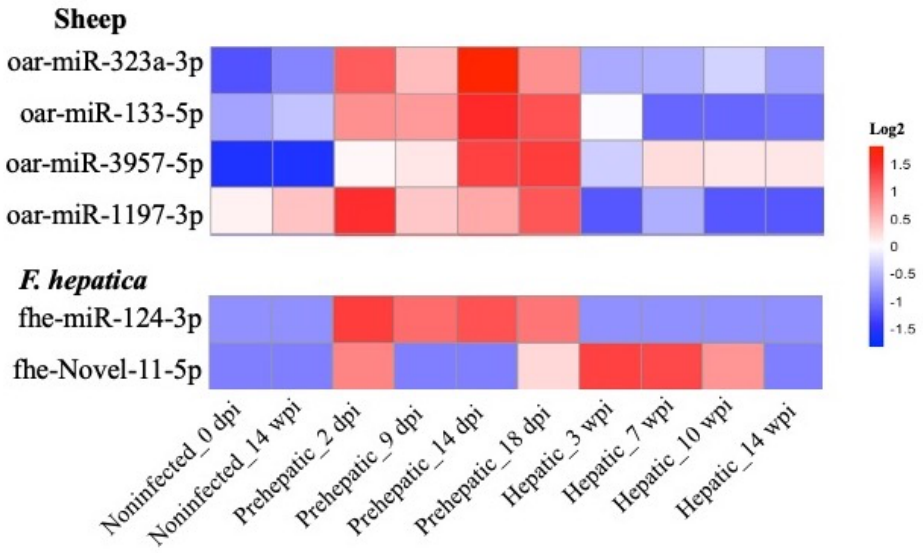


Figure 2.3. Selection of host and F. hepatica miRNAs as potential biomarkers for pre-hepatic and hepatic stages of fasciolosis. *Relative abundance of selected sheep and parasite miRNAs in uninfected animals (0 dpi-neg, 14 wpi-neg), pre-hepatic infection (2 dpi, 9 dpi, 14 dpi, 18 dpi), and hepatic infection (3 wpi, 7 wpi, 10 wpi, 14 wpi), represented as high (red) or low (blue) normalised read counts. dpi: days post infection, wpi: weeks post infection*

While sequencing analysis provided high-throughput screening of RNA sequences, it is not practical for large-scale diagnosis of fasciolosis. RT-qPCR represents a more suitable method for determining the differential expression of miRNAs in simultaneous samples of sheep sera.

On this basis, a series of qPCR primers specific to each of the selected miRNA sequences was designed. To first test the ability of these primers to specifically detect the candidate diagnostic miRNAs, lamb tissue was employed as a positive test sample for evaluating the performance of sheep miRNA specific primers, while RNA isolated from *F. hepatica* NEJs was used as the positive control to assess the efficacy of primers designed to detect the liver fluke miRNAs. This life cycle stage (NEJ) of the parasite was selected because fhe-Novel-11-5p is reportedly only expressed in NEJs and not in the juvenile or adult worms (both liver stages), while fhe-miR-124-3p is present throughout all intra-mammalian life cycle stages with the highest expression in the NEJs [231]. Based on the results from these RT-qPCR tests, oar-miR-1197-3p was excluded from further analysis due to its low copy number and late Cq (~33) in lamb tissue, with undetectable levels in non-infected sheep sera (Table 2.4). According to the sequencing data, the expression level of this miRNA was expected to decrease during the hepatic phase of infection (Figure 2.3). However, as it was not amplified in the test sera sample from non-infected sheep, a further decrease following the progression of *F. hepatica* infection would be impossible to detect by qPCR, thus negating its potential as a biomarker for hepatic infection.

In contrast, the Cq value of oar-miR-133-5p, oar-miR-323a-3p, and oar-miR-3957-5p were within an acceptable diagnostic range (Table 2.4), making them suitable for further analysis. In addition, the amplification of products from the Set A and B sera samples using these primers validated the sequencing data, as the pattern of expression was consistent with the distribution of read counts within the sequencing data. This RT-qPCR analysis verified that both oar-miR-133-5p and oar-miR-323a-3p were only present in the pre-hepatic set of samples whereas oar-miR-3957-5p was detected in samples from both the pre-hepatic and hepatic stages of infection (Figure 2.4).

Table 2.4. Assessment of primer sensitivity and specificity using lamb tissue and sheep sera.

	Lamb tissue	**Sheep sera (non-infected)**
miRNA	Avg Cq ± SEM (n = 6*)	Cq (n = 1)
oar-miR-3957	30.1 ± 0.07	35.7
oar-miR-323	28.3 ± 0.25	33.5
oar-miR-133	14.6 ± 0.41	30.8
oar-miR1197	33.3 ± 0.24	No Cq

*2 technical replicates of lamb tissue RNA, 3 technical replicates for qPCR for each sample.

Avg: Average, SEM: Standard error mean

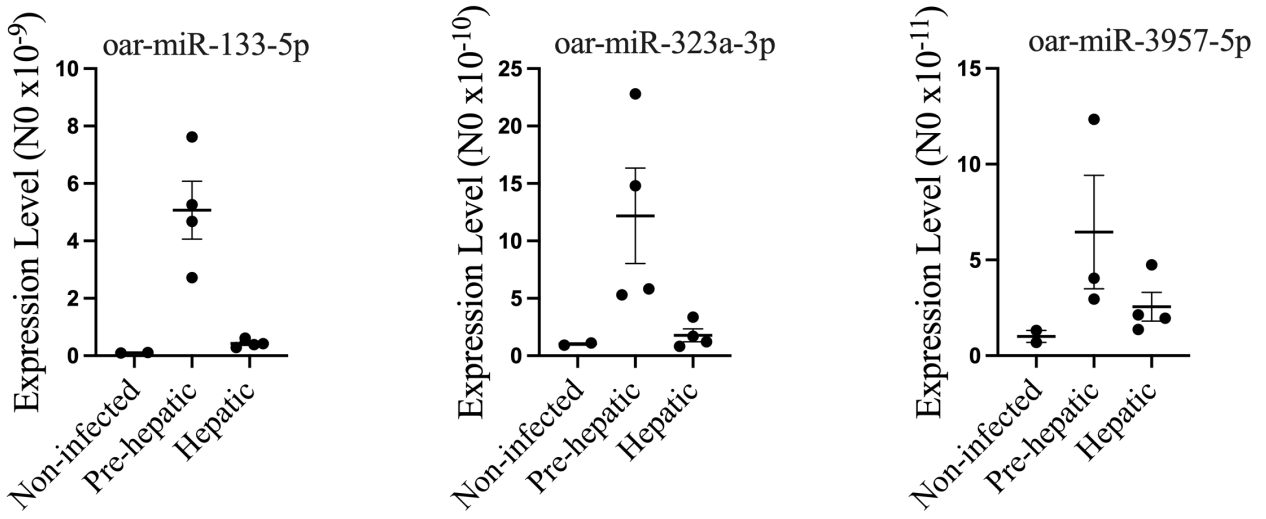


Figure 2.4. Validation of sequencing data using PCR and primers designed to detect the expression of sheep miRNAs. *RT-qPCR quantification of oar-miR-133-5p, oar-miR-323a-3p and oar-miR-2957-5p expression in the RNA isolated from the Set A and Set B sheep sera samples that had previously been sequenced. The data is presented as the starting quantity of genetic material prior to amplification (N0) as determined by LinRegPCR (v.11) This is calculated in the unit of the Y-axis of the PCR amplification plot, which are arbitrary fluorescence units. The average N0 value of two technical replicates are shown for each time point.*

Of the *F. hepatica* miRNAs, fhe-miR-124-3p and fhe-Novel-11-5p primers unexpectedly amplified products in both NEJs and lamb tissue (Figures 2.5A, 2.6A). Also, the primers designed to detect fhe-miR-124-3p produced extremely late, or no Cq, when tested further on the RNA samples from the sera from infected sheep that had been sequenced (Sets A and B; Figure 2.5B). Given these inconsistencies with the results from the test RT-qPCR in comparison to the sequencing data, a more in-depth analysis of the sequencing data for these two miRNA sequences was conducted.

This analysis revealed that the full-length canonical sequence of fhe-Novel-11-5p was not present within the sequencing reads, but a shorter variant (isomiR) missing four nucleotides at the 3' end was identified instead (Supplemental Table 5). Furthermore, by aligning this shorter sequence to the known sheep sequences using BLASTN (filtering for *Ovis aries*, txid:9940) revealed that the shortened fhe-Novel-11-5p sequence fully aligned with sheep ribosomal RNA (Figure 2.6B), which provides an explanation for the detection of fhe-Novel-11-5p in lamb tissue. In addition, as ribosomal RNAs are part (10 %) of the extracellular RNA population found in sera due to cellular turnover or secretion of microvesicles as a consequence of tissue injury (Max et al., 2018), it is likely that the detection of this sequence in the sera of infected sheep, but not uninfected sheep, reflects the host response to infection with Fasciola, or the tissue damage caused by the migrating parasite. However, due to the uncertainty of whether this result is unique to *F. hepatica* and thus indicative of infection, fhe-Novel-11-5p was omitted from subsequent analyses.

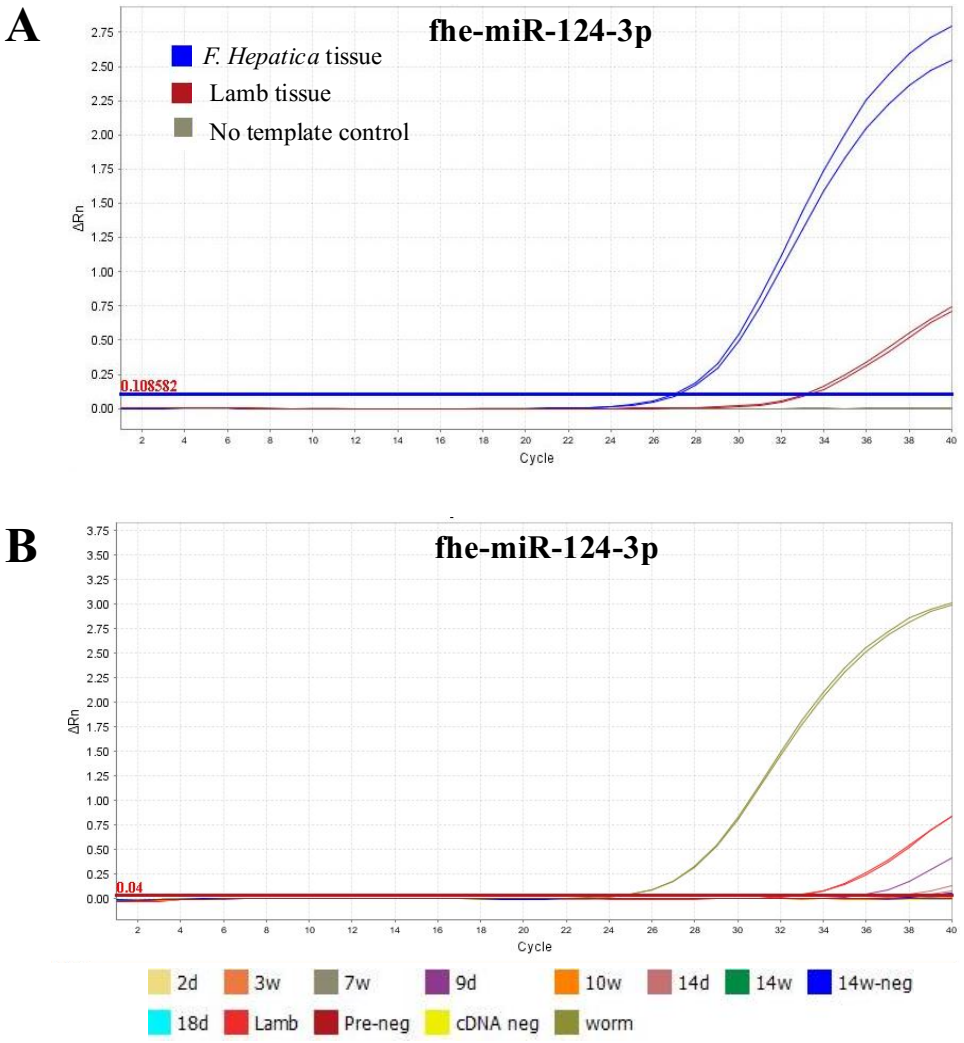
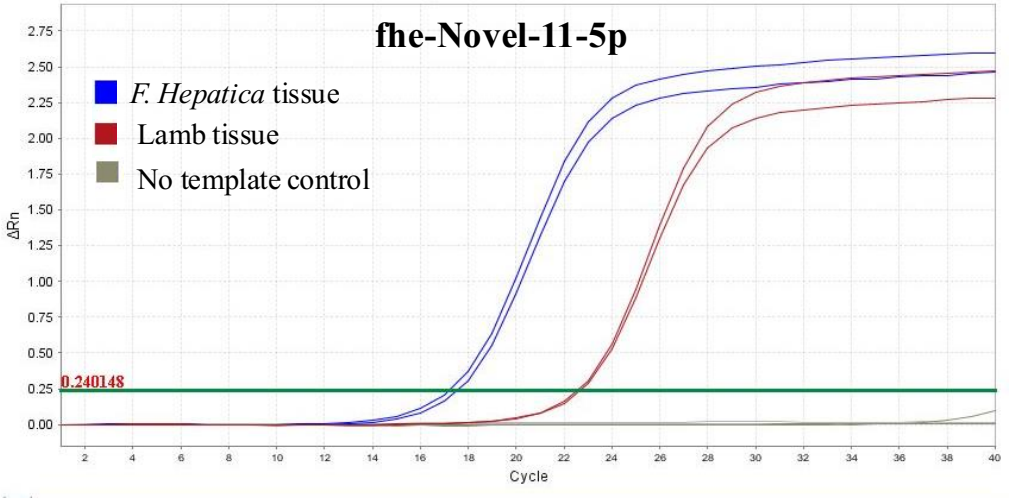


Figure 2.5. Detection of fhe-miR-124-3p. *RT-qPCR amplification plot showing (A) detection of canonical fhe-miR-124-3p in F. hepatica tissue and lamb tissue, (B) canonical fhe-miR-124-3p was poorly amplified in Set A or B sheep sera samples (n = 6 sheep sera samples pooled at each time point). d: days; w: weeks; Pre-neg: Pre-infection timepoint at day 0; 14w-neg: non-infected age-matched control at 14 weeks. Results of two technical replicates for each sample are shown in the amplification plots.*

A



B

Ovis aries 18S ribosomal RNA gene, complete sequence

Sequence ID: KY129860.1 Length: 1869 Number of Matches: 1

Range 1: 671 to 688 GenBank Graphics ▼ Next Match ▲

Score	Expect	Identities	Gaps	Strand
36.2 bits(18)	0.024	18/18(100%)	0/18(0%)	Plus/Plus

```
Query  1    AAGCTCGTAGTTGGATCT  18
           ||||||||||||||||||
Sbjct  671  AAGCTCGTAGTTGGATCT  688
```

Figure 2.6. Detection of fhe-Novel-11-5p *(A) RT-qPCR amplification plot showing amplification of canonical fhe-Novel-11-5p in F. hepatica tissue and lamb tissue. Results of two technical replicates for each sample are shown. (B) BLASTN output showing that the shorter Novel-11-5p isomiR sequence found in sheep sera matched 100% with the ribosomal RNA in sheep transcriptome.*

While the canonical sequence for fhe-miR-124-3p was not present in the sequencing reads from the sheep sera samples, this miRNA was found to be present as several sequence variants (isomiRs), missing nucleotides primarily at the 3' end and to a lesser extent at the 5' end (Figure 2.7A). Furthermore, the sequence of the canonical fhe-miR-124-3p was similar to cattle bta-miR-124-3p (Figure 2.8A), with only three nucleotides mismatched at the 3' end, suggesting that the corresponding sheep oar-miR-124-3p was likely missing from miRbase, and was thus not filtered from the sequencing reads during our initial analysis.

Consequently, a 100 % sequence identity of the bta-miR-124-3p precursor sequence to the non-coding region of sheep RNA confirmed the presence of oar-miR-124-3p and that oar-miR-124-3p is identical to bta-miR-124-3p (Figure 2.8B). Accordingly, the shorter two most dominant sequence variants of fhe-miR-124-3p found in infected sheep sera (Figure 2.7A) matched 100 % with both sheep and *F. hepatica* miR-124-3p (Figure 2.8 A). Therefore, it is impossible to determine whether the sequencing reads for the miR-124-3p variant that are increased during *F. hepatica* infection originated from sheep, parasite, or both. Nonetheless, the differential abundance of this miRNA classified it as a suitable candidate as a potential diagnostic biomarker of infection and, thus, a primer was designed for the most dominant 3' trimmed variant of miR-124-3p. This primer effectively distinguished the pre-hepatic stage of infection (Cq < 26) from both the hepatic stage and non-infected (Cq > 33) sheep using the Set A and B sequenced sera samples, an outcome that was consistent with the read counts from the sequencing data (Figure 2.7B, C; Table 2.3).

Based on these analyses, the miRNA candidate diagnostic biomarker panel for qPCR validation was refined to include four miRNAs: oar-miR-133-5p, oar-miR-323a-3p, oar-miR-3957-5p, and fhe/oar-miR-124-3p.

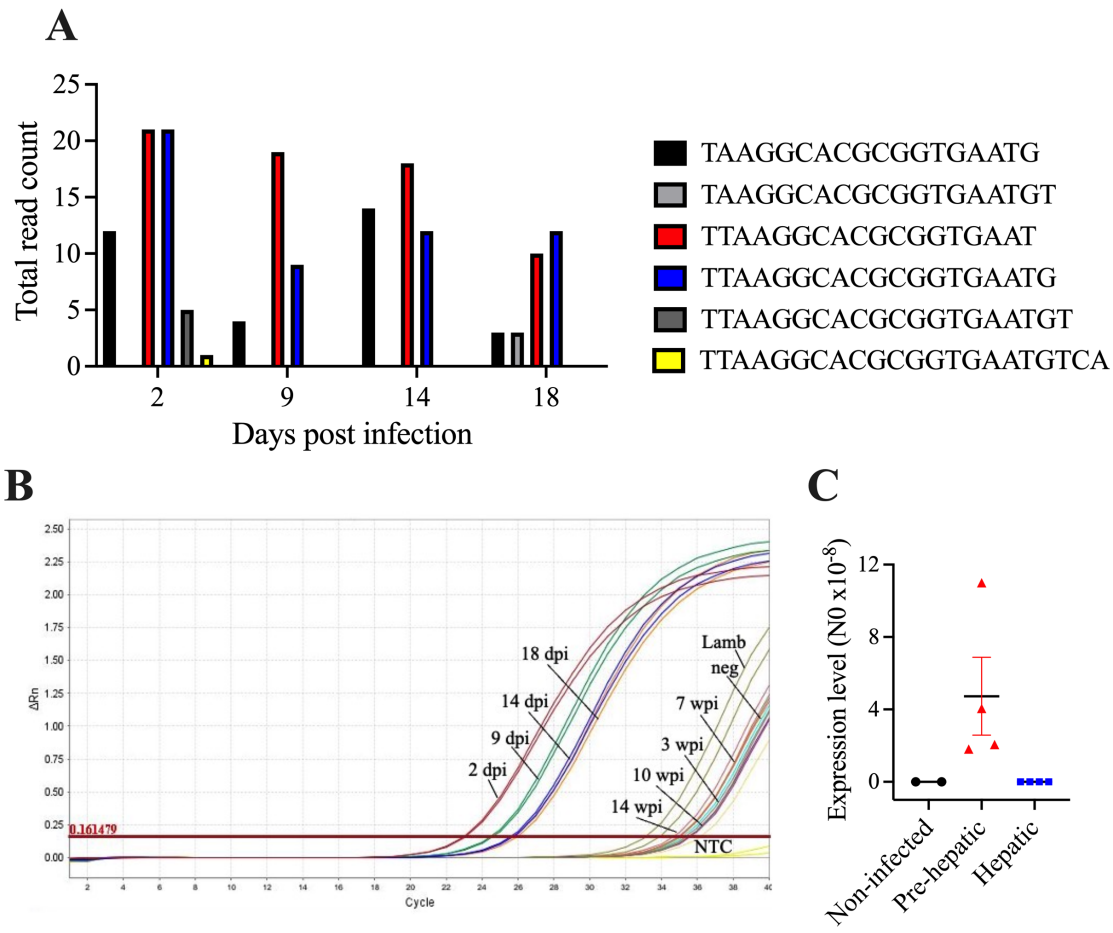


Figure 2.7. F. hepatica miR-124-3p was present as several sequence variants (isomiR) in sera of infected sheep. *(A) Total read counts of the miR-124 isomiRs present at the different time-points of infection in Set A and Set B sera. The canonical sequence is shown in yellow. The sequence of the most dominant isomiR (red bar) was used for qPCR primer design. (B) RT-qPCR amplification plot from primer test of the most dominant fhe-miR-124 isomiR in Set A and Set B sheep sera samples. dpi: days post infection; wpi: weeks post infection; neg: non-infected controls; NTC: no template control and lamb tissue. (C) RT-qPCR quantification of the dominant fhe-miR-124-3p isomiR presented as the starting quantity of genetic material prior to amplification (N0) as determined by LinRegPCR (v.11) This is calculated in the unit of the Y-axis of the PCR amplification plot, which are arbitrary fluorescence units. The average N0 value of two technical replicates are shown for each time point.*

A

fhe-miR-124-3p TTAAGGCACGCGGTGAATGTCA
bta-miR-124-3p TTAAGGCACGCGGTGAATGCCAAG

B

PREDICTED: Ovis aries uncharacterized LOC105608520 (LOC105608520), transcript variant X1, ncRNA

Sequence ID: XR_003588146.2 Length: 819 Number of Matches: 1

Range 1: 658 to 742 GenBank Graphics ▼ Next Match ▲ Previous Match

Score	Expect	Identities	Gaps	Strand
158 bits(85)	4e-38	85/85(100%)	0/85(0%)	Plus/Plus

```
Query  1    AGGCCTCTCTCTCCGTGTTCACAGCGGACCTTGATTTAAATGTCCATACAATTAAGGCAC  60
            ||||||||||||||||||||||||||||||||||||||||||||||||||||||||||||
Sbjct  658  AGGCCTCTCTCTCCGTGTTCACAGCGGACCTTGATTTAAATGTCCATACAATTAAGGCAC  717

Query  61   GCGGTGAATGCCAAGAATGGGGCTG  85
            |||||||||||||||||||||||||
Sbjct  718  GCGGTGAATGCCAAGAATGGGGCTG  742
```

Figure 2.8. Discovery of the presence of oar-miR-124-3p. *(A) Comparison of the miRBase annotated canonical sequences of miR-124-3p of F. hepatica (fhe) and Bos Tauras (cattle; bta). Red represents nucleotide(s) that did not match between the two species, blue indicates nucleotide(s) missing from the annotated canonical sequence but present in the precursor template of the miRNA. (B) Output from Blastn showing that the precursor of bta-miR-124-3p aligned 100% with the non-coding RNA region of sheep transcript.*

2.3.4. Circulating oar-miR-133-5p and oar-miR-3957-5p can diagnose fasciolosis from as early as seven days post-infection

To confirm the diagnostic potential of the selected miRNAs, RT-qPCR validation was performed on an independent archived set of sera samples harvested from individual sheep during two longitudinal infection studies; a pre-hepatic infection cohort comprised of sera collected at 0 (pre-infection), 7, and 14 days post-infection (Set C), a hepatic infection cohort with samples collected at week 3, 15, 20 and 23 post-infection (Set D), and age-matched non-infected animals for each of the timepoints.

From this analysis, the expression levels of both oar-miR-323a-3p and fhe/oar-miR-124-3p was almost identical in the sera from non-infected and infected sheep over the course of infection (Figure 2.9A, B), suggesting that these miRNAs cannot be used as indicators of fasciolosis. It is possible that this discrepancy between this RT-qPCR analysis and the sequencing data reflects the difference in sample preparation, with the sequencing performed on a pooled sample of sera from a cohort of six sheep. The variability in the expression of miRNAs across sheep samples is evident when sera from individual sheep was assessed by RT-qPCR, which in a pooled sample would create an incorrect representation of expression levels within individual samples. Furthermore, through the inclusion of age-matched non-infected sheep, it is apparent that the expression of miRNAs can change over time, irrespective of whether the animal is infected (Figure 2.9). As the sample collection that was originally sequenced lacked a full panel of age-matched controls, this alteration in expression was not fully captured, and the apparent differential abundance of miRNAs associated with infection within the sequencing data, may have simply been a variation due to age.

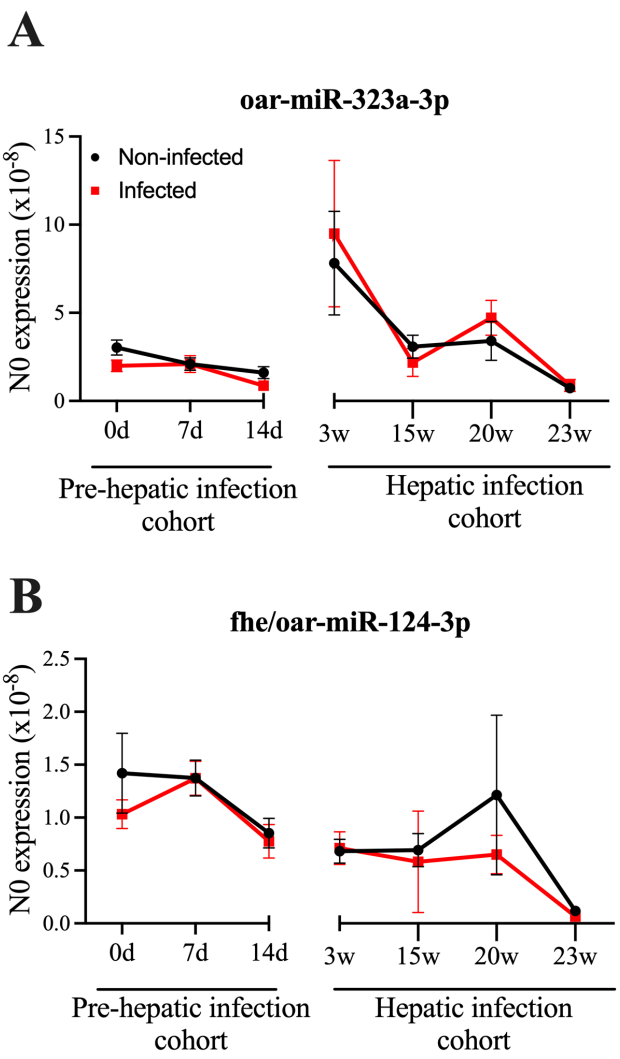


Figure 2.9. RT-qPCR assessment of sera samples invalidates the diagnostic potential of oar-miR-323a-3p and fhe-miR-124-3p. *The expression of (A) oar-miR-323a-3p, (B) fhe-miR-124-3p were determined by RT-qPCR and are presented as the starting quantity of genetic material prior to amplification (N0) as determined by LinRegPCR (v.11). This is calculated in the unit of the Y-axis of the PCR amplification plot, which are arbitrary fluorescence units. The data is presented as the mean ± SEM (n = 3-14; as shown in Table 1). The statistical significance of differences between infected and non-infected samples was determined using Welch's t-test (two-tailed).*

Consistent with the sequencing data, the RT-qPCR analysis revealed that the expression of both oar-miR-133-5p and oar-miR-3957-5p was elevated in the sera of infected animals compared to age-matched non-infected animals (Figure 2.10A, C). Furthermore, as these were longitudinal studies, the miRNA expression level in individual sheep in the pre-hepatic infection cohort could be tracked over time. As such, the fold change at 7 and 14 days compared to day 0 for each animal was examined. This approach revealed that the expression levels of both oar-miR-133-5p and oar-miR-3957-5p were significantly elevated in the infected animals at day 7 and 14 from day 0, but not in the non-infected animals (Figure 2.10B, D). Early elevation in the levels of these two miRNAs was consistent with the sequencing data, whereby an upregulation in miRNA expression was seen from 2 dpi (Figure 2.3). The sera samples representing the hepatic stage of infection were harvested from a separate infection cohort to the earlier time points, so could not be tracked in individual sheep from day 0.

Nonetheless, corroborating the sequencing data, the level of expression of oar-miR-133-5p in the sera of infected animals, other than a single peak at 20 wpi, was reduced as infection progressed, as compared to the earlier time points (Figure 2.10A). In addition, validating the sequencing data, the increase in oar-miR-3957-5p in sera from infected sheep was generally sustained throughout the entire observation period, with a lower expression level compared to the pre-hepatic phase of infection (Figure 2.10C).

In conclusion, these data indicate that both oar-miR-133-5p and oar-miR-3957-5p are potential biomarkers of early, pre-hepatic infection. In addition, the difference in expression of oar-miR-3957-5p between infected and non-infected sheep over the entire observation period suggests that this may represent an unchanging marker of infection, which, in the absence of an increase in oar-miR-133-5p, would indicate late stage/hepatic phase of infection.

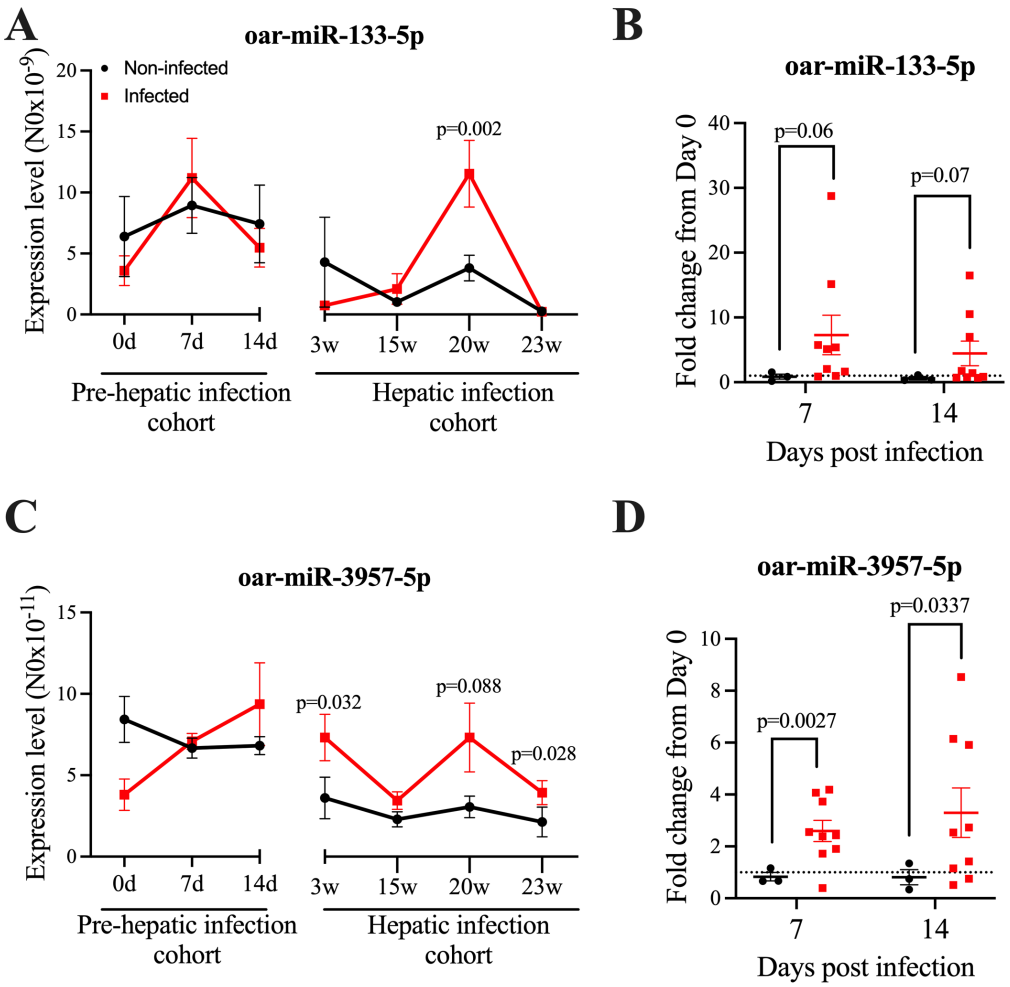


Figure 2.10. RT-qPCR demonstrates the differential expression of oar-miR-133-5p and oar-miR-3957-5p in sera from infected sheep as compared to uninfected animals. *Quantification of (A) oar-miR-133-5p and (C) oar-miR-3957-5p in the sera of individual sheep in response to infection was determined by RT-qPCR and is represented as the starting quantity of genetic material prior to amplification (N0) as determined by LinRegPCR (v.11). This is calculated in the unit of the Y-axis of the PCR amplification plot, which are arbitrary fluorescence units. The data is presented as the mean ± SEM (n = 3-14; as shown in Table 1). (B) Fold change of oar-miR-133-5p and (D) oar-miR-3957 expression at 7 or 14 dpi in comparison to 0 dpi in the sera of individual sheep in the pre-hepatic cohort. The data is presented as the mean ± SEM (n = 3 non-infected; 9 infected sheep for which data was available at all three timepoints). In all cases the statistical significance of differences between sera from infected versus uninfected sheep was determined using Welch's t-test (two-tailed).*

2.4. Discussion

The severe impact of fasciolosis on animal welfare and the significant economic cost it imposes on the livestock industry highlights the need for a reliable and robust biomarker that can effectively guide anthelmintic treatment and facilitate the management and control of liver fluke on farms [210]. The development of an accurate diagnostic method for acute infection is of paramount importance since such a tool would enable timely intervention to prevent liver flukes from inflicting liver pathology, which would mitigate the risk of sudden fatalities associated with a high liver fluke burden (in approximately 10 % of infected sheep) and disrupt the liver fluke lifecycle by preventing the parasite from reaching the bile duct to lay eggs, which in turn, would curb the spread of the infection within grazing pastures

Given this need, exploiting the differential abundance of circulating miRNAs as a biomarker of infection represents an attractive diagnostic tool. Circulating miRNAs exhibit exceptional stability, rendering them a highly suitable choice for diagnostic purposes, particularly in the setting of a farm where controlling sample collection and storage can be challenging. For this reason, miRNAs have gained significant attention for their diagnostic potential in a range of pathogenic infections, and due to their immediate alteration in expression in response to infection they are appropriate markers for the detection of early infections [226].

In this study, the utility of miRNAs in detecting both pre-hepatic and hepatic fasciolosis was assessed in sera samples collected from sheep with experimental subclinical disease. The results provide the first evidence that unique miRNA expression signatures in ruminant sera are associated with the distinct pathological stages of fasciolosis. The data supports the hypothesis that differentially expressed miRNAs can serve as prognostic markers for fasciolosis and, moreover, demonstrates that unique miRNA expression patterns emerged as early as 2 days post-infection. Therefore, miRNAs could offer superior sensitivity in fasciolosis diagnosis compared to conventional, commercial methods, such as FEC and serological ELISAs.

The analysis of sera samples from age-matched infected and non-infected sheep in the RT-qPCR validation demonstrated the paramount importance of incorporating age-matched samples in any screening protocol aimed at characterising miRNAs as diagnostic biomarkers. As demonstrated in this study, the differential expression of miRNAs quantified using RT-qPCR exhibited significant age-related variability. Specifically, the expression of oar-miR-323a-3p, which we initially described as a potential biomarker from sequencing data (without appropriate age-matched samples), was

subsequently discovered using RT-qPCR to vary significantly over time in non-infected sheep, with relatively higher expression as the animals aged.

Despite encountering challenges with variations in miRNA expression levels due to age, using a longitudinal approach of assessing miRNA expression in individual animals over time successfully addressed these issues. The findings presented here indicate that the expression of certain miRNAs in sheep increased in response to infection, irrespective of the animal's age. Given this observation, it would be recommended that for any miRNA-based diagnostics studies, it may be necessary to collect serum samples from animals on their initial exposure to pasture to set a benchmark for each animal's miRNA expression. Future serum samples can then be compared to this baseline to accurately assess the onset and progress of infection. This approach could also be effectively adapted to sentinel screening practices for monitoring liver fluke prevalence over a grazing season, as has been employed with serological tests [240].

While the potential of using host miRNA detection to support the diagnosis of fasciolosis has been established in this study, further evaluation is required to ensure specificity. The observed changes in circulating host miRNAs during infection may reflect host-driven biological processes, such as inflammatory responses, and tissue repair or remodelling in response to parasite-induced damage, rather than parasite-specific effects alone. For example, circulating oar-miR-3957-5p has been reported to be elevated in high stress responding female sheep when challenged with bacterial LPS [241, 242] suggesting that this miRNA could be upregulated in response to other broad infections. Furthermore, the sheep assessed in the current study were all male; the possibility that any differential expression in miRNAs is sex-related would need to be considered. In addition, miR-133-5p was reportedly upregulated in early bacterial infection in a marine lancelet species (*Branchiostoma belcheri*) [243], and in the plasma of chronic obstructive pulmonary disease patients, and tumour cells of various cancers, including gastric and colon cancer [244, 245]. Hence, while oar-miR-133-5p and oar-miR-3957 show promise as candidate diagnostic biomarkers for fasciolosis, their specificity to *F. hepatica* infection must be further explored.

To address the issue of specificity in another way, the results of differential expression of host miRNAs could be amalgamated with the detection of liver fluke miRNAs. Liver fluke miRNAs are likely deliberately secreted by the parasite to manipulate the host's immune response or are passively released from dying parasites. While several helminth studies have demonstrated the presence of parasite-derived miRNAs in host circulation [228, 229, 246], this is the first study to demonstrate the presence of *F. hepatica*-derived miRNAs in infected host circulation (importantly that of a ruminant).

Furthermore, the temporal expression of the liver fluke-derived miRNAs correlated with their expression pattern that was previously reported over the course of the intra-mammalian stages of development [231]. For instance, fhe-miR-124-3p and fhe-miR-71a-5p, both of which were found to be most abundant in NEJ, were detected in sheep sera at the pre-hepatic stage of infection. On the other hand, fhe-miR750-3p and fhe-Novel-102-3p, both most highly expressed by adult worms, were detected at the hepatic stage of infection. Notwithstanding that many parasite-derived miRNAs are present at very low copy numbers; it remains to be determined whether they could be amplified to detectable levels of RT-qPCR.

The analysis here also revealed that several helminth miRNAs detectable in sera, are highly conserved and, therefore, have sequences that are nearly identical to their mammalian hosts. In this study, *F. hepatica*-derived miRNAs in sheep sera were detected using a rigorous filtering process in the analysis of sequencing reads; only reads that did not align with the sheep mature miRNAs from miRBase were aligned to *F. hepatica* miRNAs, allowing zero mismatches, to eliminate any false identification of sheep miRNAs as parasite miRNAs. Furthermore, the presence of the parasite-miRNAs in sera samples from infected sheep but not in the non-infected samples provided confidence that these miRNAs exclusively originated from the parasite. However, further investigation revealed that two of the identified liver fluke miRNAs, namely fhe-miR-124-3p and fhe-Novel-11-5p, were present as trimmed isomiRs in the sheep sera, that were also conserved with sheep sequences. While previous studies have reported the presence of helminth-derived miRNAs in host circulation [228, 229, 246], the existence of such sequence variants has not yet been documented. This unique discovery raises important new considerations regarding the interpretation of sequencing data for the discovery of helminth (or pathogen)-derived miRNAs such as miR-124-3p.

In summary, the study presented in this chapter has characterised the differential abundance of parasite and host serum miRNAs during infection with *F. hepatica* in a ruminant host. Two miRNA with diagnostic biomarker potential for fasciolosis were identified following a stringent selection process. Lowering the threshold of selection from sequencing data to a 2-fold change in expression could reveal additional miRNA targets and provide an opportunity to expand the available candidate miRNA biomarker panel. The data presented here has established the suitability of developing the measurement of sheep miRNA expression into a diagnostic tool for fasciolosis, potentially through a PCR blood test. Achieving this potential will require extensive field studies to determine the precise sensitivity and specificity of this method. While our current findings are based on controlled experimental infections of sheep, the ultimate goal will be to test the effectiveness of these potential miRNA biomarkers in naturally infected animals. Such real-world conditions present a more complex

scenario for diagnosis due to varying worm burdens, infection dynamics, overlapping temporal infections, and the potential for co-infections (liver fluke and other pathogens). Accordingly, further validation in independent cohorts of naturally infected animals will be necessary to define diagnostic performance using receiver operating characteristic (ROC) analysis and to assess possible cross-reactivity with other infections. Ultimately, successful field validation of these miRNA diagnostic biomarker candidates in the field could lead to their use in point-of-care technologies at the farming level. This would be particularly beneficial in environments where access to technical expertise and resources is limited, offering a practical and user-friendly method for detecting fasciolosis in the field.

Chapter 3:

Comparing the functional activity of *F. hepatica*-derived canonical and isomiR miRNAs in the regulation of macrophage inflammatory responses

Publication statement

An edited version of this chapter is currently under review in ***PLoS Neglected Tropical Diseases***: Chowdhury, S., Sais, D., Tran, N. T., & Donnelly, S. (2025) *Fasciola hepatica* selects a sequence variant of miR-125b-5p to communicate with host immune cells, due to its enhanced efficacy as compared to the canonical miRNA.

Author Contributions:

Sumaiya Chowdhury (graduate student) designed experiments, performed, and analysed the data. Dayna Sais, Nham Tran and Sheila Donnelly made substantial contributions to the conception of the work, critical analyses of data, writing and editing of the manuscript.

The introduction and discussion presented here differ from the submitted manuscript, and the numbering of sections, style of referencing, numbering of tables and figures have been changed to align with the formatting of the thesis.

3.1. Introduction

To date, bioinformatic pipelines for the identification of miRNAs within sequencing data sets have typically assumed that individual miRNAs exist as a single defined sequence. However, recent advances in RNA sequencing have revealed that miRNAs can also exist as families of sequence variants (termed isomiRs), derived from a single miRNA locus [247-249]. Initially disregarded as sequencing artifacts, these isomiRs have since been validated through studies employing synthetic miRNA spike-in controls, which demonstrated that the observed isomiR diversity far exceeded the expected sequencing error rate, confirming that these variants are genuine biological products rather than sequencing noise. This diversity arises primarily from heterogenous cleavage of the primary or precursor miRNA transcript by the RNase III enzymes Drosha and Dicer, resulting in 5′ and 3′ end length variants with additional or missing templated nucleotides [247, 250-253]. Beyond these biogenesis-dependent variations, isomiRs are further diversified through post-transcriptional modifications, such as, addition of non-templated nucleotide i.e., nucleotides not encoded in the original transcript, by nucleotidyl transferases [254, 255], and trimming of nucleotides by exoribonucleases [256, 257].

Like their canonical miRNAs, isomiRs display expression patterns that vary according to tissue type, sex, ethnicity, and disease state [147, 258-264]. Therefore, rather than being random by-products of biogenesis, the generation of isomiRs appears to be a tightly regulated process that expands the complexity and specificity of miRNA-mediated gene regulation [248, 265-267]. The 5′ isomiRs have garnered particular interest because alterations at the 5′ end can modify the seed region, leading to redirected target specificity and consequently distinct or even opposite biological effects [268, 269]. However, 3’ isomiRs are the most prevalent type and have also been shown to have diversified gene targets compared to their canonical counterpart [250, 251, 255, 265, 270]. Besides influencing target specificity, 3’ isomiRs can also exhibit altered stability, subcellular localization, target binding affinity, and interactions with RNA-binding proteins, all of which may affect their regulatory efficiency and biological outcomes [271-273].

The discovery that fhe-miR-124-3p and fhe-Novel-11-5p were present as trimmed isomiRs in the sera of sheep infected with *F. hepatica* (Chapter 2), advocated for a re-investigation of the parasite miRNA sequences to determine the full extent of sequence variants expressed by the parasite. This analysis revealed that isomiRs are the most dominant miRNA form in NEJs, whereas a transition to canonical miRNAs occurs as the parasite matures [274]. Such a temporal variation indicates that isomiRs are critical for the NEJ life stage. Sequence analysis suggested that the generation of these isomiRs were predominantly mediated by Dicer cleavage and that the cleavage motifs in *F. hepatica* primary

miRNAs were more similar to the motifs found in mammalian cells than in the free-living nematode *C. elegans* [274]. These additional observations imply an adaptation of the miRNA sequences to function in the mammalian biogenesis machinery, and further suggests that the predominance of isomiRs in the NEJs, may reflect the host-parasite interactions that occur as the NEJs migrate from the intestine, through the peritoneal cavity, and into the liver, and in particular the ability of the parasite to modulate the activity of host immune cells at this time. Understanding the roles of isomiRs in parasitic worms is therefore important to provide new insights into parasite biology and to identify potential targets for controlling parasitic infections.

We have previously reported that peritoneal macrophages from mice infected with *F. hepatica* contain 25 parasite-derived miRNAs [63]. Of these, fhe-miR-125b, was the most abundant and was found to be loaded onto host Ago2 with functional activity that mimicked the host miR-125b resulting in the suppression of IL6 and TNF secretion from macrophages in response to inflammatory ligands [63]. However, the bioinformatic pipeline used in that study relied on simple counts of sequences that aligned exactly to the reference *F. hepatica* miRNAs, without further analysis of sequence or length variation, hence, overlooking the isomiR population. Understanding that isomiRs may potentially provide a greater breadth for the regulation of gene expression, it is important to now determine whether the increased expression of isomiRs by the NEJs is related to the immune regulation of macrophages that had been observed during the initial stages of infection.

Therefore, the aim of this study was to re-examine the sequences from the peritoneal macrophages of mice infected with *F. hepatica* for the presence of both canonical and isomiR sequences and to examine the functional role of these miRNAs in the modulation of macrophage activity.

3.2. Methods:

3.2.1. Sequencing Data and Bioinformatic Analysis

3.2.1.1. Peritoneal macrophages

Sequencing data of peritoneal macrophages from *F. hepatica* infected mice were available from our previous study (NCBI Gene Expression Omnibus Accession: GSE263895) [56]. The macrophages had been isolated from 6-7-week-old female BALB/c mice orally infected with 20 metacercariae of *F. hepatica*. Specifically, cells were harvested at 6 hours (h), 18 h, and 5 days post-infection, and from a cohort of uninfected mice (n = 25/timepoint). Peritoneal macrophages from five mice at each timepoint were pooled for RNA isolation, giving a total of five replicates for each time point. The sequencing library preparation was performed using the QIAseq prep for miRNAseq (75 M reads/ sample) and sequenced using Illumina NovaSeq 6000 platform (Ramaciotti Centre for Genomics, UNSW, Australia).

3.2.1.2. Fasciola hepatica intra-mammalian life stages

Sequencing data from the three distinct intra-mammalian life stages of *F. hepatica*: newly excysted juveniles (NEJ), juvenile and adults were available from our previous study [231]. Briefly, the NEJs (n = 1000/replicate) were obtained by excysting the metacercariae *in vitro* followed by culturing of the parasite for 24 h in media. Juvenile worms (n = 19/replicate) were isolated from the liver of *in vivo* infected BALB/c mice at 21 days post infection, and adult worms (n = 1/replicate) were isolated from infected sheep liver. Small RNA libraries were then generated (n = 3 biological replicates per life stage) using the Small RNA Library Prep Set for Illumina (Arraystar) and sequenced on the Illumina NextSeq 500 platform (Arraystar).

3.2.1.3. Fasciola hepatica isomiR profiling

The quality of the sequencing raw data (in Fastq format) was assessed using FastQC v0.11.9 [234]. Adapter sequences were excised, and reads with a Phred score below 20 were removed using CutAdapt [275]. Additionally, for miRNA detection, reads with lengths less than 18 nt or greater than 26 nt were discarded. Sequence alignment was performed using Bowtie2 [236]. For the murine macrophages, miRNA sequences were first aligned against mature mouse miRNA sequences retrieved from miRbase (Release 22.2), allowing for zero mismatches within the sequence. To identify the presence of worm-derived miRNA in the murine macrophages, the unaligned reads were subsequently aligned to known annotated *F. hepatica* miRNAs, also permitting no sequence mismatches. For the worm life stages, the sequencing data was directly aligned to the Fasciola miRNAs using Bowtie2. The read counts of the miRNAs and their respective sequences were then extracted for isomiR profiling using SamTools [275]. Each unique sequence or length variant was

treated as an individual isomiR and the quantity of the isomiRs was expressed as % of the total read count for specific miRNAs.

3.2.1.4. Target prediction and gene enrichment analysis

Target prediction of the canonical fhe-miR-125b-5p and its 3' trimmed 21 nt isomiR was performed using miRanda [276] on miRNAconsTarget (https://arn.ugr.es/srnatoolbox/amirconstarget/), filtering for a free energy score (FE) of < -20 kcal/mol. Gene enrichment analysis was performed using g:Profiler (https://biit.cs.ut.ee/gprofiler/gost) [277] on targets only found in the isomiR target list compared to the canonical fhe-miR-125b target list. GO terms for biological processes with *P* value adjusted to < 0.05 were used to graph a semantic similarity plot using Revigo (http://revigo.irb.hr) [278] (using default settings and the resulting list size as small (0.5)).

3.2.2. Isolation of bone marrow derived macrophages (BMDM)

Bone marrow was collected from the femurs and tibias of 6-7-week-old BALB/c mice. The marrow was dissociated into RPMI 1640 Medium (Gibco) containing 10% v/v heat-inactivated Fetal Bovine Serum (FBS; Gibco) by repeated aspiration through a 19-gauge needle. The resulting cell suspension was centrifuged at 300 × *g* for 5 minutes, and the cell pellet resuspended in RPMI 1640 Medium (Gibco) supplemented with 10% v/v heat-inactivated FBS, 0.005% v/v 2-mercaptoethanol (Sigma-Aldrich) and 5% v/v penicillin/streptavidin (Life Technology). To promote monocyte differentiation into macrophages, the culture medium was supplemented with 50 ng/mL recombinant macrophage colony-stimulating factor (m-CSF; Miltenyi Biotec) on days 1 and 3, and the cultures were maintained at 37 °C with 5% CO_2. On day 6, differentiated BMDMs were harvested and used for experiments as described in the figure legends. Ethics approval for these studies was granted by the UTS Animal Care and Ethics Committee (Approval Number: ETH20-4709). All experiments were conducted in accordance with the approved guidelines and in compliance with The Australian Code for the Care and Use of Animals for Scientific Purposes.

3.2.3. *In vitro* macrophage transfection and LPS stimulation

BMDMs (2 x 10^6 cells seeded overnight) were transfected with synthetic mirVana miRNA mimics (20 nM; Ambion) of fhe-miR-125b-5p canonical and its 3' trimmed isomiR (Table 3.1) using Lipofectamine RNAiMAX according to the manufacturer's protocol (Invitrogen).

Cells treated with Lipofectamine RNAiMAX alone were used as vehicle controls, and wells transfected with mmu-miR-23a-3p (Assay ID: MC10644; Thermo Fisher Scientific) served as mimic controls. After transfection, the cells were maintained at 37 °C and 5% CO_2 for 24 hours. Cells were

then washed with sterile saline and subsequently stimulated with *E. coli* lipopolysaccharide (LPS; 20ng/mL; 011:B4 strain) to induce an M1 type pro-inflammatory response. Culture supernatants were collected at 6 h and 16 h post-LPS and stored at -20 °C prior to analysis of cytokine secretion. The cells were washed with saline and collected in 500 µL RNAzol RT and stored at -80 °C prior to RNA isolation.

Table 3.1. Sequences of mature fhe-miR-125b-5p canonical and isomiR mimics

Sequence type	Abbreviation	Sequence	Sequence length (nt)
Canonical	Can	CCCCTGAGACTGATAATTGCTC	22
isomiR	Iso	CCCCTGAGACTGATAATTGCT	21

3.2.4. Cytotoxicity assay

To assess the viability of macrophages, the release of lactate dehydrogenase (LDH) activity was measured in cell supernatants using the CytoTox LDH Release Kit (Promega) following the manufacturer's instructions. Vehicle-control cells treated with lysis buffer to achieve 100% cytotoxicity served as the "maximum LDH release controls". The LDH release in the experimental samples was expressed as a percentage of the maximum LDH release control.

3.2.5. Cytokine assay

The levels of IL6 and TNF secreted by transfected BMDMs in response to subsequent LPS stimulation were quantified in the cell culture supernatant using ELISA kits, according to the manufacturer's instructions (Catalogue # 555240 and 558534; BD Biosciences). Absorbance at 450 nm was quantified using a Tecan plate reader, and background absorbance at 520nm was subtracted. Cytokine concentrations were then calculated by extrapolating from a standard curve.

3.2.6. RNA extraction

RNA extraction was performed using RNAzol RT, according to the manufacturer's instructions. Briefly, BMDMs were homogenised in 500 µL of RNAzol RT and ultrapure DNAse/RNase free distilled water (400 µL; dH_2O; Life Technologies) was added to the resulting homogenate. This combined solution was centrifuged at 12,000 × *g* for 15 min at 4 °C, to pellet DNA, proteins, and polysaccharides. The resulting supernatant containing soluble RNA was collected and combined with 4-bromoanisole (BAN; Sigma-Aldrich, USA) at 0.5% v/v and then centrifuged at 12,000 × *g* for 10 min at 4 °C to pellet residual DNA, proteins, and polysaccharides. To precipitate RNA, the resulting supernatant was collected and combined with equal volume of isopropanol (Sigma-Aldrich) and 5 µL glycogen (5 mg/mL; Life Technologies), and incubated overnight at − 20 °C. The RNA precipitate

was pelleted by centrifugation at 12,000 × *g* for 15 min at 4 °C, washed with 500 µL of 75% ethanol (Sigma-Aldrich) twice and re-solubilised in dH_2O. The quality and quantity of isolated RNA was determined using the NanoDrop One Microvolume UV-Vis spectrophotometer (Thermo Fisher Scientific).

3.2.7. Detection of fhe-miR-125b mimic in transfected cells

The levels of fhe-miR-125b-5p Canonical and IsomiR mimics in transfected cells were quantified using RT-qPCR. Custom TaqMan small RNA assays were designed for the specific detection of canonical and isomiR sequences using the Thermo Fisher Small RNA Assay Design Tool (https://www.thermofisher.com/order/custom-genomic-products/tools/small-rna/). Total RNA isolated from the transfected macrophages (25 ng) was reverse-transcribed into cDNA using the TaqMan MicroRNA Reverse Transcription Kit (Applied Biosystems) with the TaqMan stem-loop reverse transcription primer for either the canonical miRNA or the isomiR. The resulting cDNA was diluted 1:4.5 ultrapure distilled water (Thermo Fisher Scientific). For qPCR, 4.5 µL of diluted cDNA, 5 µL of TaqMan Fast Advanced Master Mix (Applied Biosystems), and 0.5 µL of the custom TaqMan primer-probe mix (specific to the mimic variants) were combined in a total reaction volume of 10 µL. All reactions were prepared in technical triplicates on a MicroAmp optical 96-well reaction plate (Life Technologies), and qPCR was conducted on a QuantStudio 6 Flex Real-Time PCR System (Life Technologies). To determine whether the transfection levels of the mimics were comparable, Cq values obtained for the canonical miRNA in canonical mimic transfected cells were compared to those of the isomiR miRNA in isomiR transfected cells.

3.2.8. Quantification of expression level of macrophage endogenous genes

Alterations to the level of several genes associated with the macrophage inflammatory response were measured in cells that were transfected and treated with bacterial LPS. Total RNA (100 ng) from macrophages was subjected to cDNA synthesis using the High-Capacity cDNA Reverse Transcription Kit (Cat. No. 4374967, Applied Biosystems). The resulting cDNA was then diluted 1:4.5 in ultrapure distilled water (Thermo Fisher Scientific), and 4.5 µL of this was used for qPCR with TaqMan Fast Advanced Mastermix (Applied Biosystems) and TaqMan primers specific for each gene (Table 3.2). Samples were prepared in technical triplicates on a MicroAmp optical 96-well reaction plate (Life Technologies) and qPCR was performed on a QuantStudio 6 flex real- time PCR system (Life Technologies). The starting concentration of the samples, presented as N0 value, was calculated from the qPCR amplification raw data using LinRegPCR software v11 [238]. Data were presented as the fold change in N0 relative to the vehicle only treated samples.

Table 3.2. Gene names and corresponding TaqMan gene expression assay IDs for qPCR

Gene name	TaqMan ID
Signal transducer and activator of transcription 3 (*Stat3*)	Mm01219775_m1
Hypoxia-inducible factor 1-alpha (*Hif1a*)	Mm00468869_m1
Runt-related transcription factor 1 (*Runx1*)	Mm01213404_m1
Peptidyl-prolyl cis-trans isomerase NIMA-interacting 1 (*Pin1*)	Mm03053328_s1
Interleukin 17 receptor D (*Il17rd*)	Mm00460340_m1
Nucleotide-binding oligomerization domain-containing protein 1 (*Nod1*)	Mm00805062_m1
P2X purinoceptor 7 (*P2rx7*)	Mm01199500_m1

3.2.9. Luciferase Assay

To validate the prediction of gene target specificity for fhe-miR-125b-5p we performed a Luciferase assay. The predicted binding sites for four murine genes (*Stat3*, *Hif1a*, *Pin1* and *Runx1*), along with 50–100 nucleotides of flanking sequences at both the 5′ and 3′ ends, were synthesized (Table 3.3) and cloned into the PsiCheck-2 vector (Promega) by GenScript Biotech (Singapore). For *Hif1a* and *Stat3*, a single binding site was included, while three binding sites were incorporated for *Pin1* and two for *Runx1*. To validate the luciferase assay, psiCheck-2 vector harbouring *Pdcd4* binding site for mmu-miR-21-5p (Thermo Fisher Scientific), obtained from a previously published study [279], was employed as a positive control. The resulting plasmids were transformed into Max Efficiency DH5α *E. coli* cells (Invitrogen, Cat. No. 18258-012) according to the manufacturer's instructions. Briefly, 50 µL of competent *E. coli* cells were thawed on ice and mixed with 10 ng of the plasmid DNA. The cells and plasmid were incubated on ice for 30 minutes, followed by heat shock at 42 °C for 30 seconds. After incubation on ice for 2 minutes, the cells were resuspended in 900 µL of Super Optimal broth with Catabolite repression (SOCs) medium (Thermo Fisher Scientific) and incubated at 37 °C for 1 h with shaking at 225 rpm. The transformed cells were then plated on LB agar plates containing ampicillin (100 µg/mL) and incubated overnight at 37 °C. Individual colonies were picked the following day and cultured in 3 mL of LB broth with ampicillin for plasmid amplification at 37 °C, shaking at 220 rpm overnight. Plasmids were purified using the GeneJet Plasmid Miniprep Kit (Thermo Fisher Scientific) following the manufacturer's instructions.

HEK293 cells were seeded at a density of 4×10^4 cells per well in a 24-well plate in Dulbecco's Modified Eagle Medium (Gibco) supplemented with 10% v/v heat-inactivated FBS (Gibco). Cells were incubated for three days to reach 60–70% confluency. Transfection was carried out using Lipofectamine 3000 (Thermo Fisher Scientific) according to the manufacturer's instructions. Each well was co-transfected with 75 ng of PsiCheck-2 plasmid containing the gene target sites (as detailed

in Table 3) in combination with 20 pmol of fhe-miR-125b-5p Canonical or IsomiR mimic, or mmu-miR-23a-3p as a mimic control. Plasmid-only transfected cells and non-transfected cells were included as negative controls.

The Dual-Luciferase Reporter Assay System (Promega, Australia) was employed to measure gene target site expression, following the manufacturer's protocol. After 24 hours, cells were lysed using Passive Lysis Buffer, and Firefly and Renilla luciferase activities were quantified on the Tecan Plate Reader M200 (Tecan, Switzerland) in luminescence mode, with an integration time of 5000, a settle time of 500 and no attenuation. The luciferase activity was calculated as the ratio of Renilla to Firefly luminescence (Van Etten et al., 2013).

Table 3.3. Cloned 3′ UTR regions of predicted fhe-miR-125b-5p target genes in psi-Check-2 vector for luciferase reporter assays.

Gene name	Transcript ID (ENST)	*Target start position	*Target sequence	Start position of cloned 3' UTR	Total cloned 3' UTR (bp)
Stat3	ENSMUST00000127638.8	1590	GGGGCTGGTGTTGTACCTCAGGGGC	1490	225
Hif1a	ENSMUST00000021530.8	1582	CAAGAGTTTTCCGCGCTCTCAGGGA	1482	225
Pin1	ENSMUST00000034689.8	182	AGGGCAGTGGGGATGGGGAGGCCCCCAGGCTCAGGGGG	132	382
		340	CAGCAACTCAGCCTCAGGGT		
		443	TGAGGTGTGGGGCCCTTGTCTCAGGGA		
Runx1	ENSMUST00000023673.14	2279	AGGCAGTATTTAGTCTCAGA	2229	864
		3022	AGGGACATTCGGTCTTAGGGA		

*Predicted target start position and target sequence for canonical fhe-miR-125b-5p is show

3.2.10. Ago2 pulldown assay

3.2.10.1. Ago2 immunoprecipitation

Mouse macrophages (RAW264.7 cell line) were seeded at 9 x 10^5 cells per well of a 6 well plate. Cells were cultured in RPMI 1640 Medium (Gibco) supplemented with 10% heat-inactivated FBS (Gibco) and maintained at 37 °C with 5% CO_2.The following day cells were transfected with fhe-miR-125b canonical and isomiR mimics as described in Section 3.2.3. After 24 h, Ago2-bound miRNAs within the macrophages were isolated using the MagCapture™ microRNA Isolation Kit, Mouse Ago2 (Cat # 297-74201, FUJIFILM Wako Pure Chemical Corporation), according to the manufacturer's instructions. To ensure the recommended number of cells for the Ago2 pulldown assay, samples from five wells were pooled together to create one sample. In total, three of these replicates per mimic were prepared. Cells were lysed in the provided lysis buffer, and endogenous Ago2 complexes were immunoprecipitated using anti-mouse Ago2 antibody-coated magnetic beads.

3.2.10.2. Quantification of Ago-bound miRNAs

RNA bound to Ago2 was eluted from the Ago2 immunoprecipitated beads using Elution Solution II in the one-step elution method. The concentration of eluted miRNAs was quantified using the Qubit™ microRNA Assay Kit (Thermo Fisher Scientific). For each sample, 4 ng of miRNA was subjected to cDNA synthesis with sequence-specific stem-loop RT primers for the Canonical and IsomiR fhe-miR-125 as described in Section 3.2.7 above. Primers to amplify endogenous mouse miR-21(TaqMan Assay ID: 00397), were included in each reaction as an internal control for miRNA loading, and qPCR was performed as described in Section 3.2.7. The relative enrichment of each miRNA variant in the Ago2-bound fraction was calculated using the comparative Cq ($^{\Delta\Delta}$Cq) method and normalized to miR-21 levels.

3.2.10.2. Western blot confirmation of Ago2 in immunoprecipitated fractions

Following RNA elution, beads were resuspended in 40 µL PBS and stored at −20 °C. For protein elution, 13 µL beads from each of three replicate samples were pooled (39 µL total) in PBS, vacuum concentrated to 14 µL and then mixed with 1 µL 1 M DTT and 4 µL 4× LDS sample buffer (Bolt, Invitrogen). Samples were heated at 80 °C for 3 min, vortexed, centrifuged, and the supernatant collected.

Proteins were separated on 4-12% Bis-Tris gels (Invitrogen) using MES SDS running buffer (Invitrogen) at 200 V for 35 min. Novex Sharp pre-stained protein ladder (Invitrogen) was included

for size estimation. Proteins were transferred to a 0.2 μm nitrocellulose membrane (Bio-Rad) using the Trans-Blot Turbo system (Bio-Rad) with the manufacturer's mini-gel program.

Membranes were blocked overnight at 4 °C with 1% BSA in PBS and incubated for 2 h at room temperature with anti-mouse Ago2 monoclonal antibody (FUJIFILM Wako Pure Chemical Corporation, 014-22023) 1:500 in 1% BSA in 1x PBS. After three washes in PBST (1x PBS + 0.1% Tween-20), membranes were incubated for 1 h at room temperature with HRP-conjugated anti-mouse IgG secondary antibody (Sigma, A4416) 1:5000 in 1% BSA/PBS. Following four PBST washes and a final PBS rinse, proteins were detected using SuperSignal West Dura chemiluminescent substrate (Thermo Fisher Scientific) according to the manufacturer's instructions.

3.2.11. Statistical analysis

Results were analysed using Graphpad Prism software (version 8). Comparisons between treatment groups were made using one-way ANOVA unless mentioned otherwise. Differences were considered significant when $p \leq 0.05$.

3.3. Results

3.3.1. Peritoneal macrophages of *Fasciola hepatica* infected mice are enriched with parasite-derived miRNAs with peak abundance at 18 hours post infection

To identify parasite-derived miRNAs in peritoneal macrophages of *Fasciola hepatica* infected mice, small RNA sequencing was performed, yielding an average of 21 million reads per sample. Of these, approximately 61% aligned to known mouse miRNAs, while the remaining unaligned reads (~39%) were mapped to the *F. hepatica* miRNA reference library using a no-mismatch alignment criterion. Across the three infection time points (6 h, 18 h, and 5 days post-infection), an average of 27 reads (0.0003% of the unaligned reads) aligned to the *F. hepatica* reference library and revealed a total of 29 *F. hepatica*-specific miRNAs present in macrophages from infected mice (Table 3.4). Of these, 28 were absent in macrophages from uninfected mice (0 h) supporting their parasitic origin. One miRNA, fhe-Novel-11-5p, was unexpectedly detected in the uninfected group (Table 3.4). However, as this sequence perfectly aligned with the mouse genome, its origin could not be confidently attributed to the parasite (Chapter 2; Section 2.3.3), and it was therefore excluded from further analysis.

Among the 28 parasite-specific miRNAs, 8 were detected at 6 hours, 22 at 18 hours, and 3 at 5 days post-infection (Table 3.4). This temporal pattern aligns with our previous study, which profiled miRNA expression at 6 h, 12 h, 24 h, 3 days, and 5 days post-infection, and reported peak levels at 12 hours [63]. However, the inclusion of the 18 h time point in the present study was primarily responsible for revealing a broader repertoire of parasite-derived miRNAs (28 versus 10 in the previous study). The peak abundance of the worm miRNAs at 18 hours (Table 3.4), coincides with the parasite's active migration through the peritoneal cavity. By day 5, the flukes have penetrated the liver capsule, likely reducing their interaction with peritoneal macrophages as evidenced in the reduced detection of miRNAs at this time point.

Notably, six of the *F. hepatica*-derived miRNAs shared identical seed sequences with mouse orthologues, suggesting the potential for functional mimicry of host miRNAs in macrophages. While most were conserved across other helminth species, six were unique to *F. hepatica* (Table 3.4), indicating that both conserved and species-specific miRNAs may contribute to host gene regulation. Moreover, 25 of these miRNAs, including the most abundant, have been previously detected in *F. hepatica* extracellular vesicles (EVs) [78, 152], supporting the concept that EVs act as the main delivery route for parasite miRNAs into host immune cells.

Members of the miR-125 family, highly conserved across mammals and helminths, were the most abundant worm-derived miRNAs in host macrophages, with fhe-miR-125a-5p and fhe-miR-125b-5p together representing 27% of all exogenous miRNA reads (Table 3.4). At 18 h post-infection, fhe-miR-125a reached the highest abundance, whereas our earlier study found fhe-miR-125b to be most abundant at 12 h post-infection. Their consistently high expression underscores *F. hepatica's* exploitation of this conserved miRNA family to modulate the host innate immune response, consistent with our prior finding that fhe-miR-125b can mimic host miR-125b in suppressing pro-inflammatory response to LPS in macrophages.

Table 3.4. *F. hepatica*-derived miRNAs were enriched in the peritoneal macrophages of infected mice.

miRNA/count	0 h (n=5)	6 h (n=5)	18 h (n=4)	Day 5 (n=5)	Total count	Present in EV[b]	Identical seed sequence in mouse miRNA
fhe-Novel-11-5p	[a]14-34	13-32	5-24	5-30	370	Yes	No
fhe-miR-125a-5p	0-0	0-0	3-7	0-0	20	Yes	Yes
fhe-miR-71a-5p	0-0	0-3	0-5	0-1	14	Yes	No
fhe-miR-125b-5p	0-0	0-1	1-6	0-0	11	Yes	Yes
fhe-miR-277b-3p	0-0	0-2	0-7	0-0	11	Yes	No
fhe-miR-71c-5p	0-0	0-0	0-2	0-0	5	Yes	No
fhe-miR-96-5p	0-0	0-0	0-5	0-0	5	Yes	Yes
fhe-miR-281-3p	0-0	0-0	0-4	0-0	5	Yes	No
fhe-miR-2162-3p	0-0	0-0	0-3	0-0	5	Yes	No
fhe-miR-3479a-3p	0-0	0-0	0-3	0-0	5	Yes	No
fhe-miR-71b-5p	0-0	0-1	0-2	0-0	4	Yes	No
fhe-miR-61-3p	0-0	0-0	0-3	0-0	3	Yes	No
fhe-miR-219-5p	0-0	0-2	0-1	0-0	3	Yes	Yes
fhe-bantam-3p	0-0	0-0	0-1	0-0	2	Yes	No
fhe-miR-2e-5p	0-0	0-0	0-2	0-0	2	Yes	No
fhe-miR-9-5p	0-0	0-0	0-1	0-0	2	Yes	Yes
fhe-miR-12-5p	0-0	0-0	0-2	0-0	2	Yes	No
fhe-miR-277a-3p	0-0	0-0	0-1	0-1	2	Yes	No
fhe-Novel-64-5p	0-0	0-0	0-2	0-0	2	Yes	No
fhe-miR-7a-5p	0-0	0-0	0-1	0-0	1	Yes	Yes
fhe-miR-87-3p	0-0	0-0	0-1	0-0	1	Yes	No
fhe-miR-3479b-5p	0-0	0-0	0-1	0-0	1	Yes	No
fhe-miR-281-5p	0-0	0-0	0-1	0-0	1	Yes	No
fhe-Novel-14-3p	0-0	0-0	0-1	0-0	1	No	No
fhe-Novel-35-3p	0-0	0-0	0-0	0-1	1	No	No
fhe-Novel-78-3p	0-0	0-1	0-0	0-0	1	No	No
fhe-Novel-78-5p	0-0	0-0	0-1	0-0	1	Yes	No
fhe-Novel-100-5p	0-0	0-0	0-1	0-0	1	Yes	No
fhe-Novel-103-5p	0-0	0-1	0-0	0-0	1	Yes	No

[a]The data is presented as the range of total read counts for each miRNA across n=5 individual RNA samples (each sample prepared from cells pooled from 5 mice) at each time point: 0 hour (h): non-infected; 6 h,and day 5 post infection, except 18h where n=4.

[b]*F. hepatica* extracellular vesicle (EV) miRNA data were obtained from [152] and [78]. Cells highlighted in pink indicate the presence of the corresponding *F. hepatica miRNA* at the specified time point.

3.3.2. Worm-derived miRNAs in the peritoneal macrophages of *Fasciola hepatica* infected mice are predominantly isomiRs

Analysis of the worm miRNA sequences, revealed notable length heterogeneity (Table 3.5). Only 28% of the worm miRNAs within the macrophages were detected in their canonical form, with the majority appearing as length variants or isomiRs (Figure 3.1; Table 3.5). The most prevalent type, representing 40% of the worm miRNAs in macrophages, was 3' trimmed isomiRs. IsomiRs trimmed at the 5' or both ends were also present, albeit at lower levels (11%) (Figure 3.1; Table 3.5). Among the worm-derived miRNAs, fhe-miR-71a-5p had the greatest number of variants, with four 3' end variants in addition to the canonical form (Table 3.5). Notably, 85% of fhe-miR-125a-5p was identified as an isomiR with a templated addition at the 3' end, i.e. the extra nucleotides at the 3' end match the genomic sequence, while fhe-miR-125b-5p was exclusively present as a 3' trimmed isomiR (Table 3.5).

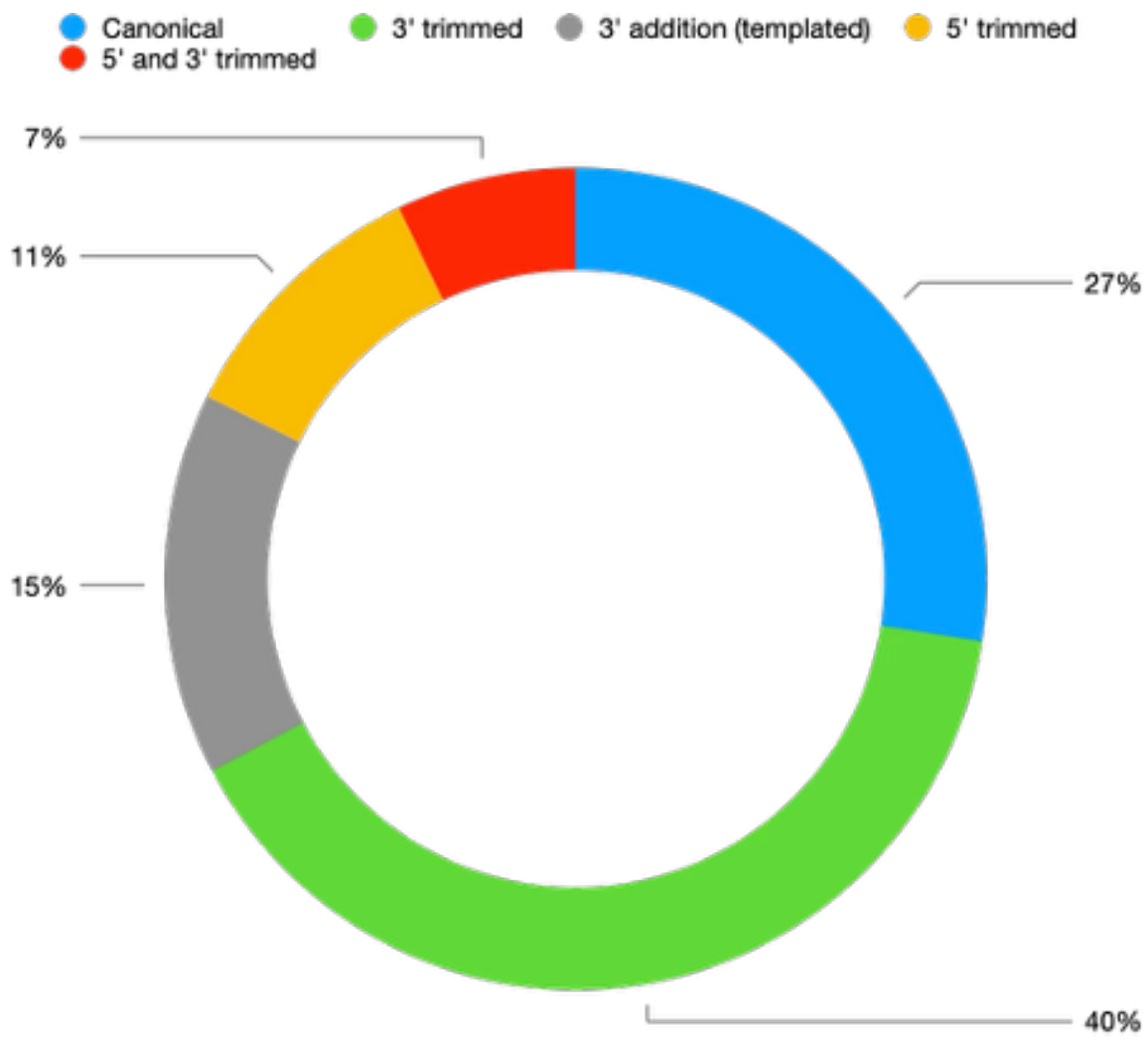


Figure 3.1. Worm-derived miRNAs detected in the peritoneal macrophages of mice infected with F. hepatica were predominantly isomiRs. *The pie chart depicts the proportion of the Fasciola-derived miRNA isoforms in peritoneal macrophages of infected mice collectively over the three different infection time points: 6 h (n = 5), 18 h (n = 4) and 5 days (n = 5) post infection.*

Table 3.5. The *Fasciola hepatica*-derived miRNAs in mouse macrophages during infection displayed length heterogeneity.

F. hepatica miRNA	miRNA sequence	Length (nt)[a]	IsomiR form	Read counts[b]	% of total count[c]
fhe-miR-125b-5p	CCCCTGAGACTGATAATTGCT	21	3' trimmed	11	100%
fhe-miR-125a-5p	TCCCTGAGACCCTAGAGTTTC	21	Canonical	3	15%
	TCCCTGAGACCCTAGAGTTTCC	22	3' extension (templated)	17	85%
fhe-miR-277b-3p	AAAATGCATCATCTACCCGAGA	22	Canonical	7	63%
	AAAATGCATCATCTACCCGAG	21	3' trimmed	4	36%
fhe-miR-71a-5p	TGAAAGACGATGGTAGTGAGATG	23	Canonical	2	14%
	TGAAAGACGATGGTAGTGA	19	3' trimmed	5	36%
	TGAAAGACGATGGTAGTGAGA	21	3' trimmed	4	29%
	TGAAAGACGATGGTAGTGAGAT	22	3' trimmed	2	14%
	TGAAAGACGATGGTAGTGAG	20	3' trimmed	1	7%
fhe-miR-61-3p	TGACTAGAAAGTGCACTCACTT	22	5' trimmed	3	100%
fhe-miR-71c-5p	TGAAAGACATGGGTAATGAGGT	22	Canonical	1	20%
	TGAAAGACATGGGTAATGAG	20	3' trimmed	4	80%
fhe-miR-281-3p	TGTCATGGAGTTGCTCTCTACA	22	5' trimmed	3	60%
	TGTCATGGAGTTGCTCTCTAC	21	5' and 3' trimmed	1	20%
	TGTCATGGAGTTGCTCTCTA	20	5' and 3' trimmed	1	20%
fhe-miR-96-5p	CTTGGCACTTTGGAATTGTCA	21	Canonical	5	100%
fhe-miR-2162-3p	TATTATGCAACATTTCACTCT	21	5' trimmed	5	100%
fhe-miR-3479a-3p	GTATTGCACTTTCCTTCGCCTTA	23	Canonical	1	20%
	TATTGCACTTTCCTTCGCCTT	21	5' and 3' trimmed	4	80%
fhe-miR-71b-5p	TGAAAGACTTGAGTAGTGAG	20	Canonical	2	50%
	TGAAAGACTTGAGTAGTGA	19	3' trimmed	2	50%
fhe-miR-219-5p	TGATTGTCCATTCGCATTTCTTG	23	Canonical	1	33%
	TGATTGTCCATTCGCATTTCTT	22	3' trimmed	2	67%
fhe-bantam-3p	TGAGATCGCGATTAAAGCTGGT	22	Canonical	1	50%
	TGAGATCGCGATTAAAGCTGG	21	3' trimmed	1	50%
fhe-miR-2e-5p	TACCAACTTAGACTGCGTTAT	21	Canonical	2	100%
fhe-miR-9-5p	TCTTTGGTTATCAAGCAGTATG	22	Canonical	1	50%
	TCTTTGGTTATCAAGCAGTAT	21	3' trimmed	1	50%
fhe-miR-12-5p	TGAGTATTTCATCAAGTAGTGA	22	Canonical	2	100%
fhe-miR-277a-3p	TAAATGCATTTTCTGGCCCG	21	5' trimmed	1	50%
	TAAATGCATTTTCTGGCCC	19	5' and 3' trimmed	1	50%
fhe-Novel-64-5p	TCCCCGATCAAAGATGCAAG	20	3' trimmed	2	100%
fhe-miR-87-3p	GTGAGCAAAGTTTCAGGTGTG	21	5' and 3' trimmed	1	100%
fhe-miR-7a-5p	TGGAAGACTGGTGATATGTTGT	22	3' trimmed	1	100%
fhe-miR-281-5p	AGGAGGGCAATTTTATGACTT	21	3' trimmed	1	100%
fhe-miR-3479b-5p	GATTGCACTACTCATAGCCTTC	22	Canonical	1	100%
fhe-Novel-14-3p	TTTGGAAAAGTAGGTTGTGC	20	3' trimmed	1	100%
fhe-Novel-35-3p	AGAAGGACGCCGCGAGAGAG	20	3' trimmed	1	100%
fhe-Novel-78-3p	AAAGTGAACACTGGTGGATG	20	3' trimmed	1	100%
fhe-Novel-78-5p	ATTTATCGGAGTTCAATAA	19	3' trimmed	1	100%
fhe-Novel-100-5p	AACACAGCGTAGTCGAAATC	20	Canonical	1	100%
fhe-Novel-103-5p	TGACCGTACCACTGAGTGACCC	22	Canonical	1	100%

[a]Shown are the sequence and length of each isoform in nucleotides (nt)

[b]The total read counts pooled across the three infection time points: 6 h (n = 5), 18 h (n = 4), and 5 days (n = 5) post-infection

[c]The percentage of each isoform relative to the total reads for the corresponding miRNA

[d]The rows representing the canonical miRNA sequences are highlighted in pink.

3.3.3. *Fasciola hepatica* selectively exports isomiRs into host peritoneal macrophages

To determine the likelihood that *F. hepatica* was actively expressing isomiRs to mediate a biological effect in host cells, sequences from NEJs, Juvenile, and adult worms [231] and their EVs [78, 152] were surveyed for the presence of the four most abundant *F. hepatica*-derived miRNAs that had been found in the mouse macrophages: fhe-miR-125b-5p, fhe-miR-125a-5p, fhe-miR-71a-5p, and fhe-miR-277b-3p (Table 3.4). This comparison revealed that the isomiRs observed in mice host cells were (i) also expressed across the developmental stages of the worm, (Figure 3.2A-D; Table 3.6) and (ii) were present in *F. hepatica*-derived EVs (Table 3.6). This finding supports the notion that isomiRs are being transported from the parasite to host cells, rather than being generated *de novo* within the host cells.

For all four miRNAs, the 3' trimmed isomiRs that were 21 nt or shorter, were more highly expressed in the NEJs as compared to the juvenile parasites (Figure 3.2A-D), which agrees with our previous observation that isomiRs are predominant in NEJs as compared to juvenile or adult worms [274]. The most prevalent isoforms of fhe-miR-125a-5p and fhe-miR-277b-3p were broadly comparable in abundance across the worm life stages, worm-derived EVs, and infected macrophages. In both cases, the top two isoforms in worms and NEJ-EVs were also present in macrophages, with the most abundant form in worms also the most abundant in host cells (Table 3.6).

For fhe-miR-71a-5p, the three most abundant variants in the worm life stages and EVs were detected in macrophages (Table 3.6). Of the five isoforms found in host cells, four corresponded to the top-expressed isoforms in NEJs (and the other worm life stages), while the most abundant isoform in macrophages was the least abundant in worms and absent from NEJ-EVs. However, the interpretation of the NEJ-EV dataset should be cautious, as it lacks biological replicates. Surprisingly, two 3′-modified isomiRs of fhe-miR-71a-5p, differing from the canonical sequence by a single nucleotide, were detected in worm life stages and adult EVs (Fig 3.2D). Although Bowtie2 was run with stringent mapping parameters, alignments with a single-nucleotide difference could be retained if the score met the threshold.

Notably, fhe-miR-125b-5p was predominantly expressed as the canonical miRNA in NEJs (and other life stages) (Figure 3.2A; Table 3.6) and EVs yet appeared exclusively as a 3′-trimmed isomiR in murine macrophages (Table 3.4). This discrepancy in isomiR profile, also observed for fhe-miR-71a-5p, suggest that *F. hepatica* selectively exports specific isomiRs to host cells, potentially to modulate the host immune response in favour of the parasite.

Table 3.6. Reported abundance of the four selected *F. hepatica* miRNA isomiRs across different worm life stages. Sequence abundance is visualized as a heat map using a red colour scale for each sample.

miRNA	Sequence	Length (nt)	[231, 274]			[78]		[152]		Infected mouse Mφ
			NEJ*	JUV*	AD*	AD EV	NEJ EV	AD EV1	AD EV2	
fhe-miR-125b-5p	CCCCTGAGACTGATAATTGCTC	22	71.54%	90.74%	80.00%	82.81%	96.15%	90.42%	90.42%	
	CCCCTGAGACTGATAATTGCT	21	26.68%	8.49%	18.44%	14.89%	2.56%	8.78%	8.78%	100%
	CCCCTGAGACTGATAATTGC	20	1.21%	0.29%	0.91%	2.04%	1.28%	0.00%	0.29%	0.00%
fhe-miR-125a-5p	TCCCTGAGACCCTAGAGTTTCC	22	43.89%	48.90%	46.79%	50.00%	20.68%	73.00%	71.15%	85%
	TCCCTGAGACCCTAGAGTTTC	21	27.45%	39.00%	26.93%	50.00%	73.96%	21.00%	23.31%	15%
	TCCCTGAGACCCTAGAGTTT	20	24.08%	9.34%	20.40%	0.00%	4.57%	5.31%	5.10%	0.00%
	TCCCTGAGACCCTAGAGT	18	2.66%	1.37%	3.76%	0.00%	0.32%	0.00%	0.10%	0.00%
fhe-miR-71a-5p	TGAAAGACGATGGTAGTGAGAT	22	44.29%	64.32%	50.49%	54.61%	33.00%	25.06%	21.21%	14%
	TGAAAGACGATGGTAGTGAGA	21	24.79%	11.94%	18.63%	21.77%	33.00%	14.44%	16.35%	29%
	TGAAAGACGATGGTAGTGAGATG	23	13.85%	13.68%	16.75%	19.68%	33.00%	37.16%	39.96%	14%
	TGAAAGACGATGGTAGTGAG	20	7.96%	2.52%	3.99%	0.46%	0.00%	16.90%	16.04%	7%
	TGAAAGACGATGGTAGTGAGATA	23	2.52%	2.63%	3.50%	0.75%	0.00%	0.71%	0.49%	0.00%
	TGAAAGACGATGGTAGTGAGATT	23	2.80%	2.24%	2.72%	2.15%	0.00%	1.58%	1.11%	0.00%
	TGAAAGACGATGGTAGTG	18	1.65%	1.42%	2.10%	0.02%	0.00%	0.22%	0.19%	0.00%
	TGAAAGACGATGGTAGTGA	19	1.48%	0.51%	1.09%	0.05%	0.00%	3.02%	3.57%	36%
fhe-miR-277b-3p	AAAATGCATCATCTACCCGAGA	22	64.57%	70.54%	70.94%	16.70%	60.77%	56.24%	62.39%	63%
	AAAATGCATCATCTACCCGAG	21	24.62%	17.10%	14.61%	33.33%	27.85%	15.78%	13.57%	36%
	AAAATGCATCATCTACCCGA	20	6.39%	8.41%	9.39%	33.33%	10.61%	23.19%	20.24%	0.00%
	AAAATGCATCATCTACCCG	19	4.11%	3.55%	4.75%	16.67%	0.69%	4.45%	3.25%	0.00%

*Averages of three biological replicates are shown for each life stage; NEJ, newly excysted juvenile; JUV, juvenile; AD, adult; EV, extracellular vesicles; Mφ, macrophage; IsomiRs are reported as percentage of the total counts for each individual miRNA. Only isomiRs comprising more than 1% of the total count in a given sample are included. The canonical sequences are highlighted in yellow.

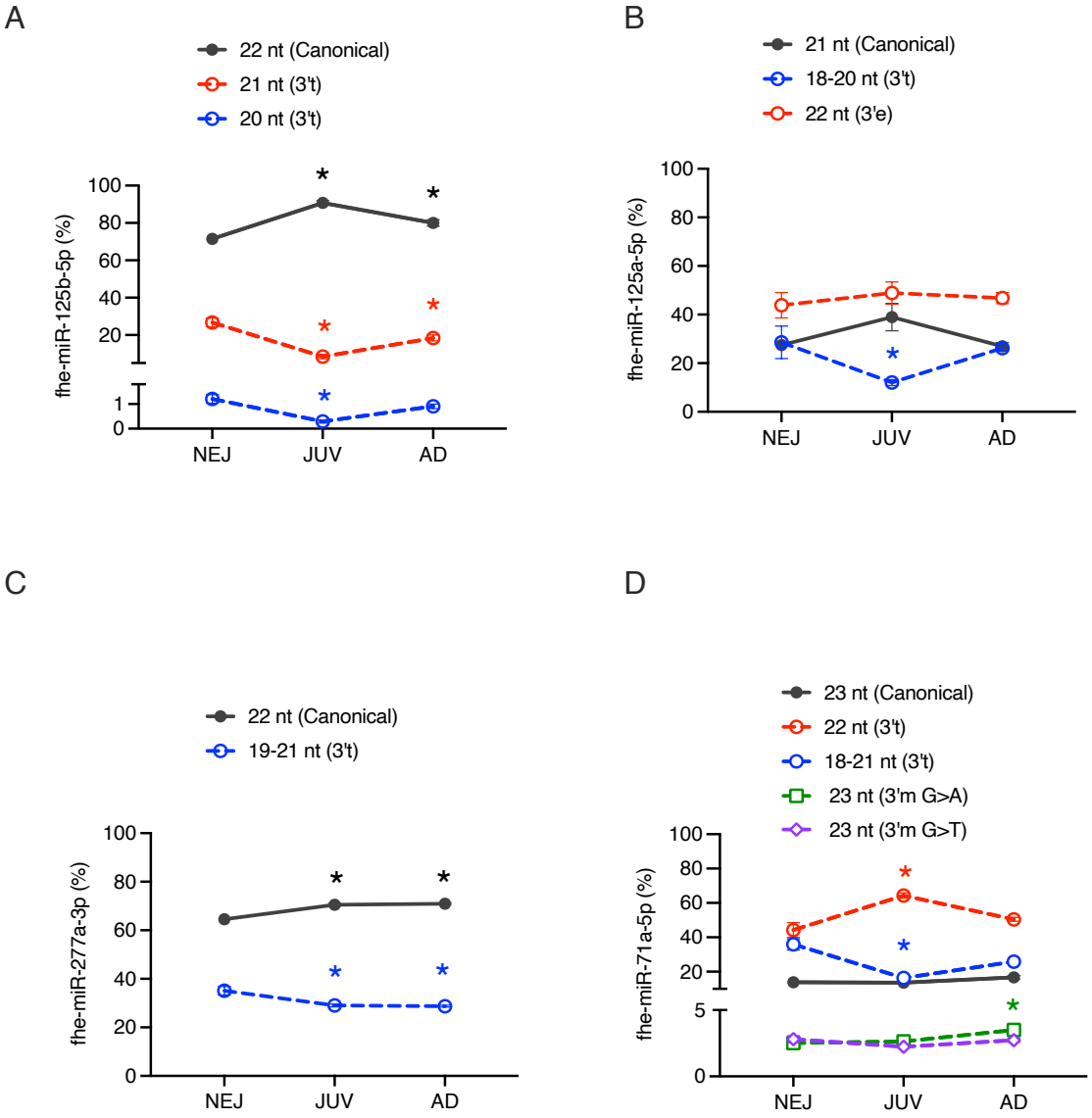


Figure 3.2. The most abundant worm-derived miRNAs in macrophages had increased 3' trimmed isomiRs expression in the NEJs, as compared to juvenile (JUV) or adult (AD) worms. *IsomiRs that accounted for more than 1% of the total read count in an individual sample are shown (n = 3 biological replicates per life stage). Canonical sequences are shown as black solid lines, and isomiRs as coloured dotted lines (t, trimmed; e, extension; m, modification). The Y-axis shows the percentage of each isoform relative to the total read count for the corresponding miRNA. Data are presented as mean ± SEM for individual replicates. Statistical analysis was performed using one-way ANOVA; asterisks (*) in the colour of the isoforms indicate a significant p value (< 0.05) compared with the NEJ life stage for that specific isoform.*

3.3.4. The 3’ trimmed fhe-miR-125b-5p isomiR is predicted to have a reduced binding affinity for host gene targets as compared to the canonical miRNA

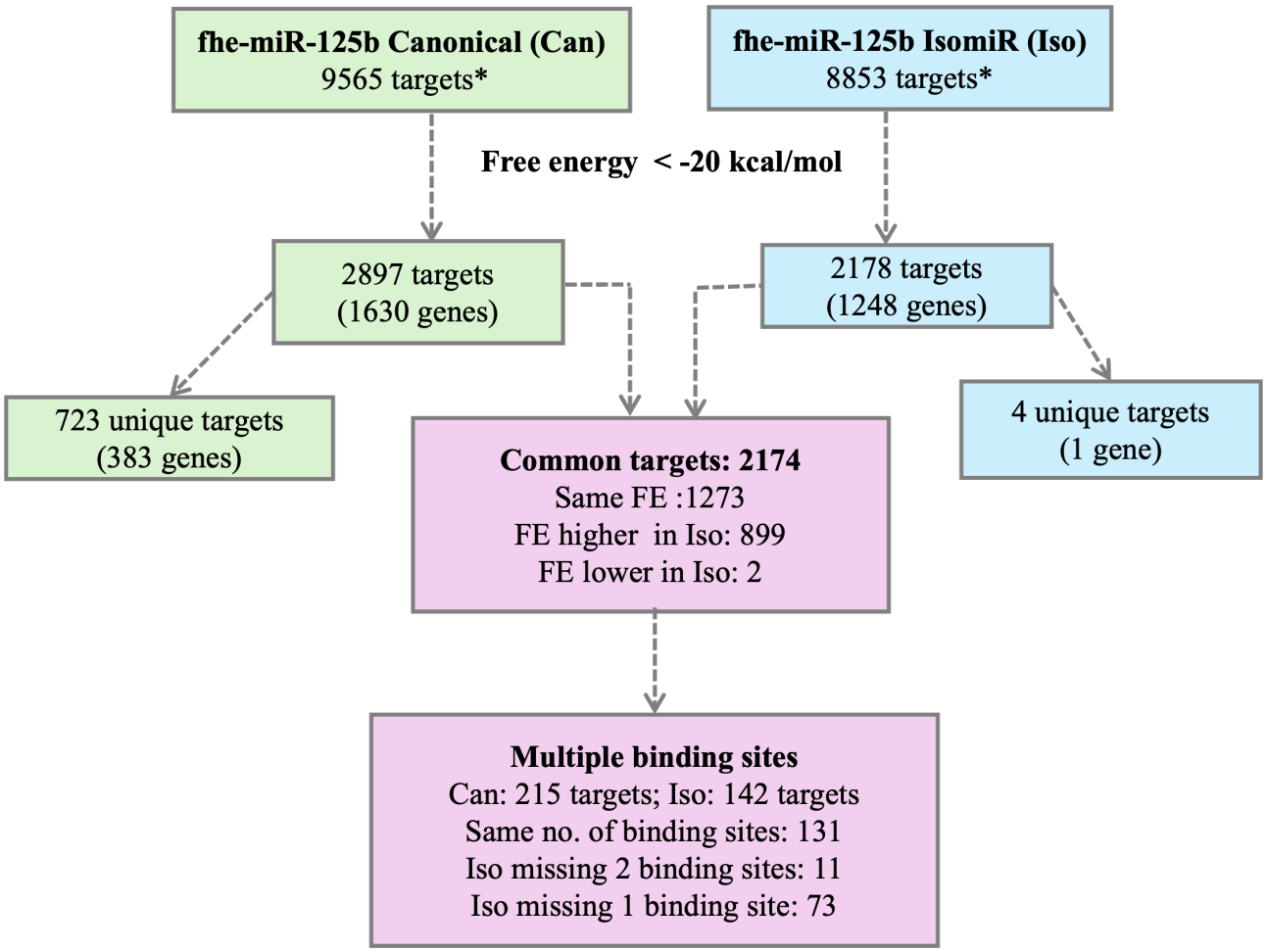
Since fhe-miR-125b-5p was exclusively present as an isomiR in host macrophages (Table 3.4) and given the previously established role for this miRNA the modulation of mammalian macrophages [63], it was selected for further characterisation. This analysis examined several known shifts in isomiR functionality as compared to their canonical counterparts, i.e. altered target specificity and binding affinity, altered efficiency in gene regulation, and altered interactions with host Ago2.

To assess whether the missing nucleotide at the 3′ end of the fhe-miR-125b-5p isomiR alters binding affinity to host target genes, target prediction was performed for both the canonical and isomiR sequences using miRanda [276], one of the earliest and most widely used miRNA target prediction tools. miRanda not only evaluates sequence complementarity but also incorporates evolutionary conservation of target sites, tolerates mismatches such as, G:U wobble pairs and gaps to detect biologically relevant targets without perfect complementarity, and, importantly, calculates the minimum free energy (FE) of miRNA-mRNA duplex formation, a key parameter for quantifying changes in binding strength.

The initial miRanda prediction identified 9,565 targets for the canonical fhe-miR-125b and 8,853 for the 3’ trimmed isomiR (Fig 3.3; Supplementary Table 3.1a and b). To compare binding strength, we focused on predicted FE values, applying the recommended −20 kcal/mol threshold to define high-confidence target sites, with more negative values indicating stronger predicted binding. This filter yielded 2,897 murine targets for the canonical sequence and 2,178 for the isomiR, representing a 25% reduction (Fig 3.3; Supplementary Table 3.1c and d). Predicted targets were distributed across multiple mRNA 3′ UTR isoforms, with several transcripts containing more than one miRNA binding site.

At the gene level, the canonical sequence was predicted to target 1,630 murine genes, compared with 1,248 for the isomiR (Fig 3.3; Supplementary Table 3.1e). Following application of the FE cutoff < -20 kcal/mol, only one gene (*Cpsf4*; four transcripts with the same binding sites) was uniquely predicted as a target for the isomiR, with an FE of −21.02 compared to −17.89 for the canonical sequence. All other isomiR-predicted genes were also identified as gene targets for the canonical miRNA. In addition to the predicted reduced affinity of the isomiR for 383 gene targets (Fig 3.3; Supplementary Table 3.1f), for some of the common genes, the FE cut-off also resulted in the a reduced affinity for one or more binding sites within the same gene (Fig 3.3; Supplementary Table 3.1g). Moreover, of the common 2174 transcript binding sites, 1273 target sites (58.6%) had the same

FE energy score, 899 target sites (41.4%) were predicted to have greater FE for isomiR; and only two transcripts (both belonging to the same gene, *Adamts17*, for the same binding site) had lower FE compared to the canonical miRNA (Fig 3.3; Supplementary Table 3.1h). Collectively, these results suggest that the loss of the 3′ nucleotide in the fhe-miR-125b isomiR primarily reduces its affinity for host targets rather than altering its target repertoire.



* Target counts include multiple mRNA 3′ UTR isoforms for the same gene, with one or more unique binding sites per transcript.

Figure 3.3. Application of the −20 kcal/mol free energy cut-off on the miRanda predicted target sites indicated that the 3'-trimmed fhe-miR-125b isomiR has reduced binding capacity for host targets compared to the canonical sequence*. The flow chart outlines the analysis workflow for predicted targets. Following free energy (FE) filtering, isomiR retained fewer targets than the canonical sequence. Among shared targets, 41% had higher FE values than the canonical miRNA, and for some transcripts with multiple binding sites, the isomiR lacked up to two binding sites.*

Gene enrichment analysis of the 383 gene targets apparently lost due to the free energy cut-off of < -20 kcal/mol (Supplementary Table 3.1f) revealed that these genes are involved in cellular responses such as cell communication, behaviour, localisation, and response to stimulus (Figure 3.4; Table 3.7). However, when the enrichment profile of the canonical and isomiR predicted targets were compared, similar pathways emerged in both, suggesting that although weaker binding efficiency may reduce the number of direct gene targets, the overall functional impact on host cellular processes may remain (Supplementary Table 3.2).

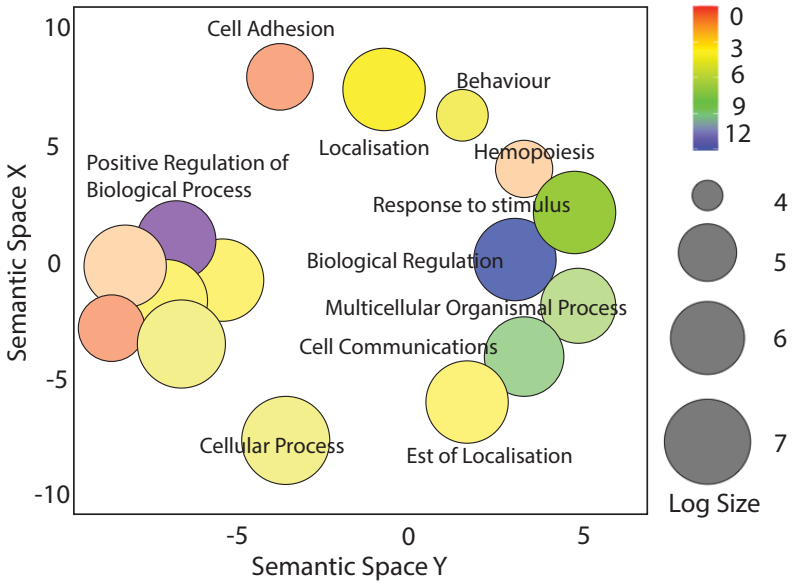


Figure 3.4. The gene targets of fhe-miR-125b-5p isomiR that were excluded after applying the FE cutoff (< −20 kcal/mol) were enriched in pathways related to host responses, including cell communication, behaviour, localisation, and response to stimulus. *Gene enrichment analysis was performed using g:Profiler [277] on targets that were predicted to have diminished binding capacity for isomiR due to the application of the FE cutoff < -20. GO terms for biological processes with P value adjusted to < 0.05 were used to graph a semantic similarity plot using Revigo [278].*

3.3.5. The fhe-miR-125b-5p canonical and isomiR sequences regulated the LPS-stimulated pro-inflammatory response in macrophages with equal efficacy

As mentioned, it has been hypothesised that *F. hepatica* miRNAs are secreted by the parasite to regulate the ability of host macrophages to mediate a classical protective, pro-inflammatory (M1-like) response to prevent the expulsion of NEJs as they migrate from the intestine to the liver (as described in Chapter 1). The diminished range of predicted gene targets for the fhe-miR-125b-5p isomiR, suggested a reduced functionality as compared to the canonical miRNA. While this was surprising given the evidence that the parasite selects isomiRs to interact with host macrophages, it may reflect a need to fine-tune immune responses with more subtlety that would be mediated by the canonical fhe-miR-125b-5p.

To further explore this idea and to compare the efficacy of the isomiR to the canonical fhe-miR-125b-5p in the modulation of innate immune responses, transfected macrophages were assessed for the secretion of cytokines and for the expression of host genes under basal and pro-inflammatory conditions. Specifically, synthetic mimics of the isomiR and canonical miRNA were transfected into BMDMs that were then stimulated with the pro-inflammatory ligand bacterial LPS, after which cytokine production and gene expression were measured. As it was expected that fhe-miR-125b would suppress/regulate the proinflammatory response, BMDMs were also transfected with a synthetic mmu-miR-23a, a miRNA that is known to promote pro-inflammatory responses [280], thus serving as a comparative and functional control.

To understand the regulatory impact of transfection, a panel of seven host genes were selected from the list of predicted gene targets for the Fasciola isomiR and canonical fhe-miR-125b (Table 3.7; Supplementary Table 3.1). These targets were chosen as they have documented involvement in macrophage polarization and proinflammatory signalling (Table 3.7). Among these genes, *Stat3*, *Hif1a*, and *Il17r* were predicted to have reduced binding affinity (FE < -20 kcal/mol) for the isomiR compared to the canonical fhe-miR-125b. In addition, *Pin1* and *Runx1* were selected as both genes possessed three predicted binding sites for fhe-miR-125b, but with at least one site per gene predicted to have higher FE score for the isomiR as compared to the canonical sequence, suggesting a reduced binding affinity. *Nod1* and *P2rx7* were also included, as they were previously identified as predicted fhe-miR-125b targets and were found to be downregulated during the pre-hepatic phase of *F. hepatica* infection in the mouse model [56].

Table 3.7. Selection of predicted host target genes of fhe-miR-125b associated with macrophage M1 polarization and proinflammatory signalling.

Gene	Transcript ID	*Target Start	Target end	Can FE	Iso FE	Biological activity associated to M1 macrophage
Stat3	ENSMUST00000127638.8	1591	1613	-23.77	-19.3	Involved in macrophage polarization [281]
Hif1a	ENSMUST00000021530.8	1582	1606	-21.49	-18.37	Regulates M1 macrophage polarization [282]
Il17rd	ENSMUST00000035336.5	1455	1478	-22.95	N/A	Suppression enhances TLR-mediated inflammation [283]
Pin1	ENSMUST00000034689.8	340	362	-23.38	-23.38	Regulates *Stat3* [284]; Activates NLRP3 inflammasome [285]
		197	218	-24.16	-22.22	
		443	464	-20.91	-17.58	
Runx1	ENSMUST00000023673.14	3919	3939	-22.69	-20.77	Enhances TLR4-induced inflammation [286]
		3022	3043	-23.89	-21.94	
		2279	2300	-21.86	N/A	
P2rx7	ENSMUST00000100737.10	2735	2755	-23.89	-21.11	Stimulates several inflammatory processes [287, 288]
Nod1	N/A					Induces pro-inflammatory cytokine production [289]

*Target start site for the canonical fhe-miR-125b. Can: Canonical; Iso: IsomiR; FE: free energy; 'N/A' indicates target not identified in the miRanda prediction. Grey-shaded cells represent FE values > –20 kcal/mol.

Initially, the effect of transfection with the miRNA mimics on the induction of pro-inflammatory responses in macrophages was determined by the quantification of IL6 and TNF in the culture media following LPS stimulation. These cytokines are typical of an anti-pathogen M1 macrophage response and are evidently inhibited in peritoneal macrophages during the NEJ stage of infection with *F. hepatica* [183, 184]. In agreement with these observations, and consistent with the previous reported effect of fhe-miR-125b on mammalian macrophages, both IL6 and TNF secretion were reduced in macrophages transfected with the canonical miRNA sequence as compared to unstimulated cells (Figure 3.5) [63]. Despite the predicted reduced binding affinity for the fhe-miR-125b-5p isomiR, there was no significant difference in the inhibition of cytokine secretion in cells transfected with the isomiR as compared to the canonical miRNA. Although, the difference between the levels of TNF secreted by the cells transfected with the isomiR and the LPS stimulated non-transfected cells were more significant than that seen in the cells transfected with the canonical. As expected, transfection with the mmu-miR-23a mimic elevated the expression of both IL6 and TNF, further supporting the regulatory effect of both the canonical and isomiR fhe-miR-125b.

To next determine if there was a differential impact on the regulation of genes associated to inflammatory pathways between the canonical and isomiR, the expression of the selected panel of target genes was quantified in the transfected cells. For six of these genes, there was no evidence of regulation in unstimulated macrophages by either the canonical or isomiR mimics (Figure 3.6A-F). However, the basal expression of *P2rx7* in macrophages was significantly downregulated to the same extent by both the fhe-miR-125b canonical and isomer (Figure 3.6 G).

Under inflammatory conditions (LPS stimulation), the expression of *Stat3*, *Hif1a*, and *Nod1*, all known positive regulators of the LPS-induced TLR4 pathway [290-292] was significantly increased. Consistent with the regulation of IL6 and TNF secretion in macrophages, both the canonical and the isomiR fhe-miR-125b mimics significantly reduced the expression of *Stat3*, *Hif1a*, and *Nod1* with equal efficacy (Figure 3.7A-C). As before, transfection with the mmu-miR-23a mimic had no effect on the expression of these genes, which again, supports the conclusion that the fhe-miR-125b mimics are specifically regulating the expression of host genes.

Although the expression of *Il17rd* was also significantly increased in macrophages following stimulation with LPS, unexpectedly, the canonical fhe-miR-125b further increased the expression of this gene (Figure 3.7 D). While the isomiR fhe-miR-125b also appeared to elevate the expression of *Il17rd* induced by LPS, this change was not statistically significant ($p = 0.24$). Once again, and as expected, transfection with mmu-miR-23a had no observable effect on the expression of *Il17rd.*

The expression of the remaining three host genes, *Pin1*, and *P2rx7* was significantly reduced in macrophages in response to LPS stimulation, and *Runx1* also appeared downregulated, although not significantly ($p = 0.09$) (Figure 3.8). No further suppression was observed in the cells transfected with the Fasciola-derived miR-125b mimics or with mmu-miR-23a.

Comparable Cq values obtained from qPCR using specific TaqMan primers for both the canonical and isomiR forms of fhe-miR-125b-5p confirmed effective transfections (Figure 3.9). Additionally, LDH assays demonstrated that cytotoxicity across all treatment groups, including those transfected with either mimic, remained below 10% and was comparable to vehicle-treated controls (Figure 3.10). These findings confirm that the observed effects of fhe-miR-125b mimics on pro-inflammatory cytokines were not influenced by differences in transfection efficiency or cytotoxicity.

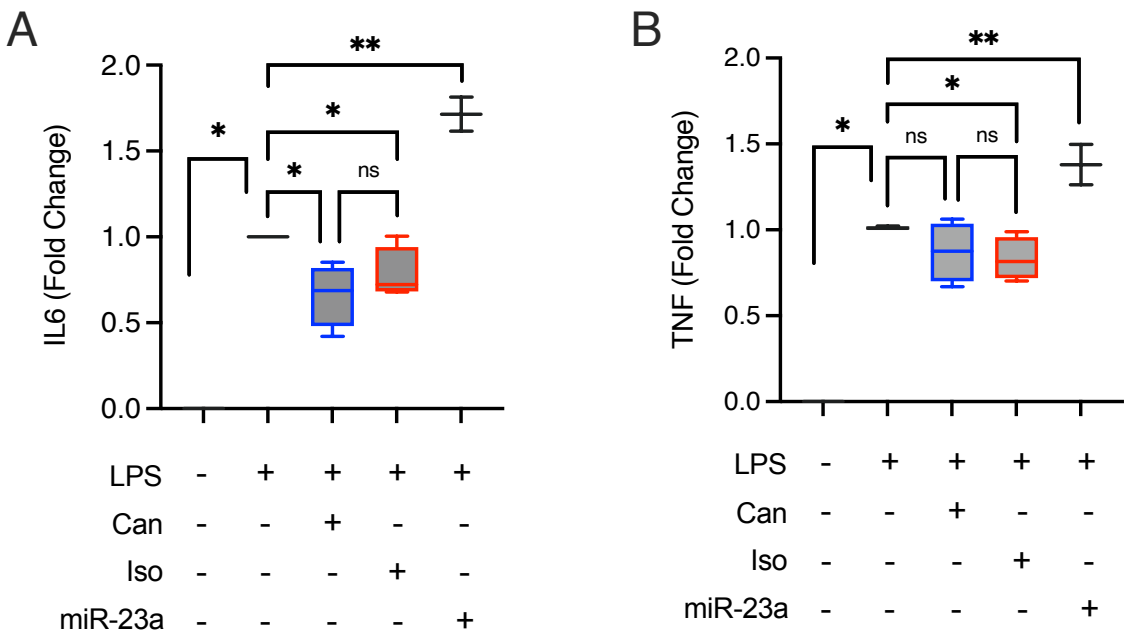


Figure 3.5. The canonical and isomiR fhe-miR-125b-5p regulated the inflammatory response to bacterial LPS in macrophages to the same extent. *BMDMs were transfected with canonical (Can) and isomiR (Iso) mimics of fhe-miR-125b-5p (20 pmol/mL) or mmu-miR-23a-3p. After 24 h, cells were stimulated with LPS (20 ng/mL) and 6 hours later, the secretion of IL6 (A) and TNF (B) was measured in the cell supernatants by ELISA. Results are presented as fold changes relative to vehicle control cells stimulated with LPS. Data are from four independent experiments, each represented by the average of three technical replicates, except for miR-23a, which is from two independent experiments. Box plots depict the data distribution, with the mean ± SEM indicated by horizontal and vertical lines. Statistical analysis was conducted using one-way ANOVA and student unpaired t test; *p < 0.05, **p < 0.005; ns, not significant.*

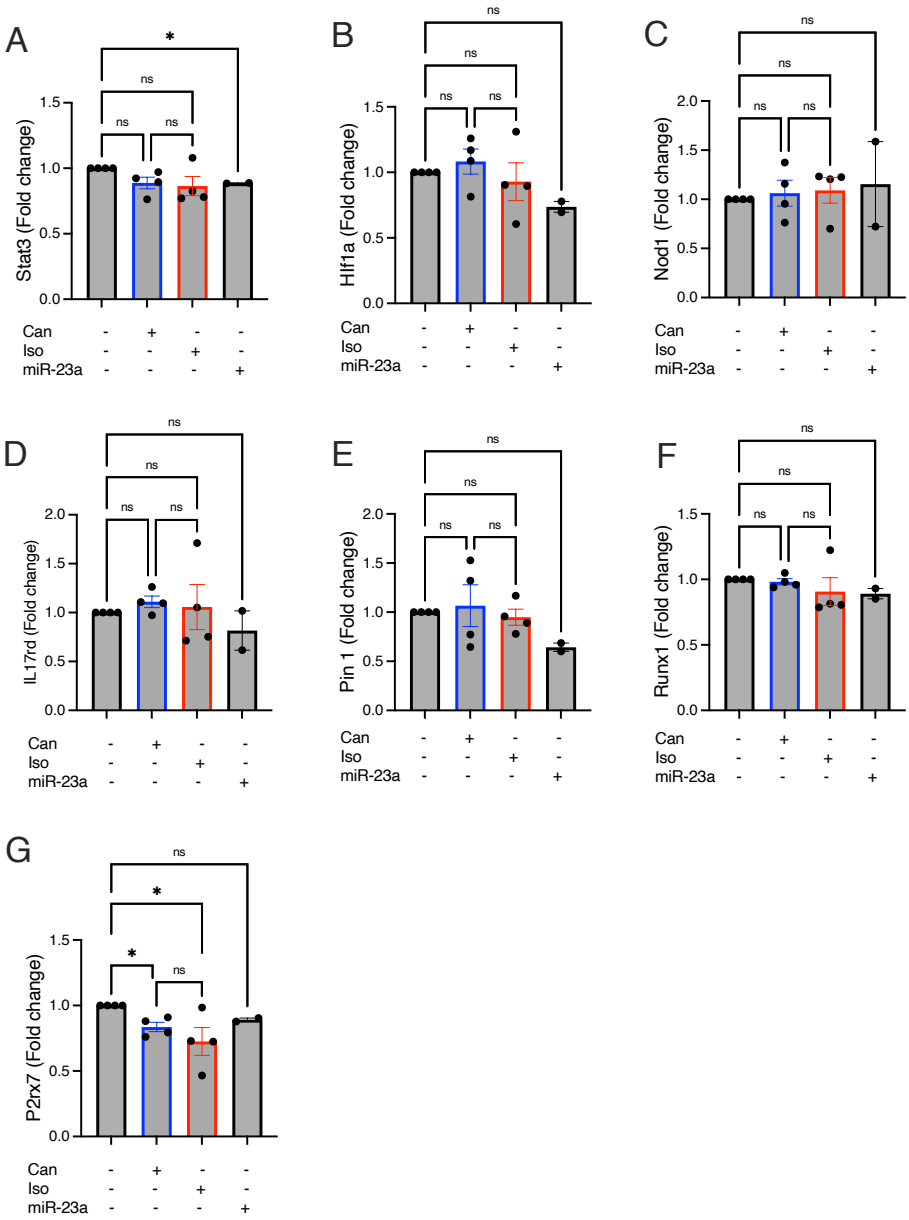


Figure 3.6. Except for the reduced expression of P2rx7, the fhe-miR-125b canonical and isomiR mimics had no effect on the expression of predicted gene targets in unstimulated BMDMs. *Gene expression was measured for A) Stats3, B) Hif1a, C) Nod1 and D) Il17d, E)Pin1, F) Runx1 and G) P2rx7 by qPCR in mouse BMDMs transfected for 24 hours with 20 pmol/mL of fhe-miR-125b canonical (Can) or isomiR (Iso) mimics, or control mimic mmu-miR-23a, followed by 6 hours in complete media (no LPS). Expression levels were quantified as starting quantities (N_0) using LinRegPCR (v.11) and presented as fold changes relative to the unstimulated vehicle control group. Each data point represents the average of three technical replicates from an independent experiment (four independent experiments for each treatment group, except miR-23a, which is from two independent experiments). Mean ± SEM are shown. Statistical analysis was performed using one-way ANOVA; *$p < 0.05$ was considered significant; ns, not significant.*

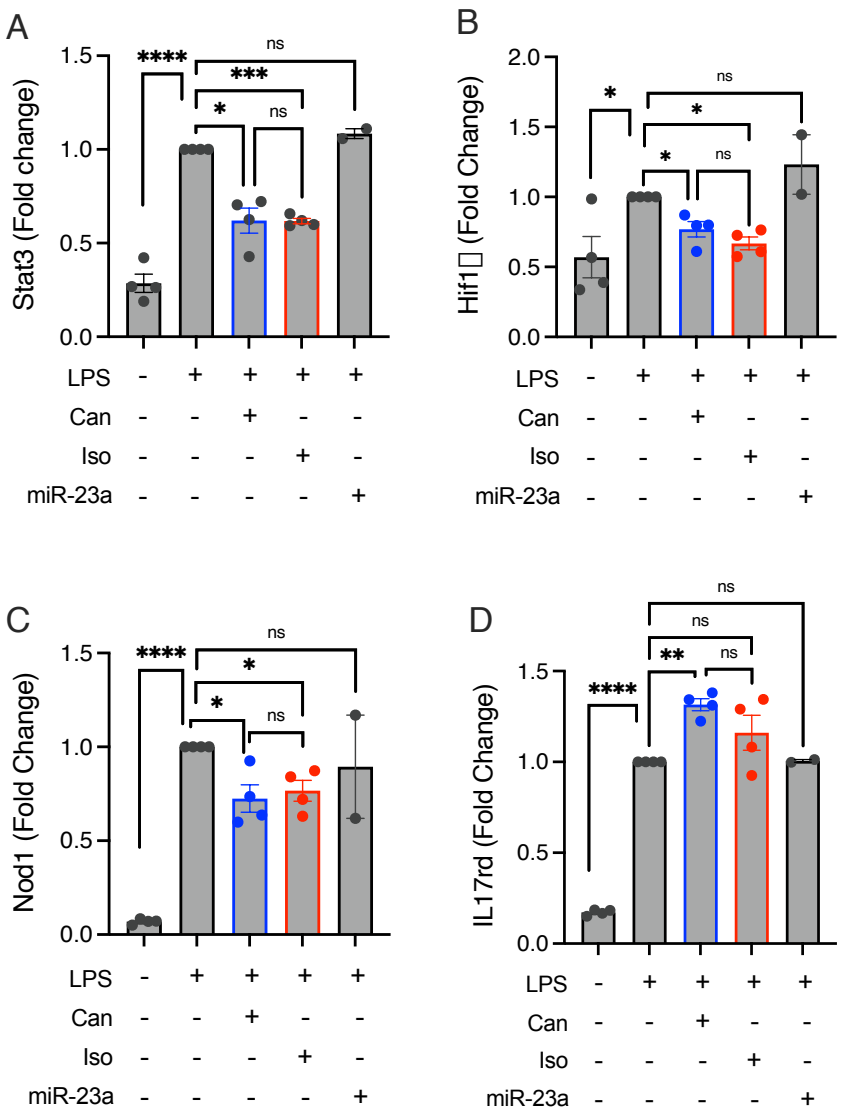


Figure 3.7. Both isomiR and canonical fhe-miR-125b-5p significantly suppressed the expression of host genes that had been increased in response to LPS stimulation of macrophages. *Gene expression was measured for A) Stats3, B) Hif1a, C) Nod1, and D) Il17d by qPCR in BMDMs transfected for 24 hours with fhe-miR-125b canonical (Can) or isomiR (Iso) mimics (20 pmol/mL), or control mimic mmu-miR-23a, followed by LPS (20ng/mL) treatment for 6 hours. Expression levels were quantified as starting quantities (N_0) using LinRegPCR (v.11) and presented as fold changes relative to the LPS-treated group without miRNA mimic. Each data point represents the average of three technical replicates from an independent experiment (four independent experiments for each treatment group, except miR-23a, which is from two independent experiments). Mean ± SEM are shown. Statistical analysis was performed using one-way ANOVA and student's unpaired t-test; *p < 0.05; **p < 0.005; ***p < 0.0005; ****p < 0.00005 was considered significant; ns, not significant.*

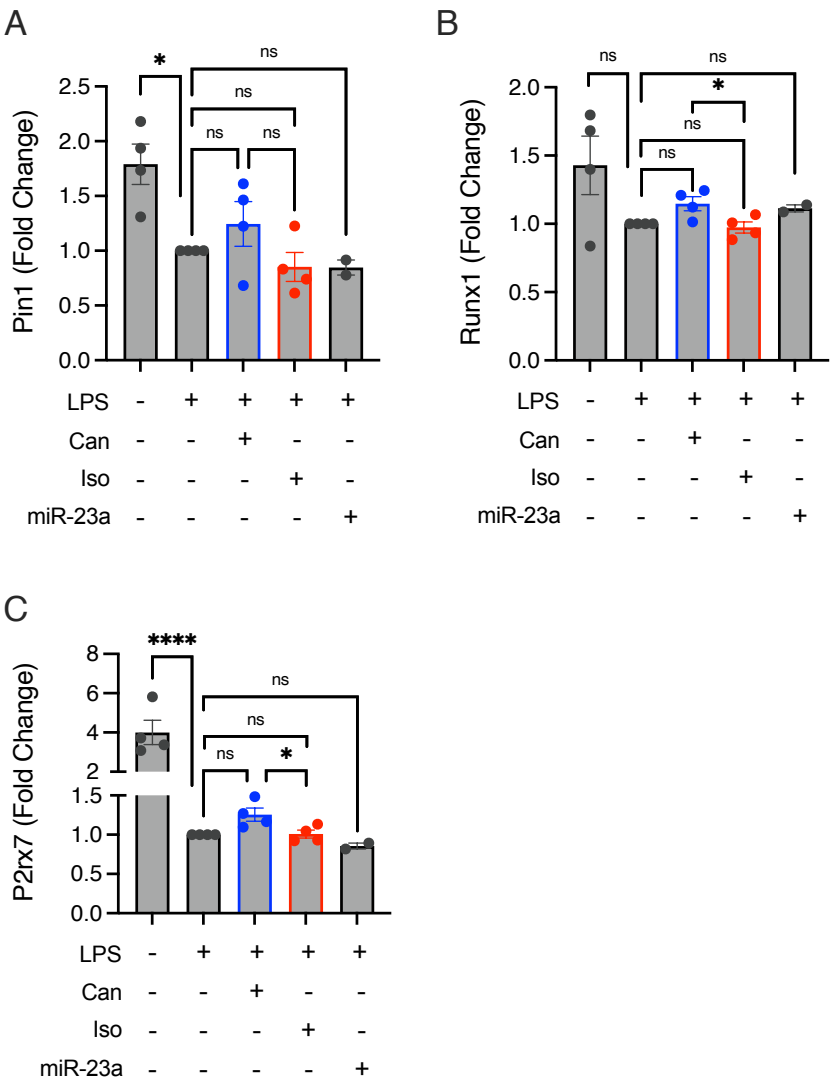


Figure 3.8. Neither the isomiR nor canonical fhe-miR-125b-5p impacted the expression of genes downregulated by LPS stimulation of macrophages. *Gene expression for A) Pin1, B) Runx1 and C) P2rx7 was measured by qPCR in mouse BMDMs transfected for 24 hours with 20 pmol/mL of fhe-miR-125b canonical (Can) or isomiR (Iso) mimics, or control mimic mmu-miR-23a, followed by LPS (20 ng/mL) treatment for 6 hours. Expression levels were quantified as starting quantities (N_0) using LinRegPCR (v.11) and presented as fold changes relative to the LPS-treated group without miRNA mimic. Each data point represents the average of three technical replicates from an independent experiment (four independent experiments for each treatment group, except miR-23a, which is from two independent experiments). Mean ± SEM are shown. Statistical analysis was performed using one-way ANOVA and student's unpaired t test; *p < 0.05 was considered significant; ns, not significant.*

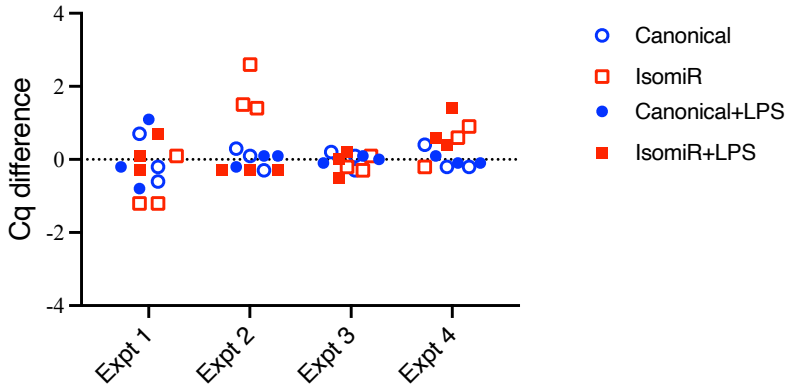


Figure 3.9. Transfected macrophages displayed the same levels of expression of fhe-miR-125b canonical (Can) and isomiR (Iso) sequences. *Cq values were obtained using TaqMan™ small RNA assays with custom primers specific to each mimic. Individual replicates from four independent experiments are shown. Data are presented as the Cq difference relative to the canonical miRNA within each treatment group.*

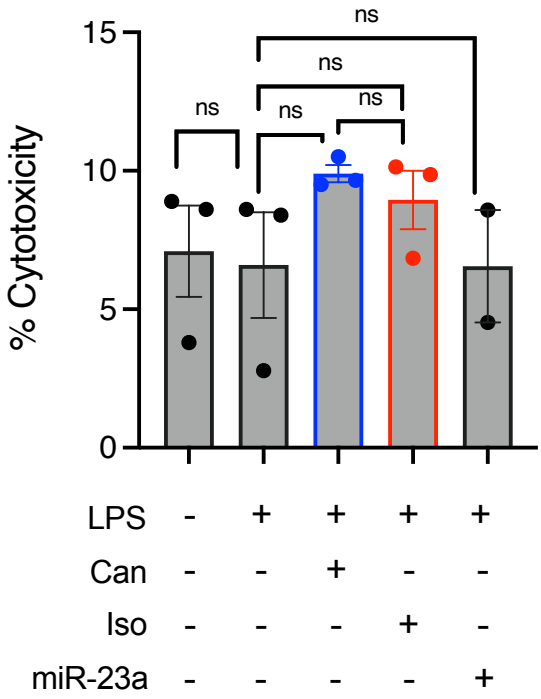


Figure 3.10. Transfection of macrophages with canonical and isomiR fhe-miR-125b mimics did not significantly impact cell viability. *Cytotoxicity was quantified as a percentage of maximum LDH release relative to vehicle and LPS-treated control cells. Data is representative of three independent experiments. Mean (n = 3) ± SEM are shown as horizontal and vertical lines. Statistical significance was determined using one-way ANOVA and student's unpaired t test, with *p < 0.05 considered significant; ns indicates non-significant results.*

3.3.6. The fhe-miR-125b-5p isomiR directly regulated the expression of host genes more efficiently than its canonical counterpart

Despite the prediction that the canonical and isomiR fhe-miR-125b-5p had different binding affinities for several host genes and thus different biological activities, this was not evident in the LPS stimulated macrophages, in which the regulation of gene expression was similar between the two miRNA forms. However, although the stimulation of macrophages with LPS is widely accepted as a model of innate inflammation and used broadly to screen for anti-inflammatory agents, several pathways and signalling cascades are activated and intersect to mediate the inflammatory response. This will include both miRNA dependent and independent mechanisms. As such, any specific regulation of a single gene by a single miRNA may be masked within this complexity.

Therefore, to more directly explore the efficiencies of gene regulation for the canonical and isomiR fhe-miR-125b-5p a more simplified luciferase reporter system was employed. Thus, the miRNA binding regions within the 3' UTRs of four selected genes were cloned into the Psi-CHECK2 luciferase reporter vector. The resulting constructs were co-transfected into HEK293 cells along with either the canonical or isomiR mimics of fhe-miR-125b. *Hif1a* and *Stat3* were selected because each contained a single predicted binding site with diminished affinity for the isomiR (Table 3.7) and, *in vitro*, were repressed by both the canonical and isomiR mimics in LPS stimulated macrophages. In contrast, *Pin1* and *Runx1* were not suppressed in LPS treated macrophages but were chosen because they harboured multiple predicted binding sites, at least one with diminished predicted binding for the isomiR based on free energy scores, and one or more with greater free energy compared to the canonical miRNA (Table 3.7). These features suggest that the canonical and isomiR forms may interact differently with these targets.

The assay was first validated using hsa-miR-21 and its well-characterized target *Pdcd4* [279]. As expected, *Pdcd4* expression was suppressed by miR-21, but not by the fhe-miR-125b mimics, confirming assay specificity (Figure 3.11A). On the other hand, the control mimic mmu-miR-23a appeared to suppress *Pdcd4*. Investigation of the cloned *Pdcd4* site for sequence complementarity with miR-23a revealed multiple potential binding sites, although all had free energy > -20 kcal/mol (Fig 3.11B). While this suggests that miR-23a is less likely to bind the cloned sequence strongly, the apparent suppression may result from these weak or non-canonical interactions.

Consistent with the qPCR analysis of host gene expression in the LPS stimulated macrophages (Figure 3.7B), the fhe-miR-125b isomiR mimicked the regulatory effect of canonical miRNA in significantly regulating the expression of *Hif1a* (Figure 3.12A). Similarly, and like the effect observed in transfected macrophages (Figure 3.8B), the expression of *Runx1* was not significantly altered by the fhe-miR-125b mimics (Figure 3.12D).

While the expression of *Stat3*, *Pin1* appeared slightly reduced by canonical fhe-miR-125b, this change was not significant ($p = 0.53$ for *Pin1*, and 0.63 for *Stat3*). In contrast, the isomiR fhe-miR-125b significantly reduced expression of both genes (Figure 3.12B and C).

As expected, miR-23a had no effect on the expression of *Hif1a*, *Pin1* and *Runx1* (Figure 3.12 A, C, and D), confirming the specificity of target sites for fhe-miR-125b. However, the expression of *Stat3* was significantly suppressed by miR-23a (Figure 3.12 B), which was explained by subsequent analysis of sequence complementarity that revealed the potential for interaction between the cloned *Stat3* 3′ UTR region and miR-23a (Figure 3.13). Therefore, to provide a validation for the specificity of *Stat3* repression by fhe-miR-125b, mmu-miR-21 was included as an additional mimic control, and as expected it did not exhibit any significant effect on *Stat3* expression (Figure 3.12B).

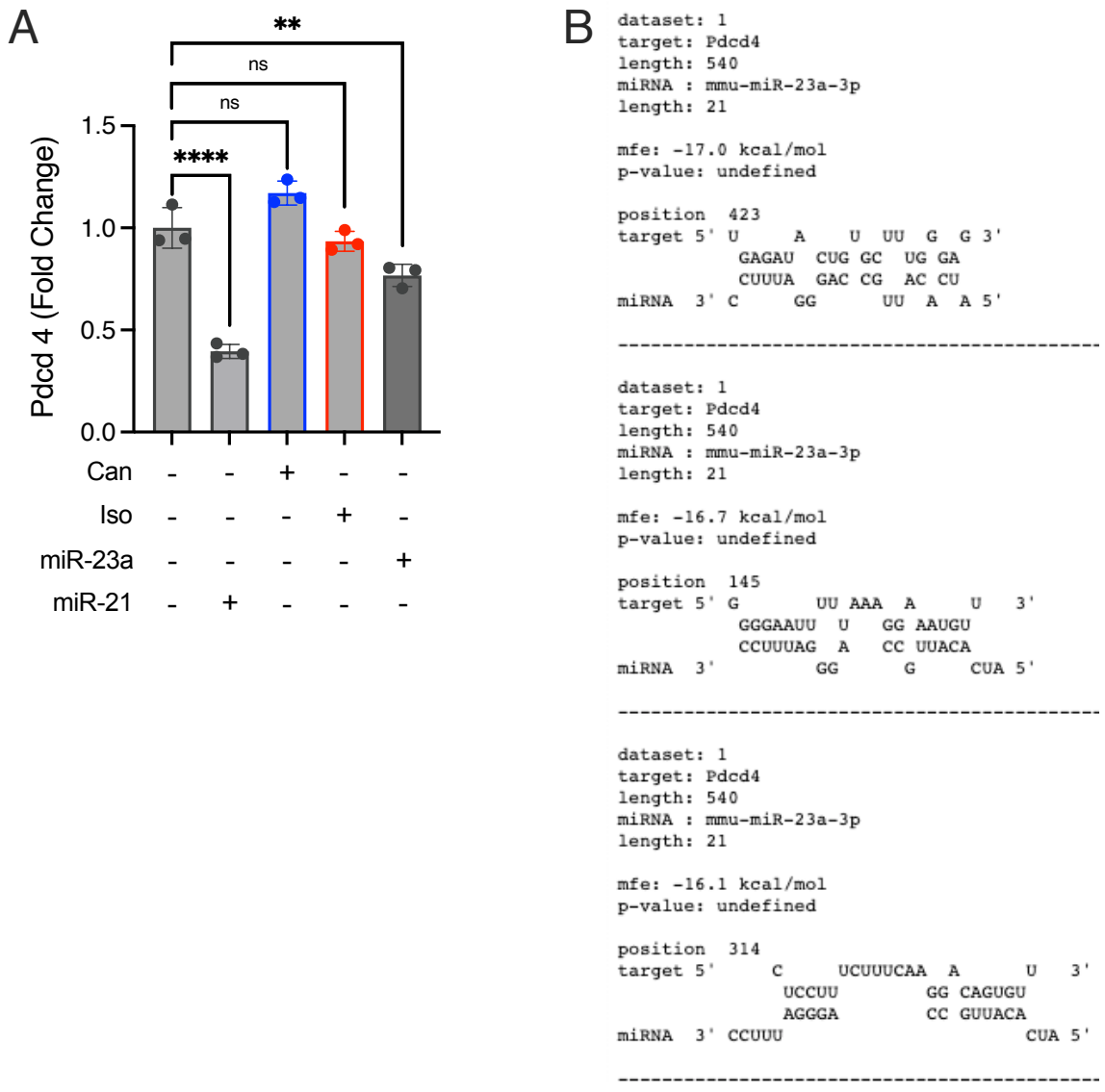


Figure 3.11. Validation of the luciferase reporter assay using hsa-miR-21 and its endogenous target Pdcd4 to assess miRNA-target direct interactions. *(A) HEK293 cells were co-transfected with miRNA mimics and the psi-CHECK2 vector containing the 3' UTR of Pdcd4, a known target of hsa-miR-21. Luciferase activity was measured as the Renilla to Firefly luminescence ratio and expressed as fold change relative to control cells transfected with the psi-CHECK2 vector alone (no miRNA mimic). The data is presented as mean (n = 3) ± SEM shown by horizontal and vertical lines. Statistical analysis was performed using one-way ANOVA; **p < 0.005, ****p < 0.00005; ns, not significant. (B) mmu-miR-23a-3p potential binding sites within the cloned Pdcd4 sequence. miRNA-mRNA interactions were predicted with RNA-hybrid (https://bibiserv.cebitec.uni-bielefeld.de/rnahybrid?id=rnahybrid_view_submission). Matches with minimum free energy (mfe) < -16 kcal/mol are shown.*

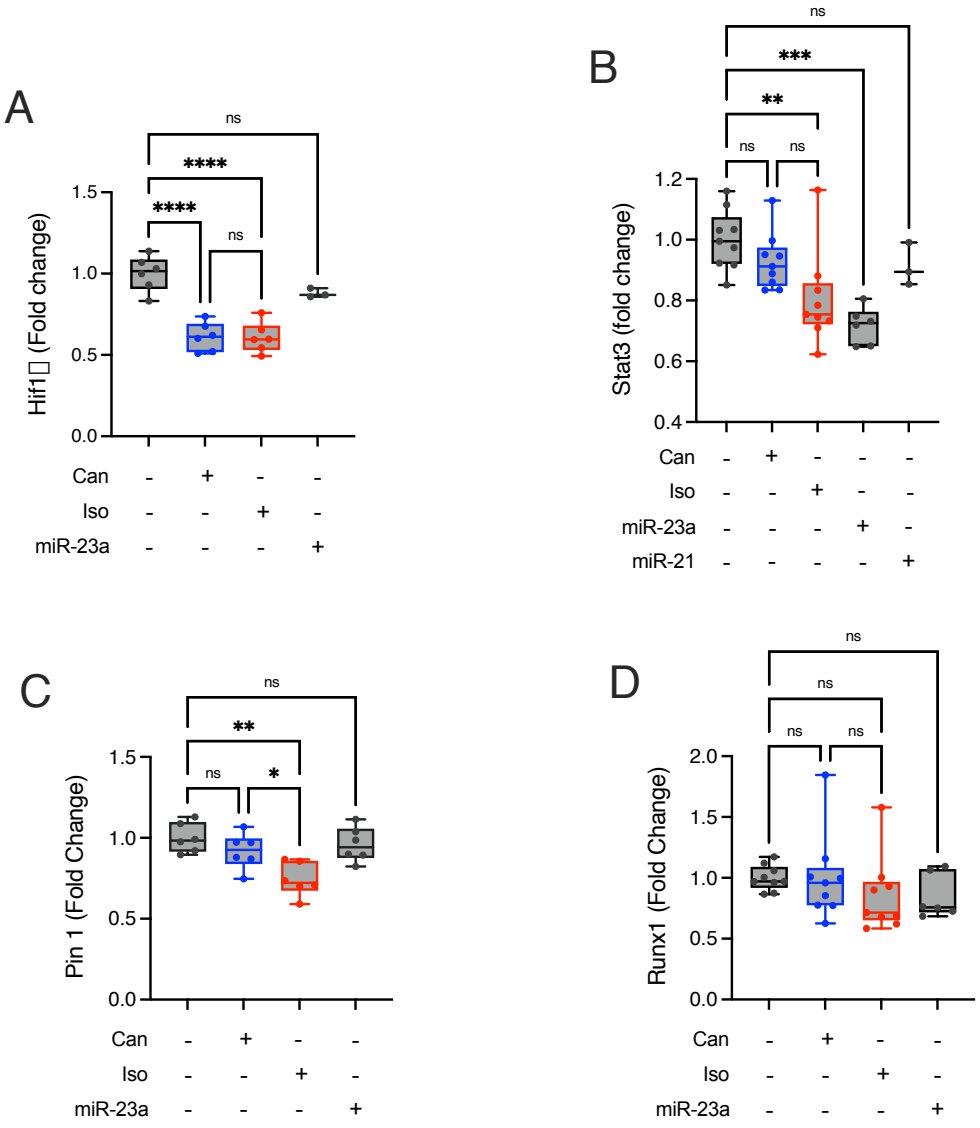


Figure 3.12. Luciferase reporter assay demonstrated that the fhe-miR-125b-5p isomiR repressed host target genes more effectively than the canonical form. *HEK293 cells were co-transfected with miRNA mimics (20 pmol) and the psi-CHECK2 vector (75 ng) containing the 3' UTR region of murine Hif1a (A), Stat3 (B), Pin1 (C), or Runx1 (D), each predicted to be targeted by fhe-miR-125b. Luciferase activity was calculated as the ratio of Renilla to Firefly luminescence and expressed as fold change relative to control cells transfected with the psi-CHECK2 vector alone (no miRNA mimic). Data are presented as box plots, with mean ± SEM indicated by horizontal and vertical lines; individual data points are shown as dots: Hif1a and Pin1, n = 6 from two independent experiments, except miR-23a (n = 3 from one experiment for Hif1a); Stat3 and Runx1, n = 9 from three independent experiments, except for miR-23a (n = 6 from two experiments). Statistical analysis was performed using one-way ANOVA;*

** $p < 0.05$, ** $p < 0.005$, *** $p < 0.0005$; ns, not significant.*

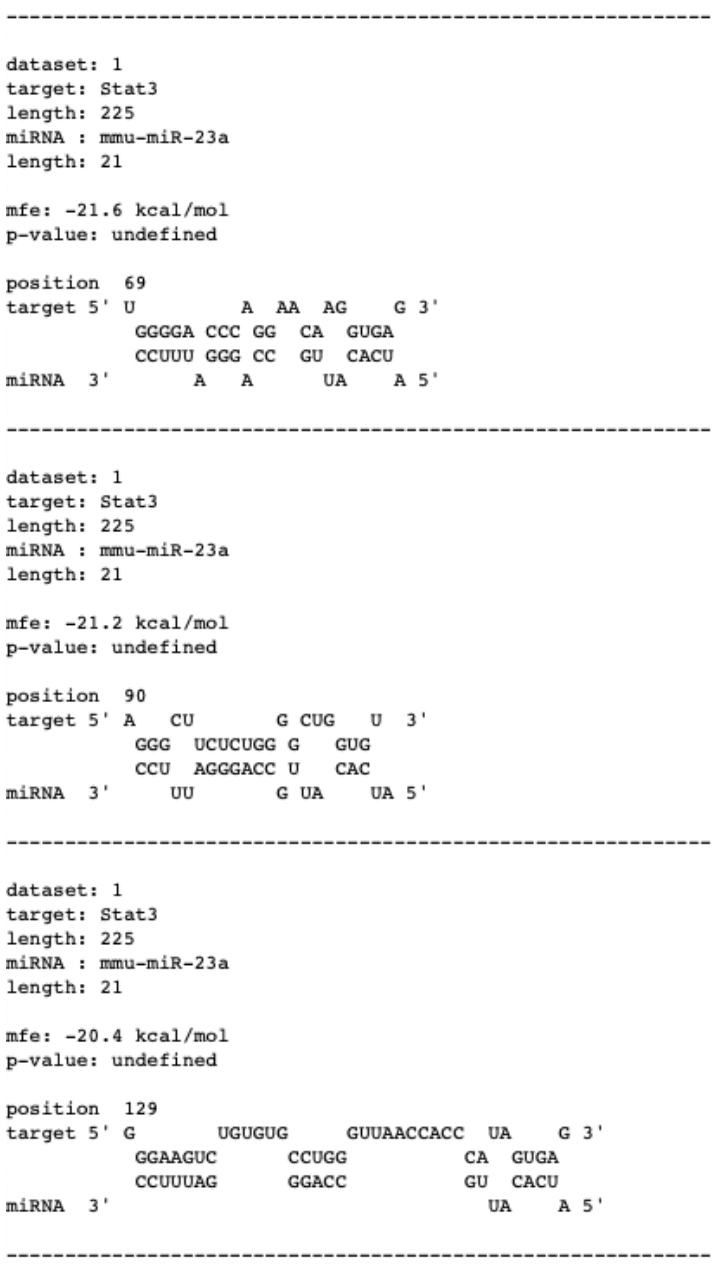


Figure 3.13. The cloned Stat3 sequence in the psiCHECK-2 vector contains multiple potential binding sites for mmu-miR-23a-3p. *miRNA-mRNA interactions were predicted with RNA-hybrid (https://bibiserv.cebitec.uni-bielefeld.de/rnahybrid?id=rnahybrid_view_submission). Matches with minimum free energy (mfe) < -20 kcal/mol are shown.*

3.3.7. The 3' trimmed isomiR fhe-miR-125b displayed enhanced interaction with host Ago2 as compared to the canonical miRNA.

Although the luciferase reporter assay showed a differential effect between the isomiR and canonical fhe-miR-125b, the increased repression of the luciferase reporter by the isomiR contrasted with the target prediction analyses. These opposing findings suggested that the greater efficacy in gene regulation displayed by the isomiR in the luciferase assay was unlikely due to sequence complementarity and/or altered binding affinity to gene targets.

To explore an alternative mechanism, we next investigated whether host Ago2 exhibits a differential binding preference for the 3′-trimmed isomiR compared to the canonical fhe-miR-125b. An Ago2 pulldown assay was performed in mouse macrophages transfected with either canonical or isomiR mimics. Immunoprecipitation of cellular Ago2 was confirmed by western blotting (Figure 3.14A). To demonstrate consistency of immunoprecipitation and elution of RNA, the quantity of loaded mmu-miR-21, a highly abundant endogenous miRNA, was quantified using RT-qPCR. This miRNA was equally abundant in cells treated with either the canonical or isomiR fhe-miR-125b (Figure 3.14B and C), which combined with the equal precipitation of the Ago2 protein, validates any comparative differences in RNA loading of the synthetic mimics.

Of the Fasciola miRNAs, the amplification of fhe-miR-125b isomiR from the Ago2 miRNA load, showed earlier Cq values compared to its canonical counterpart (Figure 3.14D), indicating a higher level of association to the Ago2 protein. Furthermore, when normalised to endogenous miR-21 levels, the isomiR was loaded with five-fold abundance as compared to the canonical miRNA (Figure 3.14E).

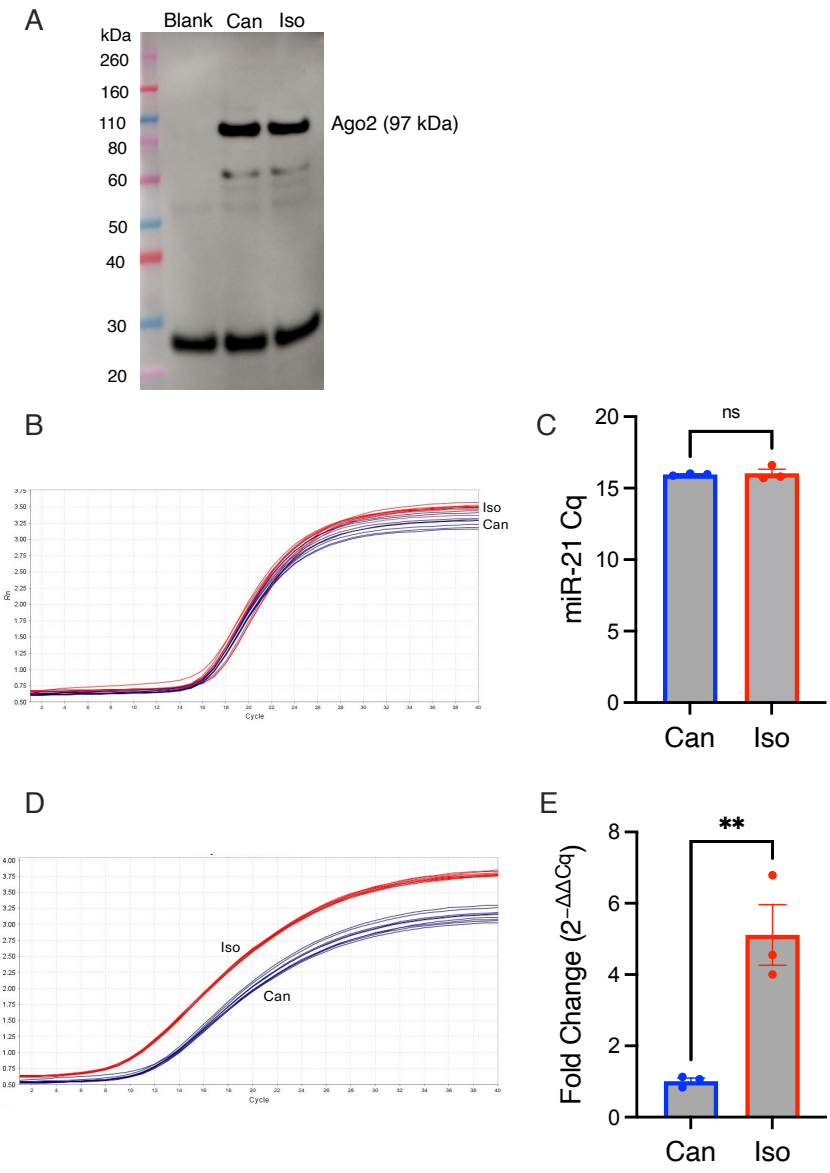


Figure 3.14. fhe-miR-125b isomiR is loaded more efficiently onto host Ago2 than the canonical form. *Macrophages (RAW264.7 cell line) were transfected for 24 hours with either the canonical (Can) or isomiR (Iso) mimic of fhe-miR-125b (20 pmol/mL), followed by Ago2 pulldown assay (A) Western blot of protein eluted from Ago2 immunoprecipitated breads showing distinct Ago2 bands at ~97 kDa. The Can and Iso lanes each represent a pooled triplicate sample of transfected cells. Blank lane represents elute from a no-cell control; (B) Amplification plots and (C) Cq values of Ago2-associated mmu-miR-21 measured by qPCR from RNA eluted from Ago2 immunoprecipitated beads; (D)Amplification plots and (E) relative levels of Ago2-associated canonical and isomiR fhe-miR-125b determined by $2^{-\Delta\Delta Cq}$ analysis normalized to miR-21. Amplification plots showing individual curves for each sample (n = 3). The bar graphs (C and E) show mean ± SEM indicated by horizontal and vertical lines; individual data points are shown as dots **p < 0.005; ns, not significant, using Student's unpaired t-test.*

3.4. Discussion

This study provides the first evidence, to our knowledge, of helminth-derived isomiRs being present within host cells. Specifically, we showed that *Fasciola hepatica* miRNAs detected in host peritoneal macrophages during the migration of NEJs are not predominantly in their canonical forms, but instead mostly exist as isomiRs. Importantly, the same isomiRs were also expressed by parasites and detected within their EVs. Notably, fhe-miR-125b appeared exclusively in macrophages as a 3′-trimmed isomiR (lacking a single nucleotide) and this variant was most abundant in host macrophages, despite the canonical form being predominant within the parasite at the corresponding timepoint. Combined, these observations strongly support a mechanism by which *Fasciola hepatica* is specifically expressing sequence variants of its miRNAs for export into host cells to mediate functional change.

It is important to note that isomiR detection in this study was limited to length variants of the canonical *F. hepatica* miRNAs, potentially underestimating the true abundance and diversity of parasite-derived miRNAs within host macrophages. This limitation arises from the use of a highly stringent alignment criterion, which allowed no mismatches against the *F. hepatica* miRNA reference library, in order to minimise the risk of misclassifying endogenous host miRNAs as parasite-derived sequences. While this conservative approach effectively reduces false positives, it restricts detection to canonical miRNAs, and isomiRs that are 3′ or 5′ trimmed or extended, provided they perfectly match the reference sequences, at least for the first 20 nucleotides [236]. As a result, the pipeline excludes isomiRs containing internal sequence variations, including single nucleotide substitutions, insertions, deletions, or RNA editing events not represented in the reference. Therefore, the isomiRs identified in this study likely represent only a subset of a broader and more complex population of *F. hepatica*-derived miRNAs. Future studies employing more permissive isomiR detection pipelines (as described in [274]), or cross-species-aware alignment strategies may reveal additional layers of sequence diversity.

Since 3′ isomiRs are commonly produced in mammalian immune cells in response to stimuli such as bacteria or viruses [147, 273], it is plausible that parasitic worms co-opt this endogenous signature to effectively integrate into the host RNAi pathway and manipulate the activity of immune cells. Supporting this hypothesis, the luciferase assay, which assesses direct interactions between miRNAs and their predicted target sites, showed that while the isomiR exerted similar effect as the canonical sequence on some gene targets (*Hif1a* and *Runx1*) it was

more efficient at downregulating specific host genes, *Stat3* and *Pin1*. These two genes are known to be functional partners: *Pin1* binds phosphorylated *Stat3* to stabilize and enhance *Stat3* activity, a key pathway regulating macrophage polarization [281, 284, 293]. The preferential suppression of this *Pin1-Stat3* axis by the isomiR points to selective targeting of a central inflammatory pathway, potentially enabling the parasite to modulate host immunity more precisely.

This functional advantage was not anticipated by thermodynamic modelling, which predicted weaker target binding by the isomiR due to its shortened 3′ end. This suggests that free energy calculations alone may be insufficient to predict regulatory activity, consistent with the gene enrichment analysis that indicated comparable biological implications for the canonical and isomiR forms. However, the free energy analysis relied solely on the miRanda tool, which, for example, did not predict *Nod1* as a target of fhe-miR-125b, in contrast to a previous study that combined three prediction tools [56]. Hence, employing a combination of *in silico* prediction tools such as RNA22 [294], combinatorial target prediction platforms like ComiR [295], and deep learning-based predictors of miRNA/isomiR targets such DMISO [296], alongside *in vitro* Ago2 FRET assays to directly assess miRNA-RISC interactions with target mRNAs [297] could provide a more comprehensive and reliable assessment of the contribution of free energy to targeting differences between the canonical and isomiR forms.

Despite the luciferase assay findings, a comparable pattern of differential gene regulation was not observed in LPS-stimulated BMDMs. This difference is not unexpected, because luciferase reporter assays measure direct miRNA-target interactions at a cloned binding site, whereas the effects observed in LPS-stimulated cells reflect the broader impact of the miRNA mimics within a complex cellular environment, including both direct and indirect regulatory influences.

The LPS stimulation model was used to evaluate the effects of the exogenous parasite-derived miRNA as LPS is a potent TLR4 agonist that induces pro-inflammatory M1-like macrophages [298]. In this sense, this model was intended to mimic the macrophage response described for the early stages of Fasciola infection, reflecting the translocation of gut bacteria as the NEJs migrate from the gut through the peritoneum to the liver.

However, this model may not fully replicate the nuanced environment encountered *in vivo*. The peritoneal cavity contains tissue-resident macrophages that are exposed to a complex mix of host- and parasite-derived signals, including cytokines, apoptotic debris, metabolites, and various pathogen-associated molecular patterns (PAMPs) [181, 299-304]. By contrast, BMDMs are homogeneous and lack this contextual diversity, which may mask subtle regulatory differences between miRNA isoforms. The strong and uniform activation induced by LPS-derived from a sole bacterial strain might override or obscure the fine-tuned effects exerted by the isomiR. These observations reinforce the context-dependent nature of parasite miRNA-mediated gene regulation and underscore the limitations of simplified *in vitro* models. Future studies should consider more physiologically relevant systems such as *in vivo* infections, 3D co-culture models, or organoid systems to better capture the complexity of host–parasite interactions.

Additionally, the expression of selected gene targets of fhe-miR-125b were not all regulated as predicted in the LPS model. While the expression of *Stat3, Hif1a,* and *Nod1*, genes upregulated by LPS, were reduced by both miRNA forms, the expression of *Il17rd, Runx1, Pin1,* and *P2rx7* were either unaffected by transfected miRNAs or unexpectedly increased. Specifically, *Pin1* and *Runx1,* were already downregulated by LPS, suggesting that repression by the isomiR may require a certain level of baseline expression. In contrast, *Il17rd* was notably upregulated by canonical miR-125b, which could be a secondary effect of miRNA, potentially due to alterations in upstream regulatory pathways or intermediate factors that influence *Il17rd* expression. Future studies should explore alternative *in vitro* models or multi-ligand stimuli that selectively induce the expression of target genes to validate targets specificity, and to better distinguish the regulatory capacity of the canonical miRNA versus the isomiR.

Our findings that the 3′-trimmed isomiR loads more efficiently onto Ago2 aligns with previous literature that demonstrated distinct Ago2 loading efficiency between miRNA isoforms [305, 306]. Since the 3′ end of the miRNA interacts with the PAZ domain of Ago proteins [307], shorter 3′ end of the fhe-miR-125b isomiR might better fit the binding pocket of Ago2, facilitating more efficient RISC assembly. From an evolutionary standpoint, the parasite's selective deployment of isomiRs that better engage host RNA silencing machinery may represent a refined strategy to manipulate host immunity.

The novel findings presented in this chapter, raises critical questions about the compatibility of parasite miRNAs within host RNAi pathways, including whether diverse canonical and isomiR repertoires are deployed by the parasite at different infection stages to tailor responses to variable host environments. Furthermore, elucidating the mechanisms of how these worm-derived miRNAs interact with, and utilise, the mammalian miRNA biogenesis machinery to mediate the processing, Ago loading and subsequent regulatory function within host cells, will be an important area for future exploration.

Chapter 4:

Deciphering the mechanisms by which parasite-derived miRNAs exploit the host RNA interference (RNAi) machinery to regulate host gene expression

4.1. Introduction

The data presented in Chapter 3 revealed that *Fasciola hepatica* strategically exploits the host Argonaute 2 (Ago2) protein by deploying isomiRs with enhanced affinity, demonstrating a sophisticated mechanism to manipulate host RNA interference (RNAi) pathways. However, the precise mechanism by which parasite-derived miRNAs are processed within the mammalian host's miRNA biogenesis machinery remain unknown. Specifically, it is now of interest to determine how these parasite-derived miRNAs engage the host RNAi pathway, which core components they utilise, and/or whether they bypass key mammalian miRNA machinery and use alternative, non-canonical processing pathways.

As previously discussed, (Section 1.4.4.1), Ago2 is the principal effector of the RNA-induced silencing complex (RISC), binding mature miRNAs and guiding them to complementary mRNA targets to mediate translational repression or degradation. Alongside Ago2, mammalian cells also express Ago1, Ago3, and Ago4, which are similarly capable of binding miRNAs and forming RISC complexes. However, only Ago2 exhibits slicer activity that enables endonucleolytic cleavage of target mRNAs, resulting in irreversible gene silencing; the other Agos primarily facilitate repression through non-cleavage mechanisms [308]. Accordingly, the Ago proteins can compensate for each other to some degree and contribute to translational repression and mRNA degradation through non-slicing mechanisms [309-312]. In mammalian cells, the loading of miRNAs onto Ago proteins tends to reflect the relative abundance of each Ago protein, rather than involving strict sequence-dependent sorting. As a result, because Ago2 is generally the most abundant Ago protein in many cell types, it associates with a larger proportion of the cellular miRNA pool, thereby underscoring its predominant role in post-transcriptional gene regulation [311].

In macrophages, Ago2, as expected, mediates miRNA-mediated regulation of macrophage activation and inflammatory responses [313, 314]. However, other Agos also contribute to immune regulation: Ago4 is essential for antiviral defence in macrophages, where its loss reduces viral RNA loading onto host RISC [315], while Ago1 is upregulated during Leishmania infection and enriched in RISCs isolated from the parasite infected cells [316]. Together, these findings suggest that *F. hepatica* miRNAs might engage multiple Ago proteins

in host cells, raising the question of whether Ago2 is uniquely indispensable or whether alternative Ago pathways could support parasite miRNA function.

Dicer, an RNase III endonuclease essential for miRNA maturation, cleaves precursor miRNAs into mature miRNA duplexes within the cytoplasm (Section 1.4.4.1). A single Dicer gene exists in humans, mice, and helminths [317], and its loss results in precursor miRNA accumulation and a marked reduction in mature miRNA levels (Kim et al., 2016). Beyond maturation, Dicer contributes to miRNA strand selection and RISC assembly by interacting with TAR RNA-binding protein (TRBP) or PKR-activating protein (PACT), guiding the correct miRNA strand to Ago2 [318, 319]. Unlike in Drosophila, where this mechanism is indispensable, in mammalian cells Dicer interaction is not essential for mature miRNA loading, as exogenous miRNAs retain gene silencing in Dicer-deficient cells [320, 321]. Whether mature parasite miRNAs require host Dicer for efficient loading onto Ago2 remains unknown.

To explore these questions surrounding the integration of *F. hepatica*-derived miRNAs into the mammalian RNAi pathway, this chapter utilised CRISPR-Cas9–mediated Ago2 and Dicer knockout macrophages. Following the successful generation of these knockout cell lines, this chapter had three main objectives: (i) to characterise the inflammatory phenotypes of Ago2 and Dicer knockout macrophages; (ii) to examine whether parasite-derived miRNAs are processed through canonical or non-canonical host RNAi pathways; (iii) to determine whether canonical parasite miRNAs and their corresponding isomiRs are processed differently by the host RNAi machinery. Together, these approaches aim to provide mechanistic insight into how *F. hepatica*-derived miRNAs engage host RNAi machinery and contribute to the modulation of macrophage inflammatory responses.

4.2. Methods

4.2.1. Generation of Ago2 and Dicer gene knockout (KO) macrophage cells.

Ago2 and Dicer knockout cell lines were generated in the RAW264.7 murine macrophage cell line by the Monash Genome Modification Platform (MGMP; Monash University, Australia) using CRISPR-Cas9 genome editing. The single-guide RNAs (sgRNAs) used for gene targeting are listed in Table 4.1.

Clones were genotyped by PCR amplification of the sgRNA1 target site, and knockout candidates were further validated by sequencing. To ensure clonal purity, confirmed knockout clones were subcloned via single-cell deposition. Subclones were subsequently genotyped and sequenced by MGMP, and verified knockout subclones were expanded and handed over to UTS for downstream applications. A summary of the received validated subclones is provided in Table 4.2, and the full reports of the KO cell lines for the two genes from MGMP are available in Appendix C and D.

4.2.2. Cell culture

Wild-type (WT) RAW264.7 cells, Ago2 knockout (KO), and Dicer KO clones were cultured in RPMI 1640 medium (Thermo Fisher Scientific), supplemented with 10% FBS and 1% P/S, hereafter referred to as complete medium. Cells were maintained under standard conditions at 37 °C in a humidified incubator with 5% CO_2.

For routine maintenance, cells were seeded in T75 tissue culture flasks and allowed to adhere. Upon reaching approximately ~80% confluency, cells were washed twice with sterile Baxter saline (0.9% NaCl), then gently detached using a sterile cell scraper. Detached cells were either passaged into fresh complete media for continued culture or resuspended at required cell number and seeded into appropriate tissue culture plates for downstream experiments. All procedures were conducted under aseptic conditions in a Class II biosafety cabinet.

Table 4.1. CRISPR-Cas9 sgRNAs used for the generation of Ago2 and Dicer1 gene knockouts in RAW264.7 cells.

Gene	sgRNA name	Target sequence	Genomic target location*	Predicted cut site	Functional effect
Ago2	sgRNA1	GTGGTGCCGAAGTCCGGCCG	Second coding exon, downstream of ATG	Between amino acid 29 and 30	Frameshift; may generate KO allele as a single guide
	sgRNA2	AAGCGCCCCTCGTCAACGAA	~890 bp upstream of stop codon	Final exon	With sgRNA1, enables deletion of majority of coding region
Dicer1	sgRNA1	GAGGTCGCCCCTGATCTGAT	Second coding exon	Early coding region	Frameshift; may generate KO allele as a single guide
	sgRNA2	ATTCCGTGCAATAGTACCCG	518 bp downstream of stop codon	3′ UTR / downstream flanking region	With sgRNA1, enables deletion of majority of coding region

* Genomic coordinates refer to Ensembl transcripts Ago2-201 and Dicer1-201

4.2.3. Assessment of cell confluency

WT, Ago2 KO, and Dicer KO clones were seeded at a density of 4,000 cells per well in 96-well plates. The following day, when cells reached ~10% confluency, real-time imaging was initiated using the Incucyte® Live-Cell Analysis System (Sartorius). Phase-contrast images were captured every 3 hours for up to 5 days. Image analysis using Incucyte software was performed to plot the percentage of confluency over time.

4.2.4. CFSE cell proliferation assay

Cell proliferation was assessed using the CellTrace™ CFSE Cell Proliferation Kit (Thermo Fisher Scientific). Briefly, 4.2×10^6 cells were resuspended in 1 mL pre-warmed PBS. To each tube, 1 µL of CFSE stock solution (5mM in DMSO) was added (final concentration 5 µM), and cells were then incubated at 37 °C for 10 minutes in the dark. Staining was quenched by adding 10 mL of ice-cold complete culture medium and incubating the samples on ice for 5 minutes. Cells were then centrifuged at 300 × *g* for 5 minutes and washed twice with 10 mL of complete medium to remove excess dye. Stained cells were resuspended in pre-warmed complete medium, and 2 mL of this cell suspension (3.5×10^5 cells/mL) was seeded into 6-well plates. Cells were then cultured under standard conditions (Section 4.2.2) and harvested at 24 and 48 h post-seeding for analysis of proliferation by flow cytometry.

Cells were washed twice in sterile saline and finally suspended into 1 mL of FACS buffer (1× PBS with 5% heat-inactivated FBS and 5 mM EDTA). Unstained cells served as negative controls. Samples were analysed on a CytoFLEX LX flow cytometer (Beckman Coulter), with CFSE fluorescence detected in the B525-40-A channel (excitation 488 nm, emission 525 ± 20 nm). Data were acquired and analysed using CytExpert software.

4.2.5. Cytotoxicity Assay

Cell viability was assessed by measuring the release of LDH into cell culture media using the CytoTox 96® Non-Radioactive Cytotoxicity Assay (Cat# G1780; Promega). Cells were seeded at 8×10^4 cells per well in 96-well plates and incubated overnight in complete media to allow for adherence. The next day, cells were washed with sterile saline and replenished with 150 µL of fresh complete medium. After 6 hours of incubation, culture supernatants were collected and the levels of LDH release was measured as described in Section 3.2.4. Maximum LDH release was obtained by lysing cells with 15 µL of the supplied 10× lysis solution (containing 9% v/v Triton X-100). LDH release in experimental wells was expressed as a percentage of the maximum release for each clone.

4.2.6. Scratch Wound Assay

Cell migration was assessed using the Incucyte® Scratch Wound Assay. Cells were seeded in 96-well plates in complete media and cultured overnight to reach 100% confluency. A uniform scratch was created in each well using the Incucyte® 96-well WoundMaker tool. Following wounding, the wells were gently washed with serum free RPMI medium to remove detached cells and debris. Cells were then maintained in serum-starved RPMI medium (supplemented with 1% penicillin-streptomycin) to minimise cell proliferation and ensure that wound closure predominantly reflected migratory activity. Live-cell imaging was performed using the Incucyte® Live-Cell Analysis System equipped with the Scratch Wound module. Images were captured every 2 hours for up to 48 hours. Wound closure was quantified using the Incucyte software to calculate the percentage of wound area over time, enabling comparison of migratory capacity between WT and KO clones.

4.2.7. Phagocytosis Assay

The phagocytic capacity of WT and KO clones was assessed using pHrodo™ Red *Escherichia coli* Bioparticles (Thermo Fisher Scientific), which fluoresce upon internalisation into acidic phagosomes. Lyophilised pHrodo™ Red *E. coli* Bioparticles were reconstituted in pre-warmed R10 medium to a stock concentration of 1 mg/mL. The suspension was vortexed, transferred to a glass tube, and sonicated for 10 minutes to disperse aggregates. The stock solution was diluted to a working concentration of 200 μg/mL.

For flow cytometry, cells were seeded at a density of 4×10^5 cells per well in 24-well plates in 500 μL of complete RPMI medium supplemented with 10% foetal bovine serum (R10 medium) and incubated overnight to allow adherence. Cells were then washed once with sterile saline and incubated with 500 μL of the diluted pHrodo™ suspension for 1 hour at 37 °C in a humidified incubator with 5% CO_2. Following incubation, cells were washed twice with sterile saline to remove uninternalised particles and replenished with fresh R10 medium. Cells were then harvested, centrifuged at 300 × *g* for 5 minutes at 4 °C, and washed twice with ice-cold phosphate-buffered saline (PBS). Cell pellets were resuspended in 500 μL of FACS buffer. Negative controls (cells incubated with pHrodo™ particles on ice) and unstained cells (cells not treated with pHrodo™) were included to control for background fluorescence. Flow cytometry was performed using a CytoFLEX LX cytometer (Beckman Coulter), with pHrodo™ Red detected in the Y585-42 channel (excitation 561 nm, emission 585 ± 21 nm).

For imaging, the phagocytosis assay was performed in black-walled, clear-bottom 96-well plates. Cells were seeded overnight at a density of 8 × 10^4 cells per well, treated with 200 µg/mL pHrodo™ Red *E. coli* Bioparticles for 1 hour at 37 °C, washed twice with sterile saline, and replenished with fresh R10 medium. Images were acquired using an EVOS™ FL fluorescence microscope (Thermo Fisher Scientific) with the RFP channel (excitation 530 nm, emission 593 nm) overlaid on phase-contrast images, using a 10× objective lens.

4.2.8. Assessment of the inflammatory response of WT and KO clones

WT and KO clones were seeded at 7 x 10^5 cells in 2 mL complete media in a 6 well plate. At 48 hours, cells were washed with saline twice and stimulated with *E. coli* lipopolysaccharide (LPS; 20ng/ml; 011:B4 strain). Culture supernatants were collected at 6 h post LPS stimulation for analysis of cytokine secretion. Cells were then washed to remove LPS, and harvested in 1 mL of fresh medium on ice, followed by two washes with 1 mL of 1× PBS by centrifugation at 300 x *g*. During the second wash, an aliquot of 20 µL of the cell suspension was pelleted and stored at -80 °C for the CyQUANT assay. The remaining cells were centrifuged, and the pellet was resuspended in 500 µL of RNAzol RT and stored at -80 °C for subsequent RNA isolation.

The quantification of TNF and IL6 secreted into the supernatants was measured by ELISA as described in Section 3.4.5.

RNA was extracted from cells to evaluate the expression of predicted host target genes of fhe-miR-125b via qPCR, as detailed in Sections 3.4.6 and 3.4.8.

4.2.9. Quantification of cell number using CyQUANT Assay

Cell numbers were quantified using the CyQUANT® Cell Proliferation Assay Kit (Thermo Fisher Scientific) following the manufacturer's instructions. The CyQUANT working solution was prepared by diluting the stock solution 1:400 in freshly prepared 1× lysis buffer and was protected from light until use. For the preparation of the cell number standard curve, RAW264.7 cells (5 × 10^5) were washed in 1× PBS, pelleted, and stored at –80 °C. Prior to the assay, cell pellets were thawed at room temperature, resuspended in 1 mL of CyQUANT working solution, and serial dilutions were prepared to achieve a range of 50 to 50,000 cells per well in 200 µL in duplicate. Wells containing CyQUANT working solution without cells served as blanks. For experimental samples, cell pellets were thawed and resuspended in 420 µL CyQUANT working solution. Aliquots of 200 µL were transferred, in duplicate, to black

96-well microplates. Samples were incubated for 2–5 minutes at room temperature, protected from light, and fluorescence was measured at 480 nm excitation and 520 nm emission. Cell numbers were calculated by reference to the standard curve.

4.2.10. Transfection of *Fasciola hepatica* miRNA mimics

WT, A3 (Ago2 KO subclone), and D3 (Dicer KO subclone) were seeded at 7 x 10^5 cells in 2 mL complete media in a 6 well plate overnight. Cells were then transfected with *F. hepatica* mature miRNA fhe-miR-125b-5p canonical (Can) and isomiR (Iso) mimics (20 nM) for 24 hours, followed by *E. coli* LPS (20 ng/mL) stimulation for 6 hours as detailed in Section 3.4.3. Cytokine secretion was quantified by ELISA, and the expression of endogenous genes were measured by RT-qPCR as previously described in Sections 3.4.5, 3.4.6 and 3.4.8.

4.2.11. Statistical analysis

All statistical analyses were performed using GraphPad Prism software (version 10). Comparisons between treatment groups were conducted using one-way ANOVA, two-way ANOVA, and/ or Student unpaired t-tests, as specified in the figure legends. Results were considered statistically significant at $p \leq 0.05$.

4.3. Results

4.3.1. Generation of Ago2 and Dicer gene knockout RAW264.7 murine macrophage cells

To investigate whether host Ago2 and Dicer are required for the maturation and RNAi activity of the *Fasciola hepatica*-derived fhe-miR-125b in host cells, we aimed to generate Ago2 and Dicer knockout cell lines. As this was not feasible in primary macrophages, the RAW264.7 macrophage cell line was selected as a model, as these are a commonly used cell line for *in vitro* analysis of macrophage inflammatory responses. However, while this cell line closely mimics the activity of BMDMs, they have some phenotypical and functional differences compared to primary cells [322, 323]. Before embarking on the creation of KO cells, the effect of transfection with the Fasciola miRNAs was first tested to ensure their regulatory activity was also evident in these cell lines. Mimicking the experimental conditions used in BMDMs to induce an M1 phenotype with LPS, RAW264.7 cells responded similarly to BMDMs, with elevated secretion of the proinflammatory cytokines TNF and IL6 (Figure 3.5). However, the levels of TNF and IL6 differed from those in BMDMs, with RAW264.7 cells producing much higher quantities of TNF and lower amounts of IL6, likely reflecting the acknowledged differences in phenotype and biological activity between immortalized macrophage cell lines and primary BMDMs. Nonetheless, using this model, fhe-miR-125b-5p exerted a suppressive effect on LPS-induced cytokine production (Figure 4.1) comparable to that observed in BMDMs (Chapter 3). Specifically, TNF expression was significantly reduced by the isomiR (Figure 4.1A), whereas IL6 was significantly suppressed by both the canonical and isomiR mimics (Figure 4.1B). These results supported the use of RAW264.7 cells to examine whether Ago2 and Dicer are required for the function of parasite-derived miRNAs in host macrophages.

The Monash Genome Modification Platform (Monash University, Australia) was contracted to generate CRISPR-Cas9-mediated knockouts of Ago2 and Dicer in RAW264.7 cells. From this effort, three Ago2 homozygous KO subclones (A2, A3, and A5), three Dicer homozygous KO subclones (D1, D2, and D3), and one heterozygous Dicer KO clone (DH) were obtained (Table 4.2). Knockout status was verified by PCR and sequencing (Table 4.2; Appendix C, D). All three Ago2 KO clones (A2, A3, A5) were derived from a single Ago2 KO clone and carried a 37 bp deletion at the sgRNA1 site, together with a 1 bp insertion at the second target site. The three Dicer homozygous KO subclones were derived from three distinct clones and exhibited distinct disruptive mutations: D1 carried a large 40,098 bp deletion at sgRNA1 and a 1 bp insertion at the second site; D2 had a 40,008 bp deletion at sgRNA1 and a 5 bp deletion at the

second site; and D3 harboured a 40,223 bp deletion with a single base change upstream of sgRNA1 and a 5 bp deletion at the second site. The heterozygous Dicer KO (DH) contained a 40,002 bp deletion at sgRNA1 but retained a wild-type allele at the second site. Collectively, these sequencing results confirmed successful generation of both Ago2 and Dicer KO RAW264.7 subclones for downstream functional assays.

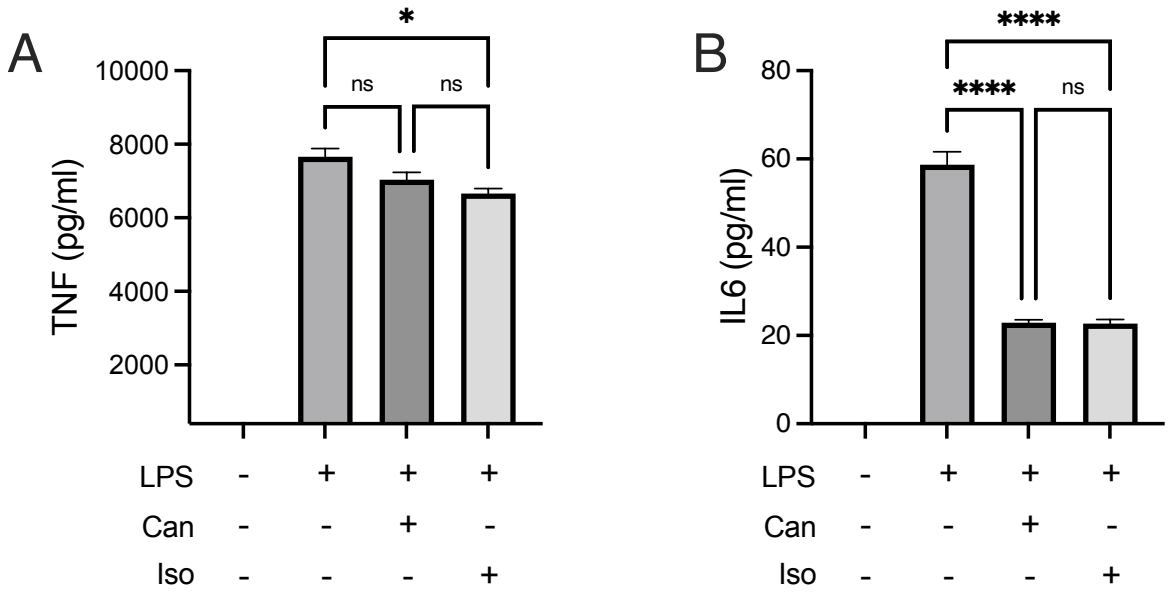


Figure 4.1. LPS induced proinflammatory cytokines were downregulated by fhe-miR-125b-5p in RAW264.7 murine macrophage cell line. *RAW264.7 cells were transfected with canonical (Can) and isomiR (Iso) mimics of fhe-miR-125b-5p (20 pmol/mL) and after 24 h, cells were stimulated with LPS (20ng/mL) for 6 h. Secretion of TNF (A) and IL6 (B) in the culture supernatant was quantified by ELISA. Data are presented as mean (n = 3 technical replicates) ± SEM. Statistical analysis was performed using one-way ANOVA followed by Student's unpaired t-test; *p < 0.05, ****p < 0.00005.*

Table 4.2. Ago2 and Dicer1 gene knockout subclones in RAW264.7 cells received from the Monash Genome Modification Platform (Monash University, Australia)

		Allele 1		Allele 2	
Sub-clones received	**Sub-clone ID**	**WT PCR**	**Mutation at sgRNA1 site**	**WT PCR**	**Mutation at sgRNA1 site**
Ago2 subclone 82-2 homozygous KO	A2	597bp	37bp deletion (-41bp/+4bp)	635bp	1bp insertion
Ago2 subclone 82-3 homozygous KO	A3	597bp	37bp deletion (-41bp/+4bp)	635bp	1bp insertion
Ago2 subclone 82-5 homozygous KO	A5	597bp	37bp deletion (-41bp/+4bp)	635bp	1bp insertion
Dicer1 subclone 22-21 homozygous KO	D1	707bp	40098bp	564bp	1bp insertion
Dicer1 subclone 166-1 homozygous KO	D2	797bp	40008bp	558bp	5bp deletion
Dicer1 subclone 173-1 homozygous KO	D3	582bp	40223bp (1bp change upstream of the mutation)	558bp	5bp deletion
Dicer1 subclone 203-1 heterozygous KO	DH	803bp	40002bp	563bp	WT

4.3.2 Growth dynamics of the Ago2 and Dicer gene knockout (KO) RAW264.7 macrophage subclones

To determine whether selecting Ago2 or Dicer had a deleterious effect on the expected biology of the RAW264.7 cells, several phenotypic and functional characteristics of macrophages were profiled prior to using them for experimental work. Cell confluency of the KO subclones was compared with the parental WT cells using Incucyte live-cell imaging. Among the Ago2 KO clones, A2 and A3 exhibited confluency patterns comparable to WT, whereas A5 showed reduced growth, becoming evident from day 3 onwards (Figure 4.2A). For the Dicer KO clones, D1 and the heterozygous clone DH displayed growth rates like WT, while D2 and D3 demonstrated markedly slower proliferation from 24 h (Figure 4.3A). Cytotoxicity levels remained minimal (< 8%) and comparable across all KO and WT cells (Figure 4.2B, 4.3B), indicating that loss of Ago2 or Dicer did not compromise cell viability. Notably, while confluency appeared similar to WT in some clones, all KO lines displayed a modest but consistent reduction in proliferation, more pronounced at 48 h compared to 24 h (Figure 4.2C, 4.3C). Together, these data indicate that disruption of the miRNA biogenesis machinery slows macrophage proliferation without affecting viability.

4.3.3. Ago2 and Dicer KOs differentially influence macrophage migration while preserving phagocytic function

To evaluate whether Ago2 and Dicer deficiency affected the essential effector roles of macrophages, two key functions – migration and phagocytosis, were examined. Migration of cells was assessed via a wound healing assay, in which Ago2 KO subclones, A2 and A3 exhibited migration comparable to WT, whereas A5 showed significantly reduced wound closure, indicating impaired motility (Figure 4.4A). Among the Dicer KO subclones, both D2 and D3 displayed accelerated wound closure from 6 h and 24 h post-wounding respectively, while D1 and the heterozygous clone DH migrated at rates that were similar to WT (Figure 4.5A).

Phagocytosis of pHrodo-labelled bioparticles was comparable across all Ago2 and Dicer KO clones, indicating that disruption of the miRNA biogenesis machinery does not affect the phagocytic capacity of macrophages in the RAW264.7 cells (Figure 4.4B, C; Figure 4.5B, C).

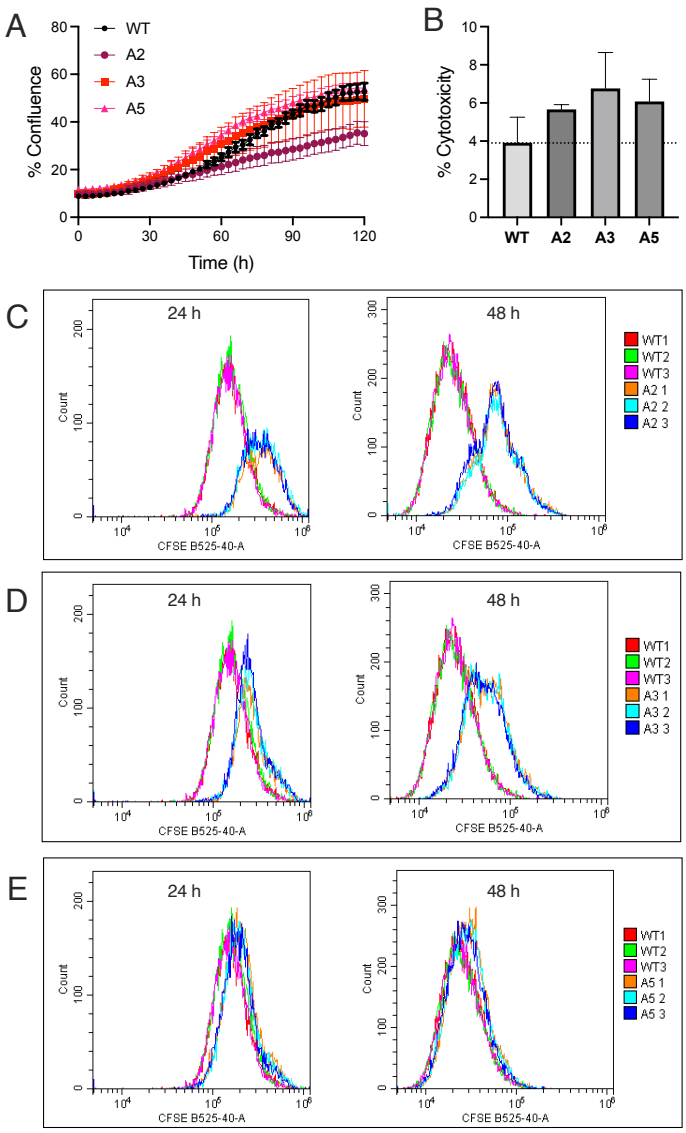


Figure 4.2. Characterization of Ago2 KO cell growth dynamics. *(A) Cell confluency over time. 4000 cells were seeded per well of a 96 well plate overnight before imaging with the Incucyte every 3 h for four days. Percentage confluence was quantified using the Incucyte image analysis module. Data are presented as mean ± SEM (n = 3 technical replicates). (B) Cytotoxicity assay. Cell death was quantified as the percentage of maximum LDH release. Data are shown as mean ± SEM (n = 3 technical replicates). Statistical significance was assessed by one-way ANOVA followed by Student's unpaired t-test. (C–E) CFSE-based cell proliferation assay. Fluorescence histograms of CFSE intensity in Ago2 KO clones A2 (C), A3 (D), and A5 (E) compared with WT cells at 24 h (left) and 48 h (right), with peaks indicating dye dilution corresponding to successive cell divisions. Individual technical replicates are shown (n = 3).*

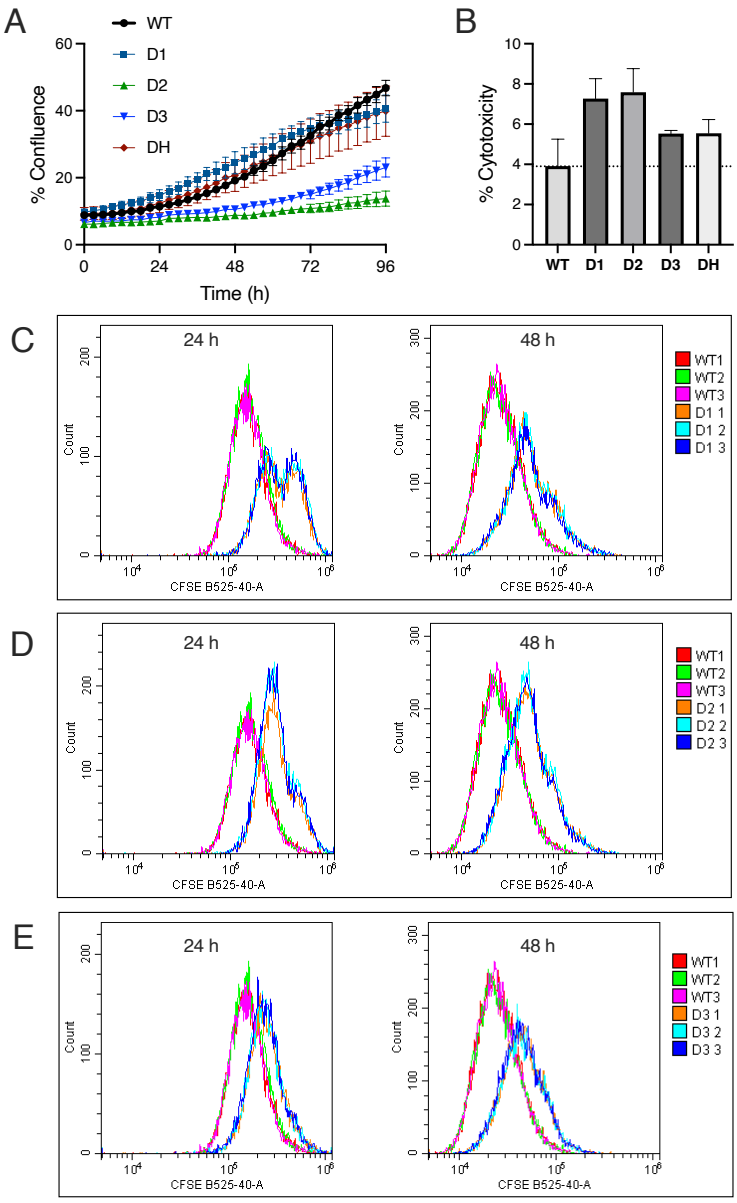


Figure 4.3. Characterization of Dicer KO cell growth dynamics. *(A) Cell confluency over time. 4000 cells were seeded per well of a 96 well plate overnight before imaging with the Incucyte every 3 h for four days. Percentage confluence was quantified using the Incucyte image analysis module. Data are presented as mean ± SEM (n = 3 technical replicates). (B) Cytotoxicity assay. Cell death was quantified as the percentage of maximum LDH release. Data are shown as mean ± SEM (n = 3 technical replicates). Statistical significance was assessed by one-way ANOVA followed by Student's unpaired t-test. (C–E) CFSE-based cell proliferation assay. Representative fluorescence histograms of CFSE intensity in Dicer KO clones: D1 (C), D2 (D), and D3 (E) compared with WT cells at 24 h (left) and 48 h (right). X-axis: CFSE fluorescence (log scale); Y-axis: event count. Peaks indicate dye dilution corresponding to successive cell divisions. Individual technical replicates are shown (n = 3).*

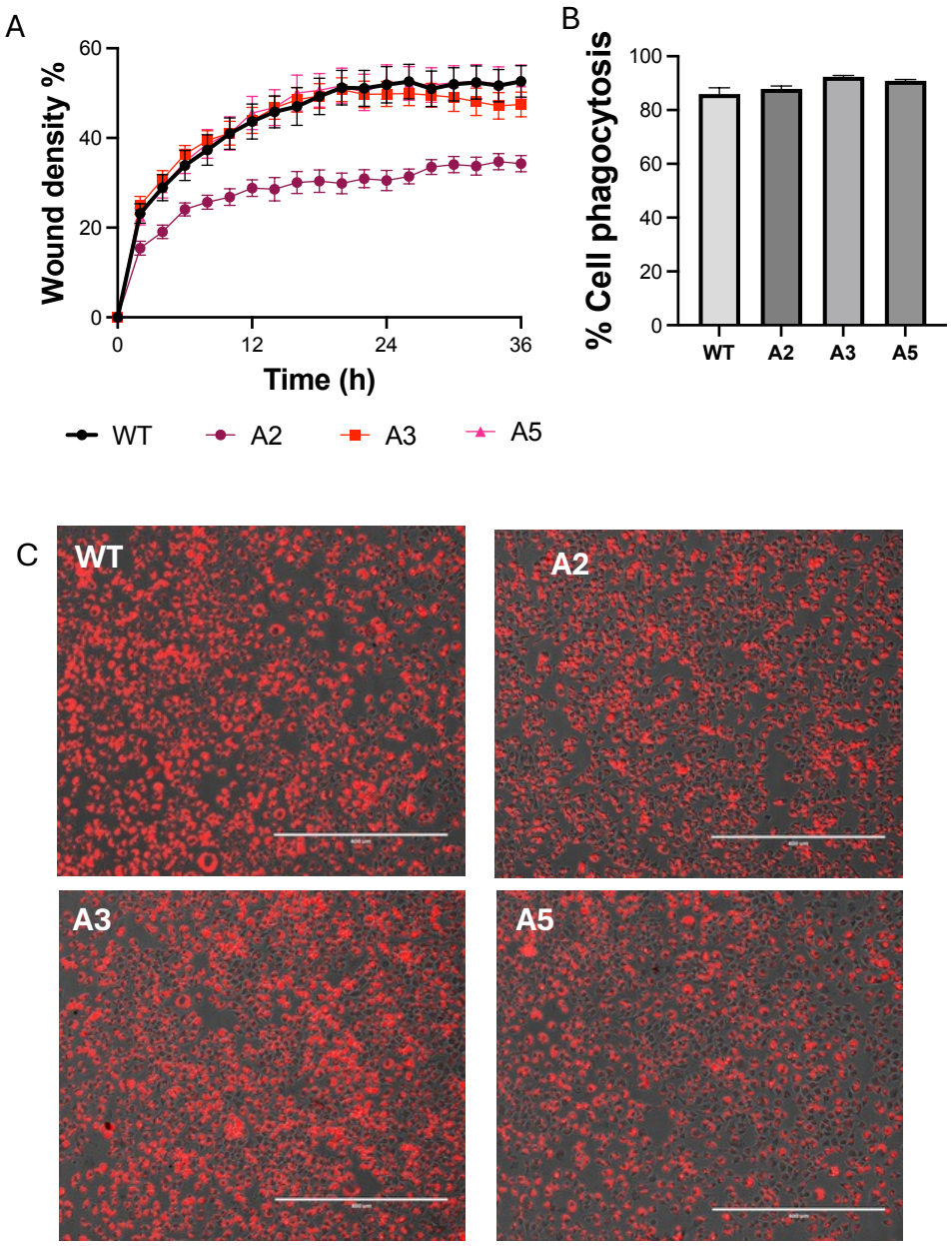


Figure 4.4. Functional characterization of Ago2 KO macrophage clones. *(A) Scratch wound assay. Confluent monolayers in 96-well plates were scratched and imaged every 3 h for up to 36 h using the Incucyte. Percentage wound closure was quantified with the Incucyte analysis module. Data are presented as mean ± SEM of technical replicates (n = 12 technical replicates). (B) Phagocytosis assay. Uptake of pHrodo Red* E. coli *bioparticles (200 µg/mL) by Ago2 KO clones was measured as the percentage of phagocytic cells at 1 h. Data are shown as mean ± SEM (n = 3 technical replicates). (C) Representative fluorescence image of bead uptake at 1 h, acquired with a 10× objective.*

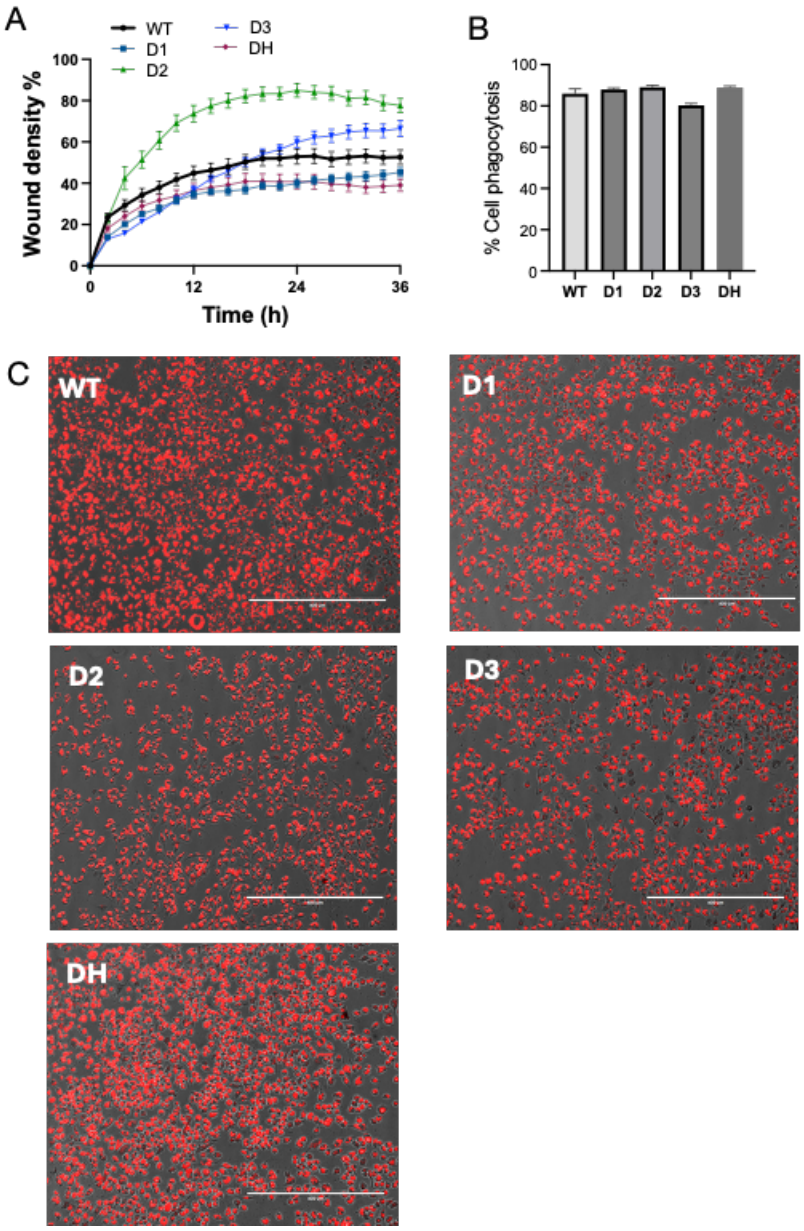


Figure 4.5. Functional characterization of Dicer KO macrophage clones. (A) Scratch wound assay. *Confluent monolayers in 96-well plates were scratched and imaged every 3 h for up to 36 h using the Incucyte. Percentage wound closure was quantified with the Incucyte analysis module. Data are presented as mean ± SEM of technical replicates (n = 12 technical replicates; for D2 and D3, n = 6 technical replicates). (B) Phagocytosis assay. Uptake of pHrodo Red* E. coli *bioparticles (200 µg/mL) by Ago2 KO clones was measured as the percentage of phagocytic cells at 1 h. Data are shown as mean ± SEM (n = 3 technical replicates). (C) Representative fluorescence image of bead uptake at 1 h, acquired with a 10× objective.*

4.3.4. Loss of Ago2 dampens, while loss of Dicer exaggerates, proinflammatory responses to LPS

The KO subclones were next evaluated for their inflammatory response to *E. coli* LPS. All three Ago2 KO clones exhibited TNF production comparable to WT cells (Figure 4.6A). In contrast, the three Dicer homozygous KO subclones produced over threefold higher TNF levels in response to LPS, whereas the heterozygous Dicer clone (DH) responded similarly to WT (Figure 4.6C). Analysis of IL6 secretion revealed that while IL6 was induced in response to LPS in both the Ago2 KO clones and Dicer KO clones, this increase was less than half the elevated level of IL6 observed in WT cells, with the exception of D1, which secreted IL6 at levels comparable to WT (Figure 4.6B, D). These findings indicate that both Ago2 and Dicer contribute to IL6 secretion in response to LPS, whereas TNF regulation is primarily influenced by Dicer in RAW264.7 macrophages.

The expression of selected fhe-miR-125b target genes associated with proinflammatory and M1 macrophage responses (identified in Chapter 3) was next examined. In WT cells, LPS stimulation induced significant upregulation of *Stat3* and *Nod1* (Figures 4.7B, C; Figure 4.8B, C), while *Hif1a*, *Pin1*, and *Runx1* expression remained comparable to untreated controls (Figure 4.7 A, D, E; Figure 4.8A, D, E). In contrast, *P2rx7* expression was significantly downregulated following LPS treatment (Figure 4.7F; Figure 4.8F).

In the Ago2 KO clones, gene expression changes were similar or reduced compared to WT, consistent with the cytokine secretion profile (Figure 4.7A-F). The LPS-induced upregulation of *Stat3* and *Nod1* observed in WT cells was absent in all three Ago2 KO clones (Figures 4.7B, C). *P2rx7* expression was further downregulated in the Ago2 KOs, with A2 and A3 showing significantly lower levels than LPS treated WT cells (Figure 4.7F), while the reduction in A5 did not reach significance ($p = 0.07$). *Runx1* was also consistently downregulated in all three Ago2 KO clones in response to LPS, with levels significantly lower than WT (Figure 4.7E). *Hif1a* expression was variable across clones: A5 responded to LPS similarly to WT, showing a slight but non-significant increase ($p = 0.14$), whereas A3 displayed significant downregulation, and both A2 and A3 had significantly lower *Hif1a* levels compared to LPS-treated WT (Figure 4.7A).

In contrast, but consistent with the cytokine data, the Dicer KO clones exhibited an exaggerated proinflammatory transcriptional response (Figure 4.8 A-F). All three homozygous Dicer KO

clones showed stronger upregulation of *Stat3* and *Pin1* (> 1.5-fold higher than WT) following LPS stimulation (Figure 4.8B, D). *Hif1a* and *Nod1* were also elevated in D2 and D3, whereas D1 responded similarly to WT (Figure 4.8A, C). Unlike WT and Ago2 KO, *P2rx7* expression was not downregulated in any of the homozygous or heterozygous Dicer KO clones after LPS treatment (Figure 4.8F). *Runx1* expression remained unchanged in response to LPS across the Dicer KOs; however, basal *Runx1* levels were elevated in the homozygous clones (Figure 4.8E). Unlike the Dicer homozygous KOs, the heterozygous Dicer clone (DH) displayed gene expression profile broadly comparable to WT (Figure 4.8A-F).

4.3.5. Selection of subclones A3 and D3 as representative Ago2 and Dicer KOs

To study the effect of fhe-miR-125b in Ago2 KO and Dicer KO macrophages, representative clones were selected to capture the defining knockout features while limiting clone-specific confounders. Clone A3 was selected as the representative Ago2 KO line. In contrast to A5, which displayed reduced proliferation and impaired migration, A3 exhibited growth and wound healing responses comparable to WT cells (Figure 4.2A; Figure 4.4A). Functionally, A3 recapitulated the defining Ago2-deficient phenotype, showing WT-like TNF secretion with reduced IL6 production (Figure 4.6A, B), absence of LPS-induced *Stat3* and *Nod1* upregulation (Figure 4.7B, C), and a more pronounced downregulation of *P2rx7* relative to WT (Figure 4.7F). Furthermore, unlike A2, which showed lower basal expression of *Stat3*, *Pin1*, *P2rx7* compared to WT in the untreated cells, A3 maintained basal expression levels closer to WT for all genes (Figure 4.7A-F). Together, these features indicate that A3 captures the canonical Ago2 loss profile while minimising clone-specific confounders.

For the Dicer KO, clone D3 was selected as the representative homozygous line. D3 exhibited a consistent Dicer-null phenotype, characterised by a 4.3-fold increase in TNF induction (Figure 4.6 C), a 0.15-fold reduction in IL6 secretion (Figure 4.6D), exaggerated LPS responses for *Stat3* and *Pin1* (> 1.7-fold relative to WT), elevated *Hif1a* and *Nod1* expression, and failure to downregulate *P2rx7* following LPS stimulation (Figure 4.8A-F). These transcriptional changes were consistent with other homozygous Dicer KOs, while the basal expression of these genes in D3 remained similar to WT. Compared with D1, which often behaved like WT, and D2, which displayed very enhanced migration, D3 most reliably reflected the core transcriptional and inflammatory features of Dicer deficiency without outlier behaviour.

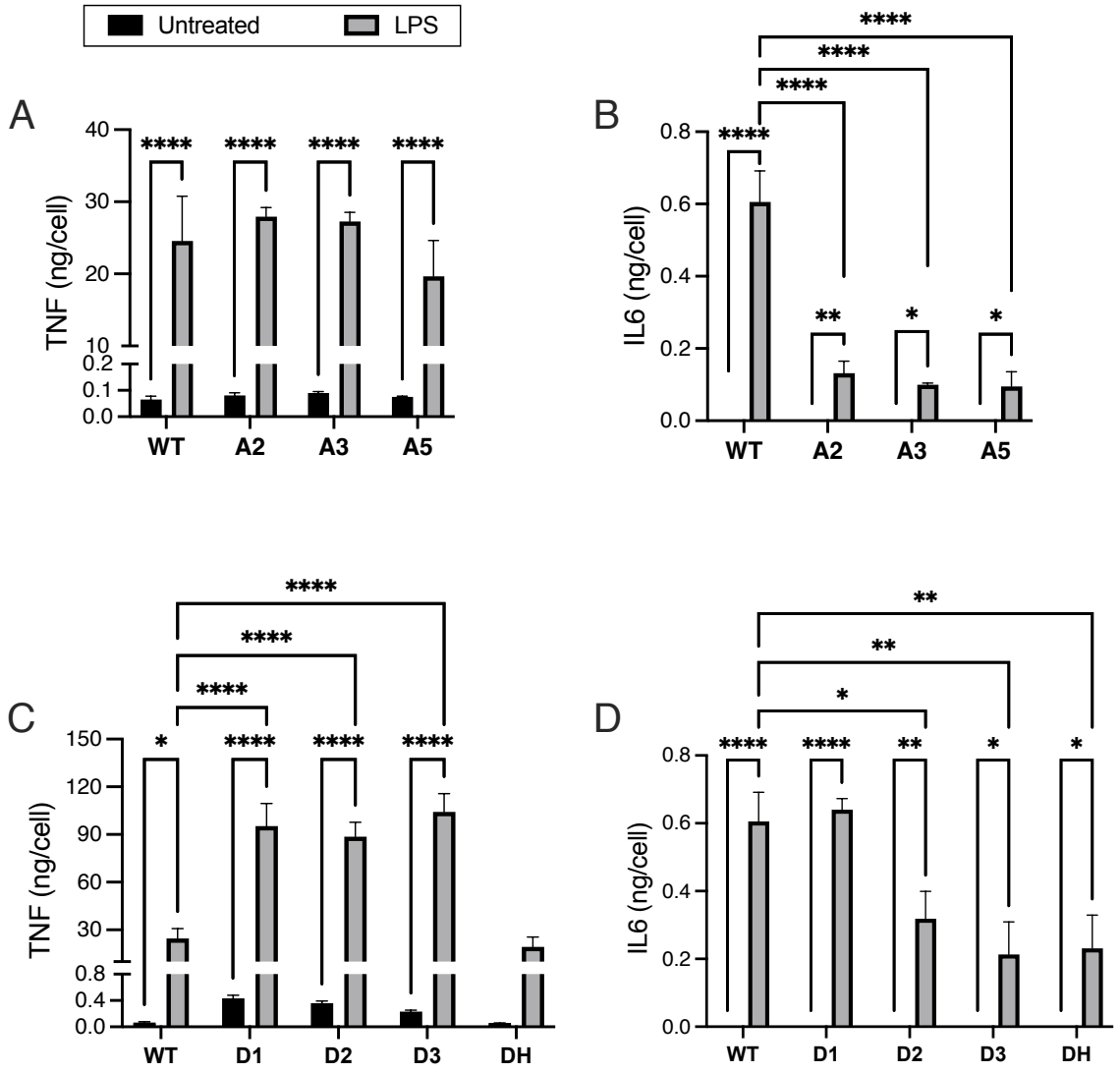


Figure 4.6. Proinflammatory cytokine production by Ago2 KO and Dicer KO clones. *(A, B) Ago2 KO and (C, D) Dicer KO macrophages were stimulated with LPS (20ng/mL) for 6 h. Secretion of TNF (A, C) and IL6 (B, D) in the culture supernatant was quantified by ELISA and normalized to cell number at the time of collection. Data are presented as mean ± SEM from six replicates from two independent experiments. Statistical analysis was performed using two-way ANOVA followed by Student's unpaired t-test; *p < 0.05, **p < 0.005; ***p < 0.0005; ****p < 0.00005.*

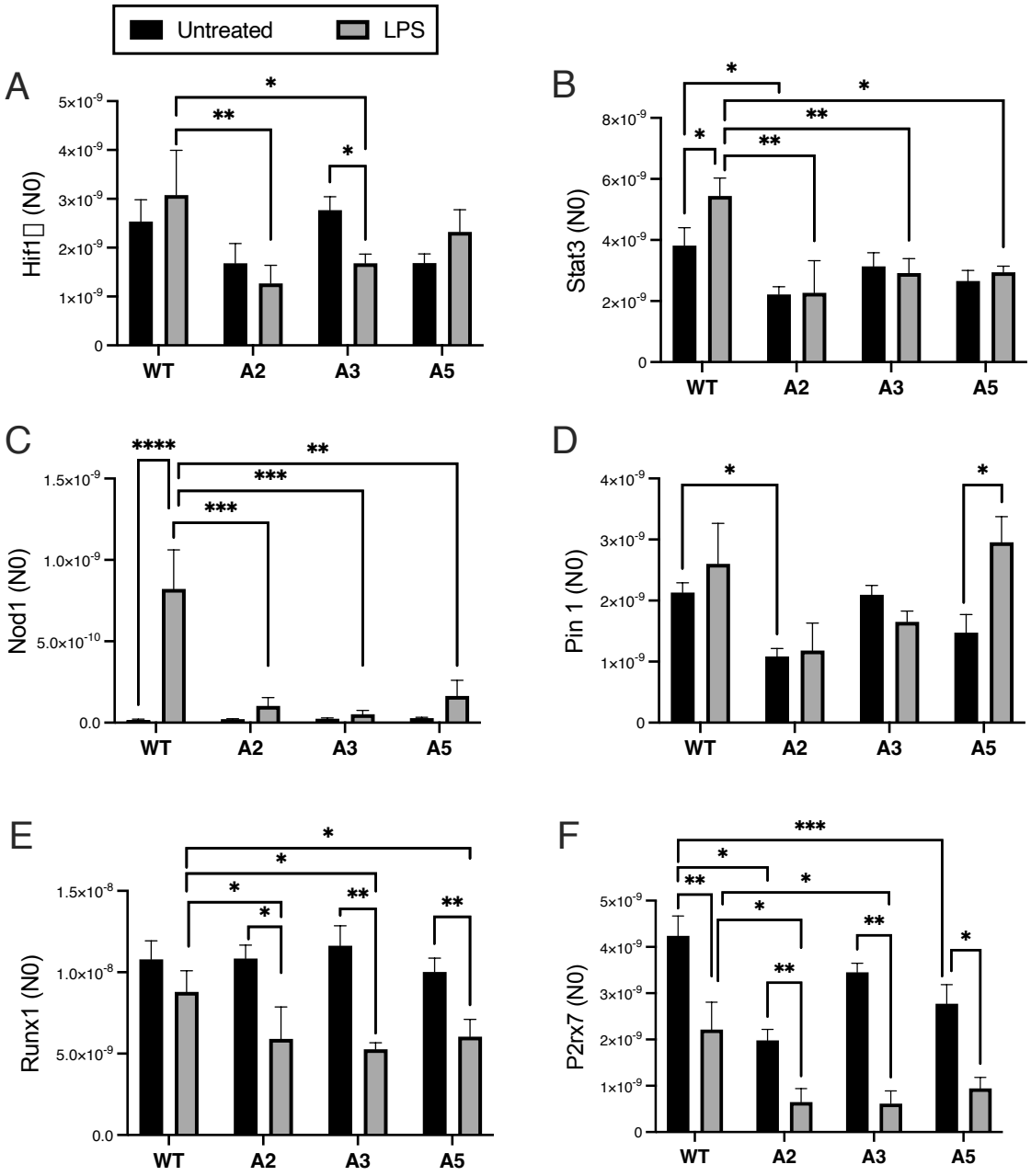


Figure 4.7. Assessment of M1 polarization and proinflammatory gene expression in Ago2 KO macrophages in response to LPS. *Gene expression was measured by qPCR in untreated and cells treated with LPS (20ng/mL) for 6 h. Expression levels are presented as starting quantities (N_0) using LinRegPCR (v.11.). Data are presented as mean ± SEM from six replicates pooled from two independent experiments. Mean ± SEM are shown. Statistical analysis was performed using two-way ANOVA followed by Student's unpaired t-test; *p < 0.05, **p < 0.005; ***p < 0,0005; ****p < 0.00005.*

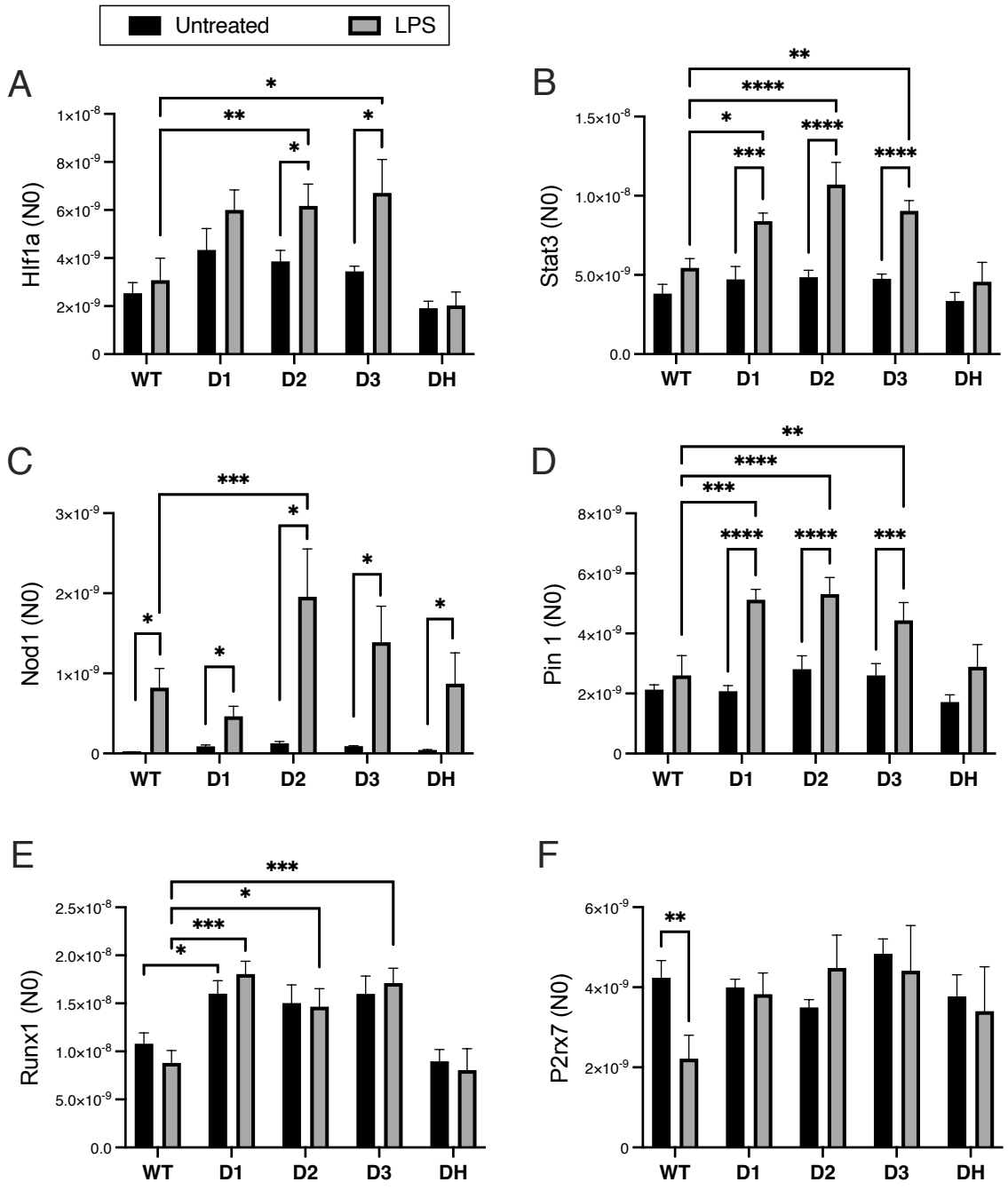


Figure 4.8. Dicer KO macrophages had elevated proinflammatory gene expression in response to LPS compared to WT. *Gene expression was measured by qPCR in untreated cells and cells stimulated with LPS (20 ng/mL) for 6 h. Expression levels are reported as starting quantities (N_0) calculated using LinRegPCR (v11). Data are presented as mean ± SEM from six replicates pooled from two independent experiments. Statistical analysis was performed using two-way ANOVA; *p < 0.05, **p < 0.005, ***p < 0.0005, ****p < 0.00005.*

4.3.6. Functional activity of fhe-miR-125b-5p was preserved in Ago2- and Dicer-deficient macrophages

To assess whether Ago2 and Dicer are required for the activity of worm-derived miRNAs in host cells, WT, Ago2 KO (A3), and Dicer KO (D3) RAW264.7 cells were transfected with canonical and isomiR mimics of fhe-miR-125b-5p for 24 hours, followed by LPS stimulation for 6 hours. As expected, both the canonical and isomiR mimic of fhe-miR-125b suppressed TNF in WT cells (Figure 4.9A; Figure 4.10A). Similarly, in Ago2 KO cells, both mimics suppressed TNF to a similar extent (Figure 4.9B). However, when fold change relative to LPS treated controls was examined, the canonical mimic exhibited a significantly greater effect in the Ago2 KO compared with WT (Figure 4.9D). Notably, in Dicer KO cells, both the canonical and isomiR mimics produced a significantly stronger suppression of TNF than in WT cells (Figure 4.9C, D). IL6 secretion was also reduced by both mimics in Ago2 KO cells (Figure 4.10 B), comparable to WT (Figure 4.10A, D), whereas IL6 levels in Dicer KO cells remained undetectable even after LPS stimulation, consistent with the very low levels produced by these KO clones. These findings indicate that *F. hepatica*-derived mature miRNAs do not require Ago2 or Dicer to exert their function in host cells. In contrast, the comparator mimic, mmu-miR-23a, upregulated TNF and IL6 in WT cells (Figure 4.9A; Figure 4.10A) but failed to do so in both Ago2 and Dicer KO cells (Figure 4.9B-D; Figure 4.10B-D), suggesting that, unlike fhe-miR-125b, miR-23a may require Ago2 and Dicer for its proinflammatory activity in macrophages.

Building on the previous observation that fhe-miR-125b downregulates specific predicted targets in LPS-stimulated bone marrow derived macrophages (BMDMs) (Chapter 3), and given that these genes were also upregulated by LPS in at least one of the three cell types (WT, Ago2 KO, Dicer KO) (Figure 4.7; Section 4.3.5), four candidate genes – *Hif1a*, *Nod1*, *Stat3*, and *Pin1* were selected for further analysis.

In WT cells, consistent with earlier findings, *Stat3* and *Nod1* were significantly upregulated following LPS stimulation (Figure 4.11D, G), although neither gene was repressed by the fhe-miR-125b mimics. The expression of *Hif1a* and *Pin1* was not significantly altered by LPS, and was unchanged following transfection of the parasite mimics (Figure 4.11A, J). In Ago2 KO cells, only *Nod1* was induced by LPS, and while the canonical mimic showed no effect, the isomiR significantly suppressed *Nod1* expression compared with the LPS-treated no-mimic control (Figure 4.11E). On the other hand, LPS had no significant impact on *Hif1a*, *Stat3*, or

Pin1 expression in Ago2 KO cells, and correspondingly, the mimics had no measurable effect (Figure 4.11B, H, K).

In contrast, Dicer KO cells displayed a robust transcriptional response to LPS, with marked upregulation of *Hif1a*, *Nod1*, and *Stat3* (Figure 4.11C, F, I). Under these conditions, both the fhe-miR-125b mimics strongly repressed all three genes. *Pin1* expression was modestly increased by LPS, although not significantly ($p = 0.07$), and neither mimic produced a significant repression (Figure 4.11L). The canonical and isomiR mimics exhibited comparable repression of all four target genes in Dicer KO cells, consistent with previous findings in BMDMs under the same experimental conditions (LPS stimulation for 6 h), suggesting that both mimics retain equivalent functional activity in the absence of Dicer.

Consistent with the results in BMDMs (Chapter 3), mmu-miR-23a did not alter the expression of the four target genes in WT or Ago2 KO cells (Figure 4.11A-L). However, in Dicer KO cells, although mmu-miR-23a failed to influence LPS-induced TNF and IL6 production (in contrast to WT), its transfection unexpectedly led to the downregulation of the four measured fhe-miR-125b target genes. Given the established proinflammatory role of mmu-miR-23a, this paradoxical repression is unlikely to be a direct effect of the mimic itself. Instead, it may reflect compensatory regulatory mechanisms triggered by the heightened basal inflammation associated with Dicer deficiency. In this altered context, secondary pathways such as enhanced activity of negative feedback regulators (e.g., suppressors of cytokine signalling) may be activated to limit further escalation of the inflammatory response.

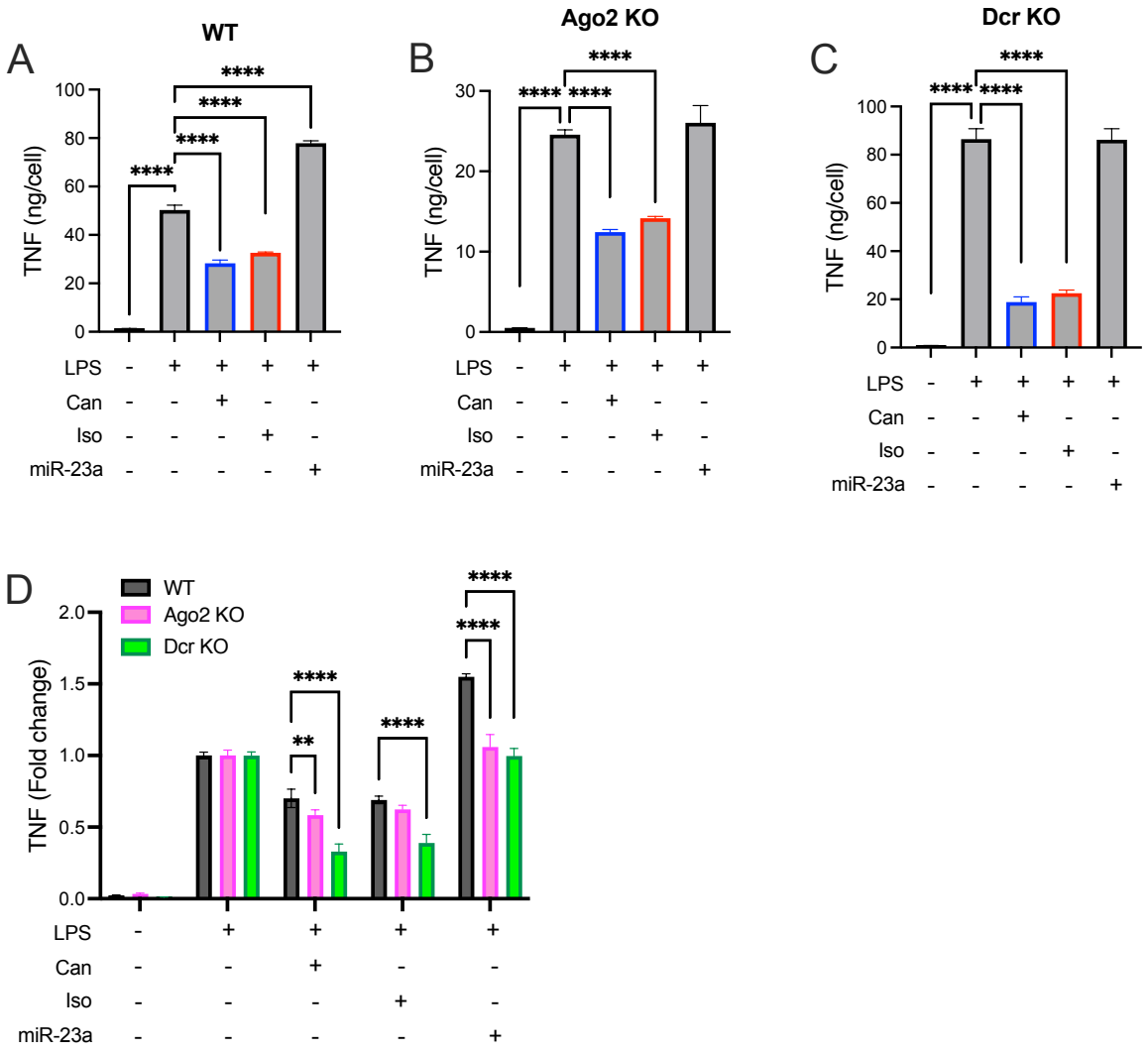


Figure 4.9. fhe-miR-125b-5p repressed LPS-induced TNF secretion in Ago2 and Dicer KO cells. *WT, Ago2 KO and Dicer (Dcr) KO macrophages were transfected with canonical (Can) and isomiR (Iso) mimics of fhe-miR-125b-5p (20 pmol/mL) or mmu-miR-23a-3p. After 24 h, cells were stimulated with LPS (20 ng/mL) and 6 hours later, the secretion. of TNF was measured in the cell supernatants by ELISA. TNF concentration normalised to cell number for each cell type at the time of supernatant collection in (A) WT, (B) Ago2 KO and (C) Dcr KO cells (n = 3 from 1 experiment). (D) Comparison of mimic effects across the three cell types shown as fold change in TNF concentration relative to LPS-stimulated vehicle controls for each cell type (n = 6, pooled from two independent experiments, except for miR-23a which had n = 3 from one experiment). Data are presented as mean ± SEM. Statistical analysis was performed using two-way ANOVA; ** p < 0.005, ***p < 0.0005, ****p < 0.00005.*

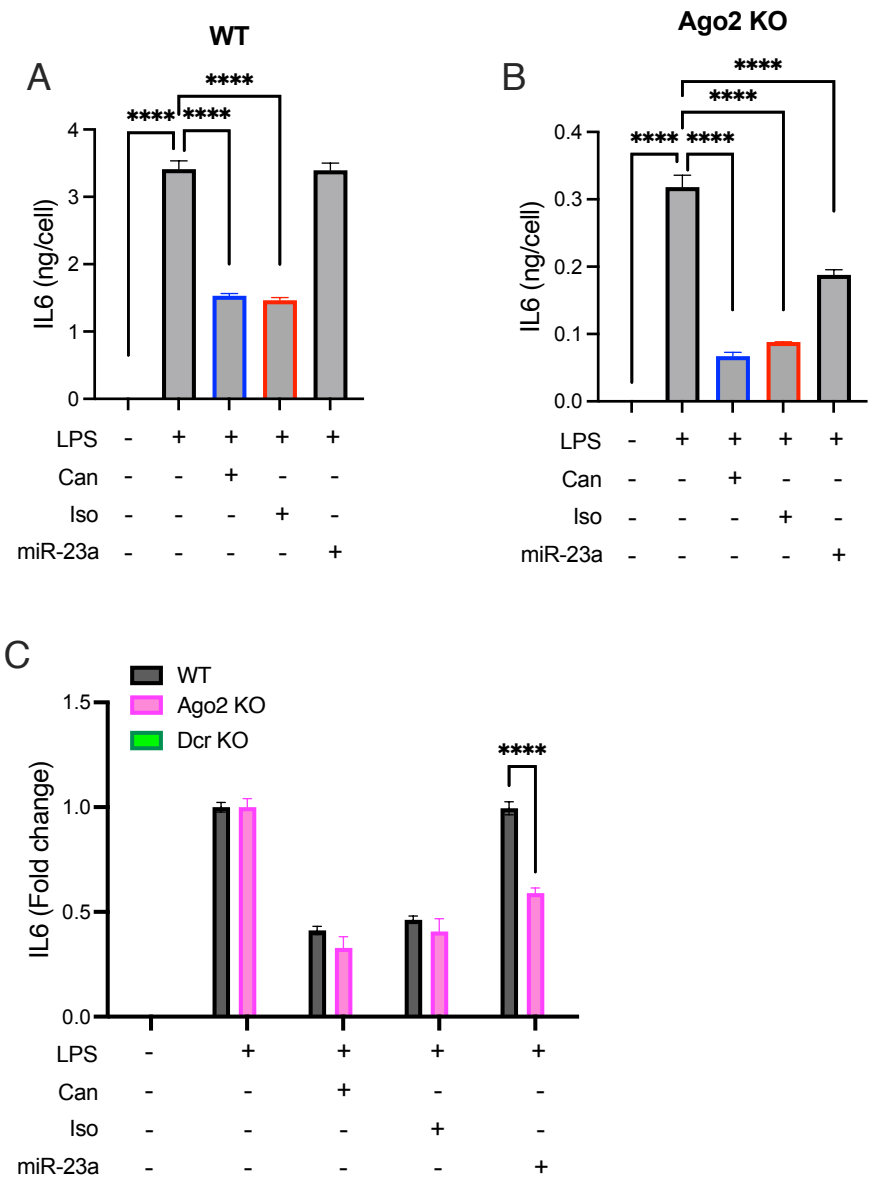


Figure 4.10. fhe-miR-125b-5p repressed LPS-induced IL6 secretion in Ago2 KO cells. *WT, Ago2 KO and Dicer KO macrophages were transfected with canonical (Can) and isomiR (Iso) mimics of fhe-miR-125b-5p (20 pmol/mL) or mmu-miR-23a-3p. After 24 h, cells were stimulated with LPS (20 ng/mL) and 6 hours later, the secretion of IL6 was measured in the cell supernatants by ELISA. IL6 concentration normalised to cell number at the time of supernatant collection in (A) WT, (B) Ago2 KO cells. IL6 was undetectable in Dicer KO cells; (D) Comparison of mimic effects across the cell types shown as fold change in IL6 concentration relative to LPS-stimulated vehicle controls for each cell type. Data are presented as mean ± SEM (n = 6, pooled from two independent experiments, except for miR-23a which had three replicates from one experiment). Statistical analysis was performed using two-way ANOVA; ****$p < 0.00005$.*

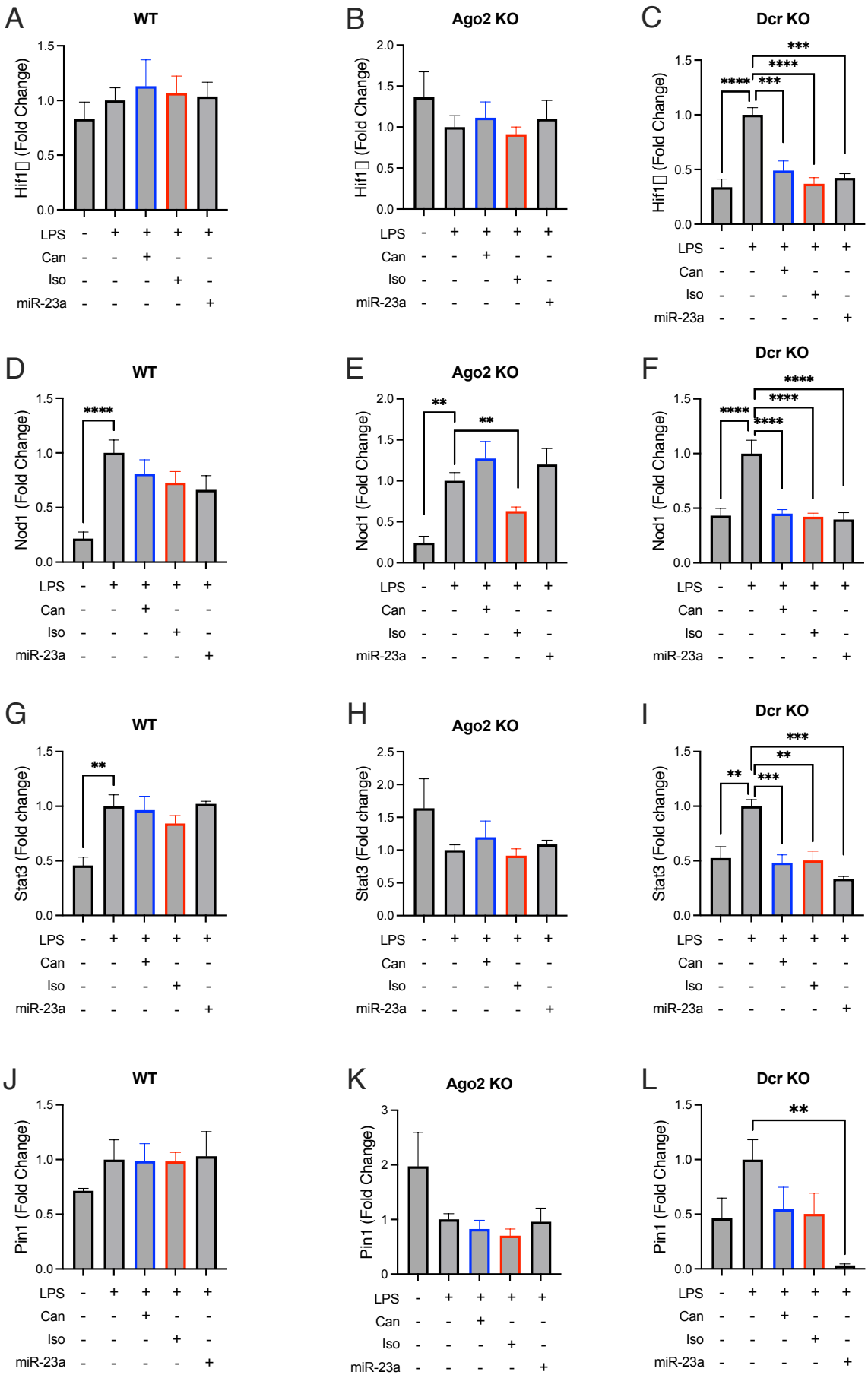

A
WT
Hif1α (Fold Change)
B
Ago2 KO
Hif1α (Fold Change)
C
Dcr KO
Hif1α (Fold Change)
D
WT
Nod1 (Fold Change)
E
Ago2 KO
Nod1 (Fold Change)
F
Dcr KO
Nod1 (Fold Change)
G
WT
Stat3 (Fold change)
H
Ago2 KO
Stat3 (Fold change)
I
Dcr KO
Stat3 (Fold change)
J
WT
Pin1 (Fold Change)
K
Ago2 KO
Pin1 (Fold Change)
L
Dcr KO
Pin1 (Fold Change)
LPS
Can
Iso
miR-23a

Figure 4.11. Assessment of fhe-miR-125b-5p mediated suppression of endogenous target genes in Ago2 and Dicer KO macrophages. *WT, Ago2 KO, and Dicer (Dcr) KO cells were transfected for 24 h with canonical (Can) or isomiR (Iso) mimics of fhe-miR-125b-5p (20 pmol/mL), or with a control mimic (mmu-miR-23a), followed by LPS stimulation (20 ng/mL) for 6 h. qPCR analysis was performed using LinRegPCR (v.11), with expression levels (N_0) reported as fold change relative to LPS stimulated controls without mimic. Data are shown as mean ± SEM (n = 6; combined from two experiments; miR-23a, n = 3 from one experiment). Statistical analysis was performed using two-way ANOVA followed by Student's unpaired t test. ** p < 0.005, ***p < 0.0005, ****p < 0.00005.*

4.4. Discussion

This chapter sought to elucidate the distinct roles of the miRNA biogenesis components Argonaute 2 (Ago2) and Dicer in processing parasite-derived miRNAs within host macrophages using CRISPR-Cas9 knockout RAW264.7 murine macrophage cells. The primary findings demonstrate that knockout (KO) of Ago2 or Dicer impairs cell proliferation, alters LPS-induced proinflammatory responses in unique ways, and that the Fasciola-derived miRNA, fhe-miR-125b-5p, maintains immune regulatory activity even in the absence of these core RNA interference (RNAi) proteins.

Characterization of Ago2- and Dicer-deficient macrophages revealed reduced proliferation with cell confluence equal to, or lower than, wild-type (WT) controls, consistent with previous reports linking Ago2 or Dicer loss to delayed proliferation via impaired miRNA processing and downstream effects on cell cycle regulators [130, 324-329]. Importantly, cell viability remained unchanged indicating reduced proliferation was not due to cytotoxicity.

Phagocytic activity remained unaffected in both Ago2 and Dicer KO macrophages, suggesting that this evolutionarily ancient and fundamental macrophage function is likely robust to disruptions in RNA interference pathways. In contrast to this data, it has been reported that Dicer-deficient primary murine macrophages show increased uptake of dextran, albeit via endocytosis rather than phagocytosis [330]. It is possible that this variability in observations arise from differences between immortalized RAW264.7 cells and primary macrophages, with the latter generally displaying higher phagocytic efficiency and more physiologically relevant responses due to inherent variation in receptor expression and signalling pathways [331]. Furthermore, other studies have reported a reduced uptake of myelin debris and apoptotic cells in Dicer-deficient macrophages [332, 333], which may reflect the distinct mechanisms employed for bacterial versus endogenous target uptake. While phagocytosis of bacteria like *E. coli* is a rapid, pathogen clearance function relying on recognition of conserved microbial patterns, clearance of cellular remnants requires more complex signalling, metabolic input, and M2-like reprogramming [334]. Collectively, these inconsistencies likely reflect differences in the targets assessed, the pathways engaged, and the cellular context.

The second functional assessment showed a variable effect of Ago/Dicer deficiency in macrophage migration, with some KO clones resembling WT, one Ago2 KO clone showing

reduced migration, and two Dicer KO clones displaying enhanced migration. miRNAs are well-established regulators of macrophage migration, and distinct miRNA signatures in conditions such as diabetes and atherosclerosis have been shown to alter migratory capacity compared to healthy cells [335, 336]. Consistent with this, the effects of Ago2 or Dicer ablation vary across cell types. For instance, Ago2 deficiency reduces migration in colorectal cancer cells [326] whereas in brain cancer cell promotes cell migration [337]. Similarly, Dicer ablation delays migration in T cells, and hepatocellular carcinoma cells [338, 339], yet enhances migration in tumour cell lines such as MCF-7, U251, and 7901 [340]. These findings highlight the tissue- and context-specific roles of Ago2, Dicer, and miRNAs in dynamically regulating cell migration. As such, the variability observed among Ago2 and Dicer KO subclones in this study likely reflects clonal heterogeneity.

Non-isogenic parental cell lines were used for the generation of Ago2 and Dicer knockouts, which would have permitted background genetic differences to be propagated and amplified during clonal selection. This highlights the importance of employing isogenic cell lines when dissecting the functional consequences of gene loss. Additional factors, such as compensatory adaptations, incomplete knockout efficiency, or stochastic effects introduced during CRISPR/Cas9 editing, may also have contributed, limitations that have been widely recognised in genome editing studies [341]. Although the KO clones were validated at the sequence level, confirmation of the absence of Ago2 and Dicer protein expression by Western blot remains necessary to fully validate the absence of these proteins.

The Ago2 and Dicer KO cells displayed divergent proinflammatory responses compared to WT cells. Ago2 deficiency dampened IL6 production and altered transcriptional responses, with *Stat3* failing to show any induction above basal levels and *Nod1* upregulated only modestly compared to the stronger induction observed in WT cells, while TNF secretion remained unaffected. This mirrors previous findings showing mutation of Ago2 (that impairs miRNA binding) in macrophages dampens expression of IL6 and IL1ß, while leaving TNF unchanged [313]. miRNAs are well established regulators of the IL6/JAK/Stat3 pathway [342]. Thus, the suppressed IL6 production and lack of *Stat3* induction are reflective of broader disruption of this regulatory axis following Ago2 loss, with reduced IL6 further compounding the effect, as IL6 is a key driver of *Stat3* activation [343]. Similarly, miRNAs and *Nod1* participate in a tightly regulated feedback loop, regulating one another to balance immune gene expression and inflammation [344, 345], the reduced *Nod1* induction in response to LPS may

reflect disruption of this regulatory balance in the Ago2 KO cells. Attenuated *Nod1* signalling could then contribute to the reduced IL6 production [346, 347], reinforcing the dampened proinflammatory profile observed in the Ago2-deficient macrophages.

In contrast, Dicer KO exaggerated TNF secretion while reducing IL6 and enhanced expression of *Stat3*, *Nod1*, *Pin1*, and *Hif1a*. This phenotype is consistent with other studies that have shown that disruption of Dicer in macrophage leads to heightened proinflammatory M1 phenotype, that has been characterised for Dicer in balancing macrophage polarization, mediating the balance between pro-inflammatory (M1) and anti-inflammatory (M2) state [320, 330, 348, 349]. Supporting this, Dicer heterozygous macrophages largely resembled WT cells in proliferation, confluence, and LPS responsiveness, with the notable exception of reduced IL6 secretion, which mirrored the Dicer homozygous KO phenotype. This suggests that while most cellular functions can tolerate partial loss of Dicer, IL6 production is particularly sensitive to reduced abundance of Dicer, reflecting the complex transcriptional and epigenetic mechanisms governing IL6 regulation and the fine balance required for effective inflammatory resolution [350, 351].

While both RAW264.7 cells and bone marrow derived macrophages (BMDMs; Chapter 3) responded to LPS with increased proinflammatory cytokine secretion and gene induction, notable differences were observed in the magnitude and profile of these responses. These differences reflect fundamental distinctions between primary macrophages and immortalised tumour-derived cell lines, underscoring the limitations of using immortalised cells as surrogates for primary macrophages, although they remain indispensable for functional studies requiring stable genetic knockouts.

Importantly, the three targets suppressed by fhe-miR-125b mimics in BMDMs, *Hif1a*, *Stat3*, and *Nod1* were not repressed in WT RAW264.7 cells. The lack of *Hif1a* repression may be attributed to its absence of LPS induced upregulation, whereas *Stat3* and *Nod1* were significantly induced by LPS but remained unaffected by the mimics. In Dicer KO cells, however, strong suppression of all four genes*, Hif1a*, *Stat3*, *Nod1*, and *Pin1* was observed, coinciding with their more robust LPS induced upregulation compared with WT cells. This pattern suggests that greater induction of proinflammatory target genes may be required for fhe-miR-125b mimics to exert detectable suppression. Varying the dose or duration of LPS stimulation or applying additional ligands (e.g. IFNγ) for stronger proinflammatory gene

induction, could clarify this threshold effect. Moreover, the suppression of these genes in Dicer KO cells, and the selective suppression of *Nod1* the only gene upregulated in Ago2 KO cells by the fhe-miR-125b isomiR, may reflect increased availability of the RNAi machinery due to disrupted miRNA biogenesis in these knockouts. Reintroducing Dicer or Ago2 into the KO cells would provide a means to validate this. Further, transcriptomic profiling of these cells, with and without fhe-miR-125b mimic treatment, would provide broader insights into global gene expression changes in WT versus knockout backgrounds and clarify the specific targets modulated by the mimic in this experimental system.

A pivotal outcome of this study is the finding that fhe-miR-125b-5p retained immune-regulatory activity despite Ago2 or Dicer ablation. These findings suggest that parasite miRNAs may not be strictly dependent on these host components and may retain function through redundant or non-canonical mechanisms. In mammalian cells, Ago2 loss impairs but does not abolish miRNA function due to compensatory activity from the remaining Ago proteins (Ago1, Ago3, and Ago4) [311, 352, 353]. Notably, Ago1 expression has been shown to increase following Ago2 ablation in various cell types [354, 355]. This raises the possibility that fhe-miR-125b's regulation of proinflammatory genes is not necessarily reliant on Ago2's catalytic slicing activity, which mediates irreversible mRNA degradation, and that the parasite miRNA may instead engage alternative Ago proteins to exert its regulatory effects.

Differences between the canonical and isomiR forms of fhe-miR-125b in in Ago2 KO cells further supports this. The canonical miRNA suppressed TNF more effectively than in WT, while the isomiR, but not the canonical mimic, repressed *Nod1* in the absence of Ago2. These discrepancies suggest selective loading preferences among remaining Agos, reflecting the Ago2 loading biases described in the previous chapter. Such Ago preferences are likely to influence the targeting efficacy and specificity, warranting further investigation into parasite miRNA interactions with individual mammalian Agos. Given that *Nod1* is critical for sensing pathogen-associated molecular patterns (PAMPs) in host cells and initiating proinflammatory and antimicrobial responses, the ability of the isomiR to selectively repress *Nod1* may provide the parasite with an adaptive advantage by dampening host defences and promoting its survival.

While traditionally it was thought that Dicer plays a crucial role in loading mature miRNAs onto Ago [356], more recent studies confirmed that exogenously introduced mature miRNAs can form functional RISCs in the absence of Dicer [357, 358], consistent with the observation

in this study. Nonetheless, Dicer independence would reduce reliance on the host miRNA biogenesis machinery, by enabling parasite-derived miRNAs to directly load onto host Ago, allowing more immediate regulation of the host target genes immediately upon entry into host cells.

In summary, this study establishes Ago2- and Dicer-deficient macrophage lines as a robust platform for interrogating RNAi machinery contributions to parasite-host interactions. The persistence of fhe-miR-125b-5p immunomodulatory function despite loss of key RNAi components suggests a degree of functional flexibility in how parasite miRNAs engage host silencing machinery, potentially involving Ago redundancy and/or non-canonical pathways. These insights advance understanding of helminth-host molecular communications while highlighting the need for further investigation into the specific pathways through which parasite miRNAs modulate host responses.

Chapter 5:
General Discussion

Parasitic worms (helminths) are highly pervasive pathogens, infecting approximately 1.5 billion people worldwide, particularly within marginalized communities, causing significant disability and morbidity (Chapter 1). These infections also affect animals, consequently threatening food security and causing significant economic loss by impairing livestock productivity. Current control methods, such as chemical drenching, pose environmental risks due to drug leaching into ecosystems and the food chain. Compounding this challenge, resistance to anthelmintic drugs is increasingly widespread. Therefore, advancing research to develop sustainable, effective control strategies is essential for safeguarding global public health, socioeconomic stability, and environmental health.

A key tenet is that the evolutionary success of these parasites hinges on their ability to establish chronic infections by artfully manipulating the host immune system (Chapter 1). Building on the growing recognition of miRNAs as pivotal regulators in this parasite-host interplay, the aims of this research project were to unravel the molecular mechanisms by which miRNAs mediate these interactions, aspiring to pave the way for novel strategies in early diagnosis and intervention against chronic helminth infections.

Fasciola hepatica was selected as the model organism due to its unique capability to infect almost all mammalian species it comes in contact with, reflecting an extensive evolutionary adaptation that facilitates universal immune regulatory mechanisms (Chapter 1). Additionally, its clearly defined developmental stages with distinct tissue migration and residency during infection provided an ideal framework for studying temporal and spatial dynamics of miRNA-mediated host modulation. Most importantly, while *C. elegans* has provided foundational insight into helminth-miRNA biology, its relevance to parasitic flatworms is limited by the deep evolutionary divergence between Ecdysozoa (nematodes) and Lophotrochozoa (including trematodes such as *F. hepatica*), which may result in differences in RNAi regulatory mechanisms [359]. Direct investigation of miRNA-mediated host modulation in a parasitic trematode system therefore addresses a critical knowledge gap beyond assumptions derived from Ecdysozoan models.

Three themes were investigated experimentally: (i) the identification and utility of circulating miRNAs as diagnostic biomarkers of infection, (ii) the functional characterisation of parasite-derived isomiRs in host immune cells, and (iii) the mechanistic dissection of how Fasciola miRNAs engage the host RNA interference (RNAi) machinery. While each chapter addressed

distinct questions, their findings converge on a unifying concept: helminths deploy a highly adaptable and multi-layered small RNA-based regulatory system to modulate host biology.

The outcomes of this research, as presented in this thesis advances understanding of miRNA-mediated host-parasite interactions in *F. hepatica* infection by bridging fundamental biological insights, innovative diagnostic biomarker discovery, and detailed mechanistic exploration of immune modulation. Together, the studies reveal mechanistic pathways by which parasite-secreted miRNAs are selectively deployed to hijack the mammalian RNA interference machinery, regulate immune signalling pathways, and establish persistent infections, thereby offering new avenues for targeted diagnosis and therapeutic intervention.

5.1. Host and parasite miRNA signatures: toward sensitive and stage-specific helminth diagnostics

The data presented in Chapter 2 of this thesis established that both host- and parasite-derived miRNAs display dynamic, stage-specific patterns during *Fasciola hepatica* infection, supporting their translational potential as early diagnostic biomarkers for fasciolosis. This is particularly significant in the context of current diagnostic limitations, where conventional approaches, such as faecal egg counts, antigen/antibody-based assays often lack sensitivity during pre-patent phase, thereby restricting timely detection and intervention (reviewed in Chapter 2). Thus, circulating miRNAs represent a promising alternative class of molecular indicators capable of capturing early and otherwise cryptic host–parasite interactions.

Importantly, the broader literature on helminth-derived small RNAs reinforces this view [55]. In serum from *Schistosoma. mansoni* infected patients, parasite-derived miRNAs has been shown to distinguish ‘egg negative’ from ‘egg positive individuals, demonstrating that helminth miRNAs can serve as robust, non-invasive infection markers [228]. Similarly, recent work in *Trichuris muris* has shown that integrated host-parasite small RNA profiling in stool can reveal associations with pathology and tissue remodelling, further supporting the concept that circulating or secreted/ excreted miRNAs reflect biologically meaningful infection states.[360]. Together, these studies situate *F. hepatica* within a growing body of evidence supporting miRNA-based diagnostics across helminth systems.

Within this framework, parasite-derived miRNAs are particularly noteworthy due to their high sequence specificity and frequent lack of mammalian orthologues, making them attractive candidates for discriminating *F. hepatica* infection in helminth-endemic settings where co-infections are common. Moreover, their temporal appearances across infection stages (Chapter 2 and 3), alongside stage-specific expression patterns reported in the parasite itself [231], suggests regulated secretion aligned with parasite development and host tissue migration. This strengthens the hypothesis that parasite miRNAs may not only serve as biomarkers of infection presence but also as indicators of parasite biological activity and developmental stage.

When the experimental findings are integrated with data obtained throughout this PhD, circulating miRNAs emerge as more than passive biomarkers of infection or tissue damage. Instead, they likely represent an active molecular interface of host-parasite communication. The detection of parasite-derived miRNAs in host biofluids, alongside evidence of their uptake and functional activity within host immune cells, (Chapters 3 and 4) supports the interpretation that at least a subset of these molecules is selectively secreted and biologically active. This aligns with established paradigms in miRNA biology, where circulating miRNAs are known to exist either in extracellular vesicles or in association with protein complexes, both of which confer stability and functional potential in extracellular environments (Chapter 1, Section 1.4.3).

However, a layer of complexity arises from the discovery that isomiRs were among the parasite-derived miRNAs in circulation. As demonstrated across Chapters 3 and 4, these sequence variants (particularly 3′-trimmed forms) may dominate in host cellular environments. In addition, isomiR profiles are known to vary across parasite life stages and can shift in mammalian hosts in response to infection and disease states [259, 260, 274], suggesting that isomiR signatures may provide enhanced sensitivity and improved temporal resolution for infection staging. This has important implications for biomarker discovery, as conventional qPCR or annotation-dependent pipelines targeting canonical sequences may fail to capture the full diversity of biologically relevant miRNA species [361].

Collectively, these findings support a model in which host and parasite miRNAs form complementary diagnostic signals: host miRNAs reflect systemic and tissue-level responses to infection, while parasite-derived miRNAs provide direct evidence of parasite presence and

activity. Integrating these signatures will likely yield a more robust diagnostic framework than either component alone, enabling improved sensitivity, specificity, and temporal discrimination of infection stages.

5.1.1. Limitations and future directions

Despite the conceptual and technical advances presented in this chapter, several limitations should be acknowledged. First, parasite-derived miRNAs were present at extremely low abundance in host circulation, which poses significant challenges for reliable detection and quantification. This is further compounded by the dynamic and context-dependent nature of circulating host miRNAs, which introduces biological variability that may obscure infection-specific signals.

Second, current analytical approaches remain largely dependent on canonical miRNA annotations. As demonstrated here, the presence of isomiRs introduces a substantial layer of molecular diversity that is often not captured by standard pipelines. This likely contributes to underestimation of true miRNA abundance and may lead to false negatives in validation studies, particularly when using targeted qPCR assays. While emerging technologies such as CRISPR-based biosensors, isothermal amplification methods, and nanomaterial-enabled detection platforms offer promising solutions for improving sensitivity [362-364], many remain at early stages of development or have not yet been validated for complex biological fluids such as serum in veterinary settings. Their integration into helminth diagnostics will therefore require further optimisation and field validation.

Finally, although temporal sampling in controlled infection models provides valuable insight into infection dynamics, translation to natural field infections introduces additional complexity, including variation in parasite burden, co-infections, and host genetic diversity. Furthermore, the high genomic heterozygosity and pronounced population structure of *F. hepatica* [365] suggest that strain-specific variation in miRNA loci is plausible. Similarly, while mature miRNA sequences in mammals are generally highly conserved, polymorphisms in pri- and pre-miRNA regions can potentially influence miRNA processing and expression [366, 367]. These factors may significantly influence circulating miRNA profiles and reduce diagnostic consistency across populations.

Future work should prioritise isomiR-resolved sequencing strategies, mechanistic studies linking circulating miRNAs to tissue and cellular sources, and large-scale validation in natural

infection settings, while incorporating mismatch tolerant and population-aware reference datasets to account for parasite and host genetic variation. In parallel, the development of multiplexed, point-of-care platforms capable of integrating host and parasite-derived miRNA signatures will be critical for translating these findings into practical diagnostic tools.

5.2. IsomiRs: expanding the paradigm of miRNA-mediated parasite-host interaction

A major conceptual advance arising from this thesis is the recognition that helminth-derived miRNAs found within host immune cells are not restricted to canonical sequences but exist predominantly as diverse isomiR populations, with clear functional relevance. Although isomiRs were first described in 2008 [249], it is only with recent advances in sequencing technologies and experimental validation that they have been accepted as a widespread and biologically significant class of miRNA variants [248]. Within the context of parasite-host communication, this significantly extends a field that has traditionally focused on canonical miRNA species since the initial discovery that helminth-derived extracellular vesicles can transfer regulatory small RNAs capable of modulating host gene expression and immune pathways [62].

The data presented in Chapter 3 provides direct evidence that *F. hepatica*-derived miRNAs detected in murine macrophages are enriched for diverse isomiRs including variants with 3′ and/or 5′ end nucleotide(s) addition, deletion, and substitutions. The detection of identical isomiR species in both parasites and their corresponding extracellular vesicles strongly supports a parasite origin rather than *de novo* generation within host cells. Although stringent alignment criteria may underestimate total isomiR diversity, the data clearly establish that a broader repertoire of parasite-derived miRNA variants is actively deployed into host environments.

A key finding of this thesis is that isomiRs are not merely structural variants of canonical miRNAs but can exhibit distinct functional properties (Chapter 3 and 4). As shown for fhe-miR-125b-5p, both canonical and 3′-trimmed forms were capable of modulating inflammatory responses; however, the isomiR displayed enhanced regulatory potency against specific immune targets and showed preferential loading into host Ago2 complexes. This challenges the classical paradigm in which miRNA function is only determined primarily by the seed sequence, and instead supports a model in which 3′-end variation can contribute to functional diversification through altered protein interactions, stability, and subcellular localisation.

From a mechanistic perspective, the selective enrichment of specific isomiRs within host immune cells suggests that their generation is unlikely to be purely stochastic. Instead, it is consistent with a model in which parasites actively shape isomiR output to expand the functional repertoire of a limited miRNA gene set. This represents a form of molecular economy, enabling fine-tuned regulation of host pathways without requiring genomic expansion. Such a strategy aligns with broader themes in parasitic adaptation, where limited genetic resources are leveraged to produce complex and context-specific host manipulation.

This hypothesis is consistent with findings across helminth systems. Parasitic helminths such as *Echinococcus* and *Mesocestoides corti* produce abundant 3′ isomiRs, including uridylated forms, highlighting that isomiR diversification is a conserved feature of helminth biology [368, 369]. Within this broader evolutionary context, *F. hepatica* appears to exploit isomiR diversity as part of its host regulatory strategy, reinforcing the concept that isomiR generation is not incidental but functionally significant. Thus, isomiR biology may represent a novel therapeutic vulnerability, enabling strategies that target parasite-specific small RNA processing pathways or disrupt functional isomiR-host protein interactions.

When integrated with the biomarker findings in Chapter 2, isomiR diversity also has important translational implications. The existence of multiple sequence variants derived from a single miRNA precursor may influence circulating stability, packaging into extracellular vesicles or protein complexes, and ultimately detectability. This variability may contribute to inconsistencies observed between sequencing-based discovery and targeted validation approaches that rely on canonical annotations, and may partially explain variability in biomarker performance across infection stages.

5.2.1. Limitations and future directions

While the experimental data presented in this chapter presents strong rationale for exploring the functional contribution of isomiRs in helminth biology, the low abundance of parasite-derived miRNAs in host cells should be acknowledged. This represents a broad challenge in cross-kingdom RNAi studies, in which host-transcripts will far exceed the presence of exogenous pathogen-derived miRNA sequences. In addition, technical limitations in library preparation and sequencing, and conservative bioinformatics pipelines that prioritise specificity over sensitivity to minimise false positives, may also underestimate the miRNA

abundance and isomiR diversity. Advances in miRNA detection technologies, including deeper sequencing approaches and more sensitive analytical methods, may improve detection and enable more comprehensive characterisation of isomiRs in future studies.

Second, this study focused primarily on a subset of isomiR classes (notably 3′ and 5′ length variants), and did not comprehensively evaluate other forms of post-transcriptional modification such as non-templated nucleotide additions or polymorphic isomiRs, which are known to be prevalent in helminths [274]. As such, the full spectrum of parasite-derived isomiR diversity within host environments remains unresolved.

Third, functional validation was limited to a small number of representative isomiRs. While fhe-miR-125b-5p provided clear evidence of functional divergence from its canonical counterpart, it remains unclear whether similar effects are generalisable across other parasite-derived miRNAs /isomiRs or represent a gene-specific phenomena. Broader experimental validation across multiple isomiR families will be required to establish general principles.

Fourth, mechanistic insights into isomiR biogenesis and selection remain incomplete. Although evidence suggests selective enrichment and differential Ago loading, the upstream processes governing isomiR generation in helminths and their sorting into host RNAi machinery are not yet defined. Disentangling contributions from parasite-driven processing versus host-mediated modification will be critical.

Future work should therefore prioritise (i) isomiR-resolved sequencing approaches with improved discrimination of host and parasite small RNAs, (ii) systematic functional interrogation of multiple isomiR families across infection stages and host tissues, and (iii) mechanistic studies addressing isomiR biogenesis, Ago sorting, and intracellular trafficking. In addition, integrating isomiR biology into multiplexed diagnostic and functional frameworks may enable more precise exploitation of parasite-derived small RNA pathways for both biomarker development and therapeutic targeting.

5.3. Ago2 and Dicer KO macrophages: a valuable platform for understanding miRNA-mediated parasite-host interaction

The research presented in Chapter 4 extends the depth of investigation in to parasite miRNA functionality in host immune cells by interrogating the interface with host RNAi machinery.

Using CRISPR–Cas9-generated Ago2 and Dicer knockout macrophages, it was discovered that *F. hepatica* miRNAs retain functional activity even in the absence of key canonical RNAi components. This challenges the prevailing model in which miRNA function is strictly dependent on Dicer-mediated processing and Ago2-driven incorporation into the RNA-induced silencing complex (RISC), and instead supports a more flexible and context-dependent model of cross-kingdom RNA regulation.

The persistence of parasite miRNA activity in Dicer-deficient macrophages is consistent with their delivery as mature, pre-processed molecules within parasite-derived extracellular vesicles. This bypasses the requirement for host miRNA biogenesis machinery and suggests that helminths export miRNAs in a configuration already optimised for immediate functionality upon entry into host cells.

More unexpectedly, parasite miRNA activity was also maintained in Ago2-deficient cells, indicating that canonical Ago2-dependent RISC formation is not essential for functional repression of host immune targets. Instead, parasite miRNAs appear capable of engaging alternative Argonaute family members (Ago1, Ago3, or Ago4), which, although lacking slicer activity, can still mediate translational repression and gene silencing. When considered alongside the evidence from Chapter 3 which showed preferential Ago2 loading of specific isomiRs, these findings suggest a dual-layered model; selective Ago preference under normal conditions, combined with functional redundancy when Ago2 is absent.

This flexibility likely reflects an adaptive strategy to ensure robust regulatory activity across heterogeneous host environments. During infection, macrophages undergo dynamic changes in protein expression, signalling pathways, and RNA-binding protein availability. The ability of parasite-derived miRNAs to function across different RNAi contexts would therefore confer a significant evolutionary advantage, ensuring consistent immune modulation regardless of host cellular state or perturbation of specific RNAi components.

Within this framework, isomiR diversity may further enhance functional plasticity. As described in earlier chapters, different isoforms of the same parasite miRNA can display distinct Ago loading preferences and regulatory potency. This suggests that sequence variation beyond the seed region may act as a tuning mechanism, allowing helminths to diversify RNAi engagement strategies without expanding their miRNA gene repertoire.

An additional implication of these findings is that parasite miRNAs may not exclusively rely on canonical RISC-mediated silencing. While Ago proteins are likely central mediators, the possibility remains that alternative RNA-binding complexes or non-canonical pathways contribute to observed regulatory effects. Resolving this will be essential for fully understanding how parasite-derived small RNAs exert their functions in host cells.

5.3.1. Limitations and future directions

Despite the mechanistic insights that emerged from the work presented in this chapter, limitations should be considered.

A key limitation is the reliance on *in vitro* macrophage models. Although these systems enable precise genetic and mechanistic interrogation, they do not fully recapitulate the complexity of *in vivo* infection where macrophages exist within dynamic tissue environments shaped by multiple immune cell populations, parasite migration, and systemic host signalling. These contextual factors may significantly influence RNAi pathway usage and miRNA activity.

A second limitation is the use of synthetic miRNA mimics for functional assays. While experimentally tractable, these constructs do not fully reflect the endogenous form in which parasite miRNAs are delivered. In natural infection, miRNAs are packaged within extracellular vesicles together with proteins, lipids, and other nucleic acids that may influence cellular uptake, intracellular trafficking, and functional stability [370, 371]. The absence of these cofactors may therefore lead to incomplete representation of physiological activity.

Furthermore, research on helminth-derived extracellular miRNAs has primarily focused on the identification and profiling of mature miRNAs, while the presence of precursor or primary miRNA species within EVs remains largely unexplored. Conserved Drosha-recognition motifs in *F. hepatica* pri-miRNAs [274] raise the possibility that host machinery could contribute to miRNA processing under certain conditions. If validated, this would imply an additional layer of host involvement in parasite miRNA maturation and potentially in isomiR generation, further blurring the distinction between host and parasite RNAi systems.

Mechanistically, future studies should focus on defining the full spectrum of miRNA-associated protein complexes. Approaches such as Ago-specific CLIP-seq, quantitative

proteomics of RNA-induced silencing complexes, and targeted genetic disruption of individual Ago paralogues will be critical for resolving canonical and non-canonical RNAi pathways. Expanding these analyses across multiple parasite-derived miRNAs and their isomiRs will further determine whether the functional flexibility observed here is a general helminth strategy or specific to particular miRNA families.

In addition, future work could provide validation in more physiologically relevant systems, including primary macrophages, organoid-based co-culture platforms, and *in vivo* infection models. In parallel, extracellular vesicle-mediated delivery of native parasite miRNAs will be essential to confirm that observed effects are not artefacts of synthetic mimics and to better replicate natural uptake pathways.

Together, these approaches will refine our understanding of RNAi pathway exploitation in parasite-host interactions and may reveal novel therapeutic entry points for disrupting parasite-driven immune modulation.

5.4. Evolutionary implications: hypotheses and emerging concepts

The findings presented within this thesis support several hypotheses regarding the evolution of miRNA pathways of helminth-host communication.

One hypothesis is that helminth miRNAs have evolved to mimic host miRNAs, enabling them to integrate seamlessly into host regulatory networks. The conservation of sequences such as miR-125b supports this idea, suggesting that parasites may exploit existing regulatory pathways rather than evolving entirely novel mechanisms. In this context, molecular mimicry would allow parasite-derived miRNAs to access pre-established gene regulatory circuits, thereby increasing the efficiency and subtlety of host modulation.

A complementary hypothesis is that isomiR generation provides an additional layer of adaptability. By producing multiple variants of a given miRNA, parasites may fine-tune their regulatory outputs in response to different host environments, developmental stages, or immune pressures. This capacity for diversification without expanding genomic content reflects an efficient evolutionary strategy, particularly advantageous for organisms with complex life cycles.

Finally, mechanistic flexibility in engagement with host RNAi pathways likely represents an evolutionary adaptation to host variability. The ability of parasite miRNAs to function independently of canonical components such as Ago2 and Dicer suggests that the ability of the parasite to interact with its host is not constrained by the molecular architecture of a single host species or cell type. Instead, they may have evolved to exploit a broader spectrum of RNA-binding proteins or alternative silencing pathways, ensuring functional robustness across diverse biological contexts.

Collectively, these hypotheses position helminth miRNAs as components of a dynamic evolutionary interface between parasite and host. Rather than acting as simple effectors, they may represent adaptable regulatory tools shaped by co-evolutionary pressures to optimise parasite survival while maintaining host viability.

5.5. Therapeutic and translational implications

Integrated insights generated from data presented in this thesis have several important implications for future diagnostic and therapeutic strategies (Figure 5.1).

From a diagnostic perspective, the combined use of host- and parasite-derived miRNAs offers a promising avenue for improving sensitivity and specificity. Incorporating isomiR profiles into diagnostic pipelines may further enhance resolution, particularly for distinguishing between infection stages or identifying early infections that are currently undetectable using conventional methods. The development of multiplexed assays that capture these diverse RNA signatures could represent a significant advancement in helminth diagnostics.

From a therapeutic standpoint, parasite-derived miRNAs themselves may serve as novel targets. Strategies aimed at inhibiting specific miRNAs, such as antisense oligonucleotides or miRNA sponges, could disrupt parasite-mediated immune modulation. Alternatively, targeting the delivery mechanisms of these miRNAs, particularly extracellular vesicles, may provide a means to block the transfer of regulatory signals from parasite to host.

The identification of RNAi pathway flexibility also opens new avenues for intervention. If parasite miRNAs utilise non-canonical pathways or alternative protein partners, these components may represent previously unrecognised therapeutic targets. Interfering with these

pathways could impair the parasite's ability to regulate host gene expression without directly targeting the parasite itself, potentially reducing selective pressure for resistance.

It is important to emphasise that these applications remain hypothetical at this stage. Substantial work is required to validate the feasibility, specificity, and safety of such approaches. Nonetheless, the conceptual advances presented here provide a foundation for exploring RNA-based strategies in helminth control.

5.6. Conclusion

In conclusion, this thesis provides an integrated exploration on the role of helminth-derived miRNAs in host-parasite interactions, bridging gaps between biomarker discovery, molecular function, and mechanistic understanding.

By demonstrating that circulating miRNAs can serve as early indicators of infection, that isomiRs represent a functionally significant and selectively deployed class of regulatory molecules, and that parasite miRNAs exhibit flexibility in their engagement with host RNAi pathways, this body of research advances current paradigms of cross-kingdom communication.

Importantly, these findings support a model in which helminth miRNAs operate as part of a dynamic and multilayered regulatory system. This system is characterised by three key features: (i) diversity, through the generation of isomiRs; (ii) selectivity, through targeted export and uptake; and (iii) flexibility, through the ability to engage multiple molecular pathways within the host. By integrating these concepts, the research conducted in this PhD has transcended descriptive observations and provided a cohesive mechanistic framework to elucidate host-parasite miRNA networks of communication.

Future research will be essential to test and refine this model, particularly through *in vivo* validation, comparative studies across species, and deeper mechanistic exploration. Ultimately, such efforts may enable the translation of these insights into innovative diagnostic and therapeutic strategies, contributing to improved control of helminth infections.

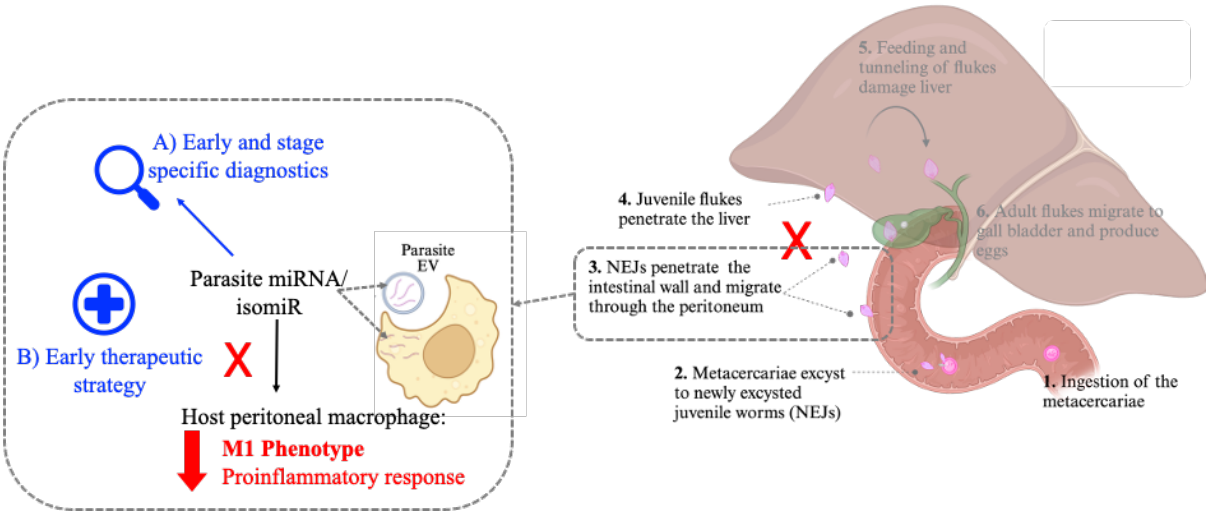


Figure 5.1. Proposed novel targeting strategies for advancing diagnostics and therapeutic intervention in Fasciola hepatica infection. *The dual opportunities identified is shown in blue: (A) Parasite-derived miRNAs and isomiRs released into the extracellular milieu represent highly specific and sensitive biomarkers, enabling early and stage-resolved detection of infection. (B) Therapeutically, intercepting these parasite miRNA/isomiR pathways during the pre-hepatic stage could block the ability of newly excysted juveniles (NEJs) to manipulate host innate immunity, thereby preventing their survival before they can enter the liver. The point of intervention in the miRNA/isomiR pathway, and the corresponding blockade of parasite life stages, is indicated with a red "X" on the schematic adapted from Figure 1.5.*

References:

1. Maizels RM, Smits HH, McSorley HJ. Modulation of Host immunity by helminths: the expanding repertoire of parasite effector molecules. Immunity. 2018;49(5):801-18.
2. Chen J, Gong Y, Chen Q, Li S, Zhou Y. Global burden of soil-transmitted helminth infections, 1990-2021. Infectious Diseases of Poverty. 2024;13(1):77.
3. Cox FE. History of human parasitology. Clinical microbiology reviews. 2002;15(4):595-612.
4. Weatherhead JE, Hotez PJ, Mejia R. The global state of helminth control and elimination in children. Pediatric clinics. 2017;64(4):867-77.
5. Gazzinelli-Guimaraes PH, Nutman TB. Helminth parasites and immune regulation. F1000Research. 2018;7.
6. King CH. Health metrics for helminth infections. Acta Tropica. 2015;141:150-60.
7. Charlier J, Rinaldi L, Musella V, Ploeger HW, Chartier C, Vineer HR, et al. Initial assessment of the economic burden of major parasitic helminth infections to the ruminant livestock industry in Europe. Preventive veterinary medicine. 2020;182:105103.
8. Kotze A, Hunt P. The current status and outlook for insecticide, acaricide and anthelmintic resistances across the Australian ruminant livestock industries: assessing the threat these resistances pose to the livestock sector. Australian Veterinary Journal. 2023;101(9):321-33.
9. Hotez PJ, Brindley PJ, Bethony JM, King CH, Pearce EJ, Jacobson J. Helminth infections: the great neglected tropical diseases. The journal of clinical investigation. 2008;118(4):1311-21.
10. Blair D. Paragonimiasis. Adv Exp Med Biol. 2019;1154:105-38.
11. Caravedo MA, Cabada MM. Human fascioliasis: current epidemiological status and strategies for diagnosis, treatment, and control. Res Rep Trop Med. 2020;11:149-58.
12. Tang ZL, Huang Y, Yu XB. Current status and perspectives of *Clonorchis sinensis* and clonorchiasis: epidemiology, pathogenesis, omics, prevention and control. Infect Dis Poverty. 2016;5(1):71.
13. Sripa B, Suwannatrai AT, Sayasone S, Do DT, Khieu V, Yang Y. Current status of human liver fluke infections in the Greater Mekong Subregion. Acta Tropica. 2021;224:106133.
14. Holland C, Sepidarkish M, Deslyper G, Abdollahi A, Valizadeh S, Mollalo A, et al. Global prevalence of Ascaris infection in humans (2010-2021): a systematic review and meta-analysis. Infect Dis Poverty. 2022;11(1):113.
15. Loukas A, Hotez PJ, Diemert D, Yazdanbakhsh M, McCarthy JS, Correa-Oliveira R, et al. Hookworm infection. Nature Reviews Disease Primers. 2016;2(1):16088.
16. Buonfrate D, Bisanzio D, Giorli G, Odermatt P, Fürst T, Greenaway C, et al. The Global Prevalence of *Strongyloides stercoralis* Infection. Pathogens. 2020;9(6).
17. Pozio E. World distribution of *Trichinella* spp. infections in animals and humans. Vet Parasitol. 2007;149(1-2):3-21.
18. James SL, Abate D, Abate KH, Abay SM, Abbafati C, Abbasi N, et al. Global, regional, and national incidence, prevalence, and years lived with disability for 354 diseases and injuries for 195 countries and territories, 1990-2017: a systematic analysis for the Global Burden of Disease Study 2017. The Lancet. 2018;392(10159):1789-858.
19. Cromwell EA, Schmidt CA, Kwong KT, Pigott DM, Mupfasoni D, Biswas G, et al. The global distribution of lymphatic filariasis, 2000-18: a geospatial analysis. The Lancet Global Health. 2020;8(9):e1186-e94.
20. Toor J, Alsallaq R, Truscott JE, Turner HC, Werkman M, Gurarie D, et al. Are we on our way to achieving the 2020 goals for Schistosomiasis morbidity control using current World Health Organization guidelines? Clinical Infectious Diseases. 2018;66(suppl_4):S245-S52.

21. Aza'ah RA, Sumo L, Ntonifor NH, Bopda J, Bamou RH, Nana-Djeunga HC. Point prevalence mapping reveals hotspot for onchocerciasis transmission in the Ndikinimeki Health District, Centre Region, Cameroon. Parasites & Vectors. 2020;13(1):519.
22. Organisation WH. Echinococcosis 2023 [Available from: https://www.who.int/news-room/fact-sheets/detail/echinococcosis.
23. Torgerson PR, Macpherson CNL. The socioeconomic burden of parasitic zoonoses: Global trends. Veterinary Parasitology. 2011;182(1):79-95.
24. Sabatini GA, de Almeida Borges F, Claerebout E, Gianechini LS, Höglund J, Kaplan RM, et al. Practical guide to the diagnostics of ruminant gastrointestinal nematodes, liver fluke and lungworm infection: interpretation and usability of results. Parasites & Vectors. 2023;16(1):58.
25. Keiser J, Utzinger J. Chapter 8 - The Drugs We Have and the Drugs We Need Against Major Helminth Infections. In: Zhou X-N, Bergquist R, Olveda R, Utzinger J, editors. Advances in Parasitology. 73: Academic Press; 2010. p. 197-230.
26. van den Enden E. Pharmacotherapy of helminth infection. Expert Opinion on Pharmacotherapy. 2009;10(3):435-51.
27. Coffeng LE, Stolk WA, de Vlas SJ. Predicting the risk and speed of drug resistance emerging in soil-transmitted helminths during preventive chemotherapy. Nature Communications. 2024;15(1):1099.
28. Zawawi A, Else KJ. Soil-transmitted helminth vaccines: are we getting closer? Frontiers in immunology. 2020;11:576748.
29. Tang B, Li J, Li T, Xie Y, Guan W, Zhao Y, et al. Vaccines as a strategy to control Trichinellosis. Front Microbiol. 2022;13:857786.
30. Bain R. Irradiated vaccines for helminth control in livestock. International journal for parasitology. 1999;29(1):185-91.
31. Bartel DP. MicroRNAs: target recognition and regulatory functions. Cell. 2009;136(2):215-33.
32. Bennett APS, de la Torre-Escudero E, Robinson MW. Helminth genome analysis reveals conservation of extracellular vesicle biogenesis pathways but divergence of RNA loading machinery between phyla. Int J Parasitol. 2020;50(9):655-61.
33. Fontenla S, Rinaldi G, Smircich P, Tort JF. Conservation and diversification of small RNA pathways within flatworms. BMC evolutionary biology. 2017;17:1-16.
34. Britton C, Winter AD, Gillan V, Devaney E. microRNAs of parasitic helminths - Identification, characterization and potential as drug targets. Int J Parasitol Drugs Drug Resist. 2014;4(2):85-94.
35. Lee RC, Feinbaum RL, Ambros V. The C. elegans heterochronic gene lin-4 encodes small RNAs with antisense complementarity to lin-14. cell. 1993;75(5):843-54.
36. Reinhart BJ, Slack FJ, Basson M, Pasquinelli AE, Bettinger JC, Rougvie AE, et al. The 21-nucleotide let-7 RNA regulates developmental timing in *Caenorhabditis elegans*. nature. 2000;403(6772):901-6.
37. Winter AD, Weir W, Hunt M, Berriman M, Gilleard JS, Devaney E, et al. Diversity in parasitic nematode genomes: the microRNAs of *Brugia pahangi* and *Haemonchus contortus* are largely novel. BMC Genomics. 2012;13(1):4.
38. Winter AD, Gillan V, Maitland K, Emes RD, Roberts B, McCormack G, et al. A novel member of the let-7 microRNA family is associated with developmental transitions in filarial nematode parasites. BMC genomics. 2015;16:1-15.
39. Zhong H, Guan G, Jin Y. Roles of helminth extracellular vesicle-derived let-7 in host-parasite crosstalk. Frontiers in Immunology. 2024;15:1449495.
40. Bai Y, Zhang Z, Jin L, Zhu Y, Zhao L, Shi B, et al. Dynamic changes in the global transcriptome and microRNAome reveal complex miRNA-mRNA regulation in early stages of

the bi-directional development of *Echinococcus granulosus* protoscoleces. Frontiers in Microbiology. 2020;11:654.
41. Ricafrente A, Nguyen H, Tran N, Donnelly S. An evaluation of the *Fasciola hepatica* miRnome predicts a targeted regulation of mammalian innate immune responses. Front Immunol. 2020;11:608686.
42. Marks ND, Winter AD, Gu HY, Maitland K, Gillan V, Ambroz M, et al. Profiling microRNAs through development of the parasitic nematode *Haemonchus* identifies nematode-specific miRNAs that suppress larval development. Scientific reports. 2019;9(1):17594.
43. Grecco A, Macchiaroli N, Pérez MG, Casulli A, Cucher MA, Rosenzvit MC. microRNA silencing in a whole worm cestode model provides insight into miR-71 function. International Journal for Parasitology. 2023;53(13):699-710.
44. Sun C, Luo F, You Y, Gu M, Yang W, Yi C, et al. MicroRNA-1 targets ribosomal protein genes to regulate the growth, development and reproduction of *Schistosoma japonicum*. International Journal for Parasitology. 2023;53(11-12):637-49.
45. Zheng Y, Fang C, Du P, Giri BR, Wu H, Ge Y, et al. Molecular characterization of miR-31 for regulating egg production in female *Schistosoma japonicum*. Acta Tropica. 2024;259:107372.
46. Zhou X, Hong Y, Shang Z, Abuzeid AM, Lin J, Li G. The potential role of MicroRNA-124-3p in growth, development, and reproduction of *Schistosoma japonicum*. Frontiers in Cellular and Infection Microbiology. 2022;12:862496.
47. Zhu L, Zhao J, Wang J, Hu C, Peng J, Luo R, et al. MicroRNAs are involved in the regulation of ovary development in the pathogenic blood fluke *Schistosoma japonicum*. PLoS pathogens. 2016;12(2):e1005423.
48. Vergani-Junior CA, Moro RDP, Pinto S, De-Souza EA, Camara H, Braga DL, et al. An intricate network involving the Argonaute ALG-1 modulates organismal resistance to oxidative stress. Nature Communications. 2024;15(1):3070.
49. Pagliuso DC, Bodas DM, Pasquinelli AE. Recovery from heat shock requires the microRNA pathway in Caenorhabditis elegans. PLoS genetics. 2021;17(8):e1009734.
50. Chiumiento L, Bruschi F. Enzymatic antioxidant systems in helminth parasites. Parasitology Research. 2009;105:593-603.
51. Gobert GN, Tran MH, Moertel L, Mulvenna J, Jones MK, McManus DP, et al. Transcriptional changes in *Schistosoma mansoni* during early schistosomula development and in the presence of erythrocytes. PLoS neglected tropical diseases. 2010;4(2):e600.
52. Littlewood DTJ, Rohde K, Bray RA, Herniou EA. Phylogeny of the Platyhelminthes and the evolution of parasitism. Biological Journal of the Linnean Society. 1999;68(1):257-87.
53. Viney M. The genomic basis of nematode parasitism. Briefings in Functional Genomics. 2017;17(1):8-14.
54. Duguet TB, Soichot J, Kuzyakiv R, Malmstrom L, Tritten L. Extracellular vesicle-xontained microRNA of *C. elegans* as a tool to decipher the molecular basis of nematode parasitism. Front Cell Infect Microbiol. 2020;10:217.
55. Mu Y, McManus DP, Gordon CA, Cai P. Parasitic helminth-derived microRNAs and extracellular vesicle cargos as biomarkers for helminthic infections. Front Cell Infect Microbiol. 2021;11:708952.
56. Sais D, Chowdhury S, Dalton JP, Tran N, Donnelly S. Both host and parasite non-coding RNAs co-ordinate the regulation of macrophage gene expression to reduce pro-inflammatory immune responses and promote tissue repair pathways during infection with *Fasciola hepatica*. RNA biology. 2024;21(1):1007-22.
57. Britton C, Winter AD, Marks ND, Gu H, McNeilly TN, Gillan V, et al. Application of small RNA technology for improved control of parasitic helminths. Veterinary parasitology. 2015;212(1-2):47-53.

58. Roth J, LeRoith D, Shiloach J, Rosenzweig JL, Lesniak MA, Havrankova J. The evolutionary origins of hormones, neurotransmitters, and other extracellular chemical messengers: implications for mammalian biology. N Engl J Med. 1982;306(9):523-7.
59. Liang H, Zen K, Zhang J, Zhang CY, Chen X. New roles for microRNAs in cross-species communication. RNA Biol. 2013;10(3):367-70.
60. Vidigal JA, Ventura A. The biological functions of miRNAs: lessons from *in vivo* studies. Trends Cell Biol. 2015;25(3):137-47.
61. Gualtieri C, Leonetti P, Macovei A. Plant miRNA cross-kingdom transfer targeting parasitic and mutualistic organisms as a tool to advance modern agriculture. Front Plant Sci. 2020;11:930.
62. Buck AH, Coakley G, Simbari F, McSorley HJ, Quintana JF, Le Bihan T, et al. Exosomes secreted by nematode parasites transfer small RNAs to mammalian cells and modulate innate immunity. Nat Commun. 2014;5:5488.
63. Tran N, Ricafrente A, To J, Lund M, Marques TM, Gama-Carvalho M, et al. *Fasciola hepatica* hijacks host macrophage miRNA machinery to modulate early innate immune responses. Sci Rep. 2021;11(1):6712.
64. Donnelly S, Tran N. Commandeering the mammalian Ago2 miRNA network: a newly discovered mechanism of helminth immunomodulation. Trends Parasitol. 2021;37(12):1031-3.
65. Nowacki FC, Swain MT, Klychnikov OI, Niazi U, Ivens A, Quintana JF, et al. Protein and small non-coding RNA-enriched extracellular vesicles are released by the pathogenic blood fluke *Schistosoma mansoni*. J Extracell Vesicles. 2015;4:28665.
66. Coakley G, Harris NL. Interactions between macrophages and helminths. Parasite immunology. 2020;42(7):e12717.
67. Nutman TB, Kumaraswami V, Ottesen EA. Parasite-specific anergy in human filariasis. Insights after analysis of parasite antigen-driven lymphokine production. The Journal of clinical investigation. 1987;79(5):1516-23.
68. Doetze A, Satoguina J, Burchard G, Rau T, Löliger C, Fleischer B, et al. Antigen-specific cellular hyporesponsiveness in a chronic human helminth infection is mediated by Th3/Tr1-type cytokines IL-10 and transforming growth factor-β but not by a Th1 to Th2 shift. International immunology. 2000;12(5):623-30.
69. Maizels RM. Regulation of immunity and allergy by helminth parasites. Allergy. 2020;75(3):524-34.
70. Taylor MD, van der Werf N, Maizels RM. T cells in helminth infection: the regulators and the regulated. Trends Immunol. 2012;33(4):181-9.
71. Donnelly S, Dalton JP, Loukas A. Proteases in helminth-and allergen-induced inflammatory responses. Parasites and Allergy. 2006;90:45-64.
72. Hewitson JP, Grainger JR, Maizels RM. Helminth immunoregulation: the role of parasite secreted proteins in modulating host immunity. Molecular and biochemical parasitology. 2009;167(1):1-11.
73. Lund ME, O'Brien BA, Hutchinson AT, Robinson MW, Simpson AM, Dalton JP, et al. Secreted proteins from the helminth *Fasciola hepatica* inhibit the initiation of autoreactive T cell responses and prevent diabetes in the NOD mouse. PloS one. 2014;9(1):e86289.
74. Ancarola ME, Lichtenstein G, Herbig J, Holroyd N, Mariconti M, Brunetti E, et al. Extracellular non-coding RNA signatures of the metacestode stage of *Echinococcus multilocularis*. PLoS Negl Trop Dis. 2020;14(11):e0008890.
75. Acuna SM, Floeter-Winter LM, Muxel SM. MicroRNAs: Biological Regulators in Pathogen-Host Interactions. Cells. 2020;9(1).

76. Ancarola ME, Marcilla A, Herz M, Macchiaroli N, Perez M, Asurmendi S, et al. Cestode parasites release extracellular vesicles with microRNAs and immunodiagnostic protein cargo. Int J Parasitol. 2017;47(10-11):675-86.
77. Ding J, He G, Wu J, Yang J, Guo X, Yang X, et al. miRNA-seq of *Echinococcus multilocularis* Extracellular Vesicles and Immunomodulatory Effects of miR-4989. Front Microbiol. 2019;10:2707.
78. Herron CM, O'Connor A, Robb E, McCammick E, Hill C, Marks NJ, et al. Developmental regulation and functional prediction of microRNAs in an expanded *Fasciola hepatica* miRNome. Front Cell Infect Microbiol. 2022;12:811123.
79. Liu J, Zhu L, Wang J, Qiu L, Chen Y, Davis RE, et al. *Schistosoma japonicum* extracellular vesicle miRNA cargo regulates host macrophage functions facilitating parasitism. PLoS Pathog. 2019;15(6):e1007817.
80. Yang B, Wang J, Jiang H, Lin H, Ou Z, Ullah A, et al. Extracellular vesicles derived From *Talaromyces marneffei* yeasts mediate inflammatory response in macrophage cells by bioactive protein components. Front Microbiol. 2020;11:603183.
81. Eichenberger RM, Ryan S, Jones L, Buitrago G, Polster R, Montes de Oca M, et al. Hookworm Secreted Extracellular Vesicles Interact With Host Cells and Prevent Inducible Colitis in Mice. Front Immunol. 2018;9:850.
82. Gu HY, Marks ND, Winter AD, Weir W, Tzelos T, McNeilly TN, et al. Conservation of a microRNA cluster in parasitic nematodes and profiling of miRNAs in excretory-secretory products and microvesicles of *Haemonchus contortus*. PLoS Negl Trop Dis. 2017;11(11):e0006056.
83. He X, Pan W. Host-parasite interactions mediated by cross-species microRNAs. Trends Parasitol. 2022;38(6):478-88.
84. Arora N, Tripathi S, Singh AK, Mondal P, Mishra A, Prasad A. Micromanagement of Immune System: Role of miRNAs in Helminthic Infections. Front Microbiol. 2017;8:586.
85. Yan C, Zhou QY, Wu J, Xu N, Du Y, Li J, et al. Csi-let-7a-5p delivered by extracellular vesicles from a liver fluke activates M1-like macrophages and exacerbates biliary injuries. Proc Natl Acad Sci U S A. 2021;118(46).
86. Meningher T, Barsheshet Y, Ofir-Birin Y, Gold D, Brant B, Dekel E, et al. Schistosomal extracellular vesicle-enclosed miRNAs modulate host T helper cell differentiation. EMBO Rep. 2020;21(1):e47882.
87. Wang L, Liao Y, Yang R, Yu Z, Zhang L, Zhu Z, et al. Sja-miR-71a in Schistosome egg-derived extracellular vesicles suppresses liver fibrosis caused by schistosomiasis via targeting semaphorin 4D. J Extracell Vesicles. 2020;9(1):1785738.
88. He X, Wang Y, Fan X, Lei N, Tian Y, Zhang D, et al. A schistosome miRNA promotes host hepatic fibrosis by targeting transforming growth factor beta receptor III. J Hepatol. 2020;72(3):519-27.
89. Jiang P, Wang J, Zhu S, Hu C, Lin Y, Pan W. Identification of a *Schistosoma japonicum* microRNA that suppresses hepatoma cell growth and migration by targeting host fzd4 gene. Frontiers in Cellular and Infection Microbiology. 2022;12:31.
90. Soichot J, Guttmann N, Rehrauer H, Joller N, Tritten L. Nematode microRNAs can individually regulate interferon regulatory factor 4 and mTOR in differentiating T helper 2 lymphocytes and modulate cytokine production in macrophages. Frontiers in Molecular Biosciences. 2022:636.
91. Wang L, Liu T, Chen G, Li Y, Zhang S, Mao L, et al. Exosomal microRNA let-7-5p from *Taenia pisiformis* Cysticercus prompted macrophage to M2 polarization through Inhibiting the Expression of C/EBP delta. Microorganisms. 2021;9(7).

92. Landa A, Navarro L, Ochoa-Sánchez A, Jiménez L. *Taenia solium* and *Taenia crassiceps*: miRNomes of the larvae and effects of miR-10-5p and let-7-5p on murine peritoneal macrophages. Bioscience reports. 2019;39(11):BSR20190152.
93. Zheng Y, Guo X, He W, Shao Z, Zhang X, Yang J, et al. Effects of *Echinococcus multilocularis* miR-71 mimics on murine macrophage RAW264.7 cells. Int Immunopharmacol. 2016;34:259-62.
94. Tkach M, Théry C. Communication by extracellular vesicles: where we are and where we need to go. Cell. 2016;164(6):1226-32.
95. Taylor PJ, Hagen J, Faruqu FN, Al-Jamal KT, Quigley B, Beeby M, et al. *Trichinella spiralis* secretes abundant unencapsulated small RNAs with potential effects on host gene expression. Int J Parasitol. 2020;50(9):697-705.
96. Mori MA, Ludwig RG, Garcia-Martin R, Brandão BB, Kahn CR. Extracellular miRNAs: From Biomarkers to Mediators of Physiology and Disease. Cell Metab. 2019;30(4):656-73.
97. Arroyo JD, Chevillet JR, Kroh EM, Ruf IK, Pritchard CC, Gibson DF, et al. Argonaute2 complexes carry a population of circulating microRNAs independent of vesicles in human plasma. Proc Natl Acad Sci U S A. 2011;108(12):5003-8.
98. Turchinovich A, Weiz L, Langheinz A, Burwinkel B. Characterization of extracellular circulating microRNA. Nucleic Acids Res. 2011;39(16):7223-33.
99. Ortiz-Quintero B. Extracellular MicroRNAs as Intercellular Mediators and Noninvasive Biomarkers of Cancer. Cancers (Basel). 2020;12(11).
100. Vickers KC, Michell DL. HDL-small RNA Export, Transport, and Functional Delivery in Atherosclerosis. Curr Atheroscler Rep. 2021;23(7):38.
101. Vickers KC, Palmisano BT, Shoucri BM, Shamburek RD, Remaley AT. MicroRNAs are transported in plasma and delivered to recipient cells by high-density lipoproteins. Nat Cell Biol. 2011;13(4):423-33.
102. Drurey C, Maizels RM. Helminth extracellular vesicles: Interactions with the host immune system. Mol Immunol. 2021;137:124-33.
103. Sanchez-Lopez CM, Trelis M, Bernal D, Marcilla A. Overview of the interaction of helminth extracellular vesicles with the host and their potential functions and biological applications. Mol Immunol. 2021;134:228-35.
104. Dagenais M, Gerlach JQ, Wendt GR, Collins JJ, 3rd, Atkinson LE, Mousley A, et al. Analysis of *Schistosoma mansoni* Extracellular vesicles surface glycans reveals potential immune evasion mechanism and new insights on their origins of biogenesis. Pathogens. 2021;10(11).
105. Cai M, Yang J, Li Y, Ding J, Kandil OM, Kutyrev I, et al. Comparative analysis of different extracellular vesicles secreted by *Echinococcus granulosus* protoscoleces. Acta Tropica. 2021;213:105756.
106. Coakley G, McCaskill JL, Borger JG, Simbari F, Robertson E, Millar M, et al. Extracellular vesicles from a helminth parasite suppress macrophage activation and constitute an effective vaccine for protective immunity. Cell reports. 2017;19(8):1545-57.
107. Loghry HJ, Yuan W, Zamanian M, Wheeler NJ, Day TA, Kimber MJ. Ivermectin inhibits extracellular vesicle secretion from parasitic nematodes. J Extracell Vesicles. 2020;10(2):e12036.
108. Cwiklinski K, de la Torre-Escudero E, Trelis M, Bernal D, Dufresne PJ, Brennan GP, et al. The Extracellular vesicles of the helminth pathogen, *Fasciola hepatica*: Biogenesis Pathways and Cargo Molecules involved in parasite pathogenesis. Mol Cell Proteomics. 2015;14(12):3258-73.
109. McKenzie AJ, Hoshino D, Hong NH, Cha DJ, Franklin JL, Coffey RJ, et al. KRAS-MEK Signaling Controls Ago2 Sorting into Exosomes. Cell Rep. 2016;15(5):978-87.

110. Chow FW, Koutsovoulos G, Ovando-Vazquez C, Neophytou K, Bermudez-Barrientos JR, Laetsch DR, et al. Secretion of an Argonaute protein by a parasitic nematode and the evolution of its siRNA guides. Nucleic Acids Res. 2019;47(7):3594-606.
111. Groot M, Lee H. Sorting Mechanisms for MicroRNAs into Extracellular Vesicles and Their Associated Diseases. Cells. 2020;9(4).
112. Garcia-Martin R, Wang G, Brandão BB, Zanotto TM, Shah S, Kumar Patel S, et al. MicroRNA sequence codes for small extracellular vesicle release and cellular retention. Nature. 2022;601(7893):446-51.
113. Zhu S, Wang S, Lin Y, Jiang P, Cui X, Wang X, et al. Release of extracellular vesicles containing small RNAs from the eggs of *Schistosoma japonicum*. Parasit Vectors. 2016;9(1):574.
114. Kumagai T, Shimogawara R, Ichimura K, Iwanaga S. Calpain inhibitor suppresses both extracellular vesicle-mediated secretion of miRNAs and egg production from paired adults of *Schistosoma japonicum*. Parasitol Int. 2022;87:102540.
115. Sotillo J, Pearson M, Becker L, Mulvenna J, Loukas A. A quantitative proteomic analysis of the tegumental proteins from *Schistosoma mansoni* schistosomula reveals novel potential therapeutic targets. Int J Parasitol. 2015;45(8):505-16.
116. Liang P, Mao L, Zhang S, Guo X, Liu G, Wang L, et al. Identification and molecular characterization of exosome-like vesicles derived from the *Taenia asiatica* adult worm. Acta tropica. 2019;198:105036.
117. Lee Y, Kim M, Han J, Yeom KH, Lee S, Baek SH, et al. MicroRNA genes are transcribed by RNA polymerase II. The EMBO journal. 2004;23(20):4051-60.
118. Han J, Lee Y, Yeom K-H, Kim Y-K, Jin H, Kim VN. The Drosha-DGCR8 complex in primary microRNA processing. Genes & development. 2004;18(24):3016-27.
119. Denli AM, Tops BB, Plasterk RH, Ketting RF, Hannon GJ. Processing of primary microRNAs by the Microprocessor complex. Nature. 2004;432(7014):231-5.
120. Zhang H, Kolb FA, Jaskiewicz L, Westhof E, Filipowicz W. Single processing center models for human Dicer and bacterial RNase III. Cell. 2004;118(1):57-68.
121. Grishok A, Pasquinelli AE, Conte D, Li N, Parrish S, Ha I, et al. Genes and mechanisms related to RNA interference regulate expression of the small temporal RNAs that control *C. elegans* developmental timing. Cell. 2001;106(1):23-34.
122. Meijer HA, Smith EM, Bushell M. Regulation of miRNA strand selection: follow the leader? Biochemical Society Transactions. 2014;42(4):1135-40.
123. O'Brien J, Hayder H, Zayed Y, Peng C. Overview of MicroRNA Biogenesis, Mechanisms of Actions, and Circulation. Front Endocrinol (Lausanne). 2018;9:402.
124. Naeli P, Winter T, Hackett AP, Alboushi L, Jafarnejad SM. The intricate balance between microRNA-induced mRNA decay and translational repression. Febs j. 2023;290(10):2508-24.
125. Xie M, Li M, Vilborg A, Lee N, Shu M-D, Yartseva V, et al. Mammalian 5′-capped microRNA precursors that generate a single microRNA. Cell. 2013;155(7):1568-80.
126. Ruby JG, Jan CH, Bartel DP. Intronic microRNA precursors that bypass Drosha processing. Nature. 2007;448(7149):83-6.
127. Salim U, Kumar A, Kulshreshtha R, Vivekanandan P. Biogenesis, characterization, and functions of mirtrons. Wiley Interdisciplinary Reviews: RNA. 2022;13(1):e1680.
128. Chen J, Zhu D, Sun Y. Cap-seq reveals complicated miRNA transcriptional mechanisms in *C. elegans* and mouse. Quantitative Biology. 2017;5:352-67.
129. Cheloufi S, Dos Santos CO, Chong MM, Hannon GJ. A dicer-independent miRNA biogenesis pathway that requires Ago catalysis. Nature. 2010;465(7298):584-9.

130. Kim Y-K, Kim B, Kim VN. Re-evaluation of the roles of DROSHA, Exportin 5, and DICER in microRNA biogenesis. Proceedings of the National Academy of Sciences. 2016;113(13):E1881-E9.
131. Stavast CJ, Erkeland SJ. The non-canonical aspects of MicroRNAs: many roads to gene regulation. Cells. 2019;8(11).
132. Snead NM, Wu X, Li A, Cui Q, Sakurai K, Burnett JC, et al. Molecular basis for improved gene silencing by Dicer substrate interfering RNA compared with other siRNA variants. Nucleic Acids Res. 2013;41(12):6209-21.
133. Weiberg A, Wang M, Lin FM, Zhao H, Zhang Z, Kaloshian I, et al. Fungal small RNAs suppress plant immunity by hijacking host RNA interference pathways. Science. 2013;342(6154):118-23.
134. Mishra R, Kumar A, Ingle H, Kumar H. The interplay between viral-derived miRNAs and host immunity during infection. Frontiers in immunology. 2020;10:3079.
135. Nakanishi K. Anatomy of RISC: how do small RNAs and chaperones activate Argonaute proteins? Wiley Interdisciplinary Reviews: RNA. 2016;7(5):637-60.
136. Lech M, Weidenbusch M, Kulkarni OP, Ryu M, Darisipudi MN, Susanti HE, et al. IRF4 deficiency abrogates lupus nephritis despite enhancing systemic cytokine production. Journal of the American Society of Nephrology: JASN. 2011;22(8):1443.
137. Nguyen TL, Nguyen TD, Ngo MK, Nguyen TA. Dissection of the *Caenorhabditis elegans* Microprocessor. Nucleic Acids Research. 2023;51(4):1512-27.
138. Luo QJ, Zhang J, Li P, Wang Q, Zhang Y, Roy-Chaudhuri B, et al. RNA structure probing reveals the structural basis of Dicer binding and cleavage. Nat Commun. 2021;12(1):3397.
139. Lee Y-Y, Kim H, Kim VN. Sequence determinant of small RNA production by DICER. Nature. 2023:1-8.
140. Shapiro JS, Varble A, Pham AM. Noncanonical cytoplasmic processing of viral microRNAs. Rna. 2010;16(11):2068-74.
141. Morales L, Oliveros JC, Fernandez-Delgado R, Robert tenOever B, Enjuanes L, Sola I. SARS-CoV-encoded small RNAs contribute to infection-associated lung pathology. Cell host & microbe. 2017;21(3):344-55.
142. Zhou L, Lim MYT, Kaur P, Saj A, Bortolamiol-Becet D, Gopal V, et al. Importance of miRNA stability and alternative primary miRNA isoforms in gene regulation during *Drosophila* development. Elife. 2018;7:e38389.
143. Stark A, Brennecke J, Bushati N, Russell RB, Cohen SM. Animal MicroRNAs confer robustness to gene expression and have a significant impact on 3′ UTR evolution. Cell. 2005;123(6):1133-46.
144. Bofill-De Ros X, Yang A, Gu S. IsomiRs: expanding the miRNA repression toolbox beyond the seed. Biochimica et Biophysica Acta (BBA)-Gene Regulatory Mechanisms. 2020;1863(4):194373.
145. Fontenla S, Dell'Oca N, Smircich P, Tort JF, Siles-Lucas M. The miRnome of *Fasciola hepatica* juveniles endorses the existence of a reduced set of highly divergent micro RNAs in parasitic flatworms. International journal for parasitology. 2015;45(14):901-13.
146. He Z, Yan T, Yuan Y, Yang D, Yang G. miRNAs and lncRNAs in *Echinococcus* and Echinococcosis. International Journal of Molecular Sciences. 2020;21(3):730.
147. Rotival M, Siddle KJ, Silvert M, Pothlichet J, Quach H, Quintana-Murci L. Population variation in miRNAs and isomiRs and their impact on human immunity to infection. Genome biology. 2020;21:1-31.
148. Liang X-h, Hart CE, Crooke ST. Transfection of siRNAs can alter miRNA levels and trigger non-specific protein degradation in mammalian cells. Biochimica et Biophysica Acta (BBA)-Gene Regulatory Mechanisms. 2013;1829(5):455-68.

149. Ovchinnikov VY, Kashina EV, Mordvinov VA, Fromm B. EV-transported microRNAs of Schistosoma mansoni and *Fasciola hepatica*: Potential targets in definitive hosts. Infect Genet Evol. 2020;85:104528.
150. Cavallero S, Bellini I, Pizzarelli A, Arcà B, D'amelio S. A miRNAs catalogue from third-stage larvae and extracellular vesicles of *Anisakis pegreffii* provides new clues for host-parasite interplay. Scientific Reports. 2022;12(1):9667.
151. Yang Y, Liu L, Liu X, Zhang Y, Shi H, Jia W, et al. Extracellular vesicles derived from *Trichinella spiralis* muscle larvae ameliorate TNBS-induced colitis in mice. Frontiers in immunology. 2020;11:1174.
152. Fontenla S, Langleib M, de la Torre-Escudero E, Dominguez MF, Robinson MW, Tort J. Role of *Fasciola hepatica* Small RNAs in the Interaction With the Mammalian Host. Front Cell Infect Microbiol. 2021;11:812141.
153. Lai EC, Wiel C, Rubin GM. Complementary miRNA pairs suggest a regulatory role for miRNA: miRNA duplexes. Rna. 2004;10(2):171-5.
154. Neeb ZT, Ritter AJ, Chauhan LV, Katzman S, Lipkin WI, Mishra N, et al. A potential role for SARS-CoV-2 small viral RNAs in targeting host microRNAs and modulating gene expression. Sci Rep. 2022;12(1):21694.
155. Takahashi T, Ichikawa H, Okayama Y, Seki M, Hijikata T. SV40 miR-S1 and cellular miR-1266 sequester each other from their targets, enhancing telomerase activity and viral replication. Non-Coding RNA. 2022;8(4):57.
156. Vitkauskaite A, McDermott E, Lalor R, De Marco Verissimo C, Dehkordi MH, Thompson K, et al. *In vitro* co-culture of *Fasciola hepatica* newly excysted juveniles (NEJs) with 3D HepG2 spheroids permits novel investigation of host–parasite interactions. Virulence. 2025;16(1):2482159.
157. Perez MG, Gillan V, Anderson WM, Gerbe F, Herbert F, McNeilly TN, et al. A secreted helminth microRNA suppresses gastrointestinal cell differentiation required for innate immunity. Frontiers in Immunology. 2025;16:1558132.
158. Britton C, Laing R, McNeilly TN, Perez MG, Otto TD, Hildersley KA, et al. New technologies to study helminth development and host-parasite interactions. International Journal for Parasitology. 2023;53(8):393-403.
159. Cai Q, He B, Weiberg A, Buck AH, Jin H. Small RNAs and extracellular vesicles: New mechanisms of cross-species communication and innovative tools for disease control. PLoS Pathog. 2019;15(12):e1008090.
160. Cai Q, Qiao L, Wang M, He B, Lin FM, Palmquist J, et al. Plants send small RNAs in extracellular vesicles to fungal pathogen to silence virulence genes. Science. 2018;360(6393):1126-9.
161. LaMonte G, Philip N, Reardon J, Lacsina JR, Majoros W, Chapman L, et al. Translocation of sickle cell erythrocyte microRNAs into *Plasmodium falciparum* inhibits parasite translation and contributes to malaria resistance. Cell Host Microbe. 2012;12(2):187-99.
162. Garcia HH, Moro PL, Schantz PM. Zoonotic helminth infections of humans: echinococcosis, cysticercosis and fascioliasis. Curr Opin Infect Dis. 2007;20(5):489-94.
163. Mas-Coma S. Epidemiology of fascioliasis in human endemic areas. Journal of Helminthology. 2005;79(3):207-16.
164. Andrews SJ, Cwiklinski K, Dalton JP. The discovery of F*asciola hepatica* and its life cycle. Fasciolosis: CABI Wallingford UK; 2021. p. 1-22.
165. Cwiklinski K, Dalton JP, Dufresne PJ, La Course J, Williams DJ, Hodgkinson J, et al. The *Fasciola hepatica* genome: gene duplication and polymorphism reveals adaptation to the host environment and the capacity for rapid evolution. Genome biology. 2015;16(1):71.

166. Cwiklinski K, Jewhurst H, McVeigh P, Barbour T, Maule AG, Tort J, et al. Infection by the helminth parasite *Fasciola hepatica* requires rapid regulation of metabolic, virulence, and invasive factors to adjust to its mammalian host. Mol Cell Proteomics. 2018;17(4):792-809.
167. Cwiklinski K, Robinson MW, Donnelly S, Dalton JP. Complementary transcriptomic and proteomic analyses reveal the cellular and molecular processes that drive growth and development of *Fasciola hepatica* in the host liver. BMC Genomics. 2021;22(1):46.
168. Xu J, Wu L, Sun Y, Wei Y, Zheng L, Zhang J, et al. Proteomics and bioinformatics analysis of *Fasciola hepatica* somatic proteome in different growth phases. Parasitol Res. 2020;119(9):2837-50.
169. Robinson MW, Tort JF, Lowther J, Donnelly SM, Wong E, Xu W, et al. Proteomics and phylogenetic analysis of the cathepsin L protease family of the helminth pathogen *Fasciola hepatica*: expansion of a repertoire of virulence-associated factors. Molecular & Cellular Proteomics. 2008;7(6):1111-23.
170. Robinson MW, Menon R, Donnelly SM, Dalton JP, Ranganathan S. An integrated transcriptomics and proteomics analysis of the secretome of the helminth pathogen *Fasciola hepatica:* proteins associated with invasion and infection of the mammalian host. Molecular & Cellular Proteomics. 2009;8(8):1891-907.
171. Young ND, Hall RS, Jex AR, Cantacessi C, Gasser RB. Elucidating the transcriptome of F*asciola hepatica*—a key to fundamental and biotechnological discoveries for a neglected parasite. Biotechnology advances. 2010;28(2):222-31.
172. Li N, Tian W, Sun L, Yan H, Hasi S. Comparative analysis of transcriptomics of *Fasciola hepatica* at different developmental stages. Trop Biomed. 2024;41(3):290-7.
173. López-García M, Cwiklinski K, Becerro-Recio D, Ruiz-Campillo MT, Molina-Hernández V, Pérez-Arévalo J, et al. Deciphering the proteomic profile of the parasite *Fasciola hepatica* after initial vertebrate host infection reveals new insights into its early-stages. Molecular & Cellular Proteomics. 2025:101005.
174. Lalor R, Cwiklinski K, Calvani NED, Dorey A, Hamon S, Corrales JL, et al. Pathogenicity and virulence of the liver flukes *Fasciola hepatica* and *Fasciola gigantica* that cause the zoonosis Fasciolosis. Virulence. 2021;12(1):2839-67.
175. Quinteros SL, O'Brien B, Donnelly S. Exploring the role of macrophages in determining the pathogenesis of liver fluke infection. Parasitology. 2022;149(10):1364-73.
176. Castro-Hermida JA, González-Warleta M, Martínez-Sernández V, Ubeira FM, Mezo M. Current challenges for fasciolicide treatment in ruminant livestock. Trends in Parasitology. 2021;37(5):430-44.
177. Molina-Hernández V, Mulcahy G, Pérez J, Martínez-Moreno Á, Donnelly S, O'Neill SM, et al. *Fasciola hepatica* vaccine: we may not be there yet but we're on the right road. Veterinary parasitology. 2015;208(1-2):101-11.
178. Everts B, Perona-Wright G, Smits HH, Hokke CH, van der Ham AJ, Fitzsimmons CM, et al. Omega-1, a glycoprotein secreted by *Schistosoma mansoni* eggs, drives Th2 responses. Journal of Experimental Medicine. 2009;206(8):1673-80.
179. Walsh R. Modulation of immune responses by *Fasciola hepatica*-derived products: Trinity College Dublin; 2019.
180. Varga T, Mounier R, Horvath A, Cuvellier S, Dumont F, Poliska S, et al. Highly dynamic transcriptional signature of distinct macrophage subsets during sterile inflammation, resolution, and tissue repair. The Journal of Immunology. 2016;196(11):4771-82.
181. Ruiz-Campillo MT, Molina Hernandez V, Escamilla A, Stevenson M, Perez J, Martinez-Moreno A, et al. Immune signatures of pathogenesis in the peritoneal compartment during early infection of sheep with *Fasciola hepatica.* Sci Rep. 2017;7(1):2782.
182. Perez-Caballero R, Javier Martinez-Moreno F, Zafra R, Molina-Hernandez V, Pacheco IL, Teresa Ruiz-Campillo M, et al. Comparative dynamics of peritoneal cell

immunophenotypes in sheep during the early and late stages of the infection with *Fasciola hepatica* by flow cytometric analysis. Parasit Vectors. 2018;11(1):640.
183. Perez-Caballero R, Buffoni L, Martinez-Moreno FJ, Zafra R, Molina-Hernandez V, Perez J, et al. Expression of free radicals by peritoneal cells of sheep during the early stages of *Fasciola hepatica* infection. Parasit Vectors. 2018;11(1):500.
184. Golden O, Flynn RJ, Read C, Sekiya M, Donnelly S, Stack C, et al. Protection of cattle against a natural infection of *Fasciola hepatica* by vaccination with recombinant cathepsin L1 (rFhCL1). Vaccine. 2010;28(34):5551-7.
185. Donnelly S, O'Neill SM, Sekiya M, Mulcahy G, Dalton JP. Thioredoxin peroxidase secreted by *Fasciola hepatica* induces the alternative activation of macrophages. Infection and immunity. 2005;73(1):166-73.
186. Stempin CC, Motrán CC, Aoki MP, Falcón CR, Cerbán FM, Cervi L. PD-L2 negatively regulates Th1-mediated immunopathology during *Fasciola hepatica* infection. Oncotarget. 2016;7(47):77721-31.
187. Frigerio S, Da Costa V, Costa M, Festari MF, Landeira M, Rodríguez-Zraquia SA, et al. Eosinophils control liver damage by modulating immune responses against *Fasciola hepatica*. Frontiers in immunology. 2020;11:579801.
188. Rodríguez E, Noya V, Cervi L, Chiribao ML, Brossard N, Chiale C, et al. Glycans from *Fasciola hepatica* modulate the host immune response and TLR-induced maturation of dendritic cells. PLoS neglected tropical diseases. 2015;9(12):e0004234.
189. Hamilton CM, Dowling DJ, Loscher CE, Morphew RM, Brophy PM, O'Neill SM. The *Fasciola hepatica* tegumental antigen suppresses dendritic cell maturation and function. Infection and immunity. 2009;77(6):2488-98.
190. Peixoto R, Silva LM, López-Osório S, Zhou E, Gärtner U, Conejeros I, et al. *Fasciola hepatica* induces weak NETosis and low production of intra-and extracellular ROS in exposed bovine polymorphonuclear neutrophils. Developmental & Comparative Immunology. 2021;114:103787.
191. Neill SM, Donnelly S. Mechanisms of Immune Modulation by *Fasciola hepatica*: the impact of innate immune cells on the developing adaptive immune response. Immunity to Helminths and Novel Therapeutic Approaches: Bentham Science Publishers; 2014. p. 51-67.
192. McSorley HJ, Blair NF, Robertson E, Maizels RM. Suppression of OVA-alum induced allergy by Heligmosomoides polygyrus products is MyD88-, TRIF-, regulatory T-and B cell-independent, but is associated with reduced innate lymphoid cell activation. Experimental parasitology. 2015;158:8-17.
193. Balic A, Harcus Y, Holland MJ, Maizels RM. Selective maturation of dendritic cells by *Nippostrongylus brasiliensis*-secreted proteins drives Th2 immune responses. European journal of immunology. 2004;34(11):3047-59.
194. Vacca F, Le Gros G. Tissue-specific immunity in helminth infections. Mucosal Immunology. 2022;15(6):1212-23.
195. Soleymani N, Sadr S, Santucciu C, Dianaty S, Lotfalizadeh N, Hajjafari A, et al. Unveiling novel insights in helminth proteomics: advancements, applications, and implications for parasitology and beyond. Biologics. 2024;4(3):314-44.
196. Yeshi K, Ruscher R, Loukas A, Wangchuk P. Immunomodulatory and biological properties of helminth-derived small molecules: Potential applications in diagnostics and therapeutics. Frontiers in Parasitology. 2022;1:984152.
197. Dalton JP, McGonigle S, Rolph TP, Andrews SJ. Induction of protective immunity in cattle against infection with *Fasciola hepatica* by vaccination with cathepsin L proteinases and with hemoglobin. Infection and immunity. 1996;64(12):5066-74.

198. Donnelly S, O'Neill SM, Stack CM, Robinson MW, Turnbull L, Whitchurch C, et al. Helminth cysteine proteases inhibit TRIF-dependent activation of macrophages via degradation of TLR3. Journal of Biological Chemistry. 2010;285(5):3383-92.
199. Lund ME, Greer J, Dixit A, Alvarado R, McCauley-Winter P, To J, et al. A parasite-derived 68-mer peptide ameliorates autoimmune disease in murine models of Type 1 diabetes and multiple sclerosis. Scientific Reports. 2016;6(1):37789.
200. Flores-Velázquez LM, Ruiz-Campillo MT, Herrera-Torres G, Martínez-Moreno Á, Martínez-Moreno FJ, Zafra R, et al. Fasciolosis: pathogenesis, host-parasite interactions, and implication in vaccine development. Frontiers in veterinary science. 2023;10:1270064.
201. Figueroa-Santiago O, Espino AM. *Fasciola hepatica* fatty acid binding protein induces the alternative activation of human macrophages. Infection and immunity. 2014;82(12):5005-12.
202. Chowdhury S, Sais D, Donnelly S, Tran N. The knowns and unknowns of helminth–host miRNA cross-kingdom communication. Trends in Parasitology. 2024;40(2):176-91.
203. Polley L, Thompson RA. Parasite zoonoses and climate change: molecular tools for tracking shifting boundaries. Trends in Parasitology. 2009;25(6):285-91.
204. Mas-Coma S, Valero MA, Bargues MD. Climate change effects on trematodiases, with emphasis on zoonotic fascioliasis and schistosomiasis. Veterinary Parasitology. 2009;163(4):264-80.
205. Robinson MW, Dalton JP. Zoonotic helminth infections with particular emphasis on fasciolosis and other trematodiases. Philos Trans R Soc Lond B Biol Sci. 2009;364(1530):2763-76.
206. Howell AK, Williams DJ. The epidemiology and control of liver flukes in cattle and sheep. Veterinary Clinics: Food Animal Practice. 2020;36(1):109-23.
207. Boray J, Crowfoot P, Strong M, Allison J, Schellenbaum M, Von Orelli M, et al. Treatment of immature and mature *Fasciola hepatica* infections in sheep with triclabendazole. The Veterinary Record. 1983;113(14):315-7.
208. McMahon C, Edgar HWJ, Hanna REB, Ellison SE, Flanagan AM, McCoy M, et al. Liver fluke control on sheep farms in Northern Ireland: A survey of changing management practices in relation to disease prevalence and perceived triclabendazole resistance. Veterinary Parasitology. 2016;216:72-83.
209. Kelley JM, Rawlin G, Beddoe T, Stevenson M, Spithill TW. *Fasciola hepatica* control practices on a sample of dairy farms in victoria, Australia. Frontiers in Veterinary Science. 2021;8:669117.
210. Stuen S, Ersdal C. Fasciolosis—an increasing challenge in the sheep industry. Animals. 2022;12(12):1491.
211. Novobilský A, Höglund J. First report of closantel treatment failure against *Fasciola hepatica* in cattle. International Journal for Parasitology: Drugs and Drug Resistance. 2015;5(3):172-7.
212. Moll L, Gaasenbeek CP, Vellema P, Borgsteede FH. Resistance of *Fasciola hepatica* against triclabendazole in cattle and sheep in The Netherlands. Veterinary parasitology. 2000;91(1-2):153-8.
213. Hanna RE, McMahon C, Ellison S, Edgar HW, Kajugu PE, Gordon A, et al. *Fasciola hepatica*: a comparative survey of adult fluke resistance to triclabendazole, nitroxynil and closantel on selected upland and lowland sheep farms in Northern Ireland using faecal egg counting, coproantigen ELISA testing and fluke histology. Vet Parasitol. 2015;207(1-2):34-43.
214. Taylor MA, Coop RL, Wall RL. Veterinary parasitology. John Wiley & Sons; 2015.
215. Mazeri S, Sargison N, Kelly RF, Bronsvoort BM, Handel I. Evaluation of the performance of five diagnostic tests for *Fasciola hepatica* Infection in naturally infected cattle using a bayesian no gold standard approach. PLoS One. 2016;11(8):e0161621.

216. Mazeri S, Rydevik G, Handel I, Bronsvoort BMD, Sargison N. Estimation of the impact of *Fasciola hepatica* infection on time taken for UK beef cattle to reach slaughter weight. Sci Rep. 2017;7(1):7319.
217. Braun U, Wolfensberger R, Hertzberg H. Diagnosis of liver flukes in cows--a comparison of the findings in the liver, in the feces, and in the bile. Schweizer Archiv fur Tierheilkunde. 1995;137(9):438-44.
218. Charlier J, De Meulemeester L, Claerebout E, Williams D, Vercruysse J. Qualitative and quantitative evaluation of coprological and serological techniques for the diagnosis of fasciolosis in cattle. Veterinary parasitology. 2008;153(1-2):44-51.
219. Sánchez-Andrade R, Paz-Silva A, Suárez J, Panadero R, Díez-Baños P, Morrondo P. Use of a sandwich-enzyme-linked immunosorbent assay (SEA) for the diagnosis of natural *Fasciola hepatica* infection in cattle from Galicia (NW Spain). Veterinary Parasitology. 2000;93(1):39-46.
220. Novobilský A, Averpil HB, Höglund J. The field evaluation of albendazole and triclabendazole efficacy against *Fasciola hepatica* by coproantigen ELISA in naturally infected sheep. Veterinary Parasitology. 2012;190(1):272-6.
221. Brockwell Y, Spithill T, Anderson G, Grillo V, Sangster N. Comparative kinetics of serological and coproantigen ELISA and faecal egg count in cattle experimentally infected with *Fasciola hepatica* and following treatment with triclabendazole. Veterinary parasitology. 2013;196(3-4):417-26.
222. Novobilský A, Engström A, Sollenberg S, Gustafsson K, Morrison DA, Höglund J. Transmission patterns of *Fasciola hepatica* to ruminants in Sweden. Veterinary Parasitology. 2014;203(3):276-86.
223. Cornelissen JBWJ, Gaasenbeek CPH, Boersma W, Borgsteede FHM, van Milligen FJ. Use of a pre-selected epitope of cathepsin-L1 in a highly specific peptide-based immunoassay for the diagnosis of *Fasciola hepatica* infections in cattle. International Journal for Parasitology. 1999;29(5):685-96.
224. Costa M, Saravia A, Ubios D, Lores P, da Costa V, Festari MF, et al. Liver function markers and haematological dynamics during acute and chronic phases of experimental *Fasciola hepatica* infection in cattle treated with triclabendazole. Experimental Parasitology. 2022;238:108285.
225. Ambros V. The functions of animal microRNAs. Nature. 2004;431(7006):350-5.
226. Tribolet L, Kerr E, Cowled C, Bean AG, Stewart CR, Dearnley M, et al. MicroRNA biomarkers for infectious diseases: from basic research to biosensing. Frontiers in microbiology. 2020;11:1197.
227. Blondal T, Nielsen SJ, Baker A, Andreasen D, Mouritzen P, Teilum MW, et al. Assessing sample and miRNA profile quality in serum and plasma or other biofluids. Methods. 2013;59(1):S1-S6.
228. Hoy AM, Lundie RJ, Ivens A, Quintana JF, Nausch N, Forster T, et al. Parasite-derived microRNAs in host serum as novel biomarkers of helminth infection. PLoS neglected tropical diseases. 2014;8(2):e2701.
229. Guo X, Guo A. Profiling circulating microRNAs in serum of *Fasciola gigantica*-infected buffalo. Molecular and Biochemical Parasitology. 2019;232:111201.
230. Ghalehnoei H, Bagheri A, Fakhar M, Mishan MA. Circulatory microRNAs: promising non-invasive prognostic and diagnostic biomarkers for parasitic infections. European Journal of Clinical Microbiology & Infectious Diseases. 2020;39:395-402.
231. Ricafrente A, Cwiklinski K, Nguyen H, Dalton JP, Tran N, Donnelly S. Stage-specific miRNAs regulate gene expression associated with growth, development and parasite-host interaction during the intra-mammalian migration of the zoonotic helminth parasite *Fasciola hepatica*. BMC Genomics. 2022;23(1):419.

232. Corrales JL, Cwiklinski K, Verissimo CDM, Dorey A, Lalor R, Jewhurst H, et al. Diagnosis of sheep fasciolosis caused by *Fasciola hepatica* using cathepsin L enzyme-linked immunosorbent assays (ELISA). Veterinary parasitology. 2021;298:109517.
233. El-Khoury V, Pierson S, Kaoma T, Bernardin F, Berchem G. Assessing cellular and circulating miRNA recovery: the impact of the RNA isolation method and the quantity of input material. Scientific reports. 2016;6(1):19529.
234. Andrews S. FastQC: a quality control tool for high throughput sequence data. Babraham Bioinformatics, Babraham Institute, Cambridge, United Kingdom; 2010.
235. Martin M. Cutadapt removes adapter sequences from high-throughput sequencing reads. EMBnet journal. 2011;17(1):10-2.
236. Langmead B. Aligning short sequencing reads with Bowtie. Current protocols in bioinformatics. 2010;32(1):11.7. 1-.7. 4.
237. Love M, Anders S, Huber W. Differential analysis of count data – the DESeq2 package. Genome Biol. 2014;15(550):10-1186.
238. Ruijter J, Ramakers C, Hoogaars W, Karlen Y, Bakker O, Van den Hoff M, et al. Amplification efficiency: linking baseline and bias in the analysis of quantitative PCR data. Nucleic acids research. 2009;37(6):e45-e.
239. Ge SX, Son EW, Yao R. iDEP: an integrated web application for differential expression and pathway analysis of RNA-Seq data. BMC Bioinformatics. 2018;19(1):534.
240. Melville L, Hayward A, Morgan E, Shaw D, McBean D, Andrews L, et al. Precision worm control in grazing lambs by targeting group treatment based on performance of sentinels. Animal. 2021;15(4):100176.
241. Shandilya UK, Sharma A, Naylor D, Canovas A, Mallard B, Karrow NA. Expression profile of miRNA from high, middle, and low stress-responding sheep during bacterial endotoxin challenge. Animals. 2023;13(3):508.
242. Sharma A, Shandilya UK, Sullivan T, Naylor D, Cánovas A, Mallard B, et al. PSXIV-20 Ovine circulatory markers regulating the acute-phase response of variable stress responding sheep to LPS challenge. Journal of Animal Science. 2021;99(Supplement_3):494-5.
243. Jin P, Li S, Sun L, Lv C, Ma F. Transcriptome-wide analysis of microRNAs in *Branchiostoma belcheri* upon *Vibrio parahemolyticus* infection. Developmental & Comparative Immunology. 2017;74:243-52.
244. Carpi S, Polini B, Nieri D, Dubbini N, Celi A, Nieri P, et al. Expression analysis of muscle-specific miRNAs in plasma-derived extracellular vesicles from patients with chronic obstructive pulmonary disease. Diagnostics. 2020;10(7):502.
245. He M-Q, Wan J-F, Zeng H-F, Tang Y-Y, He M-Q. miR-133a-5p suppresses gastric cancer through TCF4 down-regulation. Journal of Gastrointestinal Oncology. 2021;12(3):1007.
246. Alizadeh Z, Mahami-Oskouei M, Spotin A, Kazemi T, Ahmadpour E, Cai P, et al. Parasite-derived microRNAs in plasma as novel promising biomarkers for the early detection of hydatid cyst infection and post-surgery follow-up. Acta tropica. 2020;202:105255.
247. Neilsen CT, Goodall GJ, Bracken CP. IsomiRs – the overlooked repertoire in the dynamic microRNAome. Trends in Genetics. 2012;28(11):544-9.
248. Wagner V, Meese E, Keller A. The intricacies of isomiRs: from classification to clinical relevance. Trends in Genetics. 2024.
249. Morin RD, O'Connor MD, Griffith M, Kuchenbauer F, Delaney A, Prabhu A-L, et al. Application of massively parallel sequencing to microRNA profiling and discovery in human embryonic stem cells. Genome research. 2008;18(4):610-21.
250. Tomasello L, Distefano R, Nigita G, Croce CM. The MicroRNA family gets wider: the IsomiRs classification and role. Frontiers in cell and developmental biology. 2021;9:668648.

251. Zhiyanov A, Nersisyan S, Tonevitsky A. Hairpin sequence and structure is associated with features of isomiR biogenesis. RNA biology. 2021;18(sup1):430-8.
252. Starega-Roslan J, Witkos TM, Galka-Marciniak P, Krzyzosiak WJ. Sequence features of Drosha and Dicer cleavage sites affect the complexity of isomiRs. International journal of molecular sciences. 2015;16(4):8110-27.
253. Gu S, Jin L, Zhang Y, Huang Y, Zhang F, Valdmanis PN, et al. The loop position of shRNAs and pre-miRNAs is critical for the accuracy of dicer processing *in vivo*. Cell. 2012;151(4):900-11.
254. Burroughs AM, Ando Y, de Hoon MJ, Tomaru Y, Nishibu T, Ukekawa R, et al. A comprehensive survey of 3′ animal miRNA modification events and a possible role for 3′ adenylation in modulating miRNA targeting effectiveness. Genome research. 2010;20(10):1398-410.
255. Thornton JE, Du P, Jing L, Sjekloca L, Lin S, Grossi E, et al. Selective microRNA uridylation by Zcchc6 (TUT7) and Zcchc11 (TUT4). Nucleic acids research. 2014;42(18):11777-91.
256. Xie W, Sowemimo I, Hayashi R, Wang J, Burkard TR, Brennecke J, et al. Structure-function analysis of microRNA 3′-end trimming by Nibbler. Proceedings of the National Academy of Sciences. 2020;117(48):30370-9.
257. Yoda M, Cifuentes D, Izumi N, Sakaguchi Y, Suzuki T, Giraldez Antonio J, et al. Poly(A)-Specific Ribonuclease Mediates 3′-End Trimming of Argonaute2-Cleaved Precursor MicroRNAs. Cell Reports. 2013;5(3):715-26.
258. Panzade G, Li L, Hebbar S, Veksler-Lublinsky I, Zinovyeva A. Global profiling and annotation of templated isomiRs dynamics across Caenorhabditis elegans development. RNA biology. 2022;19(1):928-42.
259. Dika E, Broseghini E, Porcellini E, Lambertini M, Riefolo M, Durante G, et al. Unraveling the role of microRNA/isomiR network in multiple primary melanoma pathogenesis. Cell Death & Disease. 2021;12(5):473.
260. Siddle KJ, Tailleux L, Deschamps M, Loh Y-HE, Deluen C, Gicquel B, et al. Bacterial infection drives the expression dynamics of microRNAs and their isomiRs. PLoS genetics. 2015;11(3):e1005064.
261. Fernandez-Valverde SL, Taft RJ, Mattick JS. Dynamic isomiR regulation in Drosophila development. Rna. 2010;16(10):1881-8.
262. Guo L, Liang T, Yu J, Zou Q. A comprehensive analysis of miRNA/isomiR expression with gender difference. PloS one. 2016;11(5):e0154955.
263. Nersisyan S, Zhiyanov A, Engibaryan N, Maltseva D, Tonevitsky A. A novel approach for a joint analysis of isomiR and mRNA expression data reveals features of isomiR targeting in breast cancer. Frontiers in Genetics. 2022;13:1070528.
264. McGahon MK, Yarham JM, Daly A, Guduric-Fuchs J, Ferguson LJ, Simpson DA, et al. Distinctive profile of IsomiR expression and novel microRNAs in rat heart left ventricle. PloS one. 2013;8(6):e65809.
265. Cloonan N, Wani S, Xu Q, Gu J, Lea K, Heater S, et al. MicroRNAs and their isomiRs function cooperatively to target common biological pathways. Genome biology. 2011;12(12):1-20.
266. Guo L, Li H, Liang T, Lu J, Yang Q, Ge Q, et al. Consistent isomiR expression patterns and 3′ addition events in miRNA gene clusters and families implicate functional and evolutionary relationships. Molecular biology reports. 2012;39:6699-706.
267. Tan GC, Chan E, Molnar A, Sarkar R, Alexieva D, Isa IM, et al. 5′ isomiR variation is of functional and evolutionary importance. Nucleic acids research. 2014;42(14):9424-35.

268. Al-Modawi RN, Brinchmann JE, Karlsen TA. Extensive downregulation of immune gene expression by microRNA-140-3p 5′ isomiR in an *in vitro* model of osteoarthritis. Osteoarthritis and Cartilage Open. 2021;3(3):100189.
269. van der Kwast RV, Woudenberg T, Quax PH, Nossent AY. MicroRNA-411 and Its 5′-IsomiR have distinct targets and functions and are differentially regulated in the vasculature under ischemia. Molecular Therapy. 2020;28(1):157-70.
270. Broughton JP, Lovci MT, Huang JL, Yeo GW, Pasquinelli AE. Pairing beyond the seed supports microRNA targeting specificity. Molecular cell. 2016;64(2):320-33.
271. Liu N, Abe M, Sabin LR, Hendriks G-J, Naqvi AS, Yu Z, et al. The exoribonuclease Nibbler controls 3′ end processing of microRNAs in *Drosophila.* Current Biology. 2011;21(22):1888-93.
272. Llorens F, Bañez-Coronel M, Pantano L, del Río JA, Ferrer I, Estivill X, et al. A highly expressed miR-101 isomiR is a functional silencing small RNA. BMC genomics. 2013;14:1-14.
273. Nejad C, Pillman KA, Siddle KJ, Pépin G, Änkö M-L, McCoy CE, et al. miR-222 isoforms are differentially regulated by type-I interferon. Rna. 2018;24(3):332-41.
274. Sais D, Chowdhury S, Nguyen PT, Cwiklinski K, Nguyen TD, Nguyen TA, et al. Dynamic shifts in isomiR profiles during parasite maturation of *Fasciola hepatica*. RNA biology. 2025;22(1):1-22.
275. Li H, Handsaker B, Wysoker A, Fennell T, Ruan J, Homer N, et al. The Sequence Alignment/Map format and SAMtools. Bioinformatics. 2009;25(16):2078-9.
276. Enright A, John B, Gaul U, Tuschl T, Sander C, Marks D. MicroRNA targets in Drosophila. Genome biology. 2003;4(11):P8.
277. Kolberg L, Raudvere U, Kuzmin I, Adler P, Vilo J, Peterson H. g: Profiler—interoperable web service for functional enrichment analysis and gene identifier mapping (2023 update). Nucleic acids research. 2023;51(W1):W207-W12.
278. Supek F, Bošnjak M, Škunca N, Šmuc T. REVIGO summarizes and visualizes long lists of gene ontology terms. PloS one. 2011;6(7):e21800.
279. Ajuyah P, Hill M, Ahadi A, Lu J, Hutvagner G, Tran N. MicroRNA (miRNA)-to-miRNA regulation of programmed cell death 4 (PDCD4). Mol Cell Biol. 2019;39(18).
280. Ma S, Liu M, Xu Z, Li Y, Guo H, Ge Y, et al. A double feedback loop mediated by microRNA-23a/27a/24-2 regulates M1 versus M2 macrophage polarization and thus regulates cancer progression. Oncotarget. 2015;7(12):13502.
281. Xia T, Zhang M, Lei W, Yang R, Fu S, Fan Z, et al. Advances in the role of STAT3 in macrophage polarization. Front Immunol. 2023;14:1160719.
282. Qiu B, Yuan P, Du X, Jin H, Du J, Huang Y. Hypoxia inducible factor-1α is an important regulator of macrophage biology. Heliyon. 2023;9(6):e17167.
283. Mellett M, Atzei P, Bergin R, Horgan A, Floss T, Wurst W, et al. Orphan receptor IL-17RD regulates Toll-like receptor signalling via SEFIR/TIR interactions. Nature Communications. 2015;6(1):6669.
284. Lufei C, Koh TH, Uchida T, Cao X. Pin1 is required for the Ser727 phosphorylation-dependent Stat3 activity. Oncogene. 2007;26(55):7656-64.
285. Dong R, Xue Z, Fan G, Zhang N, Wang C, Li G, et al. Pin1 promotes NLRP3 inflammasome activation by phosphorylation of p38 MAPK pathway in septic shock. Front Immunol. 2021;12:620238.
286. Luo M-C, Zhou S-Y, Feng D-Y, Xiao J, Li W-Y, Xu C-D, et al. Runt-related Transcription Factor 1 (RUNX1) Binds to p50 in macrophages and enhances TLR4-triggered inflammation and septic shock. Journal of Biological Chemistry. 2016;291(42):22011-20.

287. de Torre-Minguela C, Barberà-Cremades M, Gómez AI, Martín-Sánchez F, Pelegrín P. Macrophage activation and polarization modify P2X7 receptor secretome influencing the inflammatory process. Scientific Reports. 2016;6(1):22586.
288. Wiley J, Sluyter R, Gu B, Stokes L, Fuller S. The human P2X7 receptor and its role in innate immunity. Tissue antigens. 2011;78(5):321-32.
289. Kang TJ, Chae GT. The Role of Intracellular Receptor NODs for cytokine production by macrophages infected with *Mycobacterium leprae*. Immune Netw. 2011;11(6):424-7.
290. Bode JG, Ehlting C, Häussinger D. The macrophage response towards LPS and its control through the p38MAPK–STAT3 axis. Cellular signalling. 2012;24(6):1185-94.
291. Harris AJ, Roger Thompson A, KB Whyte M, Walmsley SR. HIF-mediated innate immune responses: cell signaling and therapeutic implications. Hypoxia. 2014:47-58.
292. Pashenkov MV, Murugina NE, Budikhina AS, Pinegin BV. Synergistic interactions between NOD receptors and TLRs: Mechanisms and clinical implications. Journal of leukocyte biology. 2019;105(4):669-80.
293. Fan G, Li G, Li L, Da Y. Pin1 maintains the effector program of pathogenic Th17 cells in autoimmune neuroinflammation. Journal of Autoimmunity. 2024;147:103262.
294. Loher P, Rigoutsos I. Interactive exploration of RNA22 microRNA target predictions. Bioinformatics. 2012;28(24):3322-3.
295. Coronnello C, Benos PV. ComiR: combinatorial microRNA target prediction tool. Nucleic acids research. 2013;41(W1):W159-W64.
296. Talukder A, Zhang W, Li X, Hu H. A deep learning method for miRNA/isomiR target detection. Scientific reports. 2022;12(1):10618.
297. Chandradoss SD, Schirle NT, Szczepaniak M, MacRae IJ, Joo C. A dynamic search process underlies microRNA targeting. Cell. 2015;162(1):96-107.
298. Fujihara M, Muroi M, Tanamoto K-i, Suzuki T, Azuma H, Ikeda H. Molecular mechanisms of macrophage activation and deactivation by lipopolysaccharide: roles of the receptor complex. Pharmacology & Therapeutics. 2003;100(2):171-94.
299. Ruiz-Campillo MT, Molina-Hernández V, Pérez J, Pacheco IL, Pérez R, Escamilla A, et al. Study of peritoneal macrophage immunophenotype in sheep experimentally infected with Fasciola hepatica. Vet Parasitol. 2018;257:34-9.
300. Davies LC, Rice CM, Palmieri EM, Taylor PR, Kuhns DB, McVicar DW. Peritoneal tissue-resident macrophages are metabolically poised to engage microbes using tissue-niche fuels. Nature Communications. 2017;8(1):2074.
301. Louwe PA, Badiola Gomez L, Webster H, Perona-Wright G, Bain CC, Forbes SJ, et al. Recruited macrophages that colonize the post-inflammatory peritoneal niche convert into functionally divergent resident cells. Nature Communications. 2021;12(1):1770.
302. Ardavín C, Alvarez-Ladrón N, Ferriz M, Gutiérrez-González A, Vega-Pérez A. Mouse Tissue-Resident Peritoneal Macrophages in Homeostasis, Repair, Infection, and Tumor Metastasis. Adv Sci (Weinh). 2023;10(11):e2206617.
303. Escamilla A, Pérez-Caballero R, Zafra R, Bautista MJ, Pacheco IL, Ruiz MT, et al. Apoptosis of peritoneal leucocytes during early stages of *Fasciola hepatica* infections in sheep. Veterinary Parasitology. 2017;238:49-53.
304. Corral-Ruiz GM, Sánchez-Torres LE. *Fasciola hepatica*-derived molecules as potential immunomodulators. Acta Tropica. 2020;210:105548.
305. Llorens F, Bañez-Coronel M, Pantano L, del Río JA, Ferrer I, Estivill X, et al. A highly expressed miR-101 isomiR is a functional silencing small RNA. BMC Genomics. 2013;14:104.
306. Haseeb A, Makki MS, Khan NM, Ahmad I, Haqqi TM. Deep sequencing and analyses of miRNAs, isomiRs and miRNA induced silencing complex (miRISC)-associated miRNome in primary human chondrocytes. Scientific Reports. 2017;7(1):15178.

307. Wang Y, Sheng G, Juranek S, Tuschl T, Patel DJ. Structure of the guide-strand-containing argonaute silencing complex. Nature. 2008;456(7219):209-13.
308. Müller M, Fazi F, Ciaudo C. Argonaute proteins: from structure to function in development and pathological cell fate determination. Frontiers in Cell and Developmental Biology. 2020;7:360.
309. Liu J, Carmell MA, Rivas FV, Marsden CG, Thomson JM, Song J-J, et al. Argonaute2 is the catalytic engine of mammalian RNAi. Science. 2004;305(5689):1437-41.
310. Valdmanis PN, Gu S, Schüermann N, Sethupathy P, Grimm D, Kay MA. Expression determinants of mammalian argonaute proteins in mediating gene silencing. Nucleic acids research. 2012;40(8):3704-13.
311. Wang D, Zhang Z, O'Loughlin E, Lee T, Houel S, O'Carroll D, et al. Quantitative functions of Argonaute proteins in mammalian development. Genes Dev. 2012;26(7):693-704.
312. Yekta S, Shih I-h, Bartel DP. MicroRNA-directed cleavage of HOXB8 mRNA. Science. 2004;304(5670):594-6.
313. Mazumder A, Bose M, Chakraborty A, Chakrabarti S, Bhattacharyya SN. A transient reversal of miRNA-mediated repression controls macrophage activation. EMBO reports. 2013;14(11):1008-16.
314. Ranjan R, Lee Y, Karpurapu M, Syed M, Chung S, Deng J, et al. p47phox and reactive oxygen species production modulate expression of microRNA-451 in macrophages. Free radical research. 2015;49(1):25-34.
315. Adiliaghdam F, Basavappa M, Saunders TL, Harjanto D, Prior JT, Cronkite DA, et al. A requirement for Argonaute 4 in mammalian antiviral defense. Cell Rep. 2020;30(6):1690-701.e4.
316. Moradimotlagh A, Chen S, Koohbor S, Moon K-M, Foster LJ, Reiner N, et al. Leishmania infection upregulates and engages host macrophage Argonaute 1, and system-wide proteomics reveals Argonaute 1-dependent host response. Frontiers in Immunology. 2023;14:1287539.
317. Paturi S, Deshmukh MV. A glimpse of “Dicer Biology” through the structural and functional perspective. Frontiers in molecular biosciences. 2021;8:643657.
318. Sakurai K, Amarzguioui M, Kim D-H, Alluin J, Heale B, Song M-s, et al. A role for human Dicer in pre-RISC loading of siRNAs. Nucleic Acids Research. 2010;39(4):1510-25.
319. Wilson Ross C, Tambe A, Kidwell Mary A, Noland Cameron L, Schneider Catherine P, Doudna Jennifer A. Dicer-TRBP Complex Formation Ensures Accurate Mammalian MicroRNA Biogenesis. Molecular Cell. 2015;57(3):397-407.
320. Wei Y, Corbalán-Campos J, Gurung R, Natarelli L, Zhu M, Exner N, et al. Dicer in macrophages prevents atherosclerosis by promoting mitochondrial oxidative metabolism. Circulation. 2018;138(18):2007-20.
321. Guan Y, Yao H, Wang J, Sun K, Cao L, Wang Y. NF-κB-DICER-miRs axis regulates TNF-α expression in responses to endotoxin stress. International journal of biological sciences. 2015;11(11):1257.
322. Berghaus LJ, Moore JN, Hurley DJ, Vandenplas ML, Fortes BP, Wolfert MA, et al. Innate immune responses of primary murine macrophage-lineage cells and RAW 264.7 cells to ligands of Toll-like receptors 2, 3, and 4. Comp Immunol Microbiol Infect Dis. 2010;33(5):443-54.
323. Graf J, Bomb K, Trautmann-Rodriguez M, Jarai BM, Gill N, Kloxin AM, et al. Macrophage variance: investigating how macrophage origin influences responses to soluble and physical cues with immortalized vs. primary cells in 2D and 3D culture. Frontiers in Biomaterials Science. 2024;3:1399448.
324. Hwang HW, Mendell JT. MicroRNAs in cell proliferation, cell death, and tumorigenesis. Br J Cancer. 2006;94(6):776-80.

325. Peng Y, Croce CM. The role of MicroRNAs in human cancer. Signal Transduction and Targeted Therapy. 2016;1(1):15004.
326. Zhu Y, Wang G, Xu H, Guo Y. CRISPR-Cas9 mediated AGO2 knockout inhibits tumorigenesis in human colorectal cancer cells. Cellular and Molecular Biology. 2024;70(7):174-9.
327. Yang Y, Mei Q. Accumulation of AGO2 facilitates tumorigenesis of human hepatocellular carcinoma. Biomed Res Int. 2020;2020:1631843.
328. Liu YQ, Luo M, Shi Y, Guo Y, Zhang H, Yang KD, et al. Dicer deficiency impairs proliferation but potentiates anti-tumoral effect of macrophages in glioblastoma. Oncogene. 2022;41(30):3791-803.
329. Gurung C, Fendereski M, Sapkota K, Guo J, Huang F, Guo Y-L. Dicer represses the interferon response and the double-stranded RNA-activated protein kinase pathway in mouse embryonic stem cells. Journal of Biological Chemistry. 2021;296:100264.
330. Wang Z, Li W, Li J, Jin T, Chen H, Liang F, et al. Neutrophil-modulated Dicer expression in macrophages influences inflammation resolution. Cellular and Molecular Life Sciences. 2025;82(1):1-18.
331. Guo M, Härtlova A, Dill BD, Prescott AR, Gierliński M, Trost M. High-resolution quantitative proteome analysis reveals substantial differences between phagosomes of RAW 264.7 and bone marrow derived macrophages. Proteomics. 2015;15(18):3169-74.
332. Mao Q, Luo B, Mei J, Li W, Zhang X, Wang Z, et al. Macrophage Dicer promotes tolerogenic apoptotic cell clearance and immune tolerance by inhibiting pentose phosphate pathway activity. Cell Mol Immunol. 2021;18(7):1841-3.
333. Tripathi A, Rai NK, Perles A, Courtney H, Jones C, Sapra A, et al. Dicer deficiency affects microglial function during demyelination and impairs remyelination. Neurobiology of Disease. 2025;208:106879.
334. Flannagan RS, Jaumouillé V, Grinstein S. The cell biology of phagocytosis. Annual Review of Pathology: Mechanisms of Disease. 2012;7(1):61-98.
335. Nguyen M-A, Karunakaran D, Geoffrion M, Cheng HS, Tandoc K, Perisic Matic L, et al. Extracellular vesicles Secreted by atherogenic macrophages transfer MicroRNA to inhibit cell migration. Arteriosclerosis, Thrombosis, and Vascular Biology. 2018;38(1):49-63.
336. Bhattacharya S, Aggarwal R, Pal Singh V, Ramachandran S, Datta M. Downregulation of miRNAs during delayed wound healing in diabetes: role of dicer. Molecular Medicine. 2015;21(1):847-60.
337. Kim S, Kim Y, Kim W, Rin Lee W. Effect of AGO2 depletion on cell migration of A172 brain cancer cell. Cancer Res J. 2020;8:51.
338. Zhang N, Bevan MJ. Dicer controls CD8+ T-cell activation, migration, and survival. Proceedings of the National Academy of Sciences. 2010;107(50):21629-34.
339. Han X, Wu J, Sha Z, Lai R, Shi J, Mi L, et al. Dicer Suppresses Hepatocellular Carcinoma via Interleukin-8 Pathway. Clinical Medicine Insights: Oncology. 2023;17:11795549231161212.
340. Han L, Zhang A, Zhou X, Xu P, Wang G-X, Pu P-Y, et al. Downregulation of Dicer enhances tumor cell proliferation and invasion. International journal of oncology. 2010;37(2):299-305.
341. Uddin F, Rudin CM, Sen T. CRISPR gene therapy: applications, limitations, and implications for the future. Front Oncol. 2020;10:1387.
342. Kiszałkiewicz JM, Majewski S, Piotrowski WJ, Górski P, Pastuszak-Lewandoska D, Migdalska-Sęk M, et al. Evaluation of selected IL6/STAT3 pathway molecules and miRNA expression in chronic obstructive pulmonary disease. Scientific Reports. 2021;11(1):22756.
343. Johnson DE, O'Keefe RA, Grandis JR. Targeting the IL-6/JAK/STAT3 signalling axis in cancer. Nature Reviews Clinical Oncology. 2018;15(4):234-48.

344. Vlacil A-K, Vollmeister E, Bertrams W, Schoesser F, Oberoi R, Schuett J, et al. Identification of microRNAs involved in NOD-dependent induction of pro-inflammatory genes in pulmonary endothelial cells. PLoS One. 2020;15(4):e0228764.
345. Rommereim LM, Akhade AS, Dutta B, Hutcheon C, Lounsbury NW, Rostomily CC, et al. A small sustained increase in NOD1 abundance promotes ligand-independent inflammatory and oncogene transcriptional responses. Sci Signal. 2020;13(661).
346. Ahmad H, Alatshan A, Bíró E, Benkő S. Retinoic acid differently modulates NOD1/NOD2-mediated inflammatory responses in human macrophage subsets. Frontiers in Immunology. 2025;16:1609763.
347. Caruso R, Warner N, Inohara N, Núñez G. NOD1 and NOD2: signaling, host defense, and inflammatory disease. Immunity. 2014;41(6):898-908.
348. Baer C, Squadrito ML, Laoui D, Thompson D, Hansen SK, Kiialainen A, et al. Suppression of microRNA activity amplifies IFN-γ-induced macrophage activation and promotes anti-tumour immunity. Nature cell biology. 2016;18(7):790-802.
349. Xia S, Chen W, Xu Z, Gao Y, Chen J, Ding N, et al. Targeting Dicer reprograms tumor-associated macrophages to promote anti-tumoral immunity in colorectal cancer liver metastasis. Journal of Nanobiotechnology. 2025;23(1):421.
350. Luo Y, Zheng SG. Hall of Fame among Pro-inflammatory Cytokines: Interleukin-6 Gene and Its Transcriptional Regulation Mechanisms. Front Immunol. 2016;7:604.
351. Aliyu M, Zohora FT, Anka AU, Ali K, Maleknia S, Saffarioun M, et al. Interleukin-6 cytokine: An overview of the immune regulation, immune dysregulation, and therapeutic approach. International Immunopharmacology. 2022;111:109130.
352. Su H, Trombly MI, Chen J, Wang X. Essential and overlapping functions for mammalian Argonautes in microRNA silencing. Genes Dev. 2009;23(3):304-17.
353. Matsui M, Li L, Janowski BA, Corey DR. Reduced Expression of Argonaute 1, Argonaute 2 and TRBP Changes Levels and Intracellular Distribution of RNAi Factors. Scientific Reports. 2015;5(1):12855.
354. Ngondo RP, Cirera-Salinas D, Yu J, Wischnewski H, Bodak M, Vandormael-Pournin S, et al. Argonaute 2 is required for extra-embryonic endoderm differentiation of mouse embryonic stem cells. Stem Cell Reports. 2018;10(2):461-76.
355. Chu Y, Kilikevicius A, Liu J, Johnson KC, Yokota S, Corey DR. Argonaute binding within 3′-untranslated regions poorly predicts gene repression. Nucleic Acids Research. 2020;48(13):7439-53.
356. MacRae IJ, Ma E, Zhou M, Robinson CV, Doudna JA. *In vitro* reconstitution of the human RISC-loading complex. Proceedings of the National Academy of Sciences. 2008;105(2):512-7.
357. Betancur JG, Tomari Y. Dicer is dispensable for asymmetric RISC loading in mammals. Rna. 2012;18(1):24-30.
358. Kim H, Lee Y-Y, Kim VN. The biogenesis and regulation of animal microRNAs. Nature Reviews Molecular Cell Biology. 2025;26(4):276-96.
359. Hedges SB, Kumar S. The timetree of life: OUP Oxford; 2009.
360. Layton E, Goldsworthy S, Yang E, Ong WY, Sutherland TE, Bancroft AJ, et al. An optimised faecal microRNA sequencing pipeline reveals fibrosis in *Trichuris muris* infection. Nature Communications. 2025;16(1):1589.
361. Ferre A, Santiago L, Sánchez-Herrero JF, López-Rodrigo O, Sánchez-Curbelo J, Sumoy L, et al. 3'IsomiR species composition affects reliable quantification of miRNA/isomiR variants by Poly(A) RT-qPCR: impact on small RNA-Seq profiling validation. Int J Mol Sci. 2023;24(20).

362. Ai Z, Wang W, Li X, Wang X, Chen J, Wu J, et al. A CRISPR/Cas12a-coupled multiplexed amplification system for ultrasensitive detection of miRNA-155. Analytical Methods. 2025;17(19):4044-50.
363. PP ASU, Sekar D. Novel insights into biosensor-based helminth detection: implications for public health. The Lancet Microbe. 2025.
364. Ullah H, Qadeer A, Rashid M, Rashid MI, Cheng G. Recent advances in nucleic acid-based methods for detection of helminth infections and the perspective of biosensors for future development. Parasitology. 2020;147(4):383-92.
365. Beesley NJ, Williams DJ, Paterson S, Hodgkinson J. *Fasciola hepatica* demonstrates high levels of genetic diversity, a lack of population structure and high gene flow: possible implications for drug resistance. Int J Parasitol. 2017;47(1):11-20.
366. Saunders MA, Liang H, Li WH. Human polymorphism at microRNAs and microRNA target sites. Proc Natl Acad Sci U S A. 2007;104(9):3300-5.
367. Zhang W, Wang L, Zhou P, Song G, Shen M, Gan S, et al. Identification and analysis of genetic variations in pri-miRNAs expressed specifically or at a high level in sheep skeletal muscle. PLoS One. 2015;10(2):e0117327.
368. Cucher M, Macchiaroli N, Kamenetzky L, Maldonado L, Brehm K, Rosenzvit MC. High-throughput characterization of *Echinococcus* spp. metacestode miRNomes. International journal for parasitology. 2015;45(4):253-67.
369. Basika T, Macchiaroli N, Cucher M, Espinola S, Kamenetzky L, Zaha A, et al. Identification and profiling of microRNAs in two developmental stages of the model cestode parasite *Mesocestoides corti*. Molecular and Biochemical Parasitology. 2016;210(1-2):37-49.
370. Zhang J, Li J, Zheng Y, Zhu C, Wu Z, Wang T, et al. Lipid metabolism and lipid signaling in extracellular vesicles ontogeny: from biogenesis to functional execution. J Nanobiotechnology. 2025;23(1):672.
371. Dellar ER, Hill C, Melling GE, Carter DR, Baena-Lopez LA. Unpacking extracellular vesicles: RNA cargo loading and function. Journal of extracellular biology. 2022;1(5):e40.

Appendix A:

Published review article: The knowns and unknowns of helminth-host miRNA cross-kingdom communication. *Trends in Parasitology*. 2024;40(2). doi:10.1016/j.pt.2023.12.003

CellPress

Trends in Parasitology

Review

The knowns and unknowns of helminth–host miRNA cross-kingdom communication

Sumaiya Chowdhury [1,2], Dayna Sais [2], Sheila Donnelly [1,*,3] and Nham Tran [2,*,3]

MicroRNAs (miRNAs) are small noncoding RNAs that oversee gene modulation. They are integral to cellular functions and can migrate between species, leading to cross-kingdom gene suppression. Recent breakthroughs in helminth genome studies have sparked curiosity about helminth RNA regulators and their ability to regulate genes across species. Growing data indicate that helminth miRNAs have a significant impact on the host's immune system. Specific miRNAs from helminth parasites can merge with the host's miRNA system, implying that parasites could exploit their host's regulatory machinery and function. This review highlights the role of cross-kingdom helminth-derived miRNAs in the interplay between host and parasite, exploring potential routes for their uptake, processing, and consequences in host interaction.

Highlights

Helminths use small microRNAs (miRNAs) to manipulate their host's immune responses by 'cross-kingdom' gene regulation, but the exact mechanisms remain unclear.

Helminths communicate with their host cells by releasing miRNAs encapsulated in extracellular vesicles (EVs); this EV cargo is selectively packaged for specific microRNAs.

Helminth miRNAs share structural similarities with mammalian miRNAs, allowing them to be loaded onto the host's argonaute (AGO) proteins.

Helminth miRNAs use a multifaceted strategy, regulating host targets, mimicking host miRNAs to commandeer their biogenesis components, and potentially binding to other host miRNAs.

Unravelling the complex mechanism of 'cross-kingdom' gene regulation could transform our approach to combating helminth infections and deepen our insight into host–parasite dynamics.

The theory of cross-kingdom miRNA communication

'Cross-kingdom communication' refers to the transmission of extracellular chemicals and bioactive molecules resulting in the regulation of biological signals between genetically diverse species. This term was first coined in the 1980s following the realisation that distinct cells can communicate with each other through secreted hormones [1]. Subsequently, the concept expanded with the discovery that bacteria had the capacity to manipulate the signal transduction of plant and mammalian cells, while host hormones cross-signalled with quorum sensing molecules to regulate bacterial gene expression [2].

Most recently, **miRNAs** (see Glossary) have emerged as important mediators of inter-kingdom communication. miRNAs are a class of small noncoding RNAs (18-24 nucleotides) that are critical regulators of post-transcriptional gene expression [3]. By binding to the complementary 3′ untranslated region (UTR) of their mRNA target, miRNAs can either interfere with the mRNA translation process or cause mRNA cleavage and degradation [4]. However, the opposite effect has also been seen where miRNA binding to the 5′ UTR prevents mRNA degradation and promotes the translation process [5]. It is thought that, in metazoans, miRNAs originated as a defence mechanism against pathogens with predominantly antiviral functions, but over time, have evolved to target intrinsic genes. As a result, endogenous miRNAs have developed as a highly conserved mechanism of gene regulation that controls a multitude of biological functions, such as developmental processes, cell cycle processes, intracellular signalling, and homeostasis [6].

miRNAs have the ability to move between cells, acting as intermediates in cellular communication. Several studies conducted in animals and plants have provided increasing evidence that pathogens, including bacteria, viruses, fungi, and protozoa, utilise these mobile miRNAs as a mechanism to manipulate host gene expression [7]. Most recently, we, and others, have demonstrated that larger, multicellular parasitic worms (helminths) also deploy miRNAs to specifically divert and manipulate their host's immune responses to prevent their expulsion and tolerate

[1]The School of Life Sciences, University of Technology, Sydney, Australia
[2]School of Biomedical Engineering, Faculty of Engineering and Information Technology, University of Technology Sydney, Ultimo, NSW, Australia
[3]These authors contributed equally to this work.

*Correspondence:
sheila.donnelly@uts.edu.au (S. Donnelly) and
nham.tran@uts.edu.au (N. Tran).

© 2023 Elsevier Ltd. All rights reserved.

their presence; this permits the establishment of chronic infections [8–13]. However, while there has been extensive characterisation of the helminth miRNomes and their corresponding host target genes, very little is known about how these miRNAs are selected by the parasite for transfer to host cells and, once there, how they integrate into the host cell miRNA biogenesis pathway.

Helminth-derived miRNAs alter the host's immune response to establish chronic infection

Almost 300 different species of helminths have been identified with the capacity to infect humans [14]. Accordingly, helminth infections are a major global public health problem with recent estimates suggesting that 1.5 billion people harbour one or more of the most common worms: *Schistosoma* spp., *Fasciola hepatica, Ascaris lumbricoides, Necator americanus, Ancylostoma duodenale, Trichuris trichiura,* and *Strongyloides stercoralis* (see Table S1 in the supplemental information online) [15,16]. No vaccine exists for any human helminth, and although most infections can be controlled by a limited number of pharmaceutical antihelminthics, these treatments do not prevent reinfection, and as a result, the prolonged, exhaustive use of these drugs within populations has led to a concerning level of resistance [17]. Thus, new strategies for control or disease prevention are urgently needed.

Unlike bacteria or viral pathogens, helminths do not replicate in their hosts. Instead, they require time to grow to maturity, reproduce and release their offspring in the form of eggs. To accomplish this cycle, helminths have evolved mechanisms to regulate the host's immune cell signalling pathways to prevent their expulsion while also safeguarding the fitness of the host [18]. During helminth infection, the typical innate detection systems of the host are not activated as expected, and the adaptive immune response is directed towards a tolerant or hyporesponsive state [19,20]. As a result, parasitic worms establish chronic infections to complete their life cycle, while the tissue damage caused by their feeding and migration is readily repaired, and excessive inflammation is controlled [21,22]. Understanding the communication pathways between helminths and their hosts during this process will inform the development of new anthelminthic therapeutics.

Historically, the focus for this research has been on the identification and characterisation of parasite-secreted proteins as it was assumed that these were the most likely molecules to be in contact with host immune cells and operate as immune modulators [23–25]. However, more recently, helminth-derived miRNAs are emerging as key manipulators of host immune cells [8,9,13,26–37]. The miRNA profile of helminths has been characterised in over 35 species of trematodes, nematodes, and cestodes [37]. Comparative analysis of miRNA sequences has revealed that helminth miRNAs are well conserved, with many parasite miRNAs sharing sequence identity with mammalian miRNAs, and thus predicted to have the same regulatory functions as their host miRNAs, many of which target immune-modulating genes (Figure 1A, Table S2). *In silico* analysis has also predicted that several nonconserved, novel parasite miRNA sequences could target host genes involved in immune pathways, thus suggesting immune modulatory functionality (Figure 1B, Table S2) [9,27].

The breadth of miRNAs and corresponding mammalian targets suggests a high degree of redundancy, with multiple helminth miRNAs (conserved and novel) predicted to act on single host gene targets within multiple immune cells (Figure 1C, Table S2). Such findings support the hypothesis that, by hijacking the host endogenous miRNA system of gene regulation, helminths can alter host gene expression and hence modulate the host immune response to a phenotype that favours parasite survival and reproduction. There is now supporting experimental evidence for this possibility from both *in vivo* mouse infection models and *in vitro* transfections of mammalian cells (Table 1), which collectively and convincingly demonstrate that helminth-derived miRNAs

Glossary

Argonaute (AGO): a core component of the small RNA-induced silencing complexes with small RNA. The guide strand of the small RNA is loaded onto the Argonaute protein, ultimately leading to gene silencing.
Dicer: an RNase III endonuclease that processes miRNA precursors into smaller functional RNAs (21–23 nucleotides in length) that are subsequently incorporated into the RNA-induced silencing complex.
Drosha: a ribonuclease III enzyme that performs the initial step of miRNA processing in the canonical pathway of miRNA biogenesis, converting primary miRNA sequences to precursor miRNAs.
Extracellular vesicles (EVs): small membrane-bound vesicles released by cells (and helminths) to facilitate intercellular communication. They typically contain a mixture of proteins, lipids, and small RNAs.
IsomiRs: miRNA sequences that have variations (in length, sequence, or both) compared to the canonical/reference miRNA sequence.
MicroRNAs: small, single-stranded, noncoding RNA molecules containing 21–23 nucleotides. miRNAs typically interact with the 3′ untranslated region of target mRNAs to induce the degradation of gene transcripts and the repression of translation.
Precursor miRNAs: the hairpin precursors of miRNAs formed by the cleavage of primary miRNAs by ribonuclease enzymes.
Primary miRNA: the initial gene transcript of a miRNA sequence.
RNA binding proteins (RBPs): proteins that directly interact with single-stranded or double-stranded RNA, customarily regarded as important facilitators of gene expression. More recently, they have been found to mediate the packaging of miRNAs into extracellular vesicles.
Seed sequence: defined as the first 2–8 nucleotides of a miRNA starting at the 5′ end and counting toward the 3′ end. Canonically, the regulation of gene expression by miRNAs is reliant on base pairing of the seed region to sequences in the 3′ untranslated region of target mRNAs.
WAGO: an Argonaute protein subfamily that is exclusive to worms.

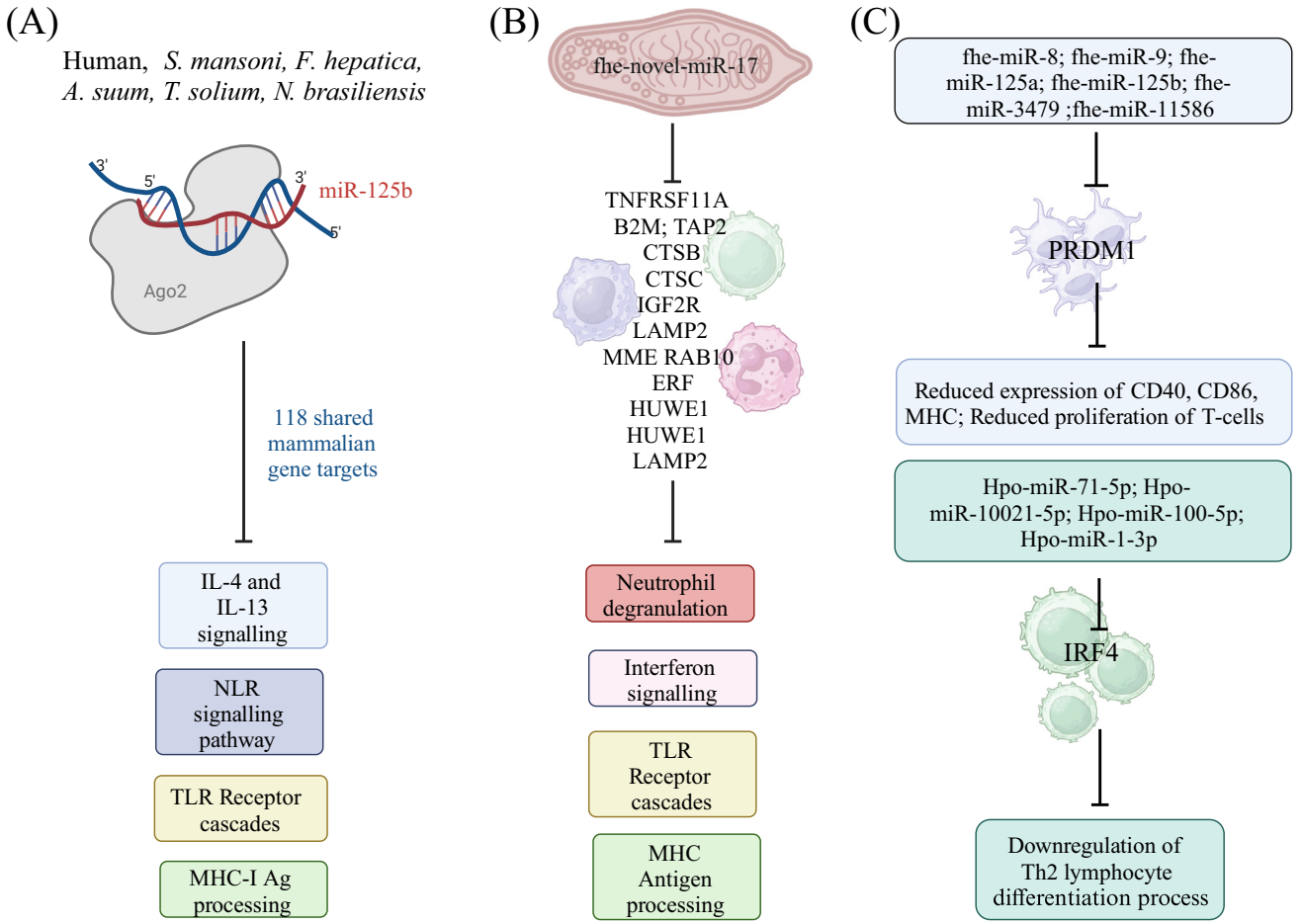


Figure 1. Helminth microRNAs (miRNAs) are predicted to target mammalian genes to regulate the immune response during infection. (A) Several parasites express miR-125b, which is a highly conserved miRNA also expressed in mammalian cells, with identified roles in the activation of multiple immune processes. The miRbase data base (https://mirdb.org) predicts that human miR-125b has 925 gene targets. Of these, the parasite miR-125b sequences have been predicted to target 118 genes (Table S2). Pathway analysis of these gene targets using Reactome suggests that the parasite miRNAs would impact the processing and presentation of antigen by major histocompatibility complex I (MHC) and cell signalling pathways activated by IL-4, IL-13, NOD-like receptors (NLRs), and Toll-like receptors (TLRs). (B) The prediction of gene targets for novel, nonconserved, parasite miRNAs suggests that they also have the capacity to regulate mammalian gene targets. For example, using miRANDA, PITA, and RNAhybrid predicted 13 mammalian gene targets for *Fasciola hepatica* novel miR-17. Reactome analysis attributed these genes to immune pathways associated with neutrophil degranulation, interferon signalling, TLR receptor signalling, and MHC I- and II-mediated antigen processing. (C) The observation that multiple parasite miRNAs are predicted to target the same mammalian gene target suggests a level of redundancy within the parasite regulation of their host's immune system. As an example, six different miRNAs expressed by *F. hepatica* have been predicted to target positive regulatory domain i-binding factor 1 (PRDM1), a protein that promotes the expression of the costimulatory molecules on dendritic cells that are necessary for efficient T cell activation, and the development of an effector adaptive immune response. Similarly, four different miRNAs produced by the nematode *Heligmosomoides polygyrus* are predicted to target interferon regulatory factor (IRF)-4, a key regulatory transcription factor in the development of immune cells. This figure was created using BioRender.com.

can be taken up by mammalian cells and, once internalised, operate to regulate gene expression to alter key immune pathways and cellular processes.

Delivery of helminth miRNAs to host cells

miRNAs are released by helminths in extracellular vesicles and nonvesicular forms

The most widely characterised mechanism of intracellular (and cross-kingdom) communication is via the secretion and uptake of **extracellular vesicles (EVs)** [38]. Encapsulation of miRNAs in

Table 1. Functional studies demonstrating cross-kingdom immunomodulatory role of helminth miRNAs in mammalian cells[a]

Parasite	Parasite-derived miRNA(s)	Host gene target(s)	Host target cell	Model used for study	Immune response	Refs
Fasciola hepatica	fhe-miR-125b-5p	TRAF6	Peritoneal macrophages	*In vitro* murine bone marrow derived macrophages	Suppression of M1 macrophage phenotype	[10]
Clonorchis sinensis	csi-let-7a-5p	Clec7a, Socs1	Hepatic macrophages	*In vitro* RAW264.7 murine macrophage cell line	Promotion of M1 phenotype by upregulation of NF-kB signalling and induction of proinflammatory cytokines TNF, Interleukin (IL)-6 and IL-1b.	[110]
Schistosoma mansoni	sma-miR-10	MAP3K7	T cells	*In vitro* human HEK-293 human embryonic kidney cell line	Suppression of host Th2 cell differentiation by regulating the Th2 transcriptional pathway	[111]
Schistosoma japonicum	sja-miR-71a	Sema4D	Hepatic stellate cells	*In vivo* murine model of *S. japonicum* infection; targets validated *in vitro* using 293T human embryonic kidney cell line	Inhibition of hepatic stellate cell activation by downregulation of the TGF-β1/SMAD and IL-13/ Signal Transducer and Activator of Transcription (STAT)6 pathways and regulation of the Th1/Th2/Th17 and regulatory T cell balance	[112]
Schistosoma japonicum	sja-miR-2162	TGFBR3	Hepatic stellate cells	*In vivo* murine model of *S. japonicum* infection and *in vitro* rat HSC-T6, human LX-2 cell line, mouse primary hepatic stellate cells	Activation of hepatic stellate cells via activation of TGF-b signalling pathway, and activation of hepatic fibrosis	[86]
Schistosoma japonicum	sja-miR-71a	FZD4	HepG2 and SMMC-7721 hepatoma cell lines	*In vivo* murine model and *in vitro* HepG2 human hepatoma cells	Anti-tumour activity: inhibit tumour proliferation by cell cycle arrest at G_0/G_1 phase	[113]
Schistosoma japonicum	sja-miR-125b, sja-bantam	Pros1, Fam212b	Circulating monocytes	*In vitro* RAW264.7 murine macrophage cell line	Increased monocyte proliferation and TNF production	[31]
Heligmosomoides polygyrus	hpo-let-7, hpo-miR-200, hpo-miR-435	Dusp1	Epithelial MODE-K cell line	*In vitro* MODE-K murine enterocyte cell line	Increased anti-inflammatory responses by repression of mitogen activated protein kinase (MAPK) signalling	[8]
Heligmosomoides polygyrus	hpo-miR-71-5p	IRF4	T cells	*In vitro* murine primary $CD4^+$ T cells	Downregulation of genes and pathways of the Th2 lymphocyte differentiation process: interferon (IFN)γ signalling, the IL-2/STAT5 signalling, and the mTOR signalling pathways.	[83]
Ascaris suum	asu-miR-791-3p	mTOR	T cells	*In vitro* murine primary $CD4^+$ T cells	Downregulation of genes and pathways of the Th2 lymphocyte differentiation process: interferon gamma signalling, the IL-2/STAT5 signalling, and the mTOR signalling pathways.	[83]
Taenia pisiformis	tpi-miR-let-7-5p	C/EBP δ	Macrophages	*In vitro* RAW264.7 murine macrophage cell line	Suppression of the host Th2 immune response by repression of M1 phenotype markers and promotion of M2 phenotype markers.	[114]
Taenia solium and Taenia crassiceps	miR-10-5p, let-7-5p	Not validated	Peritoneal macrophages	*In vitro* murine primary peritoneal macrophages	Downregulation of proinflammatory cytokines in IFN-γ treated M1 macrophages, and downregulation of anti-inflammatory cytokines in IL-4 treated M2 macrophages.	[115]
Echinococcus multilocularis	emu-miR-4989-3p	Not validated	Macrophages	*In vitro* RAW264.7 murine macrophage cell line	Inhibition of macrophage nitric oxide (NO) production and increased TNF production	[29]
E. multilocularis	emu-miR-71	Not validated	Macrophages	*In vitro* RAW264.7 murine macrophage cell line	Inhibition of macrophage NO production and altered inflammatory response	[102]

EVs protects them from degradation by RNases in the harsh extracellular environment of the bloodstream or the digestive system [8]. Furthermore, intercellular delivery of miRNA via EVs can circumvent the recipient cell's transcriptional regulations, offering a comparatively straightforward mechanism of gene regulation.

While characterised in only a few studies, the presence of nonvesicular extracellular (ex)-miRNA has also been described in all three classes of helminths [27,35,39]. Although it is possible that these ex-miRNAs have been accidently released by damaged cells or dying parasites, in humans it has been shown that miRNAs are also actively transported in highly stable complexes with proteins [40]. It has been reported that more than half of the miRNAs found in human serum is bound to ribonucleoproteins, including **argonaute (AGO)**-2 [41,42], although other proteins such as high-density lipoprotein (HDL), and AGO-1, -3, and -4 have also been implicated in ex-miRNA binding, transport, and delivery to cells [43,44]. However, there is still no direct evidence that these miRNA–protein complexes operate in a functional way to alter recipient cell gene expression. Nonetheless, the observation that the profile of miRNAs bound to HDL is distinct from that found in EVs suggests a complementary and independent mechanism of miRNA transport and gene regulation [45].

For helminths, the current data indicate that the choice to secrete miRNAs packaged in EVs or in vesicle-free form may be influenced by the requirements for different stages of their life cycle. For example, during the L4 larval stage of the *H. contortus* life cycle, ex-miRNAs are more abundant in the vesicle-free fraction of the parasite secretions as compared to the adult stage, in which miRNAs are found primarily in the vesicle-enriched fraction [35]. Similarly, the miRNAs secreted by adult *T. spiralis*, which inhabit intestinal mucosa, are primarily packaged in vesicles, whereas, the muscle-stage larvae, which live intracellularly, secrete unencapsulated miRNAs [39]. While a similar stage-specific differential abundance of free versus vesicular miRNAs has not been described for any cestodes or trematodes, analysis of the excretory/secretory products of the schistosomula of *Schistosoma mansoni* identified the presence of both forms of miRNA [12], suggesting that this process of miRNA transfer is common to all helminths. However, it is important to note that vesicle-free extracellular miRNA–protein complexes may originate from EVs that lyse during isolation and preparation. Although this could be determined by the analysis of multiple biological replicates and independent preparations of parasites and their secretory products, it is technically challenging given the paucity of material that is often obtained from these parasites. Despite this caveat, the fact that several miRNA sequences, that were identified in the EV-depleted library of L4 larvae, were not found within the EV-enriched library [35] suggests that the vesicle-free miRNAs are released independently of the EV-packaged sequences.

Helminth-derived EVs are taken up by the host's immune cells

Examination of the cargo of helminth-derived EVs revealed that miRNAs are highly represented, [8,46,47] and it has now been shown for several species of helminths that EV-encapsulated miRNAs are internalised by mammalian host cells, particularly by immune cells such as macrophages, monocytes, and dendritic cells [48]. The specificity of this cellular interaction is determined by the size of the vesicles, as is illustrated with EVs derived from *E. granulosus,* with

Note to Table 1:
[a]Abbreviations: C/EBPδ CCAAT/enhancer binding proteins δ; Clec7a, C-type lectin domain family 7 member A; Dusp1, Dual specificity phosphatase 1; Fam212b, family with sequence similarity 212 member B; FZD4, fizzled 4; IRF4, interferon regulatory factor 4; MAP3K7, mitogen-activated protein 3 kinase 7; mTOR, mammalian target of rapamycin; NF-kB, nuclear factor kappa-light-chain-enhancer of activated B cells; Pros1, protein S1; Sema4D, semaphorin 4D; Socs1, suppressor of cytokine signalling 1; STAT6 signal transducer and activator of transcription 6; TGF-b, transforming growth factor b; TGFBR3, transforming growth factor beta receptor 3; TNF, tumour necrosis factor; TRAF6, tumour necrosis factor receptor associated factor 6.

smaller EVs taken up by host hepatic cells more efficiently than larger EVs (110K) [49]. The intracellular location in host cells after uptake is influenced by the surface proteins on the parasite-derived EVs. This was shown by the addition of antibodies specific to the surface proteins of *H. polygyrus* EVs, which resulted in the enhanced uptake of the EVs but redirected them to lysosomes for degradation in the recipient cell [50]. Blocking worm EV release is detrimental to parasite survival in their hosts [51] likely because this also blocks the delivery of parasite-derived immunomodulatory miRNAs to host cells, which, in turn, would allow the development of host protective immune responses to mediate parasite expulsion.

Selective sorting of parasite-derived miRNAs into EVs

There are several pieces of evidence that suggest the selection and incorporation of miRNAs into parasite-derived EVs is an active controlled process rather than an arbitrary occurrence. Firstly, the abundance of miRNAs within helminth EVs does not reflect the profile of intracellular expression, with miRNAs that are relatively highly expressed intracellularly not found in the secreted EVs, suggesting preferential selection of miRNA for cargo [29]. Furthermore, while the proteins involved in EV biogenesis pathways have been shown to be constitutively expressed, the EV miRNA cargo is developmentally regulated [30,52]. This life-stage-specific miRNA packaging in the EVs is likely necessary to cater for the differential requirements of host gene regulation during the various life stages of the helminths.

Secondly, several miRNAs are consistently found in EVs of different species of helminths, suggesting an evolutionarily conserved mechanism for the packaging and release of specific miRNAs [33–35]. Notably, the miRNAs within the helminth EVs contain more conserved miRNAs with higher **seed sequence** identity to mammalian host miRNA compared to helminth intracellular miRNAs, which may simply correspond to the conservation of ancient miRNAs across metazoans or might reflect an active selection for compatibility with host miRNA machinery. Furthermore, the most abundant EV-encapsulated miRNAs are predicted to primarily target mammalian genes involved in the immune and inflammatory pathways (Table S2).

According to the available data, most common EV miRNAs with immune-modulatory functions are let-7, miR-125, miR-71, miR-2, miR-9, miR-10, miR-31, and miR-87 (Table S2), and the most predominant predicted pathways targeted are MAPK, TGF-beta, TNF, Wnt signalling, IGF signalling pathway (Table S2). The profile of EV miRNAs and their host targets is remarkably similar between the trematodes (flukes) and nematodes (round worms), with cestodes (tapeworms) displaying a more distinct profile of miRNA abundance and gene targets (Table S2). This is somewhat surprising as trematodes and cestodes belong to the same phyla (platyhelminth), so these differing profiles may, in fact, reflect the relative lack of characterisation of cestode miRNomes compared to the more advanced characterisation of trematodes and nematodes.

Although these observations present convincing evidence that helminth miRNAs are selectively sorted for delivery to their host cells, the mechanism by which this occurs is unknown. Research on mammalian cells has highlighted a prominent role for the AGO-2 protein in sorting miRNA via the KRAS–MEK–ERK signalling pathway [53]. While the presence of AGO-2 orthologues in the genome of most trematodes and cestodes would suggest that a similar process may be utilised by these worms, there is no evidence of this protein interacting with any miRNAs within parasite EVs [54]. However, nematodes also express a lineage-specific expansion of AGO proteins (**WAGO**), one of which reportedly mediates the export of small interfering RNAs into the EVs of *H. bakeri* [55]. The conservation of WAGO in Clade V nematodes suggests the existence of a specialised RNA secretion pathway for these helminths.

Several **RNA binding proteins (RBPs)** are also known to be involved in selective sorting of miRNAs into EVs in mammalian systems [56]. Comparing the sequences of EV-packaged miRNAs to the miRNAs that are retained in mammalian cells, revealed the presence of specific sequence motifs within miRNAs which determined whether they were exported or retained by cells. Specifically, miRNA sequences that were enriched in EVs had one to four motifs of 4–7 nucleotides with high G+C content and lower Gibbs free energy than the miRNAs that were retained in cells [57]. Pulling down interacting proteins from cell lysates with EV-enriched miRNAs displaying these motifs identified SYNCRIP, ALYREF, RBMX, and FUS as RBPs with central roles in the selective sorting of miRNAs. Other RBPs identified through their interactions with specific miRNAs include HNRNPA2B1, YBX-1, and MVP [56]. However, although transcripts for these proteins can be found in helminth genomes, only MVP is reported in platyhelminth EV proteomic data, suggesting that either these RBPs are present at undetectable levels, or they are present in helminth EVs only at certain timepoints during infection. Alternatively, other proteins may be utilised in helminth EV miRNA sorting [54].

One such candidate is calpain, a calcium-dependent cysteine protease that is detectable in several species of trematode and cestode [58]. Inhibition of calpain expression reduces the quantity of several miRNAs in *S. japonicum* EVs [59], supporting a function in miRNA shuttling into EVs. In addition, orthologues of ADP-ribosylation factor 6 and Exportin-5, proteins which interact to shuttle a **precursor-miRNA** complex into EVs in mammalian cells, have been reported in several species of platyhelminths and cestode EVs [28,60,61], suggesting that this mechanism of precursor-miRNA packaging may be operational in helminth species. However, most studies examining helminth-derived EVs have primarily focused on the detection of mature miRNA sequences. Consequently, it is not known whether helminth-derived miRNAs are also delivered to host cells as **primary miRNA** or precursor miRNA sequences. Future studies to ascertain the precise form of miRNAs within EVs will be critical to better understand their mechanisms of transcriptional regulation, and thus functional implications, in recipient cells.

miRNA-mediated regulation of gene expression

The miRNA biogenesis pathway

The miRNA biogenesis pathway is well conserved in eukaryotes and is a tightly regulated process that involves a cascade of molecular processing by enzymes and protein interactions. First, the miRNA genes are transcribed by RNA polymerase II into nascent primary (pri)-miRNA transcripts [62]. Then, in the canonical miRNA biogenesis pathway, the pri-miRNA transcript is processed in the nucleus by the microprocessor complex of **Drosha** and DGCR8 to generate an intermediary stem–loop structure called precursor (pre)-miRNA (Figure 2) [63]. This pre-miRNA is exported to the cytoplasm by an exportin-5 (XPO5)/RanGTP complex [64]. In the cytoplasm the stem–loop structure of the pre-miRNA is processed/diced by an RNase III endonuclease **Dicer** to form the ~22 bp mature miRNA duplex (Figure 2) [65]. One strand of the duplex miRNA loads onto AGO proteins and is termed the guide strand [66]. The unloaded strand, called the passenger strand, unwinds from the guide strand, and is degraded by the cellular machinery. Whether the 5p or 3p strand is loaded on AGO varies greatly depending on the thermodynamic features of the miRNA strands, cell type, or cellular environment [67]. The AGO-loaded mature miRNA, along with other proteins, forms the RNA-induced silencing complex (RISC) [68]. Finally, the RISC complex, guided by the miRNA strand, can then bind to a complementary mRNA sequence to induce mRNA degradation or translational repression. While the conventional model dictates that high sequence complementarity leads to sequence degradation, whereas low sequence complementarity leads to reversible post-transcriptional suppression, recent evidence of deviations from this model suggests a more nuanced and complex balance between degradation and repression. It is suggested that the mode of miRNA gene silencing is influenced by factors

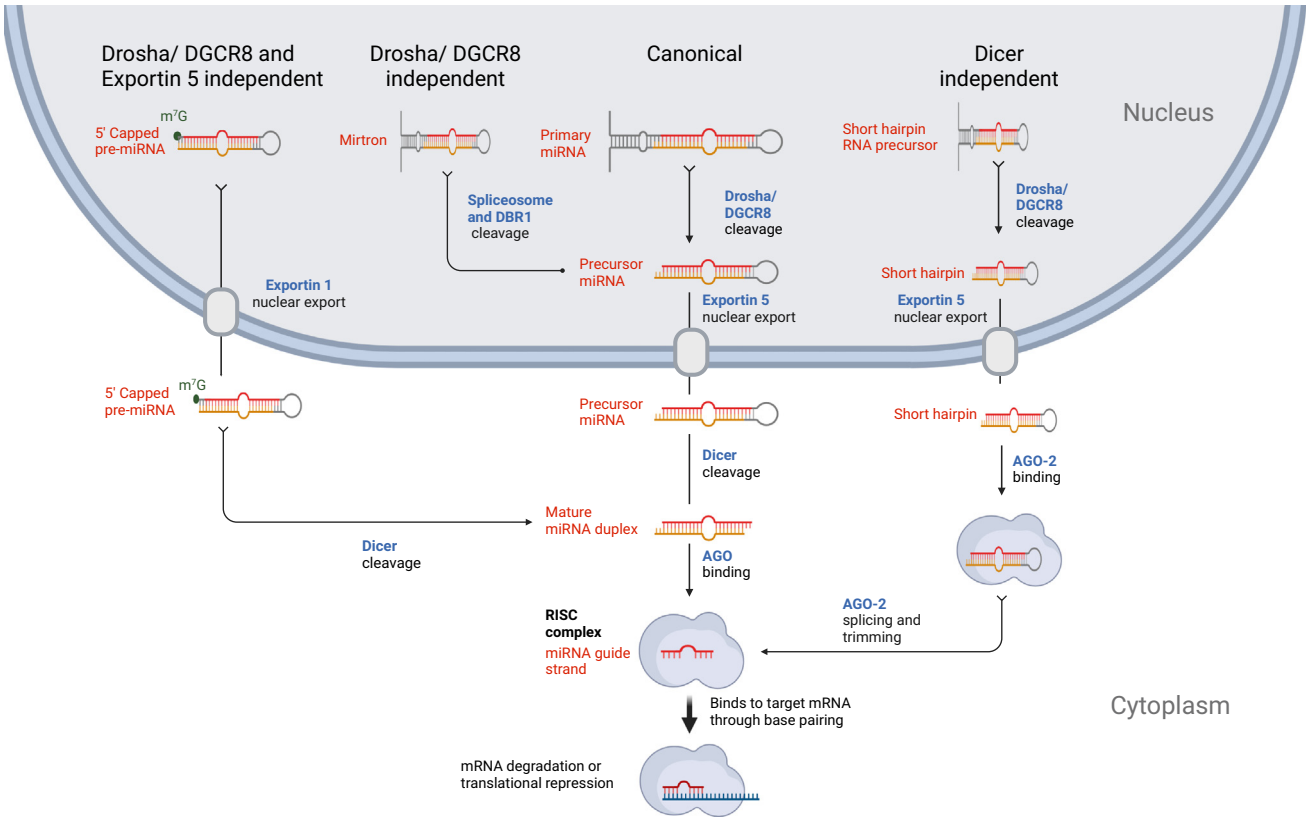


Figure 2. Mammalian microRNA (miRNA) biogenesis pathways. In the canonical miRNA biogenesis pathway, the pri-miRNA transcript is processed in the nucleus by Drosha and DGCR8 to generate an intermediary stem–loop structure called precursor (pre)-miRNA. This pre-miRNA is exported to the cytoplasm by Exportin-5. In the cytoplasm, the stem–loop structure of the pre-miRNA is cleaved off by Dicer to form a mature miRNA duplex. One strand of the duplex miRNA loads onto AGO and is termed the guide strand. The AGO loaded miRNA along with other proteins form the RISC complex. Finally, the RISC complex, guided by the miRNA strand, binds to a complementary mRNA sequence to induce mRNA degradation or translational repression. In the noncanonical miRNA biogenesis pathway, structurally diverse small RNAs can be processed into mature miRNAs by bypassing one or more of the key biogenesis enzymes, leading to alternative processing mechanisms. Mirtrons and 7-methylguanine capped (m^7G)-pre-miRNAs bypass Drosha/DGCR8 processing; while mirtrons are exported from the nucleus to the cytoplasm by canonical Exportin 5, m^7G-pre-miRNAs are alternatively shuttled via Exportin 1. In the cytoplasm, both the precursors are processed by Dicer. However, small hairpin RNAs (shRNAs) are processed by Drosha/DGCR8 complex and exported via Exportin 5, but instead of Dicer, they are alternatively processed by AGO-2. All pathways ultimately produce mature functional miRNAs that can load onto AGO and form an miRISC complex. This figure was created using BioRender.com.

such as developmental stage and environmental conditions [69]. However, the mechanistic details, particularly the criteria that determine whether a target mRNA is degraded or translationally repressed by a cognate miRNA, remain to be elucidated.

Besides the canonical pathway, several noncanonical miRNA biogenesis pathways are responsible for the production of mature miRNAs from structurally diverse small RNAs. The most common noncanonical pathways are Drosha/DGCR8-independent and Dicer-independent pathways [70]. Mirtrons are small RNA hairpin structures that arise from introns during mRNA splicing events; as such, they resemble Dicer substrate and do not require Drosha/DGCR8 processing (Figure 2) [71]. Mirtrons contribute to ~15% of the total mature miRNA population in humans and are prevalent in *Caenorhabditis elegans* [72]. Another unique class of miRNAs that bypass the microprocessor cleavage step are 5′ 7-methylguanosine (m^7G) capped pre-miRNAs, derived directly from the RNA polymerase II transcript. Unlike the canonical miRNAs, the capped pre-miRNAs are transported to the cytoplasm via Exportin-1 for Dicer processing (Figure 2) [70]. The observation

that 5′ m^7G pre-miRNAs identified in *C. elegans* are lineage specific miRNAs suggested that these miRNA genes are newly acquired, and that this pathway of biogenesis may have emerged later in evolution [73]. Conversely, Dicer-independent miRNAs are processed by Drosha from endogenous short hairpin RNA (shRNA) transcripts (Figure 2). These pre-miRNAs require AGO-2 to complete their maturation within the cytoplasm because they are of insufficient length to be Dicer substrates [74]. This, in turn, promotes loading of the entire pre-miRNA into AGO-2 and AGO-2-dependent slicing of the 3p strand [75]. The 3′-5′ trimming of the 5p strand completes their maturation [76]. However, Dicer-processed small interfering (si)-RNAs are more efficient at gene silencing than the dicer-independent siRNAs [77].

There is strong bioinformatic evidence that several key proteins in the miRNA biogenesis pathway are expressed by helminths, with a comparison to early diverging free-living parasites, suggesting that the production of small miRNAs is an ancestral mechanism of gene regulation in helminths which has had a contributory role in the transition to parasitism [78,79]. However, despite abundant information on the phylogenetic similarities and differences in protein expression in different parasites, there is no functional information on how the miRNA biogenesis pathway operates in helminths.

Processing of helminth miRNAs in mammalian cells

The notion that the miRNA biogenesis pathway can be hijacked by foreign miRNAs to mediate cross-kingdom communication was first demonstrated in plants whereby fungal miRNAs were found to load onto plant AGO proteins leading to silencing of mitogen-activated protein kinase genes and consequent suppression of protective immunity [80]. Subversion of host cell miRNA machinery by pathogen-derived miRNAs has now been identified in viral, bacterial, and plasmodium infections [2,7,81]. The detection of fhe-miR-125b, a highly conserved parasite-derived miRNA, in AGO-2 pull down products from macrophages of *F. hepatica*-infected mice [10] – and the identification of sja-miR-125b from *S. japonicum* in AGO-pulldown products from macrophages treated with parasite-derived EVs *in vitro* [31] – now provide evidence that miRNAs from parasitic worms can also be incorporated into the miRISC machinery of mammalian cells.

The loading of miRNAs to AGO protein is a very precise process that involves thermodynamics and base-match composition and is partially dictated by the sequence and structure of the miRNA [82]. As the seed sequence of both Fasciola fhe-miR-125b and schistosome sja-miR-125b is identical to mammalian miR-125 [10], and as conserved miRNA sequences are the most abundant in helminth EVs, it was initially proposed that only helminth miRNAs that are close homologues to mammalian sequences may be functional in their host cells. However, the recent detection of *H. polygyrus* miR-71 loaded onto Ago-2 in transfected Th2 cells implies that this conservation may not be essential as this helminth miRNA is specifically expressed by nematodes and does not have a homologue in mammalian cells [83].

In addition to the influence of miRNA sequence and structure, loading onto AGO is also partly dictated by the functional requirements of the cell at any particular time. In this way, miRNA mechanisms of gene regulation can be spatially and temporally controlled as required. A cell-specific functionality for helminth miRNAs has not been explored, as most experimental studies of helminth miRNAs have focused on the modulation of the biological activity of a single cell type (Table 1). However, the biological outcome of *H. polygyrus* miR-71 transfection was examined in both Th2 cells and macrophages, although similar measures of functionality were not assessed in both cell types [83]. While transfection of Th2 cells resulted in a significant reduction in expression of the transcription factor IRF4, transfection of macrophages had no significant effect on the

production of cytokines, although their expression would be expected to be altered because of changes in expression of IRF4 [84]. Despite these caveats, the results provide a suggestion of varied efficacy for helminth miRNA that is dependent on the cell type, a notion that requires further consideration.

Loading onto AGO-2 represents the final step in the canonical miRNA biogenesis pathway (Figure 2) and supports the presence of mature helminth miRNAs in mammalian cells and alludes to potential functionality within the mammalian miRNA machinery. However, it does not determine whether the worm miRNAs are delivered to their host cells as mature sequences that are directly loaded to AGO-2 or as pri-miRNA transcripts or **precursor miRNAs** that are processed by Drosha and/or Dicer. While some sequence features for Drosha cleavage are common between *C. elegans* and human miRNAs, *C. elegans* lacks other structures and sequence motifs that are critical for efficient cleavage by human Drosha [85]. Moreover, despite the high similarity in domain structures and polypeptide sequences of *C. elegans* and human Drosha, the *C. elegans* enzyme has different substrate recognition approaches and cleavage mechanisms compared to the human microprocessor [85]. In contrast, the observation that a schistosome-specific pri-miRNA mimic (pri-sja-miR-2162) was processed into a mature functional miRNA in hepatocytes suggests that, unlike the miRNAs of the free-living *C. elegans*, miRNAs secreted by parasitic worms can be fully embedded into the mammalian miRNA biogenesis pathway [86]. This further indicates that the capacity to utilise host miRNA biogenesis pathways evolved as an adaptation to parasitism and builds on the proposal that this functionality is not solely dependent on conservation with specific mammalian miRNA sequences.

The pre-miRNAs released by Drosha typically comprise of a near-perfectly based-paired stem, a large terminal loop, and a 2 nt overhang at the 3′ end, which is essential for efficient Dicer cleavage [87]. Given that the large majority of helminth miRNAs (conserved and novel) have these precursor characteristics, processing by mammalian Dicer could be expected [11]. Moreover, a position-dependent 3-bp motif in pre-miRNAs, termed the GYM motif, recently determined to influence the cleavage site and efficiency of human Dicer cleavage, is positionally conserved in nematodes [88] – which further validates the possibility that helminth-derived miRNAs can be efficiently processed by the human miRNA biogenesis pathway.

The possibility that parasite-derived miRNAs are also processed via noncanonical pathways in host cells cannot be excluded. Although knowledge of noncanonical miRNA processing of exogenous pathogen-derived miRNAs within host cells remains limited, evidence of noncanonical miRNA processing of viral miRNAs by host cells has been reported. For instance, a mirtron-like viral product from *Sindbis* virus is processed in a Dicer-dependent and Drosha-independent manner in infected murine fibroblast cells *in vitro* [89]. Conversely, *SARS-CoV-2* small viral RNA biogenesis is not affected by Drosha and Dicer deficiency in infected host cells and it is suggested that viral factors or other cytoplasmic proteases during infection could be involved in the maturation of viral miRNAs [90].

In addition to the control of miRNA functionality by aspects of the biogenesis pathway such as enzyme cleavage, and selection for AGO-loading, the stability of miRNAs also shapes the biological impact to cells by influencing the evolution of target sites in the 3′ UTR of genes [91]. Since miRNAs target the 3′ UTRs of genes, target genes that are coexpressed with an miRNA evolve to selectively avoid complementary base pairing with miRNAs that are coexpressed with the gene [92]. *H. polygyrus* miRNA, hpo-miR-71-5p, was detected continually for several days after transfection into recipient mouse cells, suggesting that the helminth miRNAs are highly stable in host cells. As such, it is plausible that the helminth miRNAs can influence the evolution of

target sites of host genes. Of interest, the production of miRNA sequence variants (**isomiRs**) is emerging as a mechanism to regulate miRNA stability and degradation [93]. While some miRNA variants arise from different loci, other isomiRs are produced from the same loci as the canonical sequence and occur due to variabilities in miRNA biogenesis or by post-transcriptional modifications [93]. A lineage-specific high sequence variation rate has been observed in platyhelminths; this is proposed to be a result of coevolution with their hosts [94], and uridylation (addition of a uridine at the 3′ end) of certain miRNAs, a variation which determines miRNA stability, is conserved among cestode species [95]. Furthermore, trimmed 3′ isomiRs have been found to be increased in response to immune activation, bacterial and viral infection, and these 3′ shorter isomiRs reportedly display greater stability than the canonical miRNAs [96]. Based on these observations, it is evident that further exploration is needed to determine the exact nature of the exogenous helminth miRNAs (mature, pri-, or pre-; canonical or isomiR) that is being delivered to the host cells. In addition, understanding the cellular location of these miRNAs (nucleus or cytoplasm) would help to elucidate the point at which they are incorporated into the mammalian miRNA machinery.

Mechanisms of helminth miRNA-mediated regulation of host gene expression

As the expected correlation to an increased expression of an miRNA is the reduced expression of its target gene, to date, the functional validation of a helminth miRNA in host cells has been assessed by measuring the expression of its predicted host gene target(s) within transfected or infected cells. This has typically been supported by the demonstration of a specific interaction by the helminth miRNA with the host gene 3′-UTR using *in vitro* luciferase reporter systems.

While this is certainly an acceptable approach, it gives only one possible outcome. An alternative mechanism could be that, by sequestering the host cell components of the miRNA biogenesis pathway, worm miRNAs prevent their occupation by mammalian miRNAs, thus altering the concentration levels of functional endogenous host miRNAs. This effect has been observed following the transfection of cells with siRNAs [97] which resulted in the rapid reduction of AGO-2 associated endogenous miRNAs. This alteration in AGO loading appeared to impact most highly expressed miRNAs, with low-abundant miRNAs unchanged, repressed, or even increased. Due to this competition for AGO loading, the expression of many miRNA target genes is altered, resulting in an effect on the biology of the cell.

Furthermore, some worm miRNAs have been shown to regulate the transcriptional levels of the miRNA biogenesis components either by direct binding or as a downstream effect. Target prediction software predicts that AGO1-4 and Dicer-1 are direct targets of several worm EV miRNAs, notably, miR-277, let-7, miR-10, and miR190 [33,98–101]. Moreover, overexpression of an *E. multilocularis* miR-71 mimic in mouse macrophages resulted in the enhanced expression of genes that encode the RISC components, AGO-1 and AGO-4, which in turn caused downregulation of several host miRNAs involved in the activation and regulation of inflammatory responses [102].

Finally, miRNAs indirectly alter the expression of gene targets by binding to other miRNAs by sequence complementarity, thus preventing their interaction with the 3′-UTR of their gene targets [103]. There is growing evidence of viral miRNA:host miRNA direct interactions. For instance, in SARS-CoV-2 infection, small viral RNAs have been predicted to form stable duplexes with host miRNAs, and concurrently, many of the predicted target host miRNAs are also found to be downregulated during SARS-CoV-2 infection [104]. Similarly, a Simian virus 40-encoded miRNA binds to host cell miRNAs and prevents their binding to target mRNAs, leading to increased telomerase

activity and viral replication. There is also evidence that the miRNA:miRNA binding happens within Ago-2-associated RISC [105]. In such a manner, parasite-derived miRNAs might bind host miRNAs to directly regulate the abundance and availability of the host miRNAs, and hence affect host gene expression.

Thus, the regulatory interplay between helminth miRNAs and host gene expression likely unfolds through multifaceted mechanisms (Figure 3). Even though helminth miRNA-targeted host gene regulation is becoming more and more evident, further exploration into the miRNA pathway will unveil the full spectrum of intricate mechanisms by which parasitic miRNAs exert control over host gene expression.

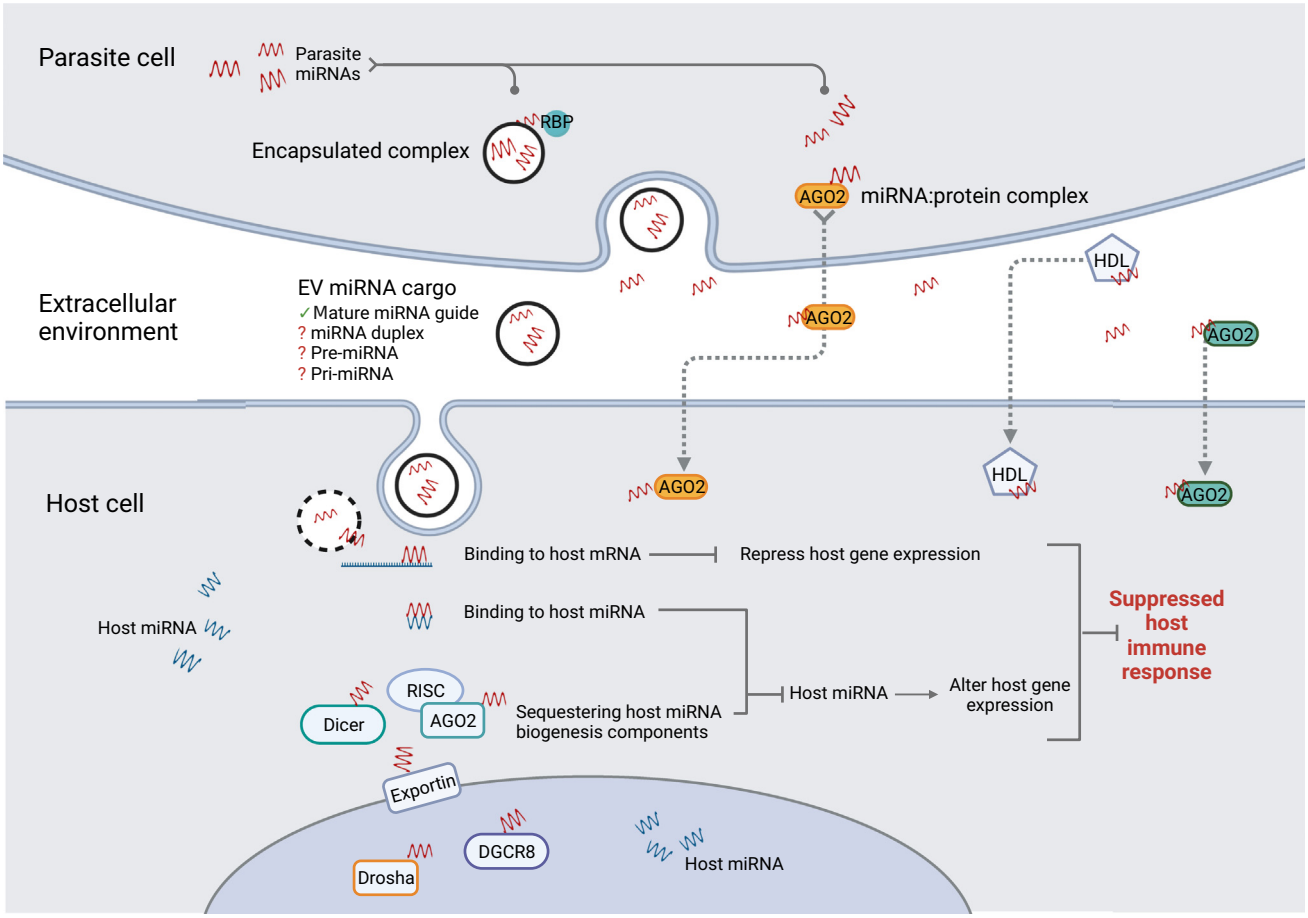


Figure 3. Proposed mechanism of helminth–miRNA mediated cross-kingdom regulation of the host's immune response. Parasite miRNAs are selectively sorted and transported to host cells via extracellular vesicles (EVs) or by forming stable miRNA:protein (e.g., AGO-2 and HDL) complexes with both parasite-derived and host-derived proteins. Once internalised by the host cells, the helminth-derived miRNAs can mimic host miRNAs and incorporate into the host cell miRNA biogenesis pathway to form a functional miRISC complex and consequently repress host gene expression. Beyond their direct interaction with host genes, the exogenous helminth miRNAs may exert their influence on host miRNAs in multiple ways. They can sequester the host's miRNA biogenesis components, including AGO and Dicer. Alternatively, these parasitic miRNAs may directly bind host miRNAs by complementary base pairing. Through these mechanisms, the extracellular miRNAs from helminths may orchestrate manipulation of both host cell mRNAs and miRNAs. As such, this intricate process serves to finely regulate the host gene function to ultimately manipulate the host's immune response, ensuring the parasite's prolonged survival and successful establishment of chronic infection. This figure was created using BioRender.com.

Concluding remarks

The expanding characterisation of helminth miRNomes and their corresponding predicted mammalian gene targets, combined with the increased detection of parasite-derived miRNA sequences within the cells of infected mammalian hosts, is providing growing validation to the hypothesis that parasitic worms can effectively manipulate their host's miRNA machinery to regulate the protective immune response to benefit their long-term survival. However, there are many unknowns regarding the mechanisms by which helminth miRNAs enter and function within their host cells (see Outstanding questions). Mechanistic approaches can be guided by models of miRNA biogenesis in mammalian cells and in the model worm *C. elegans*. However, it will be also important to consider the diversity between helminth species. As mentioned here, at the most fundamental level, understanding the impact of sequence, structure, and cellular localisation of helminth miRNAs on the interaction with host AGO, will be critical to fully elucidate the mechanism of loading and functionality. In addition, a deeper understanding of helminth miRNA sequences will provide more detailed information on the specific form (pri-, pre-, or mature; canonical or isomiR) that is packaged into EVs for transfer and will reveal potential cleavage sites for enzymes of the mammalian miRNA biogenesis pathway. These insights will predict the specific entry point for the helminth miRNA into the mammalian processing system, which can then be supported by *in vitro* assessment using cells deficient/overexpressing different components of the biogenesis pathway. Finally, the broad impact that helminth miRNAs have on their host cells should be fully assessed, beyond the simple characterisation of predicted gene targets and their level of expression. Consideration should also be given to a likely shift in the AGO loading of endogenous host miRNAs, and the possible regulation of host miRNAs activity by direct interaction. Once again, the determination of these outcomes can be achieved through the application of standard *in vitro* assays already established for mammalian miRNAs and a more comprehensive understanding of the sequences of parasite miRNAs.

While these studies will undoubtedly provide new insights into the functionality of helminth miRNAs, it is important to consider that these *in vitro/in silico* analyses may not reflect the complex dynamic microenvironment of an infection. Unlike free-living *C. elegans*, the model worm commonly used for the characterisation of miRNA biogenesis and function, parasitic worms require a mammalian host for survival, which challenges the ability to perform and assess the contribution that individual miRNAs make to the modulation of host immune cells *in vivo* and thus the parasite's survival. However, these studies will become more achievable in the future with the development of organoid culturing systems that better mimic the *in vivo* environment of the host, thus allowing for extended *in vitro* survival and the support of developmental processes and interactions with immune cells [106].

Not discussed in this review, but of relevance to a holistic understanding of the host–parasite relationship, is the observation that cross-kingdom communication of miRNAs is bidirectional [107]. Plant hosts use miRNAs as part of their defence systems, transporting miRNAs into fungal pathogens to inhibit the expression of virulence genes [108]. Similarly, mammalian hosts have been shown to transfer miRNAs to malaria parasites, which consequently mediates resistance to infection [109]. While this pathway of communication has not been reported between host and helminths, it is plausible that mammalian miRNAs (extracellular or vesicular) could be taken up by helminths as they feed on host blood and tissue. However, given the success of helminth parasites in colonising their mammalian hosts and establishing chronic infections, it is equally likely that this mechanism of host defence is less effective against worms as compared to the microbial, and intracellular pathogens such as malaria.

Overcoming the technical challenges raised here and solving some of the unknowns highlighted in this review will unravel this sophisticated mechanism of communication between helminths and

Outstanding questions

What mechanisms do helminths use to transfer their miRNA to host cells? The journey of helminth miRNAs from the parasite into mammalian host cells is intriguing. The mechanisms that enable these miRNAs to cross cellular boundaries, whether in EVs or tethered, need to be deciphered. Identifying the pathways will help us better understand host–parasite interactions at a molecular level.

Does the sequence and structure of helminth miRNAs determine how they are processed by mammalian cells? The attributes of an miRNA, such as its structure, sequence, and cellular location, determine its behaviour and interactions. There is still a knowledge gap in the characterisation of these for helminth miRNAs. Are there isomiRs? Are they processed as clusters? And what is the helminth miRNA machinery involved in this biogenesis? Decoding these characteristics could offer insights into their activity, stability, and how they are recognised or differentiated from host miRNAs by the host's machinery.

How do helminth miRNAs operate to regulate host gene expression? Are helminth miRNAs multifaceted in terms of their regulation? Can helminth miRNAs bind to host miRNA to elicit miRNA-to-miRNA regulation? *In silico* predictions may provide support for this mode of action.

Does helminth–host cross communication extend to other noncoding RNAs? miRNAs represent just one segment of the noncoding RNA tapestry present in helminths. Another component, the long noncoding RNAs (lncRNAs), found within helminths, may have potent regulatory capabilities that influence the dynamics of host–parasite relationships. Interestingly, these lncRNAs might have functionalities that mirror those of mammalian lncRNAs. To understand such parallels and gain a deeper understanding of their potential roles, an in-depth analysis of the helminth transcriptome would be required.

Is there an inverse pathway of communication? Do host miRNAs impact parasite development and/or survival?

their hosts. Addressing these considerations will also ascertain whether interfering with the functions of parasite miRNAs and/or manipulating the expression of their gene targets offers a new strategy to achieve therapeutic control of these pathogens and regulation of mammalian inflammatory responses.

Acknowledgments

S.D. and N.T. are supported by an Australian Research Council Discovery Project Grant (DP210101337). S.C. is a recipient of an Australian Government RTPS Scholarship from the University of Technology Sydney. The funders had no role in study design, data collection and analysis, decision to publish, or preparation of the manuscript.

Declaration of interests

The authors declare no competing interests.

Supplemental information

Supplemental information associated with this article can be found online at https://doi.org/10.1016/j.pt.2023.12.003.

References

1. Roth, J. *et al.* (1982) The evolutionary origins of hormones, neurotransmitters, and other extracellular chemical messengers: implications for mammalian biology. *N. Engl. J. Med.* 306, 523–527
2. Liang, H. *et al.* (2013) New roles for microRNAs in cross-species communication. *RNA Biol.* 10, 367–370
3. Ambros, V. and Horvitz, H.R. (1987) The lin-14 locus of *Caenorhabditis elegans* controls the time of expression of specific postembryonic developmental events. *Genes Dev.* 1, 398–414
4. Ameres, S.L. *et al.* (2010) Target RNA-directed trimming and tailing of small silencing RNAs. *Science* 328, 1534–1539
5. Ørom, U.A. *et al.* (2008) MicroRNA-10a binds the 5'UTR of ribosomal protein mRNAs and enhances their translation. *Mol. Cell* 30, 460–471
6. Vidigal, J.A. and Ventura, A. (2015) The biological functions of miRNAs: lessons from in vivo studies. *Trends Cell Biol.* 25, 137–147
7. Gualtieri, C. *et al.* (2020) Plant miRNA cross-kingdom transfer targeting parasitic and mutualistic organisms as a tool to advance modern agriculture. *Front. Plant Sci.* 11, 930
8. Buck, A.H. *et al.* (2014) Exosomes secreted by nematode parasites transfer small RNAs to mammalian cells and modulate innate immunity. *Nat. Commun.* 5, 5488
9. Britton, C. *et al.* (2014) microRNAs of parasitic helminths – identification, characterization and potential as drug targets. *Int. J. Parasitol. Drugs Drug Resist.* 4, 85–94
10. Tran, N. *et al.* (2021) *Fasciola hepatica* hijacks host macrophage miRNA machinery to modulate early innate immune responses. *Sci. Rep.* 11, 6712
11. Donnelly, S. and Tran, N. (2021) Commandeering the mammalian Ago2 miRNA network: a newly discovered mechanism of helminth immunomodulation. *Trends Parasitol.* 37, 1031–1033
12. Nowacki, F.C. *et al.* (2015) Protein and small non-coding RNA-enriched extracellular vesicles are released by the pathogenic blood fluke *Schistosoma mansoni*. *J. Extracell. Vesicles* 4, 28665
13. Ricafrente, A. *et al.* (2020) An evaluation of the *Fasciola hepatica* miRnome predicts a targeted regulation of mammalian innate immune responses. *Front. Immunol.* 11, 608686
14. Cox, F.E. (2002) History of human parasitology. *Clin. Microbiol. Rev.* 15, 595–612
15. Weatherhead, J.E. *et al.* (2017) The global state of helminth control and elimination in children. *Pediatr. Clin.* 64, 867–877
16. Gazzinelli-Guimaraes, P.H. and Nutman, T.B. (2018) Helminth parasites and immune regulation. *F1000Research* 7, F1000 Faculty Rev-1685
17. Fissiha, W. and Kinde, M.Z. (2021) Anthelmintic resistance and its mechanism: a review. *Infect Drug Resist* 14, 5403–5410
18. Coakley, G. and Harris, N.L. (2020) Interactions between macrophages and helminths. *Parasite Immunol.* 42, e12717
19. Nutman, T.B. *et al.* (1987) Parasite-specific anergy in human filariasis. Insights after analysis of parasite antigen-driven lymphokine production. *J. Clin. Invest.* 79, 1516–1523
20. Doetze, A. *et al.* (2000) Antigen-specific cellular hyporesponsiveness in a chronic human helminth infection is mediated by Th3/Tr1-type cytokines IL-10 and transforming growth factor-β but not by a Th1 to Th2 shift. *Int. Immunol.* 12, 623–630
21. Maizels, R.M. (2020) Regulation of immunity and allergy by helminth parasites. *Allergy* 75, 524–534
22. Taylor, M.D. *et al.* (2012) T cells in helminth infection: the regulators and the regulated. *Trends Immunol.* 33, 181–189
23. Donnelly, S. *et al.* (2006) Proteases in helminth-and allergen-induced inflammatory responses. *Parasites Allergy* 90, 45–64
24. Hewitson, J.P. *et al.* (2009) Helminth immunoregulation: the role of parasite secreted proteins in modulating host immunity. *Mol. Biochem. Parasitol.* 167, 1–11
25. Lund, M.E. *et al.* (2014) Secreted proteins from the helminth *Fasciola hepatica* inhibit the initiation of autoreactive T cell responses and prevent diabetes in the NOD mouse. *PLoS One* 9, e86289
26. Ancarola, M.E. *et al.* (2020) Extracellular non-coding RNA signatures of the metacestode stage of *Echinococcus multilocularis*. *PLoS Negl. Trop. Dis.* 14, e0008890
27. Acuna, S.M. *et al.* (2020) MicroRNAs: biological regulators in pathogen–host interactions. *Cells* 9, 113
28. Ancarola, M.E. *et al.* (2017) Cestode parasites release extracellular vesicles with microRNAs and immunodiagnostic protein cargo. *Int. J. Parasitol.* 47, 675–686
29. Ding, J. *et al.* (2019) miRNA-seq of *Echinococcus multilocularis* extracellular vesicles and immunomodulatory effects of miR-4989. *Front. Microbiol.* 10, 2707
30. Herron, C.M. *et al.* (2022) Developmental regulation and functional prediction of microRNAs in an expanded *Fasciola hepatica* miRNome. *Front. Cell. Infect. Microbiol.* 12, 811123
31. Liu, J. *et al.* (2019) *Schistosoma japonicum* extracellular vesicle miRNA cargo regulates host macrophage functions facilitating parasitism. *PLoS Pathog.* 15, e1007817
32. Yang, B. *et al.* (2020) Extracellular vesicles derived from *Talaromyces marneffei* yeasts mediate inflammatory response in macrophage cells by bioactive protein components. *Front. Microbiol.* 11, 603183
33. Eichenberger, R.M. *et al.* (2018) Hookworm secreted extracellular vesicles interact with host cells and prevent inducible colitis in mice. *Front. Immunol.* 9, 850
34. Duguet, T.B. *et al.* (2020) Extracellular vesicle-contained microRNA of *C. elegans* as a tool to decipher the molecular basis of nematode parasitism. *Front. Cell. Infect. Microbiol.* 10, 217
35. Gu, H.Y. *et al.* (2017) Conservation of a microRNA cluster in parasitic nematodes and profiling of miRNAs in excretory-secretory products and microvesicles of *Haemonchus contortus*. *PLoS Negl. Trop. Dis.* 11, e0006056

36. He, X. and Pan, W. (2022) Host–parasite interactions mediated by cross-species microRNAs. *Trends Parasitol.* 38, 478–488
37. Arora, N. *et al.* (2017) Micromanagement of immune system: role of miRNAs in helminthic infections. *Front. Microbiol.* 8, 586
38. Tkach, M. and Théry, C. (2016) Communication by extracellular vesicles: where we are and where we need to go. *Cell* 164, 1226–1232
39. Taylor, P.J. *et al.* (2020) *Trichinella spiralis* secretes abundant unencapsulated small RNAs with potential effects on host gene expression. *Int. J. Parasitol.* 50, 697–705
40. Mori, M.A. *et al.* (2019) Extracellular miRNAs: from biomarkers to mediators of physiology and disease. *Cell Metab.* 30, 656–673
41. Arroyo, J.D. *et al.* (2011) Argonaute2 complexes carry a population of circulating microRNAs independent of vesicles in human plasma. *Proc. Natl. Acad. Sci. U. S. A.* 108, 5003–5008
42. Turchinovich, A. *et al.* (2011) Characterization of extracellular circulating microRNA. *Nucleic Acids Res.* 39, 7223–7233
43. Ortiz-Quintero, B. (2020) Extracellular microRNAs as intercellular mediators and noninvasive biomarkers of cancer. *Cancers (Basel)* 12, 3455
44. Vickers, K.C. and Michell, D.L. (2021) HDL-small RNA export, transport, and functional delivery in atherosclerosis. *Curr. Atheroscler. Rep.* 23, 38
45. Vickers, K.C. *et al.* (2011) MicroRNAs are transported in plasma and delivered to recipient cells by high-density lipoproteins. *Nat. Cell Biol.* 13, 423–433
46. Drurey, C. and Maizels, R.M. (2021) Helminth extracellular vesicles: interactions with the host immune system. *Mol. Immunol.* 137, 124–133
47. Sanchez-Lopez, C.M. *et al.* (2021) Overview of the interaction of helminth extracellular vesicles with the host and their potential functions and biological applications. *Mol. Immunol.* 134, 228–235
48. Dagenais, M. *et al.* (2021) Analysis of Schistosoma mansoni extracellular vesicles surface glycans reveals potential immune evasion mechanism and new insights on their origins of biogenesis, Pathogens. *Pathogens* 10, 1401
49. Cai, M. *et al.* (2021) Comparative analysis of different extracellular vesicles secreted by *Echinococcus granulosus* protoscoleces. *Acta Trop.* 213, 105756
50. Coakley, G. *et al.* (2017) Extracellular vesicles from a helminth parasite suppress macrophage activation and constitute an effective vaccine for protective immunity. *Cell Rep.* 19, 1545–1557
51. Loghry, H.J. *et al.* (2020) Ivermectin inhibits extracellular vesicle secretion from parasitic nematodes. *J. Extracell. Vesicles* 10, e12036
52. Cwiklinski, K. *et al.* (2015) The extracellular vesicles of the helminth pathogen, *Fasciola hepatica*: biogenesis pathways and cargo molecules involved in parasite pathogenesis. *Mol. Cell. Proteomics* 14, 3258–3273
53. McKenzie, A.J. *et al.* (2016) KRAS-MEK signaling controls Ago2 sorting into exosomes. *Cell Rep.* 15, 978–987
54. Bennett, A.P.S. *et al.* (2020) Helminth genome analysis reveals conservation of extracellular vesicle biogenesis pathways but divergence of RNA loading machinery between phyla. *Int. J. Parasitol.* 50, 655–661
55. Chow, F.W. *et al.* (2019) Secretion of an Argonaute protein by a parasitic nematode and the evolution of its siRNA guides. *Nucleic Acids Res.* 47, 3594–3606
56. Groot, M. and Lee, H. (2020) Sorting mechanisms for microRNAs into extracellular vesicles and their associated diseases. *Cells* 9, 1044
57. Garcia-Martin, R. *et al.* (2022) MicroRNA sequence codes for small extracellular vesicle release and cellular retention. *Nature* 601, 446–451
58. Zhu, S. *et al.* (2016) Release of extracellular vesicles containing small RNAs from the eggs of Schistosoma japonicum. *Parasit. Vectors* 9, 574
59. Kumagai, T. *et al.* (2022) Calpain inhibitor suppresses both extracellular vesicle-mediated secretion of miRNAs and egg production from paired adults of *Schistosoma japonicum*. *Parasitol. Int.* 87, 102540
60. Sotillo, J. *et al.* (2015) A quantitative proteomic analysis of the tegumental proteins from Schistosoma mansoni schistosomula reveals novel potential therapeutic targets. *Int. J. Parasitol.* 45, 505–516
61. Liang, P. *et al.* (2019) Identification and molecular characterization of exosome-like vesicles derived from the *Taenia asiatica* adult worm. *Acta Trop.* 198, 105036
62. Lee, Y. *et al.* (2004) MicroRNA genes are transcribed by RNA polymerase II. *EMBO J.* 23, 4051–4060
63. Han, J. *et al.* (2004) The Drosha-DGCR8 complex in primary microRNA processing. *Genes Dev.* 18, 3016–3027
64. Denli, A.M. *et al.* (2004) Processing of primary microRNAs by the Microprocessor complex. *Nature* 432, 231–235
65. Zhang, H. *et al.* (2004) Single processing center models for human Dicer and bacterial RNase III. *Cell* 118, 57–68
66. Grishok, A. *et al.* (2001) Genes and mechanisms related to RNA interference regulate expression of the small temporal RNAs that control *C. elegans* developmental timing. *Cell* 106, 23–34
67. Meijer, H.A. *et al.* (2014) Regulation of miRNA strand selection: follow the leader? *Biochem. Soc. Trans.* 42, 1135–1140
68. O'Brien, J. *et al.* (2018) Overview of microRNA biogenesis, mechanisms of actions, and circulation. *Front. Endocrinol. (Lausanne)* 9, 402
69. Naeli, P. *et al.* (2023) The intricate balance between microRNA-induced mRNA decay and translational repression. *FEBS J.* 290, 2508–2524
70. Xie, M. *et al.* (2013) Mammalian 5′-capped microRNA precursors that generate a single microRNA. *Cell* 155, 1568–1580
71. Ruby, J.G. *et al.* (2007) Intronic microRNA precursors that bypass Drosha processing. *Nature* 448, 83–86
72. Salim, U. *et al.* (2022) Biogenesis, characterization, and functions of mirtrons. *Wiley Interdiscip. Rev. RNA* 13, e1680
73. Chen, J. *et al.* (2017) Cap-seq reveals complicated miRNA transcriptional mechanisms in C. elegans and mouse. *Quant. Biol.* 5, 352–367
74. Cheloufi, S. *et al.* (2010) A dicer-independent miRNA biogenesis pathway that requires Ago catalysis. *Nature* 465, 584–589
75. Kim, Y.-K. *et al.* (2016) Re-evaluation of the roles of DROSHA, Exportin 5, and DICER in microRNA biogenesis. *Proc. Natl. Acad. Sci.* 113, E1881–E1889
76. Stavast, C.J. and Erkeland, S.J. (2019) The non-canonical aspects of microRNAs: many roads to gene regulation. *Cells* 8, 1465
77. Snead, N.M. *et al.* (2013) Molecular basis for improved gene silencing by Dicer substrate interfering RNA compared with other siRNA variants. *Nucleic Acids Res.* 41, 6209–6221
78. Fontenla, S. *et al.* (2021) Lost and found: Piwi and Argonaute pathways in flatworms. *Front. Cell. Infect. Microbiol.* 11, 653695
79. Britton, C. *et al.* (2020) Small RNAs in parasitic nematodes – forms and functions. *Parasitology* 147, 855–864
80. Weiberg, A. *et al.* (2013) Fungal small RNAs suppress plant immunity by hijacking host RNA interference pathways. *Science* 342, 118–123
81. Mishra, R. *et al.* (2020) The interplay between viral-derived miRNAs and host immunity during infection. *Front. Immunol.* 10, 3079
82. Nakanishi, K. (2016) Anatomy of RISC: how do small RNAs and chaperones activate Argonaute proteins? *Wiley Interdiscip. Rev. RNA* 7, 637–660
83. Soichot, J. *et al.* (2022) Nematode microRNAs can individually regulate interferon regulatory factor 4 and mTOR in differentiating T helper 2 lymphocytes and modulate cytokine production in macrophages. *Front. Mol. Biosci.* 9, 909312
84. Lech, M. *et al.* (2011) IRF4 deficiency abrogates lupus nephritis despite enhancing systemic cytokine production. *J Am Soc Nephrol* 22, 1443
85. Nguyen, T.L. *et al.* (2023) Dissection of the *Caenorhabditis elegans* microprocessor. *Nucleic Acids Res.* 51, 1512–1527
86. He, X. *et al.* (2020) A schistosome miRNA promotes host hepatic fibrosis by targeting transforming growth factor beta receptor III. *J. Hepatol.* 72, 519–527
87. Luo, Q.J. *et al.* (2021) RNA structure probing reveals the structural basis of Dicer binding and cleavage. *Nat. Commun.* 12, 3397

88. Lee, Y.-Y. *et al.* (2023) Sequence determinant of small RNA production by DICER. *Nature* 615, 323–330
89. Shapiro, J.S. *et al.* (2010) Noncanonical cytoplasmic processing of viral microRNAs. *RNA* 16, 2068–2074
90. Morales, L. *et al.* (2017) SARS-CoV-encoded small RNAs contribute to infection-associated lung pathology. *Cell Host Microbe* 21, 344–355
91. Zhou, L. *et al.* (2018) Importance of miRNA stability and alternative primary miRNA isoforms in gene regulation during Drosophila development. *Elife* 7, e38389
92. Stark, A. *et al.* (2005) Animal microRNAs confer robustness to gene expression and have a significant impact on 3′ UTR evolution. *Cell* 123, 1133–1146
93. Bofill-De Ros, X. *et al.* (2020) IsomiRs: expanding the miRNA repression toolbox beyond the seed. *Biochim. Biophys. Acta (BBA) Gene Regul. Mech.* 1863, 194373
94. Fontenla, S. *et al.* (2015) The miRnome of *Fasciola hepatica* juveniles endorses the existence of a reduced set of highly divergent micro RNAs in parasitic flatworms. *Int. J. Parasitol.* 45, 901–913
95. He, Z. *et al.* (2020) miRNAs and lncRNAs in *Echinococcus* and Echinococcosis. *Int. J. Mol. Sci.* 21, 730
96. Rotival, M. *et al.* (2020) Population variation in miRNAs and isomiRs and their impact on human immunity to infection. *Genome Biol.* 21, 1–31
97. Liang, X.-h. *et al.* (2013) Transfection of siRNAs can alter miRNA levels and trigger non-specific protein degradation in mammalian cells. *Biochim. Biophys. Acta (BBA) Gene Regul. Mech.* 1829, 455–468
98. Fontenla, S. *et al.* (2021) Role of *Fasciola hepatica* small RNAs in the interaction with the mammalian host. *Front. Cell. Infect. Microbiol.* 11, 812141
99. Ovchinnikov, V.Y. *et al.* (2020) EV-transported microRNAs of *Schistosoma mansoni* and *Fasciola hepatica*: potential targets in definitive hosts. *Infect. Genet. Evol.* 85, 104528
100. Cavallero, S. *et al.* (2022) A miRNAs catalogue from third-stage larvae and extracellular vesicles of *Anisakis pegreffii* provides new clues for host-parasite interplay. *Sci. Rep.* 12, 9667
101. Yang, Y. *et al.* (2020) Extracellular vesicles derived from *Trichinella spiralis* muscle larvae ameliorate TNBS-induced colitis in mice. *Front. Immunol.* 11, 1174
102. Zheng, Y. *et al.* (2016) Effects of *Echinococcus multilocularis* miR-71 mimics on murine macrophage RAW264.7 cells. *Int. Immunopharmacol.* 34, 259–262
103. Lai, E.C. *et al.* (2004) Complementary miRNA pairs suggest a regulatory role for miRNA: miRNA duplexes. *RNA* 10, 171–175
104. Neeb, Z.T. *et al.* (2022) A potential role for SARS-CoV-2 small viral RNAs in targeting host microRNAs and modulating gene expression. *Sci. Rep.* 12, 21694
105. Takahashi, T. *et al.* (2022) SV40 miR-S1 and cellular miR-1266 sequester each other from their targets, enhancing telomerase activity and viral replication. *Non-Coding RNA* 8, 57
106. Britton, C. *et al.* (2023) New technologies to study helminth development and host–parasite interactions. *Int. J. Parasitol.* 53, 393–403
107. Cai, Q. *et al.* (2019) Small RNAs and extracellular vesicles: new mechanisms of cross-species communication and innovative tools for disease control. *PLoS Pathog.* 15, e1008090
108. Cai, Q. *et al.* (2018) Plants send small RNAs in extracellular vesicles to fungal pathogen to silence virulence genes. *Science* 360, 1126–1129
109. LaMonte, G. *et al.* (2012) Translocation of sickle cell erythrocyte microRNAs into *Plasmodium falciparum* inhibits parasite translation and contributes to malaria resistance. *Cell Host Microbe* 12, 187–199
110. Yan, C. *et al.* (2021) Csi-let-7a-5p delivered by extracellular vesicles from a liver fluke activates M1-like macrophages and exacerbates biliary injuries. *Proc. Natl. Acad. Sci. U. S. A.* 118, e2102206118
111. Meningher, T. *et al.* (2020) Schistosomal extracellular vesicle-enclosed miRNAs modulate host T helper cell differentiation. *EMBO Rep.* 21, e47882
112. Wang, L. *et al.* (2020) Sja-miR-71a in schistosome egg-derived extracellular vesicles suppresses liver fibrosis caused by schistosomiasis via targeting semaphorin 4D. *J. Extracell. Vesicles* 9, 1785738
113. Jiang, P. *et al.* (2022) Identification of a *Schistosoma japonicum* microRNA that suppresses hepatoma cell growth and migration by targeting host fzd4 gene. *Front. Cell. Infect. Microbiol.* 12, 31
114. Wang, L. *et al.* (2021) Exosomal microRNA let-7-5p from *Taenia pisiformis* cysticercus prompted macrophage to M2 polarization through inhibiting the expression of C/EBP delta. *Microorganisms* 9, 1403
115. Landa, A. *et al.* (2019) *Taenia solium* and *Taenia crassiceps*: miRNomes of the larvae and effects of miR-10-5p and let-7-5p on murine peritoneal macrophages. *Biosci. Rep.* 39, BSR20190152

Appendix B:

Published original article: Exploring the utility of circulating miRNAs as diagnostic biomarkers of fasciolosis. *Scientific reports* (2024) 14:7431; doi: 10.1038/s41598-024-57704-9

scientific reports

Check for updates

OPEN

Exploring the utility of circulating miRNAs as diagnostic biomarkers of fasciolosis

Sumaiya Chowdhury[1], Alison Ricafrente[1], Krystyna Cwiklinski[2,4], Dayna Sais[3], John P. Dalton[2], Nham Tran[3,5]✉ & Sheila Donnelly[1,5]✉

Effective management and control of parasitic infections on farms depends on their early detection. Traditional serological diagnostic methods for *Fasciola hepatica* infection in livestock are specific and sensitive, but currently the earliest detection of the parasite only occurs at approximately three weeks post-infection. At this timepoint, parasites have already entered the liver and caused the tissue damage and immunopathology that results in reduced body weight and loss in productivity. Here, we investigated whether the differential abundance of micro(mi)miRNAs in sera of *F. hepatica*-infected sheep has potential as a tool for the early diagnosis of infection. Using miRNA sequencing analysis, we discovered specific profiles of sheep miRNAs at both the pre-hepatic and hepatic infection phases in comparison to non-infected sheep. In addition, six *F. hepatica*-derived miRNAs were specifically identified in sera from infected sheep. Thus, a panel of differentially expressed miRNAs comprising four sheep (miR-3231-3p; miR133-5p; 3957-5p; 1197-3p) and two parasite miRNAs (miR-124-3p; miR-Novel-11-5p) were selected as potential biomarkers. The expression of these candidates in sera samples from longitudinal sheep infection studies collected between 7 days and 23 weeks was quantified using RT-qPCR and compared to samples from age-matched non-infected sheep. We identified oar-miR-133-5p and oar-miR-3957-5p as promising biomarkers of fasciolosis, detecting infection as early as 7 days. The differential expression of the other selected miRNAs was not sufficient to diagnose infection; however, our analysis found that the most abundant forms of fhe-miR-124-3p in sera were sequence variants (IsomiRs) of the canonical miRNA, highlighting the critical importance of primer design for accurate diagnostic RT-qPCR. Accordingly, this investigative study suggests that certain miRNAs are biomarkers of *F. hepatica* infection and validates miRNA-based diagnostics for the detection of fasciolosis in sheep.

The liver fluke parasite, *Fasciola hepatica*, is a trematode that causes fasciolosis, a major public health issue and neglected tropical disease affecting over 2.4 million people in over 70 countries[1–3]. Prevalence of liver fluke infection is thought to be on the rise due to the spread of drug-resistant parasites and climate change[4,5]. While *F. hepatica* has adapted to infect every mammalian host that it has encountered[2,6], grazing ruminants are most susceptible to *F. hepatica* infection due to their ingestion of pasture and water contaminated with the infective metacercariae. As such, fasciolosis is a significant economic burden to the livestock industry, with global losses of over US $3 billion per annum[7,8].

Within hours of ingestion, the *F. hepatica* metacercariae excyst in the gut, releasing the newly excysted juveniles (NEJ), which penetrate the intestinal wall to migrate through the peritoneal cavity to the liver. This pre-hepatic stage takes approximately two weeks, after which the pathology resulting from the parasite's penetration into the liver becomes evident[9–11]. Fasciolosis results from the tissue damage and bleeding caused by the parasite's burrowing and feeding in the liver and the associated immune-mediated pathology[12–14]. Within the liver, the juvenile flukes grow and mature, and by 8–12 weeks, the adult parasites enter the bile ducts to establish chronic infection, during which time they produce eggs that are excreted within the faeces, consequently contaminating

[1]The School of Life Sciences, University of Technology, Sydney, Australia. [2]Centre for One Health, School of Natural Sciences, Ryan Institute, National University of Ireland Galway, Galway, Ireland. [3]School of Biomedical Engineering, Faculty of Engineering and Information Technology, University of Technology Sydney, Ultimo, NSW, Australia. [4]Present address: Institute of Infection, Veterinary and Ecological Sciences, University of Liverpool, Liverpool, UK. [5]These authors contributed equally: Nham Tran and Sheila Donnelly. ✉email: Nham.Tran@uts.edu.au; Sheila.Donnelly@uts.edu.au

pasture and continuing the life cycle[9]. Once established in their ruminant hosts, the parasites can survive for months and even years if the infection is untreated[11,15].

Several methods are currently employed to diagnose fasciolosis in ruminants. While these techniques are effective, they have notable limitations, especially for the detection of early infection[16,17]. The gold standard for liver fluke detection is the faecal egg count (FEC), which is a preferred technique as the presence of liver fluke eggs represents a definitive diagnosis[18,19]. It is inexpensive, and both the sample collection and protocol are uncomplicated[16]. However, this method only detects infection at 8–12 weeks[20]. In addition, due to the uneven distribution of eggs in the faeces when the worm burden is low this method lacks sensitivity[21]. Coproantigen ELISAs can detect liver flukes two to three weeks earlier than FEC[22] but this antigen-based assay lacks sensitivity due to the low and inconsistent abundance of the liver fluke antigens in the host samples[23,24]. Higher sensitivity can be obtained using serological techniques[25]. Detection of anti-liver fluke antibodies in serum is a more sensitive alternative, and ELISAs for these have been proven to detect infection from three to four weeks post-infection. However, this method cannot distinguish between new and previous infections[24]. Additionally, maternal antibodies can persist in lambs for up to 12 weeks post-birth, limiting the applicability of this assay during the first 2 months on pasture[26]. Another complication of antibody detection is the lack of specificity due to cross-reaction with antibodies raised in response to other infections[27]. Finally, although the presence of liver enzymes within sera samples, including glutamate dehydrogenase (GLDH), gamma-glutamyl transferase (GGT) and albumin, are a good indication of liver damage, these changes are transient, variable, and not specific for the liver fluke[28].

As there is currently no effective vaccine against *F. hepatica*[29], liver fluke control relies heavily on the available chemical drugs, such as triclabendazole (TCBZ), closantel, and clorsulon[30]. Due to the challenge of detecting prepatent infection, farmers opt for preventative treatment measures involving blanket treatment of animals before release onto pasture and further treatment depending on factors such as housing time, local climate, fasciolosis prevalence, age of herd, and grazing period[17,31,32]. Apart from the financial burden of drenching an entire herd with flukicides, this practice is driving the emergence of drug resistance against these available chemical treatments. As such, 'test before you treat' strategies are now being advocated for sustainable parasite control[33–37]. If early diagnosis was possible, anthelmintics could be administered to infected animals only, which would prevent/minimise the parasites from breaching the liver capsule. This approach would reduce liver damage and avert the loss of animals. Additionally, it would decrease the number of eggs dispersed onto pasture and curtail the unwarranted use of flukicides. Thus, there is a clear industry requirement for new diagnostic tools that can reliably identify *F. hepatica* infections, particularly at the pre-hepatic phase of infection.

Micro(mi)RNAs are small non-coding RNAs that play a central role in all biological processes[38] and offer great promise as markers of disease. Importantly, changes in their expression profiles have been correlated to several pathologies, including infectious diseases[39]. In addition, circulating miRNAs are present and highly stable in most bodily fluids, including blood, saliva, urine, and milk, making them robust candidates for non-invasive diagnostic and prognostic biomarkers[40].

Several studies have reported alterations in the abundance of both host and parasite-derived miRNAs in circulation during helminth infections, suggesting their utility as biomarkers for detecting infection[41–44]. While the diagnostic potential of circulating miRNAs during fasciolosis has not yet been explored, we have previously shown that *F. hepatica* miRNAs are expressed in a life cycle stage-specific manner and that fluke-derived miRNAs can be detected in host cells during the pre-hepatic stage of infection[45,46]. Therefore, in this study, we explored whether a differential abundance of host and *F. hepatica* miRNAs in sera was evident in experimental infected sheep that could be used to diagnose *F. hepatica* infection, particularly from the early pre-hepatic stage of infection. This would enable prompt and effective intervention before the parasite causes significant liver pathology.

Materials and methods

Sheep sera samples from experimental *F. hepatica* infections

The sheep sera samples were taken from previous experimental infection studies, which were all carried out according to standardised protocols to ensure consistency and reproducibility between studies. Male sheep were orally infected with *F. hepatica* metacercariae, and blood samples collected by jugular venepuncture at various time points (Table 1), using appropriate blood collection tubes for serum collection. The blood was allowed to clot at room temperature, followed by centrifugation at 1000 × g for 10 min in a refrigerated centrifuge. The serum was collected and aliquoted into 1 ml aliquots that were frozen at − 80 °C. Four sets of sheep sera samples were used in this study, with each set representing an independent infection cohort (Table 1). The samples from sets A, B and D, were processed in the Molecular Parasitology Laboratory, Ireland. The samples collected in Spain (Set C) were transported to the Molecular Parasitology Laboratory in Ireland frozen on dry ice. Upon delivery, they were placed at − 80 °C. Samples used for this study were defrosted in the fridge the evening before RNA extraction; this process was the first time they had been thawed since collection. Samples from Set A and Set B were used to prepare the small RNA sequencing library. Set C (pre-hepatic time points) and Set D (hepatic time points) were used for RT-qPCR validation of the diagnostic potential of selected miRNAs. Sets C and D were obtained from longitudinal sheep *F. hepatica* infection studies that included non-infected age-matched animals as field controls.

Ethics statement

Experimental procedures at Agri-Food and Biosciences Institute (AFBI; UK) were carried out under license from the Department of Health, Social Services and Public by the Animal (Scientific Procedures) Act 1986 (License No. PPL 2771; PPL 2801), after ethical review by the AFBI Animal Ethics Committee. Experimental procedures at the University of Cordoba, Spain were carried out under license from 22-12-2015-381 in accordance with EU Directive 2012/707/UE and RD 53/2013 following ethical approval from the University of Cordoba Bioethics Committee (code no, 2015-PI-038).

Samples for sequencing		
	Set A	**Set B**
Study type	Cross-sectional	Longitudinal
Cohort (infection type)	Pre-hepatic infection	Hepatic infection
Sheep breed	Dorset cross sheep	Dorset cross sheep
Sheep age (at day 0)	6 months	6 months
F. hepatica isolate	Italian isolate (Ridgeway Research, UK)	South Gloucester isolate (Ridgeway Research, UK)
Infection dose	150 metacercariae	150 metacercariae
Collection time points	0, 2, 9, 14, 18 dpi (n = 6/timepoint)	3, 7, 10, 14 wpi, Neg-14 wpi (n = 6/timepoint)
Study location	AFBI, UK	AFBI, UK
Study reference	[47]	[47]
Samples for qPCR validation		
	Set C	**Set D**
Study type	Longitudinal	Longitudinal
Cohort (infection type)	Pre-hepatic infection	Hepatic infection
Sheep breed	Merino-breed sheep	Dorset cross sheep
Sheep age (at day 0)	8 months	6 months
F. hepatica isolate	Italian isolate	Italian isolate
Infection dose	150 metacercariae	120 metacercariae
Collection time points	0dpi (n = 3 non-infected; 9 infected) 7, 14 dpi (n = 14 non-infected; 11 infected)	3, 15, 20, 23 wpi (n = 6 non-infected; 4–5 infected/timepoint)
Study location	Cordoba, Spain	AFBI, UK
Study reference	Not published	[47]

Table 1. Details of the experimental *F. hepatica* infections in sheep. *dpi* Days post-infection, *wpi* Weeks post-infection, *Neg-14wpi* Non-infected age-matched control at 14 weeks.

RNA isolation from sheep sera, lamb tissue, and newly excysted juveniles

Small RNA extraction was performed on sheep sera using Tri-Reagent as described previously[48]. Frozen serum samples were thawed and 400 µl aliquots were treated with proteinase K (1 mg/mL) for 20 min at 37 °C to degrade proteins. Then, 750 µL Tri-Reagent RT LS (Molecular Research, US) and 100 µL 4-bromoanisole was added to each 400 µL of serum samples to solubilise the nucleic acids. The homogenate was gently mixed and centrifuged at 12,000 × *g* for 20 min. The nucleic acids were precipitated with 5 µL of glycogen (5 mg/µL) and 500 µL of 100% isopropanol at − 20 °C overnight. The RNA precipitate was pelleted by centrifugation at 12,000 × *g*, for 15 min, washed twice with 70% ethanol and reprecipitated by centrifugation at 12,000 × *g* for 10 min, and finally re-suspended in RNase free H_2O. For each serum sample, the RNA extracted from a total of 800 µL starting volume of sera was combined for subsequent analysis. All samples were processed at the same time, and each 400 µl aliquot was processed in the same manner. This process on average yielded 50 ng/µl of RNA per individual serum sample. The quality and quantity of RNA was assessed by POLARstar® Omega Multimode Microplate Reader (for small RNA sequencing library preparation) or NanoDrop reader (for RT-qPCR).

RNA was extracted from a sample of lamb rump using RNAzol RT (Molecular Research Centre Inc, USA). Approximately 100 mg of tissue was snap-frozen with liquid nitrogen and homogenised in 1 mL of RNAzol RT with a mortar and pestle for RNA extraction, which was performed as described previously[46] and yielded 2 µg of RNA.

The NEJ RNA had been previously isolated, as described by Ricafrente et al.[45]. NEJs were excysted using our standardised protocols. The *Fasciola hepatica* metacercariae (Italian isolate), sourced from Ridgeway Research Ltd (UK) were used for excystment and 24 h culture of NEJ. Specifically, metacercariae were removed from the visking tubing and incubated for a maximum of 10 min in 2% sodium hypochlorite with agitation at room temperature to remove the outer cyst wall. The parasites were then washed in distilled water by sedimentation to remove all traces of sodium hypochlorite. The washed parasites were re-suspended in excystment medium (1.2% sodium bicarbonate, 0.9% sodium chloride, 0.2% sodium tauroglycocholate, 0.07% concentrated hydrochloric acid, 0.006% L-cysteine) and incubated for up to 3 h at 37 °C in 5% CO_2. NEJ were recovered using a pipette and washed several times in PBS by sedimentation to remove all traces of the excystment media. The NEJ were then transferred to pre-warmed (37 °C) culture medium (RPMI 1640 medium (ThermoFisher Scientific) containing 2 mM L-glutamine, 30 mM HEPES, 0.1% (w/v) glucose, and 2.5 µg/ml gentamycin) and incubated for 24 h at 37 °C in 5% CO2. Following the incubation, the NEJ were centrifuged at 400 × g for 5 min to pellet the NEJ and the media was removed. The NEJ pellet was washed three times with PBS and stored at − 80 °C prior to RNA extraction. This process was carried out in triplicate using 1000 NEJ per replicate. No serum was used in the culture media as these samples were also used for proteomic analyses as described by Cwiklinski et al.[49]. RNA was extracted using the miRNeasy mini kit (Qiagen) according to the manufacturer's instructions. The QIAzol Lysis Reagent was added directly to the frozen NEJ pellet for lysis and homogenization, and the RNA eluted into a final volume of 50 µl RNase-free water. RNA integrity and concentration were verified using the 260/280 LVis

plate functionality of the PolarStar Omega Spectrophotometer (BMG LabTech) and the Quant-iT RiboGreen RNA Assay Kit (TermoFisher Scientifc). The RNA was transported to University of Technology, Sydney frozen on dry ice and stored at − 80 °C upon delivery.

Sequencing and bioinformatics

RNA extracted from each time point (representing six animals) was pooled into a single representative sample to provide sufficient yield of RNA for sequencing. RNA library preparation was performed by Macrogen Oceania (NSW, Australia) using 1 µg of total RNA with the TruSeq Small RNA library Prep Kit according to manufacturer's instruction (Part#15,004,197 Rev. G) and sequenced using Illumina NextSeq 500. The quality of the raw FASTq files was assessed using FastQC[50], and consequently the adaptor sequences were excised, and low-quality sequences were removed (< 20 phred score, and short read length < 18 nt) using the bioinformatic tool CutAdapt (v3.4)[51]. The cleaned sheep sera sequence reads were then aligned against known sheep mature miRNAs from miRBase: *Ovis aries* (Oar_V4.0) using Bowtie (v1)[52], allowing zero mismatches. The miRNA sequence reads that did not align against the sheep miRNAs were then aligned against *F. hepatica* mature miRNA sequences from miRBase (Fhepatica_v1) and other published sources[45,53–55] (Supplemental Table 1) allowing zero mismatches. The counts for the sheep and *F. hepatica* miRNAs were extracted from the resultant Sam files using SamTools[56].

Characterisation of the differential expression of miRNAs in sheep sera

DESeq2[57] was performed on the sheep miRNA read counts to assess the differential expression of circulating host-miRNAs during infection in comparison to non-infected sheep. The sequencing data from Set A, infection cohort (2, 9, 14, and 18 days post infection; dpi) were grouped as "pre-hepatic infection", and samples in the Set B cohort (3, 7, 10, 14 weeks post infection; wpi) were grouped as "hepatic infection", while the sequencing data from 0 dpi (pre-infection) and 14 days non-infected animals were grouped to provide a duplicate set of "non-infected" samples. Only miRNAs with a sum of > 10 counts across all samples and with an adjusted p-value < 0.05 were included in the subsequent analyses. Log2Fold change of 2 (Log2FC2) or fourfold cut-off was applied to identify the most differentially expressed miRNAs.

RT-qPCR

Custom Taqman small RNA primers were designed for sheep and *F. hepatica* miRNAs, as listed in Table 2. The custom Taqman RT primers and TaqMan™ MicroRNA Reverse Transcription Kit (Applied Biosystems, US) were used for the synthesis of cDNA from 150 ng of RNA extracted from each sample (Set A and B were pooled RNA samples; Set C and D were individual samples), as per manufacturer's instructions. Then 4.5 µl of cDNA was used for qPCR, with undiluted cDNA used for *F. hepatica* miRNAs, while for the sheep miRNAs the cDNA was diluted 1:2 in dH_2O. The qPCR was performed using the custom TaqMan primer and TaqMan™ Fast Advanced Master Mix. Samples were prepared on a MicroAmp optical 96-well reaction plate as technical triplicates (Life Technologies, USA) and analysed using the QuantStudio 6 Flex real-time PCR system (Life Technologies, USA). Default settings on the instrument software for Taqman® reagent Fast was used for qPCR reaction, initial denaturation at 95 °C for 20 s, followed by 40 cycles of 1 s denaturation at 95 °C and a 20 s annealing/extension at 60 °C. The starting concentration of the samples, presented as N0 value, was calculated from the qPCR amplification raw data using LinRegPCR software v11[58].

Statistical analysis

Statistical analysis of RT-qPCR data was performed with GraphPad Prism (v 10). Non-parametric Welch's two tailed t-test was performed to compare infected versus non-infected samples at each timepoint. p value < 0.05 was considered as statistically significant.

Results

Differential abundance of host circulating miRNAs during *F. hepatica* infection

To identify the presence of circulating miRNAs that are associated with developing fasciolosis, that may be considered as candidate diagnostic biomarkers, small RNA sequencing was performed on RNA extracted from sera of experimentally infected sheep. Sera collected from two distinct *F. hepatica* infection studies (Set A and B; Table 1) was used for this analysis; Sera in the Set A samples were collected at 2, 9, 14, 18 dpi, and Set B comprised

Species	miRNA	Canonical/isomiR	Sequence
Ovis aries	oar-miR-133-5p	Canonical	UUGGUCCCCUUCAACCAGCUGU
	oar-miR-323a-3p	Canonical	CACAUUACACGGUCGACCUCU
	oar-miR-3957-5p	Canonical	CUCGGAGAGUGGAGCUGUGGGUGU
	oar-miR-1197-3p	Canonical	CCCUUCCUGGUAUUUGAAGACG
F. hepatica	fhe-Novel-11-5p	Canonical	AAGCUCGUAGUUGGAUCUGGGU
	fhe-miR-124-3p	Canonical	UUAAGGCACGCGGUGAAUGUCA
	fhe-miR-124-3p	IsomiR	UUAAGGCACGCGGUGAAU

Table 2. Mature miRNA sequences used to design custom TaqMan primers.

of sera taken at 3, 7, 10, 14 wpi[47]. Sera was also collected from uninfected animals in each study, harvested at time points coincident with a pre-infection (0 dpi,Set A) and 14 weeks (Set B) timepoint.

As the initial RNA sequencing analysis of these individual samples was unsuccessful due to low RNA yield, RNA from six sera samples at each time point was pooled for preparation of the small RNASeq library. The resulting sequencing data was screened against the 153 mature miRNA sheep sequences registered in miRBase (Oar_V4.0). On average, 104 and 108 out of 153 sheep miRNAs were detected in the uninfected and infected sheep samples, respectively (Supplemental Table 2). Hierarchal clustering of the sequencing data from the different time points revealed a distinct separation in the miRNA expression between early and late infection (Fig. 1A). To measure differential expression (DE) during disease progression, the sequencing reads were grouped as pre-hepatic (2, 9, 14 and 18 dpi; thus n = 4) and hepatic (3, 7, 10 and 14 wpi; n = 4) samples. Comparative analysis was then conducted using the expression profile from the sera from non-infected sheep (pre-infection 0 dpi and 14 wpi; n = 2). Principal component analysis (PCA) verified that samples produced distinct clusters, correctly grouping the pre-hepatic and hepatic samples (Fig. 1B).

Comparing the sheep miRNAs between the non-infected, pre-hepatic, and hepatic stages of infection revealed several distinct miRNAs that were significantly increased or decreased in their abundance during the progression of infection. A four-fold cut-off (Log2FC2) was applied to these miRNA profiles to distinguish the subset of miRNAs that were most highly altered in expression and, therefore, most likely to be above a threshold of differential abundance to support the diagnosis of infection and potentially differentiate between the pre-hepatic and hepatic stages of disease.

This revealed the presence of six miRNAs that significantly increased during the pre-hepatic stage of the infection phase when compared to non-infected animals (Fig. 2A; Supplemental Table 3A). Of these, the change in expression ranged from 2 to sixfold, but the differential expression of oar-miR-323a-3p, oar-miR-133-5p, and oar-miR-3957-5p were the most significantly increased in the infected animals. The increased expression of oar-miR-3957-5p and oar-miR-541-3p, seen in the pre-hepatic samples, was also evident during the hepatic stage in infected sheep as compared to non-infected sheep, albeit at a reduced level (Fig. 2B; Supplemental Table 3B). In contrast, the presence of oar-miR-133-5p, and oar-miR-323a-3p were significantly downregulated during the hepatic stage of infection, as compared to the pre-hepatic timepoints (Fig. 2C; Supplemental Table 3C). Additionally, oar-miR-1197-3p was identified as the only miRNA significantly reduced during the hepatic stage of infection compared to uninfected animals and pre-hepatic infection (Fig. 2B,C; Supplemental Table 3B,C).

Small RNA sequencing revealed the presence of *F. hepatica* derived miRNAs in the serum of infected sheep

To determine if miRNAs derived from *F. hepatica* were present in the sera from infected sheep, sequencing reads that did not align to sheep mature miRNAs were screened against known *F. hepatica* miRNAs (Supplemental Table 1). Critically, no parasite-derived miRNA sequences were identified within the sera samples collected from non-infected sheep and, thus, validated this approach. In contrast, six liver fluke miRNAs were found within the sera from infected sheep (Table 3). These miRNAs displayed a distinct pattern of expression correlating to the division of samples into pre-hepatic and hepatic phases of infection. Specifically, two miRNAs were detected only at the pre-hepatic stage of infection: fhe-miR-124-3p and fhe-miR-71a-5p; however, fhe-miR-124-3p had higher read counts and was observed at all the timepoints, suggesting it may be a more robust infection marker than fhe-miR-71a-5p. While three microRNAs (fhe-Novel-102-3p, fhe-miR-277a-3p, and fhe-miR-750-3p) were linked to the hepatic phase of the infection, their counts per million (CPM) were all below 13, suggesting a low abundance. Only fhe-Novel-11-5p, was found throughout the entire infection, detected in all serum samples from both the pre-hepatic and hepatic stages.

Selection of sheep and *F. hepatica* derived miRNAs as potential biomarkers of fasciolosis

Based on our sequence analysis, a panel of sheep and parasite-derived miRNAs were curated as potential biomarkers of *F. hepatica* infection due to their differential abundance in infected compared to non-infected sheep and their presence across the different stages of infection (Fig. 3). This panel comprised four sheep miRNAs and two *F. hepatica* miRNAs. The sheep miRNAs included oar-miR-133-5p and oar-miR-323a-3p, which were the most significantly upregulated miRNAs in pre-hepatic infection versus non-infected animals; oar-miR-3957-5p which was consistently elevated (log2FC4) in pre-hepatic and hepatic infection; and oar-miR-1197-3p which was downregulated in hepatic infection compared to both non-infected and pre-hepatic infection. The parasite miRNAs for the selected biomarker panel included fhe-miR-124-3p and fhe-novel-11-5p, which had the highest read numbers in sheep sera.

While sequencing analysis provided high-throughput screening of RNA sequences, it is not practical for large-scale diagnosis of fasciolosis. RT-qPCR represents a more suitable method for determining the differential expression of miRNAs in simultaneous samples of sheep sera. On this basis, a series of qPCR primers specific to each of the selected miRNA sequences was designed. To first test the ability of these primers to specifically detect the candidate diagnostic miRNAs, lamb tissue was employed as a positive test sample for evaluating the performance of sheep miRNA specific primers, while RNA isolated from *F. hepatica* NEJ was used as the positive control to assess the efficacy of primers designed to detect the liver fluke miRNAs. This life cycle stage (NEJ) of the parasite was selected because fhe-Novel-11-5p is reportedly only expressed in NEJ and not in the juvenile or adult worms (both liver stages), while fhe-miR-124-3p is present throughout all intra-mammalian life cycle stages with the highest expression in the NEJ[45]. Based on the results from these RT-qPCR tests, oar-miR-1197-3p was excluded from further analysis due to its low copy number and late Cq (~ 33) in lamb tissue, with undetectable levels in non-infected sheep sera (Supplemental Table 4). According to the sequencing data, the expression level of this miRNA was expected to decrease during the hepatic phase of infection (Fig. 3).

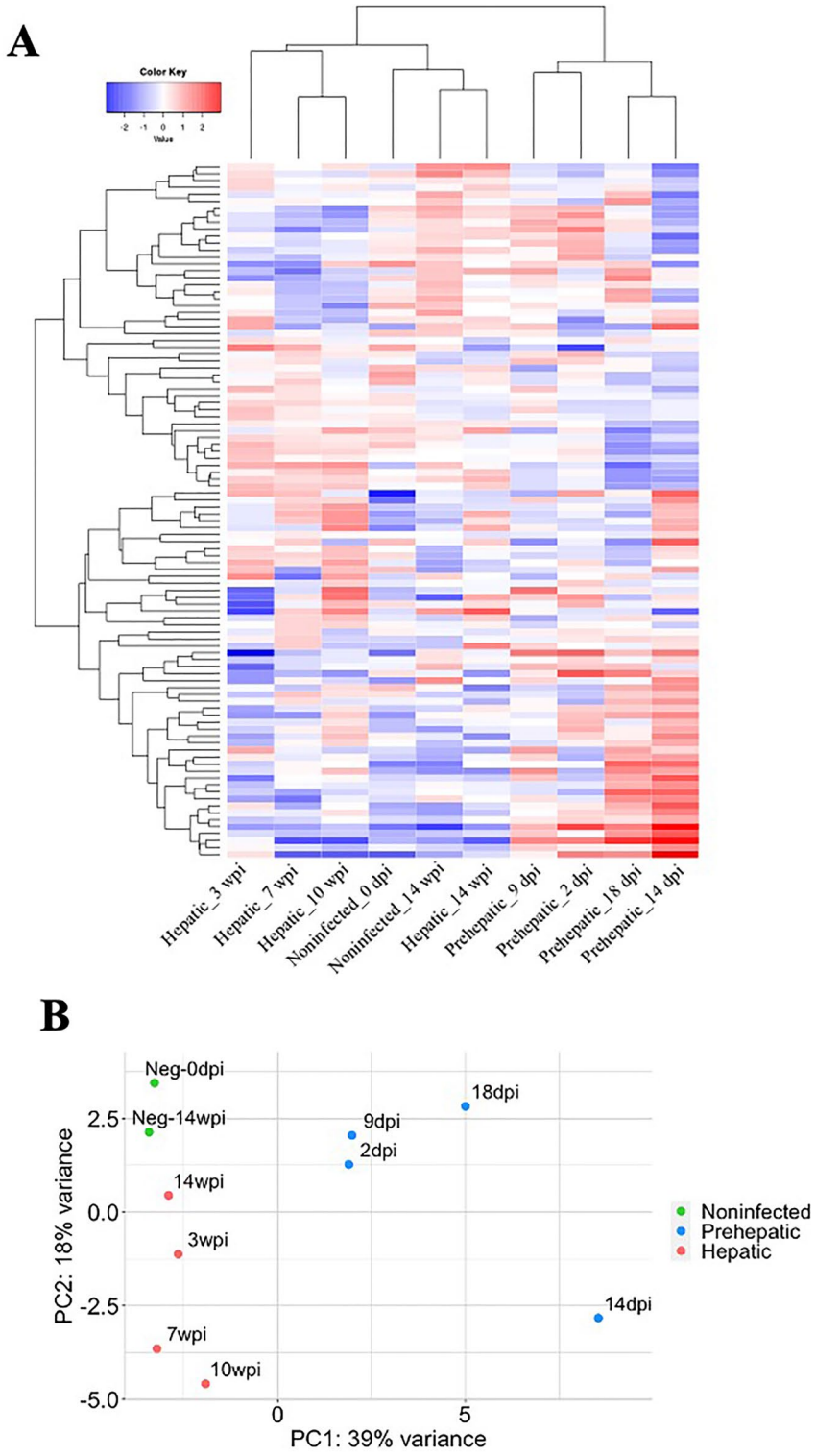


Figure 1. Differential abundance of sheep miRNAs in sera during *Fasciola hepatica* infection. (**A**) Heatmap of relative abundance of sheep miRNAs (CPM) in non-infected sheep (0 day-Neg, 14 week-Neg), early/pre-hepatic infection (2 days post infection (dpi), 9 dpi, 14 dpi, 18 dpi), and late/hepatic infection (3 weeks post infection (wpi), 7 wpi, 10 wpi, 14 wpi). The heatmap was created using idep.96[59], miRNAs were ranked by their standard deviation across all samples and hierarchical clustering carried out for the top 100 miRNAs . Expression of miRNAs represented as high (red) or low (blue) relative to total expression of miRNA across infection groups. (**B**) Principal component analysis (PCA) plot of total sheep miRNA abundance in non-infected sheep (green), pre-hepatic infection (2–18 days post infection) (blue), and hepatic infection (3–14 weeks post infection) (red).

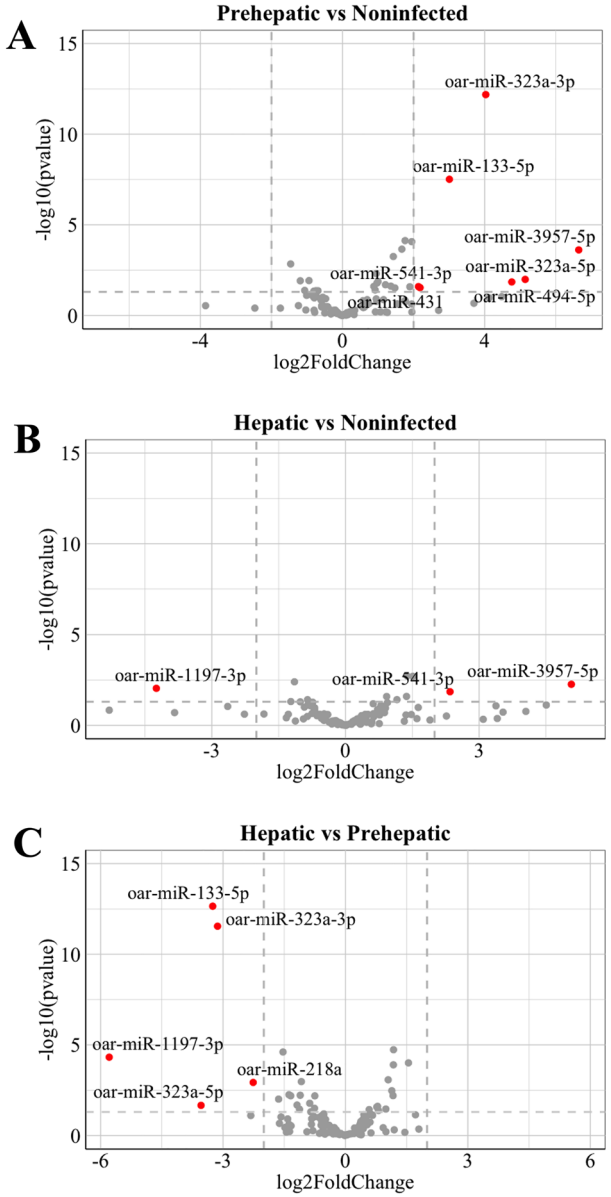


Figure 2. Circulating host-miRNA profiles are distinct during early and late *F. hepatica* infection compared to non-infected animals. Volcano plots show differential expression of sheep miRNAs using DESeq2 in (**A**) pre-hepatic infection compared to non-infected sera samples, (**B**) hepatic infection vs non-infected sera samples, and (**C**) hepatic infection vs pre-hepatic infection. Genes that are more than ± log2 fold change 2 (FC) with significant *p* value (< 0.05) are denoted in red.

	Non-infected		Pre-hepatic				Hepatic			
miRNA	Neg-0 dpi	Neg-14 wpi	2 dpi	9 dpi	14 dpi	18 dpi	3 wpi	7 wpi	10 wpi	14 wpi
fhe-miR-124-3p	0	0	59	32	44	28	0	0	0	0
fhe-Novel-11-5p	0	0	7	0	0	3	13	12	6	0
fhe-Novel-102-3p	0	0	0	0	0	0	0	13	9	0
fhe-miR-277a-3p	0	0	0	0	0	0	0	8	5	7
fhe-miR-750-3p	0	0	0	0	0	0	0	5	0	4
fhe-miR-71a-5p	0	0	0	8	0	0	0	0	0	0

Table 3. Total read counts of *Fasciola hepatica* miRNAs detected within sheep sera samples. (n = 6 sheep sera pooled/ time point); *dpi* Days post-infection, *wpi* Weeks post-infection, *Neg-0 dpi* Pre-infection timepoint, *Neg-14 wpi* 14 Weeks age-matched non-infected control.

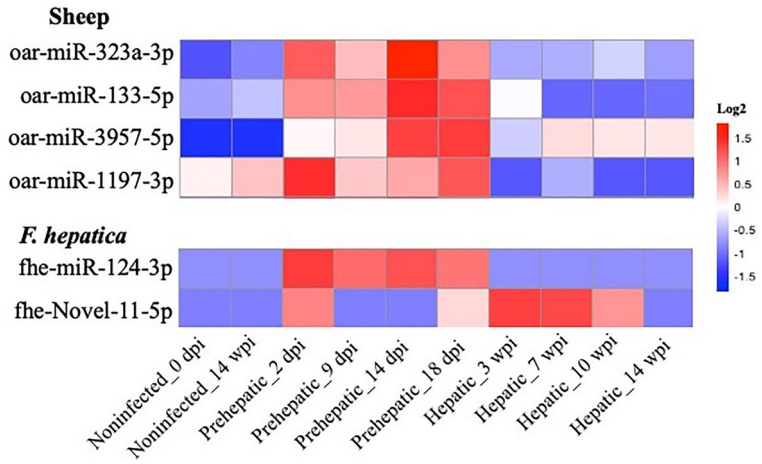


Figure 3. Selection of host and *F. hepatica* miRNAs as biomarkers for pre-hepatic and hepatic stages of fasciolosis. Relative abundance of selected sheep and parasite miRNAs in uninfected animals (0 dpi-neg, 14 wpi-neg), pre-hepatic infection (2 dpi, 9 dpi, 14 dpi, 18 dpi), and hepatic infection (3 wpi, 7 wpi, 10 wpi, 14 wpi), represented as high (red) or low (blue) normalised read counts. *dpi* Days post infection, *wpi* Weeks post infection.

However, as it was not amplified in the test sera sample from non-infected sheep, a further decrease following the progression of *F. hepatica* infection would be impossible to detect by qPCR, thus negating its potential as a biomarker for hepatic infection.

In contrast, the Cq value of oar-miR-133-5p, oar-miR-323a-3p, and oar-miR-3957-5p were within an acceptable diagnostic range (Supplemental Table 4), making them suitable for further analysis. In addition, the amplification of products from the Set A and B sera samples using these primers validated the sequencing data, as the pattern of expression was consistent with the distribution of read counts within the sequencing data. This RT-qPCR analysis verified that both oar-miR-133-5p and oar-miR-323a-3p were only present in the pre-hepatic set of samples whereas oar-miR-3957-5p was detected in samples from both the pre-hepatic and hepatic stages of infection (Supplemental Fig. 1).

Of the *F. hepatica* miRNAs, fhe-miR-124-3p and fhe-Novel-11-5p primers unexpectedly amplified products in both NEJ and lamb tissue (Supplemental Figs. 2A, 3A). Also, the primers designed to detect fhe-miR-124-3p produced extremely late, or no Cq, when tested further on the RNA samples from the sera from infected sheep that had been sequenced (Sets A and B; Supplemental Fig. 2B). Given these inconsistencies with the results from the test RT-qPCR in comparison to the sequencing data, a more in-depth analysis of the sequencing data for these two miRNA sequences was conducted.

This analysis revealed that the full-length canonical sequence of fhe-Novel-11-5p was not present within the sequencing reads, but a shorter variant (isomiR) missing four nucleotides at the 3′ end was identified instead. Furthermore, by aligning this shorter sequence to the known sheep sequences using BLASTN (filtering for *Ovis aries*, txid:9940) revealed that the fhe-Novel-11-5p sequence fully aligned with sheep ribosomal RNA (Supplemental Fig. 3B), which provides an explanation for the detection of fhe-Novel-11-5p in lamb tissue. In addition, as ribosomal RNAs are part (10%) of the extracellular RNA population found in sera due to cellular turnover or secretion of microvesicles as a consequence of tissue injury[60], it is likely that the detection of this sequence in the sera of infected sheep, but not uninfected sheep, reflects the host response to infection with Fasciola, or the tissue damage caused by the migrating parasite.

However, due to the uncertainty of whether this result is unique to *F. hepatica* and thus indicative of infection, fhe-Novel-11-5p was omitted from subsequent analyses.

While the canonical sequence for fhe-miR-124-3p was not present in the sequencing reads from the sheep sera samples, this miRNA was found to be present as several sequence variants (isomiRs), missing nucleotides primarily at the 3′ end and to a lesser extent at the 5′ end (Fig. 4A). Furthermore, the sequence of the canonical fhe-miR-124-3p was similar to cattle bta-miR-124-3p (Supplemental Fig. 4A), with only three nucleotides mismatched at the 3′ end, suggesting that the corresponding sheep oar-miR-124-3p was likely missing from miRbase, and was thus not filtered from the sequencing reads during our initial analysis.

Consequently, a 100% sequence identity of the bta-miR-124-3p precursor sequence to the non-coding region of sheep RNA confirmed the presence of oar-miR-124-3p and that oar-miR-124-3p is identical to bta-miR-124-3p (Supplemental Fig. 4B). Accordingly, the shorter two most dominant sequence variants of fhe-miR-124-3p found in infected sheep sera matched 100% with both sheep and *F. hepatica* miR-124-3p (Fig. 4A). Therefore, it is impossible to determine whether the sequencing reads for the miR-124-3p variant that are increased during *F. hepatica* infection originated from sheep, parasite, or both. Nonetheless, the differential abundance of this miRNA classified it as a suitable candidate as a potential biomarker of infection and, thus, a primer was designed for the most dominant 3′ trimmed variant of miR-124-3p. This primer effectively distinguished the pre-hepatic stage of

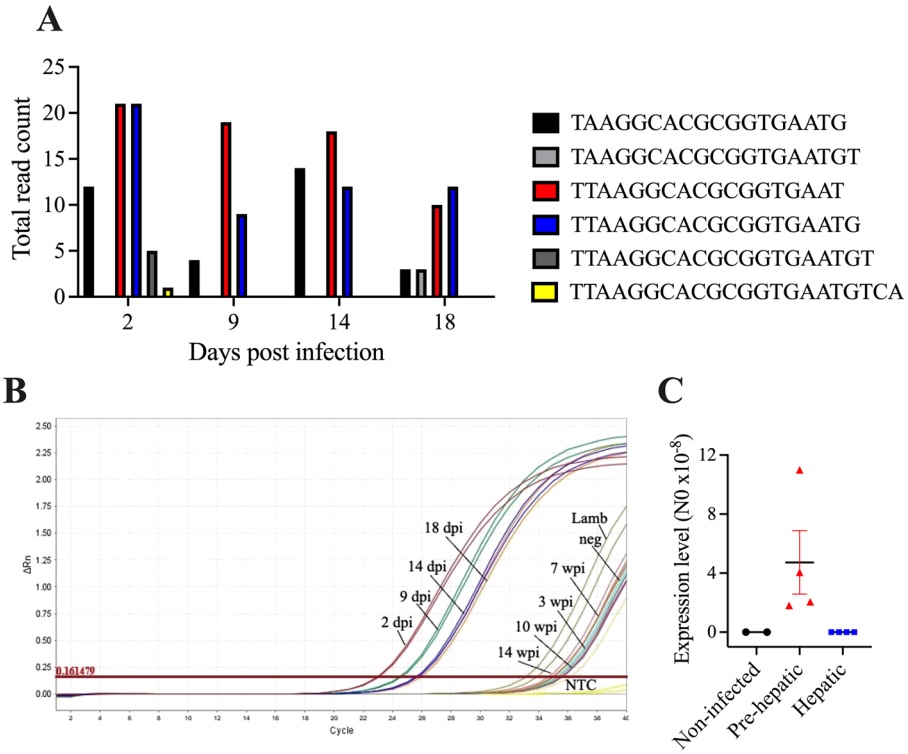


Figure 4. *F. hepatica* miR-124-3p was present as several sequence variants (isomiR) in sera of infected sheep. (**A**) Total read counts of the miR-124 isomiRs present at the different time-points of infection in Set A and Set B sera. The canonical sequence is shown in yellow. The sequence of the most dominant isomiR (red bar) was used for qPCR primer design. (**B**) RT-qPCR amplification plot from primer test of the most dominant fhe-miR-124 isomiR in Set A and Set B sheep sera samples. *dpi* Days post infection, *wpi* Weeks post infection, *neg* Non-infected controls, *NTC* No template control and lamb tissue. (**C**) RT-qPCR quantification of the dominant fhe-miR-124-3p isomiR presented as the starting quantity of genetic material prior to amplification (N0) as determined by LinRegPCR (v.11) This is calculated in the unit of the Y-axis of the PCR amplification plot, which are arbitrary fluorescence units. The average N0 value of two technical replicates are shown for each time point.

infection (Cq < 26) from both the hepatic stage and non-infected (Cq > 33) sheep using the Set A and B sequenced sera samples, an outcome that was consistent with the read counts from the sequencing data (Fig. 4B,C; Table 3).

Based on these analyses, the miRNA biomarker panel for qPCR validation was refined to include four miRNAs: oar-miR-133-5p, oar-miR-323a-3p, oar-miR-3957-5p, and fhe/oar-miR-124-3p.

Circulating oar-miR-133-5p and oar-miR-3957-5p can diagnose fasciolosis from as early as 7 days post-infection

To confirm the diagnostic potential of the selected miRNAs, RT-qPCR validation was performed on an independent archived set of sera samples harvested from individual sheep during two longitudinal infection studies; a pre-hepatic infection cohort comprised of sera collected at 0 (pre-infection), 7, and 14 days post-infection (Set C), a hepatic infection cohort with samples collected at week 3, 15, 20 and 23 post-infection (Set D), and age-matched non-infected animals for each of the timepoints.

From this analysis, the expression levels of both oar-miR-323a-3p and fhe/oar-miR-124-3p was almost identical in the sera from non-infected and infected sheep over the course of infection (Fig. 5A,B), suggesting that these miRNAs cannot be used as indicators of fasciolosis. It is possible that this discrepancy between this RT-qPCR analysis and the sequencing data reflects the difference in sample preparation, with the sequencing performed on a pooled sample of sera from a cohort of six sheep. The variability in the expression of miRNAs across sheep samples is evident when sera from individual sheep was assessed by RT-qPCR, which in a pooled sample would create an incorrect representation of expression levels within individual samples. Furthermore, through the inclusion of age-matched non-infected sheep, it is apparent that the expression of miRNAs can change over time, irrespective of whether the animal is infected (Fig. 5). As the sample collection that was originally sequenced lacked a full panel of age-matched controls, this alteration in expression was not fully captured, and the apparent differential abundance of miRNAs associated with infection within the sequencing data, may have simply been a variation due to age.

Consistent with the sequencing data, the RT-qPCR analysis revealed that the expression of both oar-miR-133-5p and oar-miR-3957-5p was elevated in the sera of infected animals compared to age-matched non-infected animals (Fig. 6A,C). Furthermore, as these were longitudinal studies, the miRNA expression level in individual

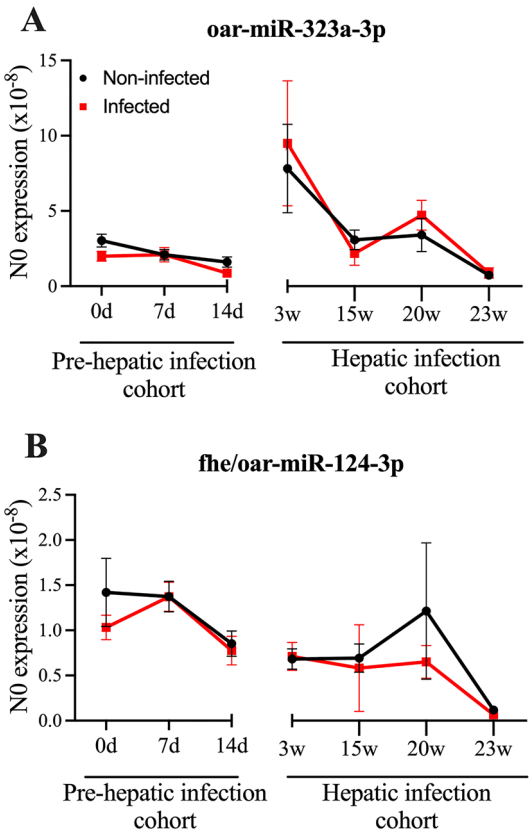


Figure 5. RT-qPCR assessment of sera samples invalidates the diagnostic potential of oar-miR-323a-3p and fhe-miR-124-3p. The expression of (**A**) oar-miR-323a-3p, (**B**) fhe-miR-124-3p were determined by RT-qPCR and are presented as the starting quantity of genetic material prior to amplification (N0) as determined by LinRegPCR (v.11). This is calculated in the unit of the Y-axis of the PCR amplification plot, which are arbitrary fluorescence units. The data is presented as the mean ± SEM (n = 3–14; as shown in Table 1). The statistical significance of differences between infected and non-infected samples was determined using Welch's t-test (two-tailed).

sheep in the pre-hepatic infection cohort could be tracked over time. As such, the fold change at 7 and 14 days compared to day 0 for each animal was examined. This approach revealed that the expression levels of both oar-miR-133-5p and oar-miR-3957-5p were significantly elevated in the infected animals at day 7 and 14 from day 0, but not in the non-infected animals (Fig. 6B,D). Early elevation in the levels of these two miRNAs was consistent with the sequencing data, whereby an upregulation in miRNA expression was seen from 2 dpi (Fig. 3). The sera samples representing the hepatic stage of infection were harvested from a separate infection cohort to the earlier time points, so could not be tracked in individual sheep from day 0.

Nonetheless, corroborating the sequencing data, the level of expression of oar-miR-133-5p in the sera of infected animals, other than a single peak at 20 wpi, was reduced as infection progressed, as compared to the earlier time points (Fig. 6A). In addition, validating the sequencing data, the increase in oar-miR-3957-5p in sera from infected sheep was generally sustained throughout the entire observation period, with a lower expression level compared to the pre-hepatic phase of infection (Fig. 6C).

In conclusion, these data indicate that both oar-miR-133-5p and oar-miR-3957-5p are biomarkers of early, pre-hepatic infection. In addition, the difference in expression of oar-miR-3957-5p between infected and non-infected sheep over the entire observation period suggests that this may represent an unchanging marker of infection, which, in the absence of an increase in oar-miR-133-5p, would indicate late stage/hepatic phase of infection.

Discussion

The severe impact of fasciolosis on animal welfare and the significant economic cost it imposes on the livestock industry highlights the need for a reliable and robust biomarker that can effectively guide anthelmintic treatment and facilitate the management and control of liver fluke on farms[17]. The development of an accurate diagnostic method for acute infection is of paramount importance since such a tool would enable timely intervention to prevent liver flukes from inflicting liver pathology, which would mitigate the risk of sudden fatalities associated with a high liver fluke burden (in approximately 10% of infected sheep) and disrupt the liver fluke lifecycle by preventing the parasite from reaching the bile duct to lay eggs, which in turn, would curb the spread of the infection within grazing pastures.

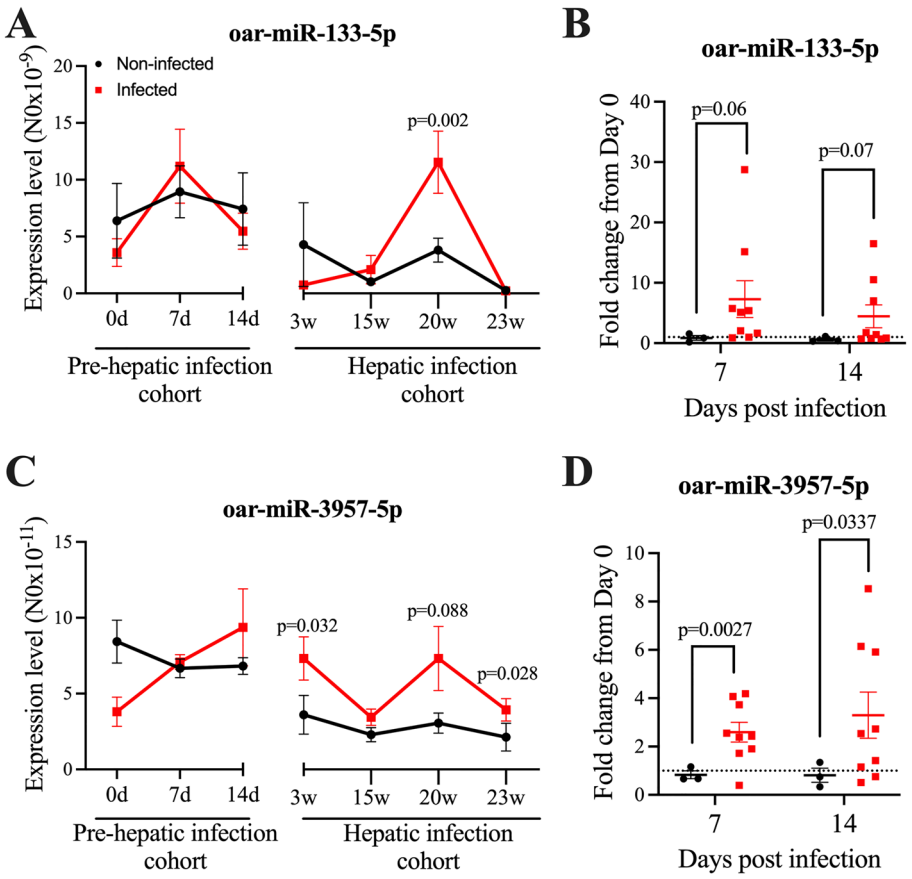


Figure 6. RT-qPCR demonstrates the differential expression of oar-miR-133-5p and oar-miR-3957-5p in sera from infected sheep as compared to uninfected animals. Quantification of (**A**) oar-miR-133-5p and (**C**) oar-miR-3957-5p in the sera of individual sheep in response to infection was determined by RT-qPCR and is represented as the starting quantity of genetic material prior to amplification (N0) as determined by LinRegPCR (v.11). This is calculated in the unit of the Y-axis of the PCR amplification plot, which are arbitrary fluorescence units. The data is presented as the mean ± SEM (n = 3–14; as shown in Table 1). (**B**) Fold change of oar-miR-133-5p and (**D**) oar-miR-3957 expression at 7 or 14 dpi in comparison to 0 dpi in the sera of individual sheep in the pre-hepatic cohort. The data is presented as the mean ± SEM (n = 3 non-infected; 9 infected sheep for which data was available at all three timepoints). In all cases the statistical significance of differences between sera from infected versus uninfected sheep was determined using Welch's t-test (two-tailed).

Given this need, exploiting the differential abundance of circulating miRNAs as a biomarker of infection represents an attractive diagnostic tool. Circulating miRNAs exhibit exceptional stability, rendering them a highly suitable choice for diagnostic purposes, particularly in the setting of a farm where controlling sample collection and storage can be challenging. For this reason, miRNAs have gained significant attention for their diagnostic potential in a range of pathogenic infections, and due to their immediate alteration in expression in response to infection they are appropriate markers for the detection of early infections[39].

In this study, we assessed the utility of miRNAs in detecting both pre-hepatic and hepatic fasciolosis using sera samples collected from sheep with experimental subclinical disease. The results provide the first evidence that unique miRNA expression signatures in ruminant sera are associated with the distinct pathological stages of fasciolosis. The data supports the hypothesis that differentially expressed miRNAs can serve as prognostic markers for fasciolosis and, moreover, demonstrates that unique miRNA expression patterns emerged as early as 2 days post-infection. Therefore, miRNAs could offer superior sensitivity in fasciolosis diagnosis compared to conventional, commercial methods, such as FEC and serological ELISAs.

The analysis of sera samples from age-matched infected and non-infected sheep in the RT-qPCR validation demonstrated the paramount importance of incorporating age-matched samples in any screening protocol aimed at characterising miRNAs as diagnostic biomarkers. As demonstrated in this study, the differential expression of miRNAs quantified using RT-qPCR exhibited significant age-related variability. Specifically, the expression of oar-miR-323a-3p, which we initially described as a potential biomarker from sequencing data (without appropriate age-matched samples), was subsequently discovered using RT-qPCR to vary significantly over time in non-infected sheep, with relatively higher expression as the animals aged.

Despite encountering challenges with variations in miRNA expression levels due to age, our longitudinal approach of assessing miRNA expression in individual animals over time successfully addressed these issues.

Our findings indicate that the expression of certain miRNAs in sheep increased in response to infection, irrespective of the animal's age. Given this observation, we would recommend that for any miRNA-based diagnostics studies, it may be necessary to collect serum samples from animals at their initial exposure to pasture to set a benchmark for each animal's miRNA expression. Future serum samples can then be compared to this baseline to accurately assess the onset and progress of infection. This approach could also be effectively adapted to sentinel screening practices for monitoring liver fluke prevalence over a grazing season, as we have employed with serological tests[61,62].

While the potential of using miRNA detection to support the diagnosis of fasciolosis has been established in this study, further evaluation is required to ensure specificity. For example, circulating oar-miR-3957-5p has been reported to be elevated in high stress responding female sheep when challenged with bacterial LPS[63,64] suggesting that this miRNA could be upregulated in response to other broad infections. Furthermore, the sheep in our study were all male; the possibility that any differential expression in miRNAs is sex-related would need to be considered. In addition, miR-133-5p was reportedly upregulated in early bacterial infection in a marine lancelet species (*Branchiostoma belcheri*)[65], and in the plasma of chronic obstructive pulmonary disease patients, and tumour cells of various cancers, including gastric and colon cancer[66,67]. Hence, while oar-miR-133-5p and oar-miR-3957 are indicated as promising biomarkers for fasciolosis, their specificity to fasciolosis must be further explored.

To address the issue of specificity in another way, the results of differential expression of host miRNAs could be amalgamated with the detection of liver fluke miRNAs. Liver fluke miRNAs are likely deliberately secreted by the parasite to manipulate the host's immune response or are passively released from dying parasites. While several helminth studies have demonstrated the presence of parasite-derived miRNAs in host circulation[42,43,68], this is the first study to demonstrate the presence of *F. hepatica* derived miRNAs in infected host circulation (importantly that of a ruminant). Furthermore, the temporal expression of the liver fluke-derived miRNAs correlated with their expression pattern that we previously reported over the course of the intra-mammalian stages of development[45]. For instance, fhe-miR-124-3p and fhe-miR-71a-5p, both of which were found to be most abundant in NEJ, were detected in sheep sera at the pre-hepatic stage of infection. On the other hand, fhe-miR750-3p and fhe-Novel-102-3p, both most highly expressed by adult worms, were detected at the hepatic stage of infection. Notwithstanding that many parasite-derived miRNAs are present at very low copy numbers, it remains to be determined whether they could be amplified to detectable levels of RT-qPCR.

We also discovered that several helminth miRNAs are highly conserved and, therefore, have sequences that are nearly identical to their mammalian hosts. In this study, *F. hepatica*-derived miRNAs in sheep sera were detected using a rigorous filtering process in the analysis of sequencing reads; only reads that did not align with the sheep mature miRNAs from miRBase were aligned to *F. hepatica* miRNAs, allowing zero mismatches, to eliminate any false identification of sheep miRNAs as parasite miRNAs. Furthermore, the presence of the parasite-miRNAs in sera samples from infected sheep but not in the non-infected samples provided confidence that these miRNAs exclusively originated from the parasite. However, further investigation revealed that two of the identified liver fluke miRNAs, namely fhe-miR-124-3p and fhe-Novel-11-5p, were present as trimmed isomiRs in the sheep sera, that were also conserved with sheep sequences. While previous studies have reported the presence of helminth-derived miRNAs in host circulation[42,43,68], the existence of such sequence variants has not yet been documented. This unique discovery raises important new considerations regarding the interpretation of sequencing data for the discovery of helminth (or pathogen)-derived miRNAs such as miR-124-3p.

In summary, our research has characterised the differential abundance of parasite and host serum miRNAs during infection with *F. hepatica* in a ruminant host. Two miRNA biomarkers with diagnostic potential for fasciolosis were identified following a stringent selection process. Lowering the threshold of selection from sequencing data to a twofold change in expression could reveal additional miRNA targets and provides an opportunity to expand the available miRNA biomarker panel. The data presented here has established the suitability of developing the measurement of sheep miRNA expression into a diagnostic tool for fasciolosis, potentially through a PCR blood test. Achieving this potential will require extensive field studies to determine the precise sensitivity and specificity of this method. While our current findings are based on controlled experimental infections of sheep, the ultimate goal will be to test the effectiveness of these miRNA biomarkers in naturally infected animals. Such real-world conditions present a more complex scenario for diagnosis due to varying worm burdens, infection dynamics, overlapping temporal infections, and the potential for co-infections (liver fluke and other pathogens). Importantly, validation of these miRNA biomarkers in the field could lead to their use in point-of-care technologies at the farming level. This would be particularly beneficial in environments where access to technical expertise and resources is limited, offering a practical and user-friendly method for detecting fasciolosis in the field.

Data availability

The RNA sequencing data have been deposited in NCBI's Gene Expression Omnibus and are accessible through GEO Series accession number GSE254115. All other data is available from the corresponding author on reasonable request.

Received: 26 January 2024; Accepted: 21 March 2024
Published online: 28 March 2024

References

1. Fürst, T., Keiser, J. & Utzinger, J. Global burden of human food-borne trematodiasis: A systematic review and meta-analysis. *Lancet. Infect. Dis* **12**(3), 210–221 (2012).
2. Mas-Coma, S. Epidemiology of fascioliasis in human endemic areas. *J. Helminthol.* **79**(3), 207–216. https://doi.org/10.1079/JOH2005296 (2005).

3. WHO. *Foodborne Parasitic Infections: Fascioliasis (Liver Fluke)*. World Health Organization. https://www.who.int/publications/i/item/WHO-UCN-NTD-VVE-2021.4 (2021).
4. Mas-Coma, S., Valero, M. A. & Bargues, M. D. Climate change effects on trematodiases, with emphasis on zoonotic fascioliasis and schistosomiasis. *Vet. Parasitol.* **163**(4), 264–280. https://doi.org/10.1016/j.vetpar.2009.03.024 (2009).
5. Polley, L. & Thompson, R. A. Parasite zoonoses and climate change: Molecular tools for tracking shifting boundaries. *Trends Parasitol.* **25**(6), 285–291 (2009).
6. Robinson, M. W. & Dalton, J. P. Zoonotic helminth infections with particular emphasis on fasciolosis and other trematodiases. *Philos. Trans. R. Soc. Lond. B Biol. Sci.* **364**(1530), 2763–2776. https://doi.org/10.1098/rstb.2009.0089 (2009).
7. Charlier, J. *et al.* Initial assessment of the economic burden of major parasitic helminth infections to the ruminant livestock industry in Europe. *Prev. Vet. Med.* **182**, 105103. https://doi.org/10.1016/j.prevetmed.2020.105103 (2020).
8. Howell, A. K. & Williams, D. J. The epidemiology and control of liver flukes in cattle and sheep. *Vet. Clin. Food Anim. Pract.* **36**(1), 109–123 (2020).
9. Andrews, S. J., Cwicklinski, K. C. & Dalton, J. P. The discovery of *Fasciola hepatica* and its life cycle. In *Fasciolosis* (ed. Dalton, J. P.) 1–22 (CABI, 2021).
10. Dixon, K. E. The physiology of excystment of the metacercaria of *Fasciola hepatica* L. *Parasitology* **56**(3), 431–456. https://doi.org/10.1017/s0031182000068931 (1966).
11. Robinson, M. W., Hanna, R. E. & Fairweather, I. Development of *Fasciola hepatica* in the mammalian host. In *Fasciolosis* (ed. Dalton, J. P.) 65–111 (CABI, 2021).
12. Dawes, B. & Hughes, D. Fascioliasis: The invasive stages of *Fasciola hepatica* in mammalian hosts. *Adv. Parasitol.* **2**, 97–168 (1964).
13. Dow, C., Ross, J. & Todd, J. The pathology of experimental fascioliasis in calves. *J. Comp. Pathol.* **77**(4), 377–385 (1967).
14. Martinez-Moreno, A. *et al.* Liver pathology and immune response in experimental *Fasciola hepatica* infections of goats. *Vet. Parasitol.* **82**(1), 19–33. https://doi.org/10.1016/S0304-4017(98)00262-3 (1999).
15. Happich, F. & Boray, J. Quantitative diagnosis of chronic fasciolosis. 2. The estimation of daily total egg production of *Fasciola hepatica* and the number of adult flukes in sheep by faecal egg counts. *Aust. Vet. J.* **45**(7), 329–331 (1969).
16. Sabatini, G. A. *et al.* Practical guide to the diagnostics of ruminant gastrointestinal nematodes, liver fluke and lungworm infection: Interpretation and usability of results. *Parasites Vectors* **16**(1), 58 (2023).
17. Stuen, S. & Ersdal, C. Fasciolosis—An increasing challenge in the sheep industry. *Animals* **12**(12), 1491 (2022).
18. Mazeri, S., Sargison, N., Kelly, R. F., Bronsvoort, B. M. & Handel, I. Evaluation of the performance of five diagnostic tests for *Fasciola hepatica* infection in naturally infected cattle using a bayesian no gold standard approach. *PLoS One* **11**(8), e0161621. https://doi.org/10.1371/journal.pone.0161621 (2016).
19. Taylor, M. A., Coop, R. L. & Wall, R. L. *Veterinary Parasitology* (Wiley, 2015).
20. Mazeri, S., Rydevik, G., Handel, I., Bronsvoort, B. M. D. & Sargison, N. Estimation of the impact of *Fasciola hepatica* infection on time taken for UK beef cattle to reach slaughter weight. *Sci. Rep.* **7**(1), 7319. https://doi.org/10.1038/s41598-017-07396-1 (2017).
21. Braun, U., Wolfensberger, R. & Hertzberg, H. Diagnosis of liver flukes in cows–a comparison of the findings in the liver, in the feces, and in the bile. *Schweizer Archiv. fur Tierheilkunde* **137**(9), 438–444 (1995).
22. Charlier, J., De Meulemeester, L., Claerebout, E., Williams, D. & Vercruysse, J. Qualitative and quantitative evaluation of coprological and serological techniques for the diagnosis of fasciolosis in cattle. *Vet. Parasitol.* **153**(1–2), 44–51 (2008).
23. Novobilský, A., Averpil, H. B. & Höglund, J. The field evaluation of albendazole and triclabendazole efficacy against *Fasciola hepatica* by coproantigen ELISA in naturally infected sheep. *Vet. Parasitol.* **190**(1), 272–276. https://doi.org/10.1016/j.vetpar.2012.06.022 (2012).
24. Sánchez-Andrade, R. *et al.* Use of a sandwich-enzyme-linked immunosorbent assay (SEA) for the diagnosis of natural *Fasciola hepatica* infection in cattle from Galicia (NW Spain). *Vet. Parasitol.* **93**(1), 39–46. https://doi.org/10.1016/S0304-4017(00)00326-5 (2000).
25. Brockwell, Y., Spithill, T., Anderson, G., Grillo, V. & Sangster, N. Comparative kinetics of serological and coproantigen ELISA and faecal egg count in cattle experimentally infected with *Fasciola hepatica* and following treatment with triclabendazole. *Vet. Parasitol.* **196**(3–4), 417–426 (2013).
26. Novobilský, A. *et al.* Transmission patterns of *Fasciola hepatica* to ruminants in Sweden. *Vet. Parasitol.* **203**(3), 276–286. https://doi.org/10.1016/j.vetpar.2014.04.015 (2014).
27. Cornelissen, J. B. W. J., Gaasenbeek, C. P. H., Boersma, W., Borgsteede, F. H. M. & van Milligen, F. J. Use of a pre-selected epitope of cathepsin-L1 in a highly specific peptide-based immunoassay for the diagnosis of *Fasciola hepatica* infections in cattle. *Int. J. Parasitol.* **29**(5), 685–696. https://doi.org/10.1016/S0020-7519(99)00017-X (1999).
28. Costa, M. *et al.* Liver function markers and haematological dynamics during acute and chronic phases of experimental *Fasciola hepatica* infection in cattle treated with triclabendazole. *Exp. Parasitol.* **238**, 108285. https://doi.org/10.1016/j.exppara.2022.108285 (2022).
29. Molina-Hernández, V. *et al. Fasciola hepatica* vaccine: We may not be there yet but we're on the right road. *Vet. Parasitol.* **208**(1–2), 101–111 (2015).
30. Boray, J. *et al.* Treatment of immature and mature *Fasciola hepatica* infections in sheep with triclabendazole. *Vet. Rec.* **113**(14), 315–317 (1983).
31. Kelley, J. M., Rawlin, G., Beddoe, T., Stevenson, M. & Spithill, T. W. Fasciola hepatica control practices on a sample of dairy farms in Victoria, Australia. *Front. Vet. Sci.* **8**, 669117 (2021).
32. McMahon, C. *et al.* Liver fluke control on sheep farms in Northern Ireland: A survey of changing management practices in relation to disease prevalence and perceived triclabendazole resistance. *Vet. Parasitol.* **216**, 72–83. https://doi.org/10.1016/j.vetpar.2015.11.018 (2016).
33. COWS. Control of worms sustainabily. Promoting the sustainable control of cattle parasites. https://www.cattleparasites.org.uk (2023).
34. Hanna, R. E. *et al.* Fasciola hepatica: A comparative survey of adult fluke resistance to triclabendazole, nitroxynil and closantel on selected upland and lowland sheep farms in Northern Ireland using faecal egg counting, coproantigen ELISA testing and fluke histology. *Vet. Parasitol.* **207**(1–2), 34–43. https://doi.org/10.1016/j.vetpar.2014.11.016 (2015).
35. Moll, L., Gaasenbeek, C. P., Vellema, P. & Borgsteede, F. H. Resistance of *Fasciola hepatica* against triclabendazole in cattle and sheep in The Netherlands. *Vet. Parasitol.* **91**(1–2), 153–158 (2000).
36. Novobilský, A. & Höglund, J. First report of closantel treatment failure against *Fasciola hepatica* in cattle. *Int. J. Parasitol. Drugs Drug Resist.* **5**(3), 172–177 (2015).
37. SCOPS. The principles of sustainable control of parasites. https://www.scops.org.uk (2023).
38. Ambros, V. The functions of animal microRNAs. *Nature* **431**(7006), 350–355 (2004).
39. Tribolet, L. *et al.* MicroRNA biomarkers for infectious diseases: From basic research to biosensing. *Front. Microbiol.* **11**, 1197 (2020).
40. Blondal, T. *et al.* Assessing sample and miRNA profile quality in serum and plasma or other biofluids. *Methods* **59**(1), S1–S6 (2013).
41. Ghalehnoei, H., Bagheri, A., Fakhar, M. & Mishan, M. A. Circulatory microRNAs: Promising non-invasive prognostic and diagnostic biomarkers for parasitic infections. *Eur. J. Clin. Microbiol. Infect. Dis.* **39**, 395–402 (2020).
42. Guo, X. & Guo, A. Profiling circulating microRNAs in serum of *Fasciola gigantica*-infected buffalo. *Mol. Biochem. Parasitol.* **232**, 111201 (2019).

43. Hoy, A. M. *et al.* Parasite-derived microRNAs in host serum as novel biomarkers of helminth infection. *PLoS Negl. Trop. Dis.* **8**(2), e2701 (2014).
44. Mu, Y., McManus, D. P., Gordon, C. A. & Cai, P. Parasitic helminth-derived microRNAs and extracellular vesicle cargos as biomarkers for helminthic infections. *Front. Cell. Infect. Microbiol.* **11**, 708952 (2021).
45. Ricafrente, A. *et al.* Stage-specific miRNAs regulate gene expression associated with growth, development and parasite-host interaction during the intra-mammalian migration of the zoonotic helminth parasite *Fasciola hepatica*. *BMC Genomics* **23**(1), 1–19 (2022).
46. Tran, N. *et al.* Fasciola hepatica hijacks host macrophage miRNA machinery to modulate early innate immune responses. *Sci. Rep.* **11**(1), 6712 (2021).
47. Corrales, J. L. *et al.* Diagnosis of sheep fasciolosis caused by *Fasciola hepatica* using cathepsin L enzyme-linked immunosorbent assays (ELISA). *Vet. Parasitol.* **298**, 109517 (2021).
48. El-Khoury, V., Pierson, S., Kaoma, T., Bernardin, F. & Berchem, G. Assessing cellular and circulating miRNA recovery: The impact of the RNA isolation method and the quantity of input material. *Sci. Rep.* **6**(1), 19529 (2016).
49. Cwiklinski, K. *et al.* Infection by the helminth parasite *Fasciola hepatica* requires rapid regulation of metabolic, virulence, and invasive factors to adjust to its mammalian host. *Mol. Cell Proteomics* **17**(4), 792–809 (2018).
50. Andrews, S. FastQC: A quality control tool for high throughput sequence data. In *Babraham Bioinformatics*. Babraham Institute (2010).
51. Martin, M. Cutadapt removes adapter sequences from high-throughput sequencing reads. *EMBnet J.* **17**(1), 10–12 (2011).
52. Langmead, B. Aligning short sequencing reads with Bowtie. *Curr. Protoc. Bioinform.* **32**(1), 11–17 (2010).
53. Fontenla, S. *et al.* Role of *Fasciola hepatica* small RNAs in the interaction with the mammalian host. *Front. Cell. Infect. Microbiol.* **11**, 812141 (2022).
54. Herron, C. M. *et al.* Developmental regulation and functional prediction of microRNAs in an expanded Fasciola hepatica miRNome. *Front. Cell. Infect. Microbiol.* **12**, 56 (2022).
55. Ricafrente, A., Nguyen, H., Tran, N. & Donnelly, S. An evaluation of the *Fasciola hepatica* miRnome predicts a targeted regulation of mammalian innate immune responses. *Front. Immunol.* **11**, 608686 (2021).
56. Li, H. *et al.* The sequence alignment/map format and SAMtools. *Bioinformatics* **25**(16), 2078–2079. https://doi.org/10.1093/bioinformatics/btp352 (2009).
57. Love, M., Anders, S. & Huber, W. Differential analysis of count data—The DESeq2 package. *Genome Biol.* **15**(550), 10–1186 (2014).
58. Ruijter, J. *et al.* Amplification efficiency: Linking baseline and bias in the analysis of quantitative PCR data. *Nucleic Acids Res.* **37**(6), e45–e45 (2009).
59. Ge, S. X., Son, E. W. & Yao, R. iDEP: An integrated web application for differential expression and pathway analysis of RNA-Seq data. *BMC Bioinform.* **19**(1), 534. https://doi.org/10.1186/s12859-018-2486-6 (2018).
60. Max, K. E. A. *et al.* Human plasma and serum extracellular small RNA reference profiles and their clinical utility. *Proc. Natl. Acad. Sci. U. S. A.* **115**(23), E5334–E5343 (2018).
61. Melville, L. *et al.* Precision worm control in grazing lambs by targeting group treatment based on performance of sentinels. *Animal* **15**(4), 100176 (2021).
62. Corrales, J. L. *et al.* The use of cathepsin L1 (FhCL1) serological ELISA in sentinel screening for liver fluke on sheep farms. *Vet. Parasitol. Reg. Stud. Reports*. **45**, 100924. https://doi.org/10.1016/j.vprsr.2023.100924 (2023).
63. Shandilya, U. K. *et al.* Expression profile of miRNA from high, middle, and low stress-responding sheep during bacterial endotoxin challenge. *Animals* **13**(3), 508 (2023).
64. Sharma, A. *et al.* PSXIV-20 Ovine circulatory markers regulating the acute-phase response of variable stress responding sheep to LPS challenge. *J. Anim. Sci.* **99**(Supplement_3), 494–495 (2021).
65. Jin, P., Li, S., Sun, L., Lv, C. & Ma, F. Transcriptome-wide analysis of microRNAs in *Branchiostoma belcheri* upon *Vibrio parahemolyticus* infection. *Dev. Comp. Immunol.* **74**, 243–252 (2017).
66. Carpi, S. *et al.* Expression analysis of muscle-specific miRNAs in plasma-derived extracellular vesicles from patients with chronic obstructive pulmonary disease. *Diagnostics* **10**(7), 502 (2020).
67. He, M.-Q., Wan, J.-F., Zeng, H.-F., Tang, Y.-Y. & He, M.-Q. miR-133a-5p suppresses gastric cancer through TCF4 down-regulation. *J. Gastrointest. Oncol.* **12**(3), 1007 (2021).
68. Alizadeh, Z. *et al.* Parasite-derived microRNAs in plasma as novel promising biomarkers for the early detection of hydatid cyst infection and post-surgery follow-up. *Acta Trop.* **202**, 105255 (2020).

Author contributions

Study conception and design: S.D., N.T., J.P.D. Sample collection: K.C., J.P.D. Sample processing: A.R., K.C., S.C. Acquisition of data: A.R., S.C., D.S. Data analysis and interpretation: S.C., D.S., N.T., S.D. All authors contributed to and approved the submitted version of the manuscript.

Funding

This work was supported by an Australian Research Council Discovery Project Grant (DP210101337). J.P.D. and K.C. are supported from Science Foundation Ireland (SFI) Professorship award 17/RP/5368. S.C. is a recipient of an Australian Government Research Training Program Scholarship.

Competing interests

The authors declare no competing interests.

Additional information

Supplementary Information The online version contains supplementary material available at https://doi.org/10.1038/s41598-024-57704-9.

Correspondence and requests for materials should be addressed to N.T. or S.D.

Reprints and permissions information is available at www.nature.com/reprints.

Publisher's note Springer Nature remains neutral with regard to jurisdictional claims in published maps and institutional affiliations.

Open Access This article is licensed under a Creative Commons Attribution 4.0 International License, which permits use, sharing, adaptation, distribution and reproduction in any medium or format, as long as you give appropriate credit to the original author(s) and the source, provide a link to the Creative Commons licence, and indicate if changes were made. The images or other third party material in this article are included in the article's Creative Commons licence, unless indicated otherwise in a credit line to the material. If material is not included in the article's Creative Commons licence and your intended use is not permitted by statutory regulation or exceeds the permitted use, you will need to obtain permission directly from the copyright holder. To view a copy of this licence, visit http://creativecommons.org/licenses/by/4.0/.

© The Author(s) 2024

Appendix C:

Monash Genome Modification Platform Final Report: Generation of Ago2 Knockout RAW264.7 Cells



Ago2 knock-out (KO)

RAW264.7 cells (client cell line)

Project design

Ago2 KO (RAW264.7 cells)

Ago2 mouse gene

Gene: Ago2 ENSMUSG00000036698

Description argonaute RISC catalytic subunit 2 [Source:MGI Symbol;Acc:MGI:2446632]

Gene Synonyms 1110029L17Rik, 2310051F07Rik, Eif2c2, argonaute 2

Location Chromosome 15: 72,967,693-73,056,784 reverse strand.
GRCm39:CM001008.3

About this gene This gene has 3 transcripts (splice variants), 209 orthologues, 3 paralogues and is associated with 18 phenotypes.

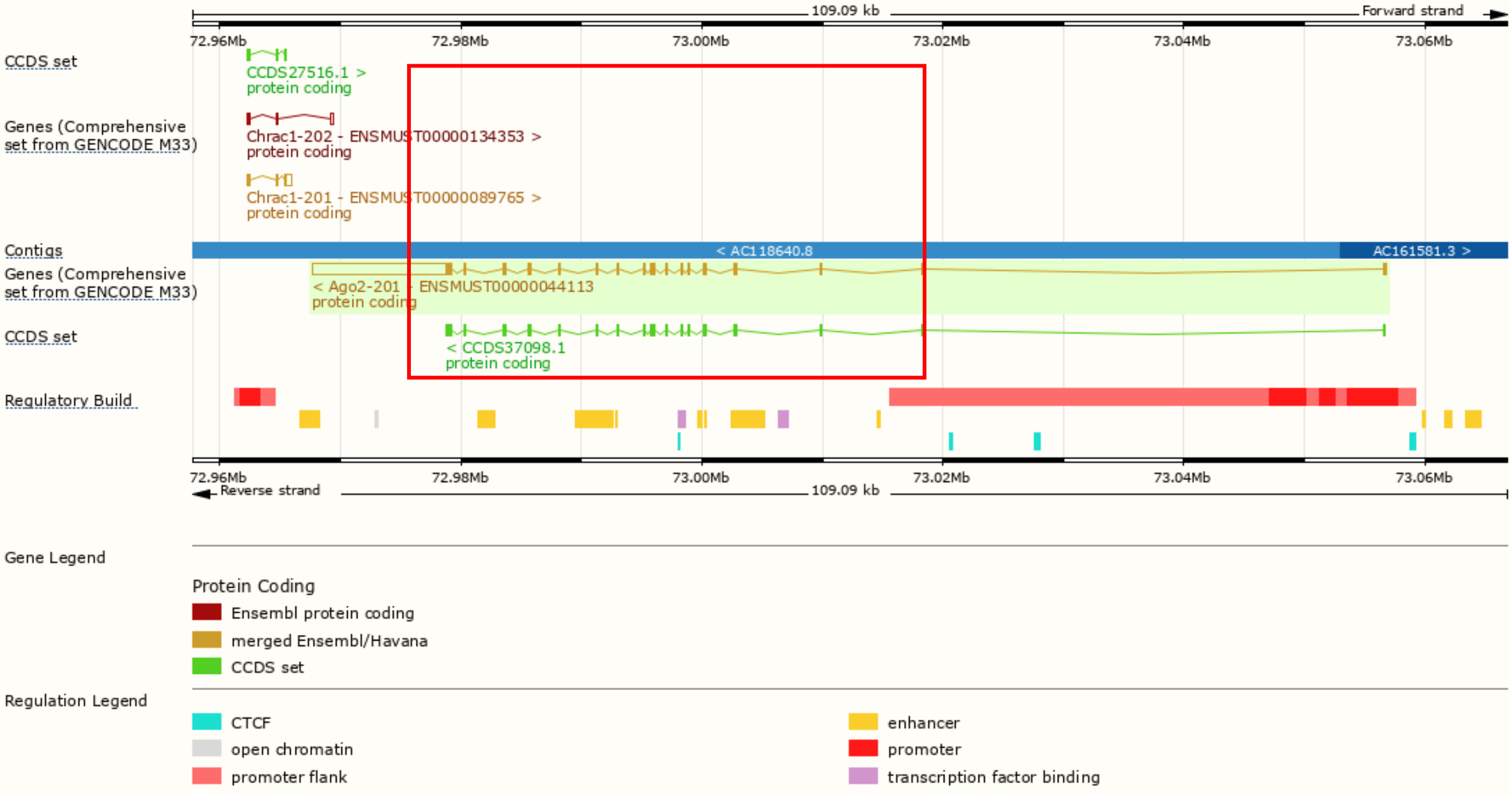
Transcripts Hide transcript table

Show/hide columns (1 hidden) Filter

Transcript ID	Name	bp	Protein	Biotype	CCDS	UniProt Match	Flags
ENSMUST00000044113.12	Ago2-201	13800	860aa	Protein coding	CCDS37098	Q8CJG0	Ensembl Canonical, GENCODE basic, APPRIS P1, TSL:1
ENSMUST00000230464.2	Ago2-203	617	No protein	Protein coding CDS not defined		-	-
ENSMUST00000230158.2	Ago2-202	616	No protein	Protein coding CDS not defined		-	-

Ago2 transcript 201

Piece of DNA that will be deleted if both sgRNA guides cut at the same time is shown in the red box



sgRNAs for Ago2 KO

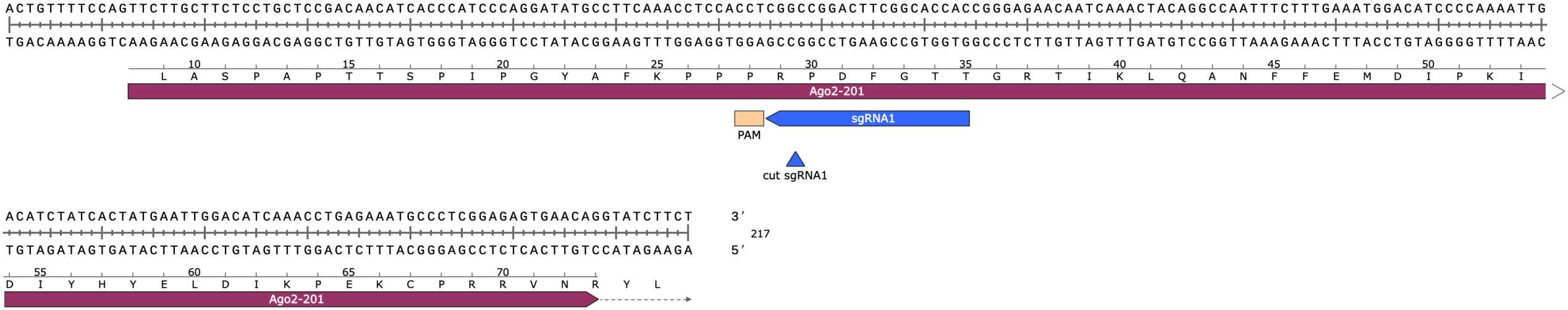
Ago2 sgRNA1: GTGGTGCCGAAGTCCGGCCG

This guide cuts downstream of the ATG of Ago2 (transcript 201) in the second coding exon between amino acid 29 and amino acid 30.
If sgRNA2 does not cut, a frameshift may still be created, resulting in a KO allele.

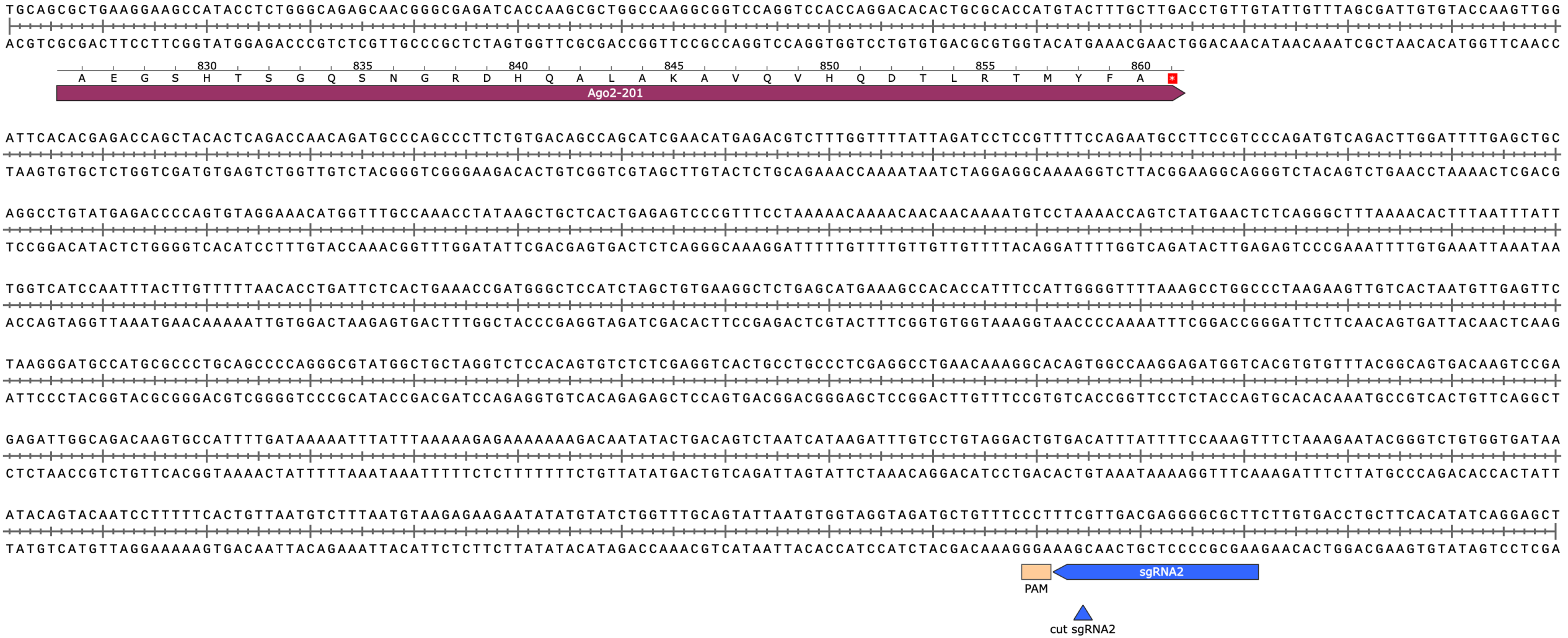
Ago2 sgRNA2: AAGCGCCCCTCGTCAACGAA

This guide cuts 890bp upstream of the Ago2 stop codon (transcript 201).
Simultaneous cutting of sgRNA1 and sgRNA2 would remove the majority of the Ago2 gene.

sgRNA1 for Ago2 shown on genomic DNA



sgRNA2 for Ago2 shown on genomic DNA

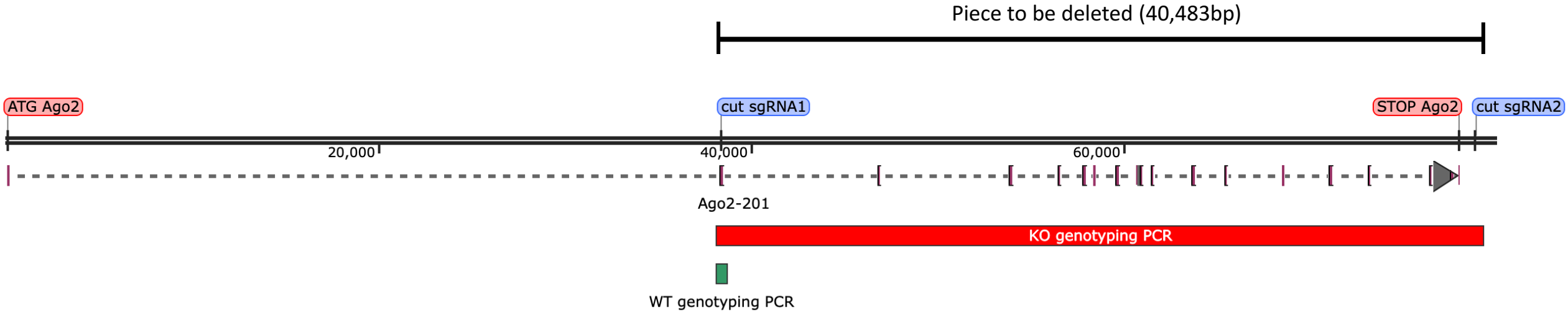


Genotyping PCRs

Ago2 KO (RAW264.7 cells)

Ago2 KO genotyping strategy

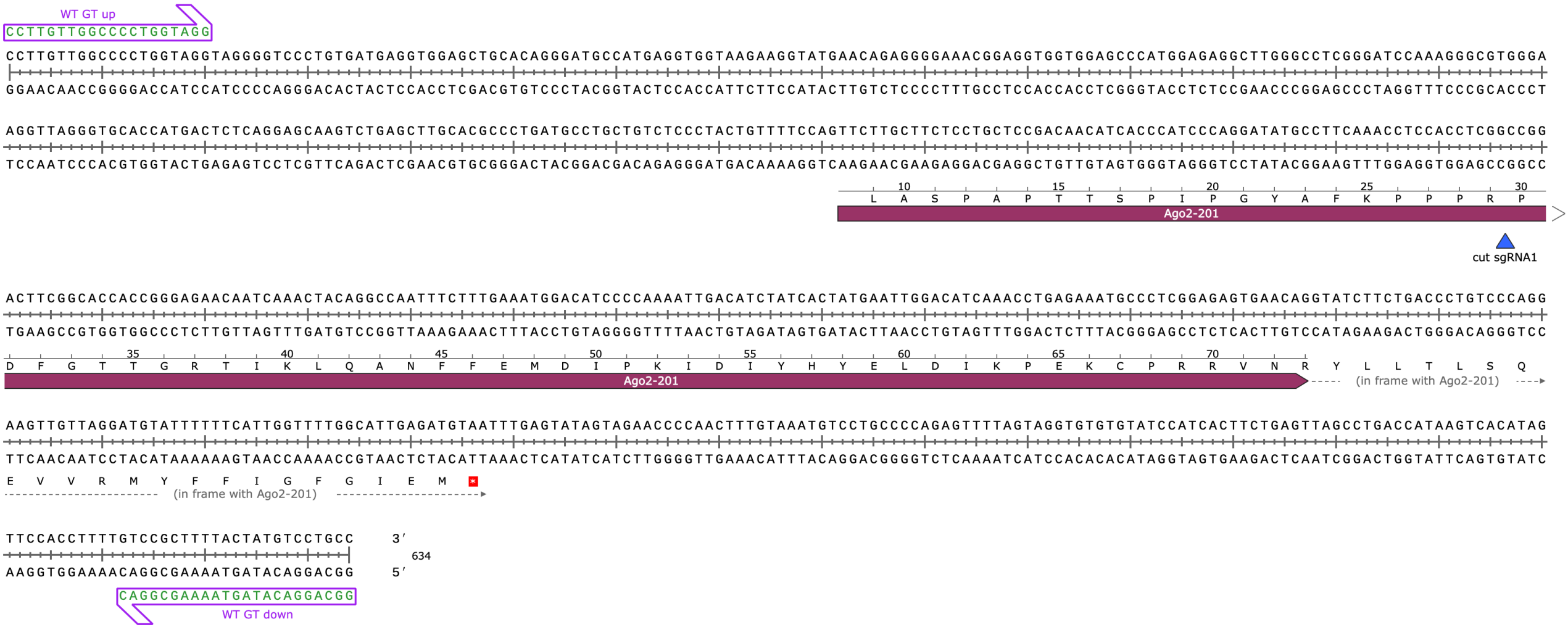
Shown on WT genomic DNA



Ago2 genotyping overview

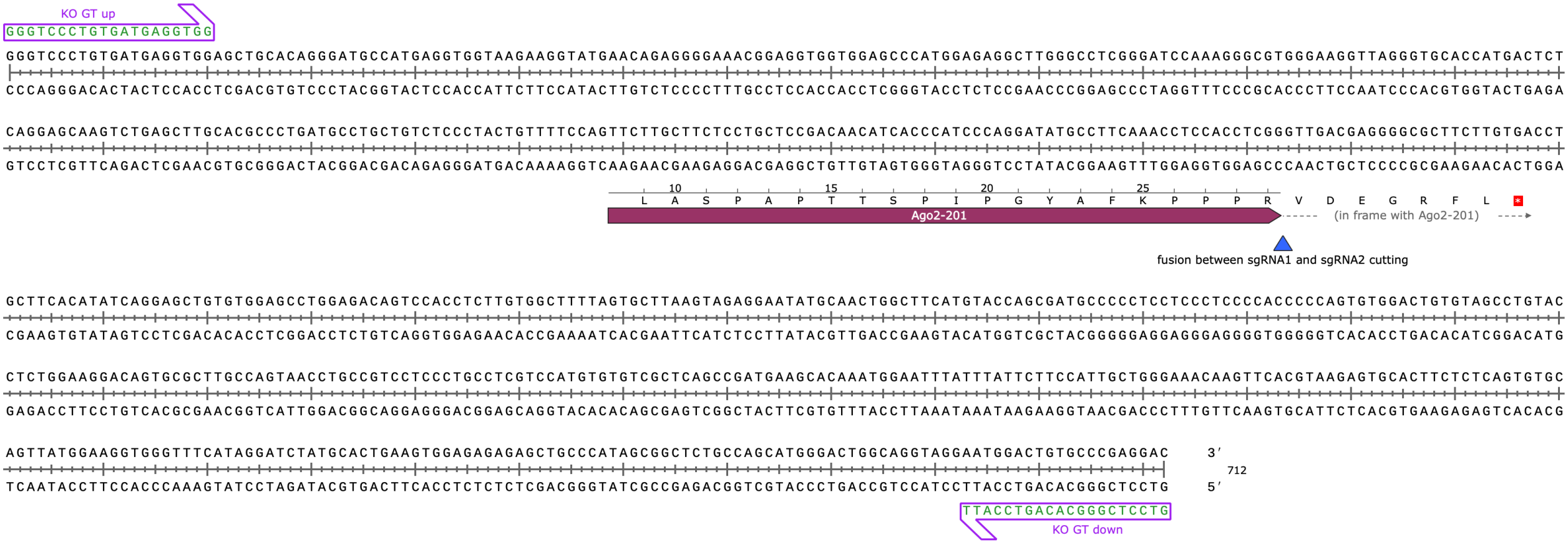
WT cells:	WT PCR works / KO PCR doesn't work and sgRNA1 has not caused a frame shift
Heterozygous KO cells:	WT PCR works and sgRNA1 has not caused a frameshift / KO PCR works OR
Heterozygous KO cells:	WT PCR works / sgRNA1 has caused a frameshift and KO PCR doesn't work
Homozygous KO cells:	WT PCR doesn't work / KO PCR works OR
Homozygous KO cells:	WT PCR works / sgRNA1 has caused a frameshift and KO PCR works OR
Homozygous KO cells:	WT PCR works / sgRNA1 has caused a frameshift on both alleles and KO PCR doesn't work

Ago2 WT genotyping PCR (634bp)



Ago2 KO genotyping PCR (around 712bp)

WT band for this PCR would be 41Kb, this PCR will not work



Running of project

Ago2 KO (RAW264.7 cells)

Ago2 KO project summary

Species	Mouse
Gene modified	Argonaute-2 (Ago2)
Modification	Knock-out
Cell line	RAW264.7 mouse cells
Medium	DMEM + 10% FBS + 1% P/S
Transfection	Cas9-GFP (protein) + 2x sgRNAs (synthetic) using Lipofectamine CRISPRMAX
Selection	FACS sorting for GFP-high cells and single cell deposition
Genotyping	A total of 676 clones were genotyped from 2 transfections. 1 clone was found to be homozygous KO
Sequencing	sgRNA1 product was sequenced for homozygous clone 82. Clone 82 has a 37bp deletion in the sgRNA1 site on one allele. On the second allele there is a 1bp insertion in the sgRNA1 site.
Subcloning	Clone 82 was subcloned by single cell deposition; subclones were genotyped and sequenced. 3 subclones were expanded for handover.
Mycoplasma testing	Absence of mycoplasma is shown by two PCR-based detection protocols
Frozen vials	Homozygous KO subclones 82-2, 82-3 and 82-5; 2 vials each

Ago2 KO Transfection

Lipofectamine CRISPRMAX transfection	
Solution I	37.5µg Cas9-GFP protein
	3.6µg sgRNA1
	3.6µg sgRNA2
	75µl Plus reagent
	750µl OPTI-MEM
Solution II	45µl Lipofectamine CRISPRMAX
	750µl OPTI-MEM
Combined Solution I and Solution II are incubated at RT for 10min, then added to a 10cm plate with ~70% confluent cells	
2 days after transfections the cells are FACS sorted for GFP-high cells into 12x 96-well plates (single cell deposition)	
Bulk cells are collected for gDNA extraction and PCR.	

Ago2 KO - screening of individual clones

Individual clones screened (1st transfection)	257
Homozygous KO	0
Individual clones screened (2nd transfection)	419
Homozygous KO	1

Homozygous clone 82 was subcloned to ensure that there was no WT contamination

Genotyping of the KO subclones

Ago2 KO (RAW264.7 cells)

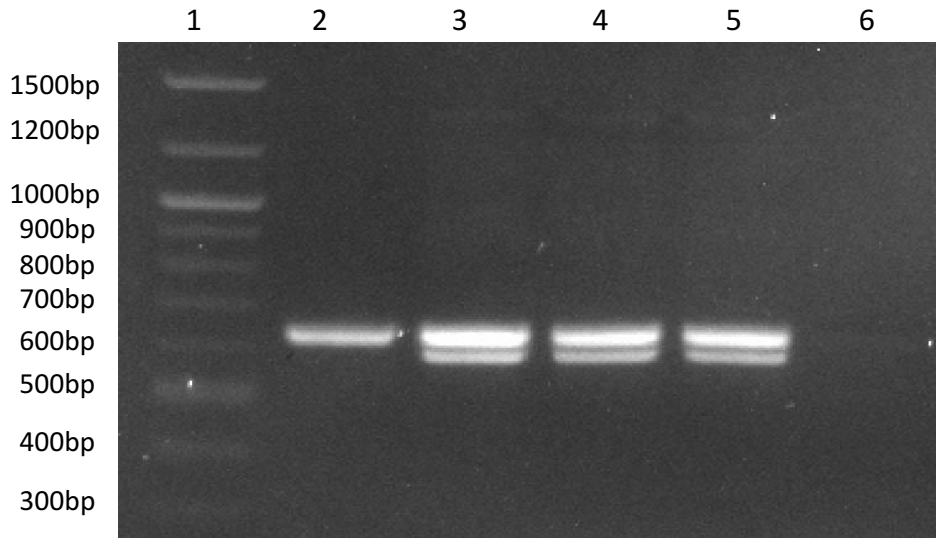
Genotyping of subclones – WT PCR (634bp)

All subclones are derived from clone 82

PCR PRIMERS		
TC59 WT GT up	20	CCTTGTTGGCCCCTGGTAGG
TC59 WT GT down	23	GGCAGGACATAGTAAAAGCGGAC

Reagents	
AccuStartII Geltrack PCR Supermix (Quantabio)	15.0 µl
TC59 WT GT up (10µM)	1.0 µl
TC59 WT GT down (10µM)	1.0 µl
Template	4.0 µl
Water	9.0 µl
Total	30.0 µl

Cycling conditions			
Denature	94˚C	2 min	
Denature	94˚C	20 sec	35 cycles
Anneal	66˚C	30 sec	
Extension	72˚C	60 sec	
Extension	72˚C	5 min	



Lane 1 Marker
Lane 2 WT
Lane 3 Subclone 82-2
Lane 4 Subclone 82-3
Lane 5 Subclone 83-5
Lane 6 Negative control

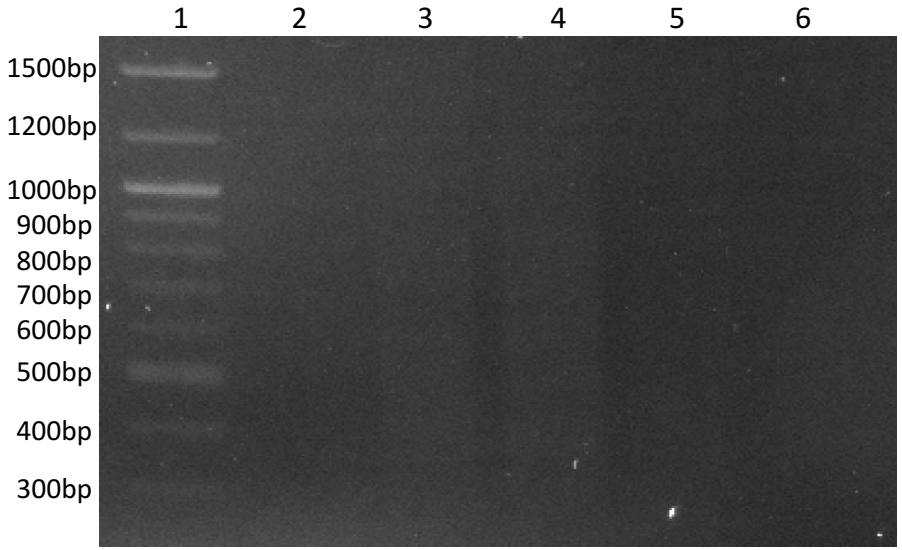
Genotyping of subclones – KO PCR (around 712bp)

All subclones are derived from clone 82

PCR PRIMERS		
TC59 KO GT up	20	GGGTCCCTGTGATGAGGTGG
TC59 KO GT down	20	GTCCTCGGGCACAGTCCATT

Reagents	
AccuStartII Geltrack PCR Supermix (Quantabio)	15.0 µl
TC59 KO GT up (10µM)	1.0 µl
TC59 KO GT down (10µM)	1.0 µl
Template	4.0 µl
Water	9.0 µl
Total	30.0 µl

Cycling conditions			
Denature	94˚C	2 min	
Denature	94˚C	20 sec	35 cycles
Anneal	64˚C	30 sec	
Extension	72˚C	60 sec	
Extension	72˚C	5 min	

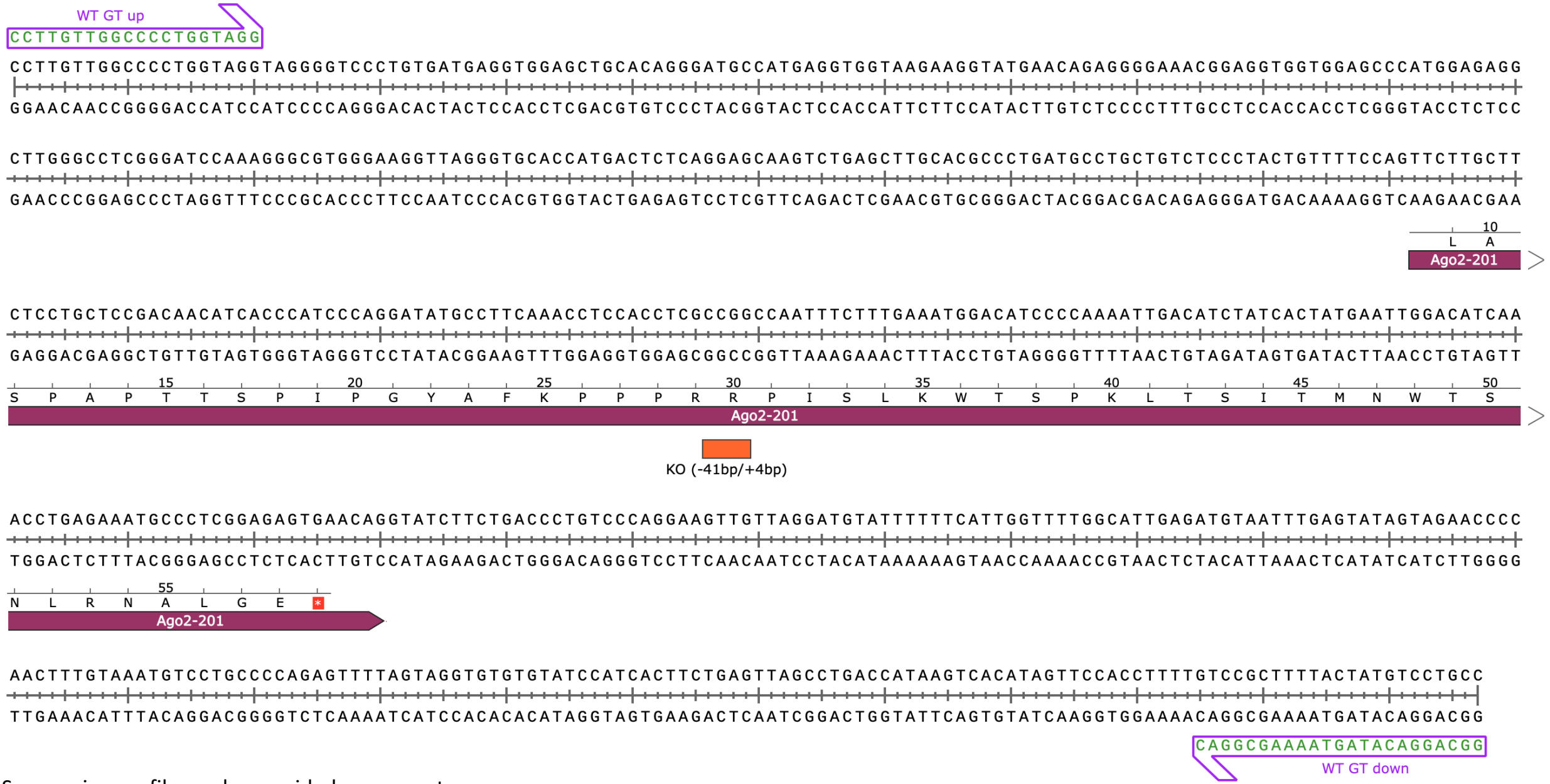


Lane 1 Marker
Lane 2 WT
Lane 3 Subclone 82-2
Lane 4 Subclone 82-3
Lane 5 Subclone 83-5
Lane 6 Negative control

Sequencing of subclones

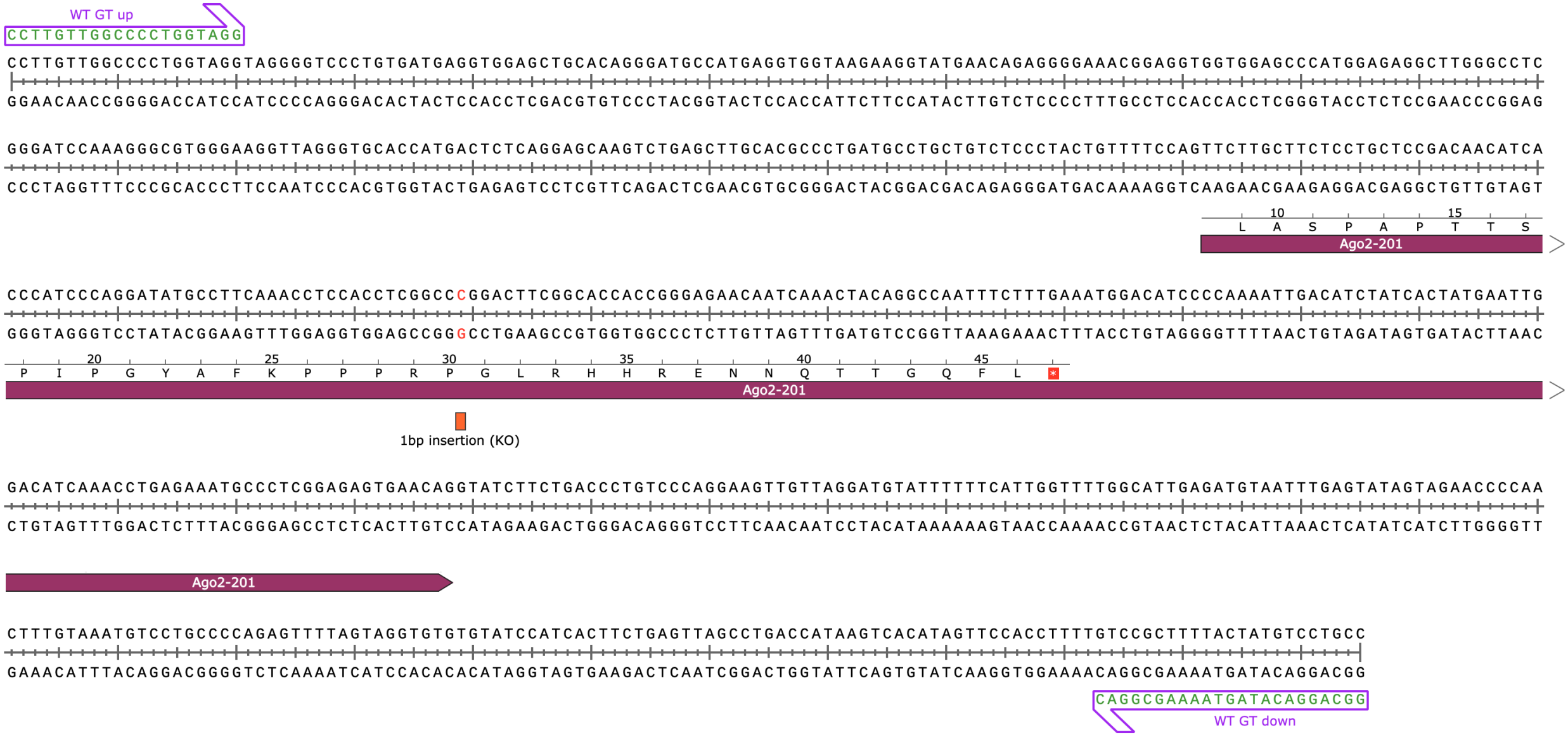
Ago2 KO (RAW264.7 cells)

Subclones 82-2, 82-3 and 82-5 - allele 1



Sequencing profile can be provided on request

Subclones 82-2, 82-3 and 82-5 - allele 2



Sequencing profile can be provided on request

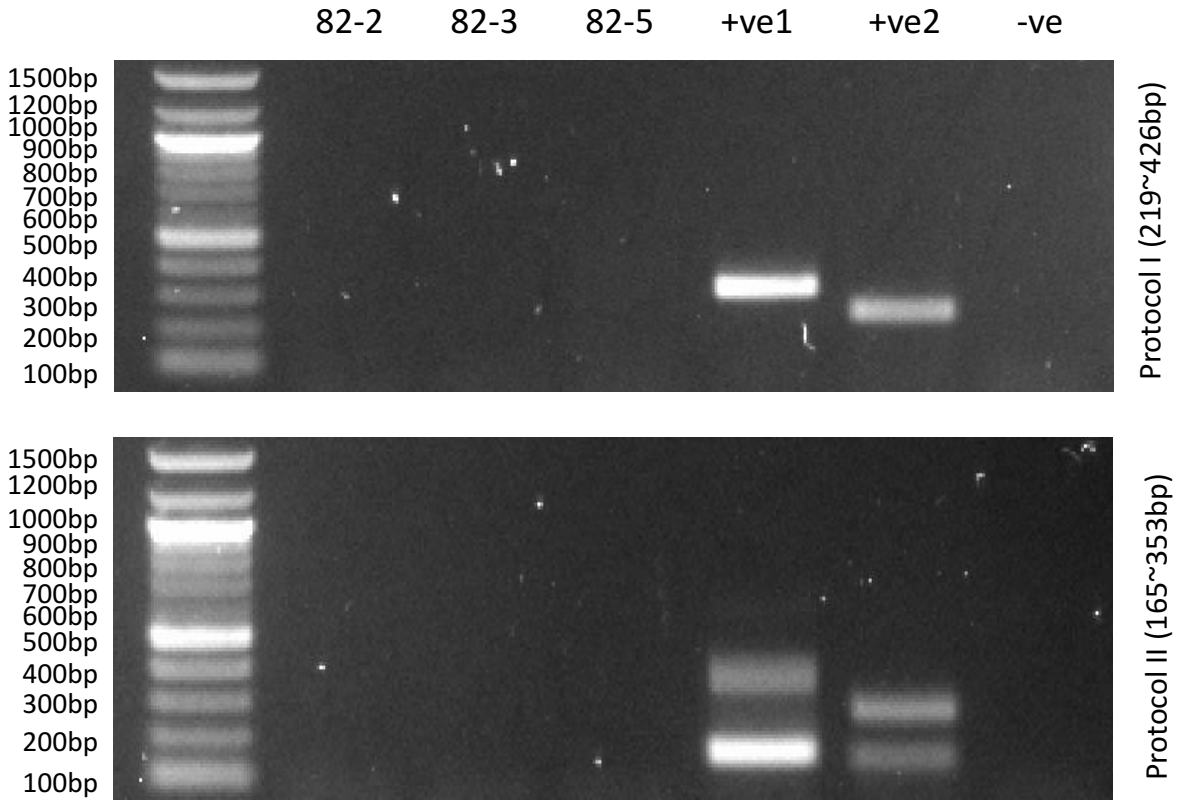
Subclones provided

Ago2 KO (RAW264.7 cells)

Ago2 KO subclones for handover

	Allele 1		Allele 2		Handover
	WT PCR	**Mutation at sgRNA1 site**	**WT PCR**	**Mutation at sgRNA1 site**	**Frozen vials**
Subclone 82-2 homozygous KO	597bp	37bp deletion (-41bp/+4bp)	635bp	1bp insertion	2
Subclone 82-3 homozygous KO	597bp	37bp deletion (-41bp/+4bp)	635bp	1bp insertion	2
Subclone 82-5 homozygous KO	597bp	37bp deletion (-41bp/+4bp)	635bp	1bp insertion	2

Mycoplasma screening



Protocol I and II are two independent PCR-based methods for detecting *Mycoplasma/Acholeplasma* species. +ve1 and +ve2 are two *Mycoplasma* positive samples, giving the expected products at 219-426bp (protocol I) and 165-355bp (protocol II).

None of the clones give a positive band, indicating they are mycoplasma-free.

Materials

Ago2 KO (RAW264.7 cells)

MATERIALS:

- DMEM (ThermoFisher, #10569044)
- Cas9-GFP (IDT Alt-R®S.p., #10008161)
- sgRNAs (IDT Alt-R® CRISPR-Cas9 sgRNA)
- Lipofectamine CRISPRMAX (ThermoFisher, #CMAX00015)

As per the Terms and Conditions of Phenomics Australia CRISPR Services, clause 16 (shown below), please include the relevant acknowledgement statement(s) in all publications.

In receiving the Material, you agree to include the following acknowledgement in any publication, presentation or press release concerning the Material: *"The [insert-e.g. mutant animals (including rats, mice and rabbits)] were produced via CRISPR genome editing by the Monash Genome Modification Platform (MGMP), Monash University as a node of Phenomics Australia. Phenomics Australia is supported by the Australian Government Department of Education through the National Collaborative Research Infrastructure Strategy, the Super Science Initiative and the Collaborative Research Infrastructure Scheme".*

Appendix D:

Monash Genome Modification Platform Final Report: Generation of Dicer Knockout RAW264.7 Cells



Dicer1 knock-out (KO)

RAW264.7 cells (client cell line)

Project design

Dicer1 KO (RAW264.7 cells)

bsi. ISO 9001 Quality Management
FS 729759

Dicer1 mouse gene

This gene has multiple transcripts, we will be working with transcript 201

Gene: Dicer1 ENSMUSG00000041415

Description dicer 1, ribonuclease type III [Source:MGI Symbol;Acc:MGI:2177178]

Gene Synonyms 1110006F08Rik, D12Ertd7e, Dicer1

Location Chromosome 12: 104,654,001-104,718,211 reverse strand.
GRCm39:CM001005.3

About this gene This gene has 9 transcripts (splice variants), 205 orthologues and is associated with 48 phenotypes.

Transcripts Hide transcript table

Show/hide columns (1 hidden) Filter

Transcript ID	Name	bp	Protein	Biotype	CCDS	UniProt Match	Flags
ENSMUST00000222528.2	Dicer1-206	4724	No protein	Protein coding CDS not defined		-	TSL:1
ENSMUST00020183813.1	Dicer1-209	691	No protein	Protein coding CDS not defined		-	-
ENSMUST00000222519.2	Dicer1-205	647	No protein	Protein coding CDS not defined		-	TSL:3
ENSMUST00020183808.1	Dicer1-207	626	No protein	Protein coding CDS not defined		-	-
ENSMUST00000041987.8	Dicer1-201	9851	1916aa	Protein coding LoF		F8VQ54	Ensembl Canonical GENCODE basic APPRIS P2 TSL:1
ENSMUST00000222002.3	Dicer1-203	1460	421aa	Protein coding LoF		A0A1Y7VJD6	APPRIS ALT2 TSL:1 CDS 3' incomplete
ENSMUST00020183809.1	Dicer1-208	446	57aa	Protein coding LoF		A0A8I4YZW9	APPRIS ALT2 CDS 3' incomplete
ENSMUST00000221293.2	Dicer1-202	6904	No protein	Retained intron		-	TSL:1
ENSMUST00000222115.2	Dicer1-204	2543	No protein	Retained intron		-	TSL:1

Dicer1 transcripts

Piece of DNA that will be deleted if both sgRNA guides cut at the same time is shown in the red box



sgRNAs for Dicer1 KO

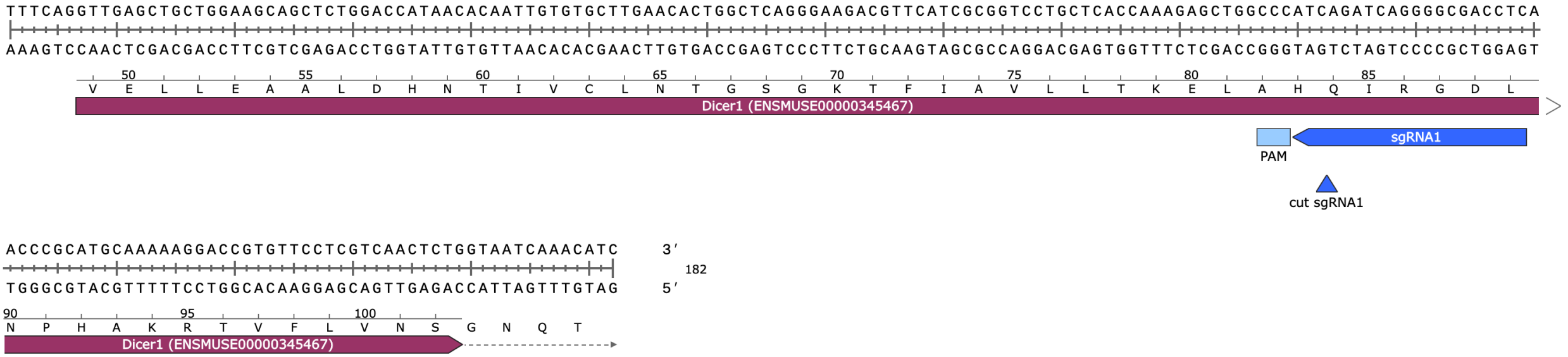
Dicer1 sgRNA1: GAGGTCGCCCCTGATCTGAT

This guide cuts in the second coding exon of Dicer1 (transcript 201).
If sgRNA2A does not cut, a frameshift may still be created, resulting in a KO allele.

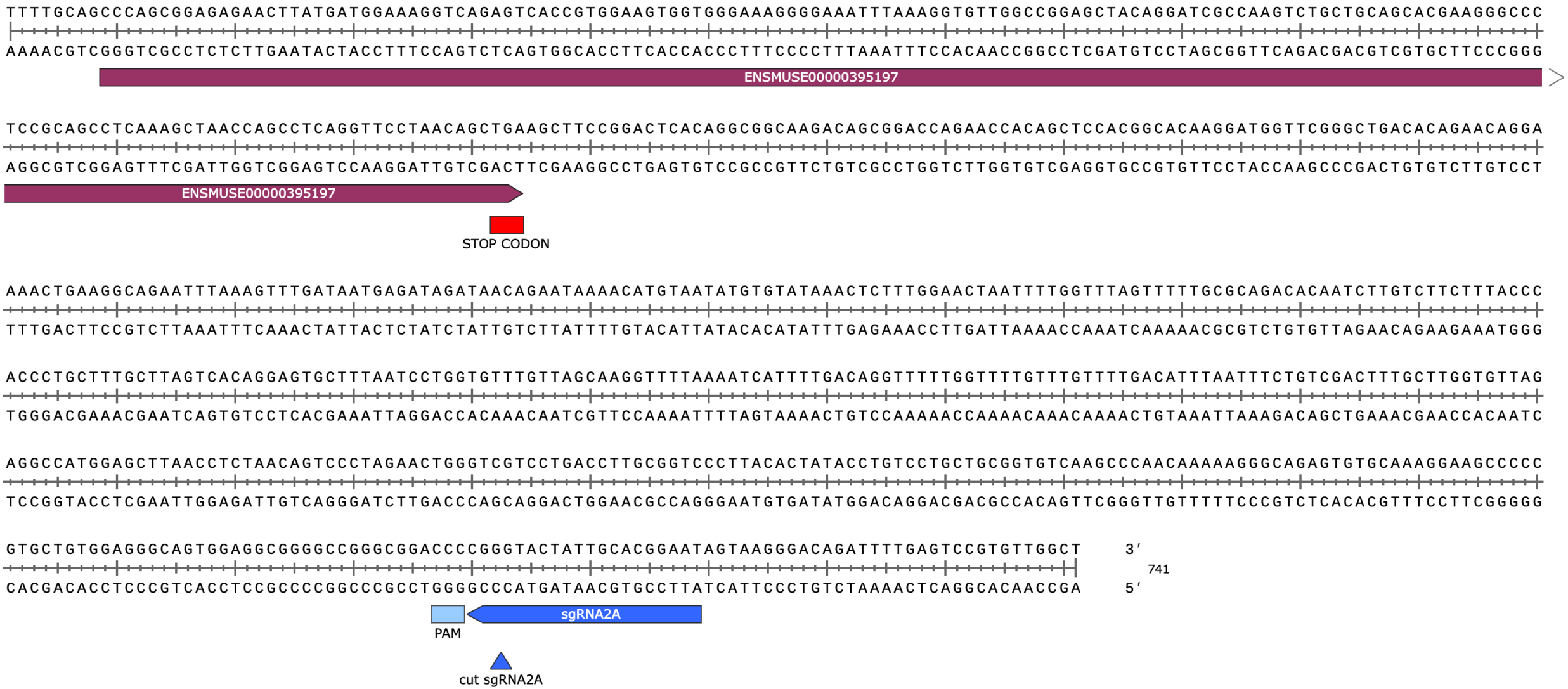
Dicer1 sgRNA2A: ATTCCGTGCAATAGTACCCG

This guide cuts 518bp downstream of the Dicer1 stop codon (transcript 201).
Simultaneous cutting of sgRNA1 and sgRNA2A would remove the majority of the Dicer1 gene.

sgRNA1 for Dicer1 shown on genomic DNA



sgRNA2A for Dicer1 shown on genomic DNA



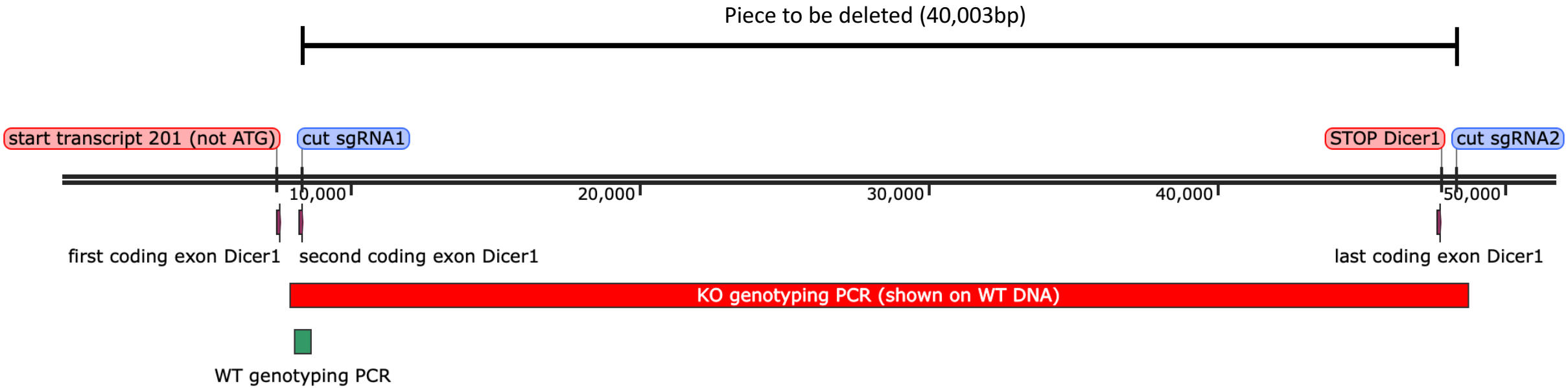
Genotyping PCRs

Dicer1 KO (RAW264.7 cells)

bsi. ISO 9001 Quality Management
FS 729759

Dicer1 KO genotyping strategy

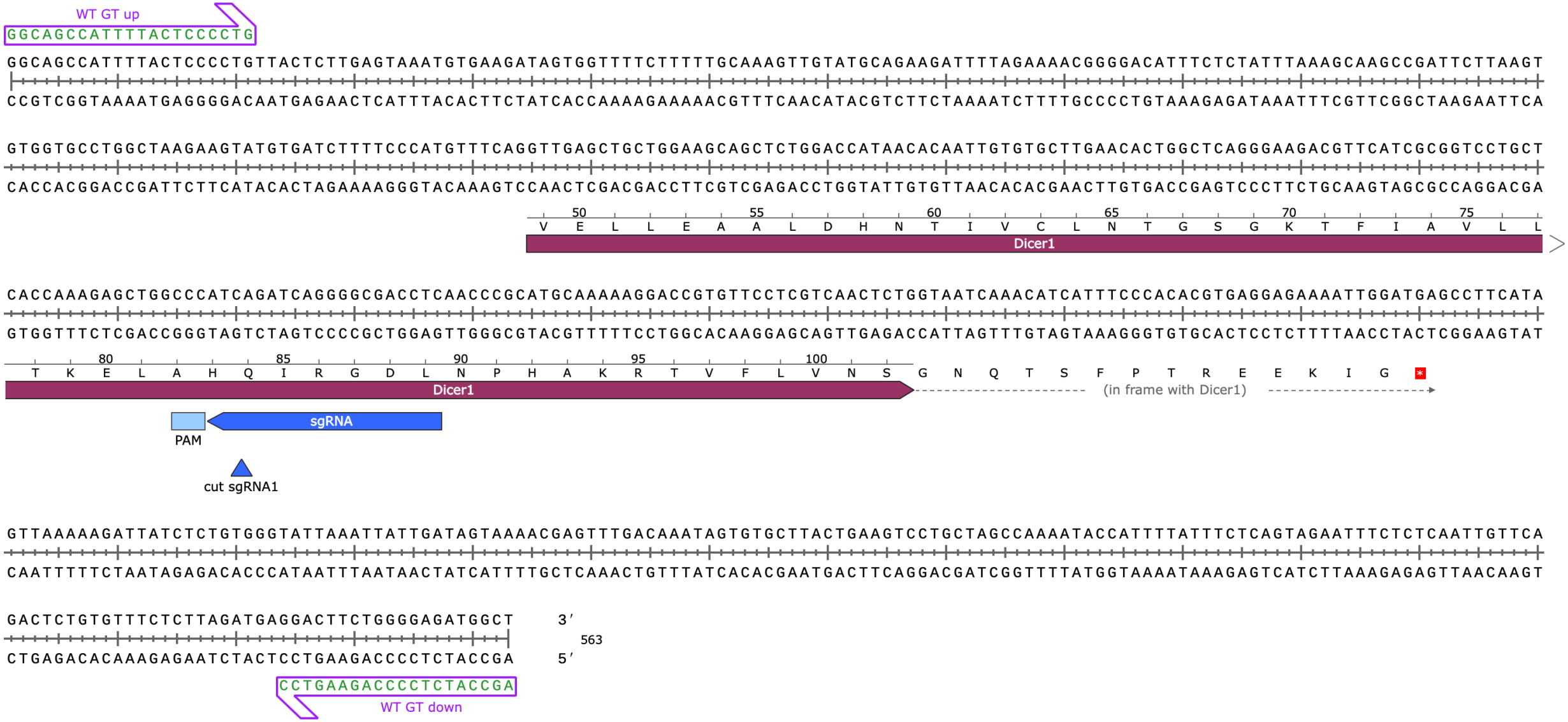
Shown on WT genomic DNA



Dicer1 genotyping overview

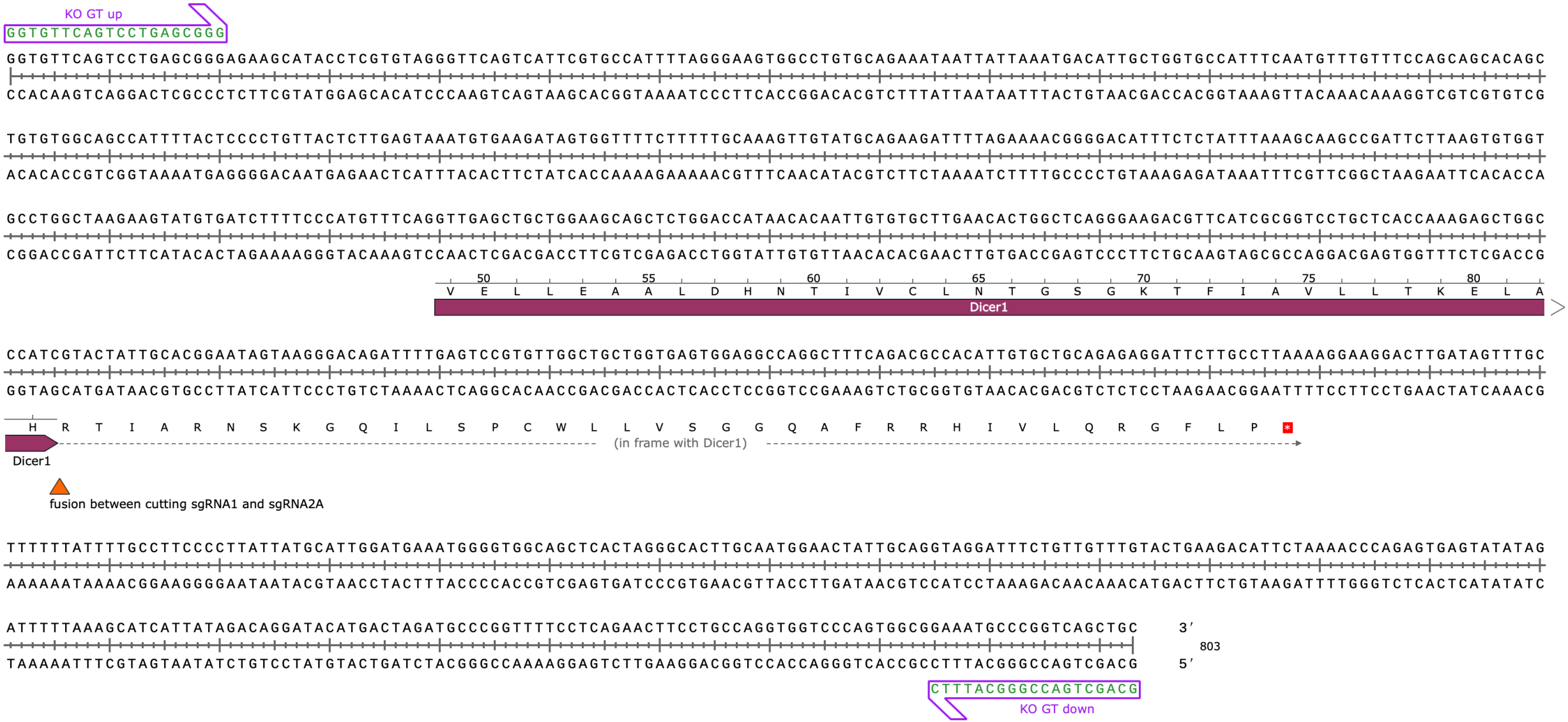
WT cells:	WT PCR works / KO PCR doesn't work and sgRNA1 has not caused a frame shift
Heterozygous KO cells:	WT PCR works and sgRNA1 has not caused a frameshift / KO PCR works OR
Heterozygous KO cells:	WT PCR works / sgRNA1 has caused a frameshift and KO PCR doesn't work
Homozygous KO cells:	WT PCR doesn't work / KO PCR works OR
Homozygous KO cells:	WT PCR works / sgRNA1 has caused a frameshift and KO PCR works OR
Homozygous KO cells:	WT PCR works / sgRNA1 has caused a frameshift on both alleles and KO PCR doesn't work

Dicer1 WT genotyping PCR (563bp)



Dicer1 KO genotyping PCR (around 803bp)

WT band for this PCR would be over 40Kb, this PCR will not work



Running of project

Dicer1 KO (RAW264.7 cells)

Dicer1 KO project summary

Species	Mouse
Gene modified	Dicer1, Ribonuclease type III
Modification	Knock-out
Cell line	RAW264.7 mouse cells
Medium	DMEM + 10% FBS + 1% P/S
Transfection	Cas9-GFP (protein) + 2x sgRNAs (synthetic) using Lipofectamine CRISPRMAX
Selection	FACS sorting for GFP-high cells and single cell deposition
Genotyping	A total of 218 clones were genotyped; 18 clones were potentially positive (positive for KO PCR or with WT PCR products at various sizes).
Sequencing	2 potential homozygous KO clones : Clones 166 and 173 3 potential heterozygous KO clones : Clones 18, 22 and 203
Subcloning and sequencing	Clones 18, 22, 166, 173 and 203 were subcloned by single cell deposition to ensure they were not a mixture. Genotyping and sequencing identified 3 homozygous KO subclones (subclones 22-21, 166-1 and 173-1) and 1 heterozygous KO subclone (subclone 203-1)
Mycoplasma testing	Absence of mycoplasma is shown by two PCR-based detection protocols
Frozen vials	Homozygous KO subclones 22-21, 166-1 and 173-1; heterozygous KO subclone 203-1; 2 vials each.

Dicer1 KO Transfection

Lipofectamine CRISPRMAX transfection	
Solution I	37.5µg Cas9-GFP protein
	3.6µg sgRNA1
	3.6µg sgRNA2A
	75µl Plus reagent
	750µl OPTI-MEM
Solution II	45µl Lipofectamine CRISPRMAX
	750µl OPTI-MEM
Combined Solution I and Solution II are incubated at RT for 10min, then added to a 10cm plate with ~70% confluent cells	
1 day after transfections the cells are FACS sorted for GFP-high cells into 12x 96-well plates (single cell deposition)	
Bulk cells are collected for gDNA extraction and PCR	

Dicer1 KO - screening of individual clones

Individual clones screened	218
Potential homozygous KO	2
Potential heterozygous KO	3

All 5 clones were subcloned to ensure that there was no WT contamination

Subcloning of the KO clones

Dicer1 KO (RAW264.7 cells)

Dicer1 KO - screening of subclones

	subclones screened	positive subclones
Clone 18	42	0
Clone 22 (homozygous KO)	44	1
Clone 166 (homozygous KO)	3	3
Clone 173 (homozygous KO)	1	1
Clone 203 (heterozygous KO)	6	6

Genotyping of the KO subclones

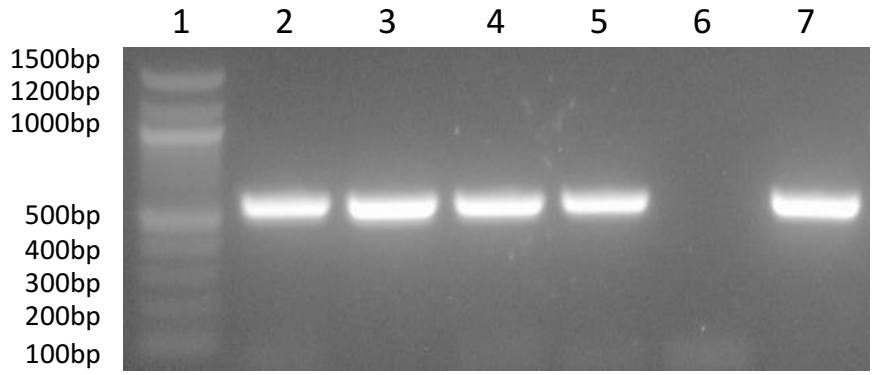
Dicer1 KO (RAW264.7 cells)

Genotyping of subclones – WT PCR (563bp)

PCR PRIMERS		
TC65 WT GT up	21	GGCAGCCATTTTACTCCCCTG
TC65 WT GT down	20	AGCCATCTCCCCAGAAGTCC

PCR REAGENTS	
AccuStartII Geltrack PCR Supermix (Quantabio)	15.0 µl
TC65 WT GT up (10µM)	1.0 µl
TC65 WT GT down (10µM)	1.0 µl
Template	4.0 µl
Water	9.0 µl
Total	30.0 µl

CYCLING CONDITIONS			
Denature	94˚C	2 min	
Denature	94˚C	20 sec	35 cycles
Anneal	64˚C	30 sec	
Extension	72˚C	60 sec	
Extension	72˚C	5 min	



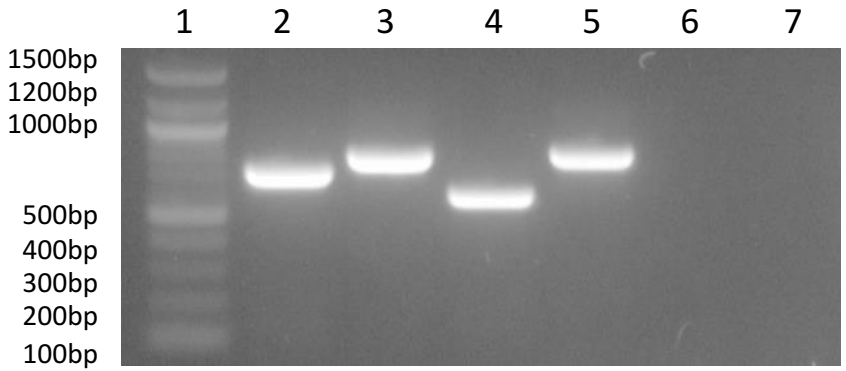
Lane 1 Marker
Lane 2 Subclone 22-21
Lane 3 Subclone 166-1
Lane 4 Subclone 173-1
Lane 5 Subclone 203-1
Lane 6 Negative control
Lane 7 WT

Genotyping of subclones– KO PCR (around 803bp)

PCR PRIMERS		
TC65 KO GT up	20	GGTGTTCAGTCCTGAGCGGG
TC65 KO GT down	19	GCAGCTGACCGGGCATTTC

PCR REAGENTS	
AccuStartII Geltrack PCR Supermix (Quantabio)	15.0 µl
TC65 KO GT up (10µM)	1.0 µl
TC65 KO GT down (10µM)	1.0 µl
Template	4.0 µl
Water	9.0 µl
Total	30.0 µl

CYCLING CONDITIONS			
Denature	98˚C	10 sec	35 cycles
Anneal	62˚C	15 sec	
Extension	68˚C	60 sec	
Extension	68˚C	5 min	



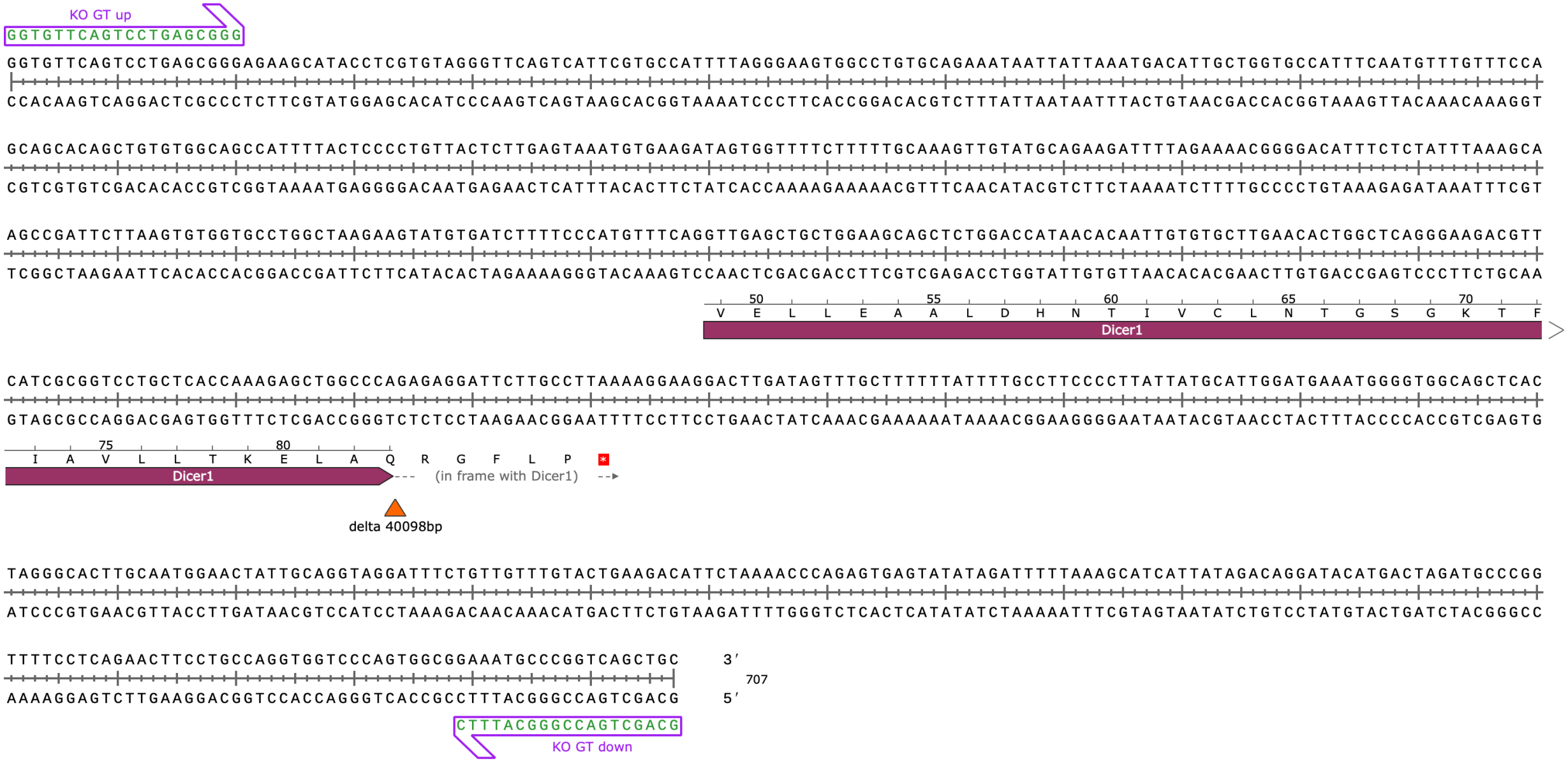
Lane 1 Marker
Lane 2 Subclone 22-21
Lane 3 Subclone 166-1
Lane 4 Subclone 173-1
Lane 5 Subclone 203-1
Lane 6 Negative control
Lane 7 WT

Sequencing of subclones

Dicer1 KO (RAW264.7 cells)

Subclone 22-21 – allele 1

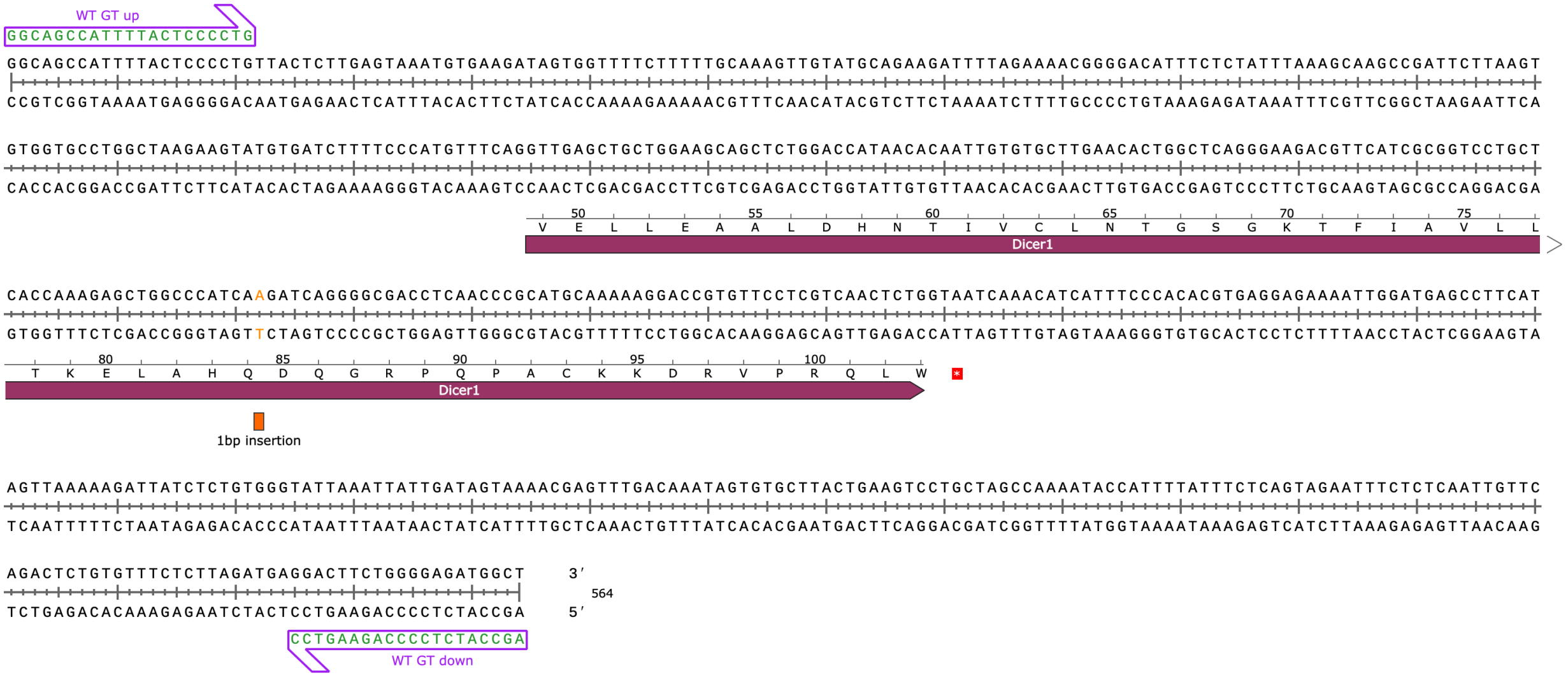
KO PCR band 707bp



Sequencing profile can be provided on request

Subclone 22-21 – allele 2

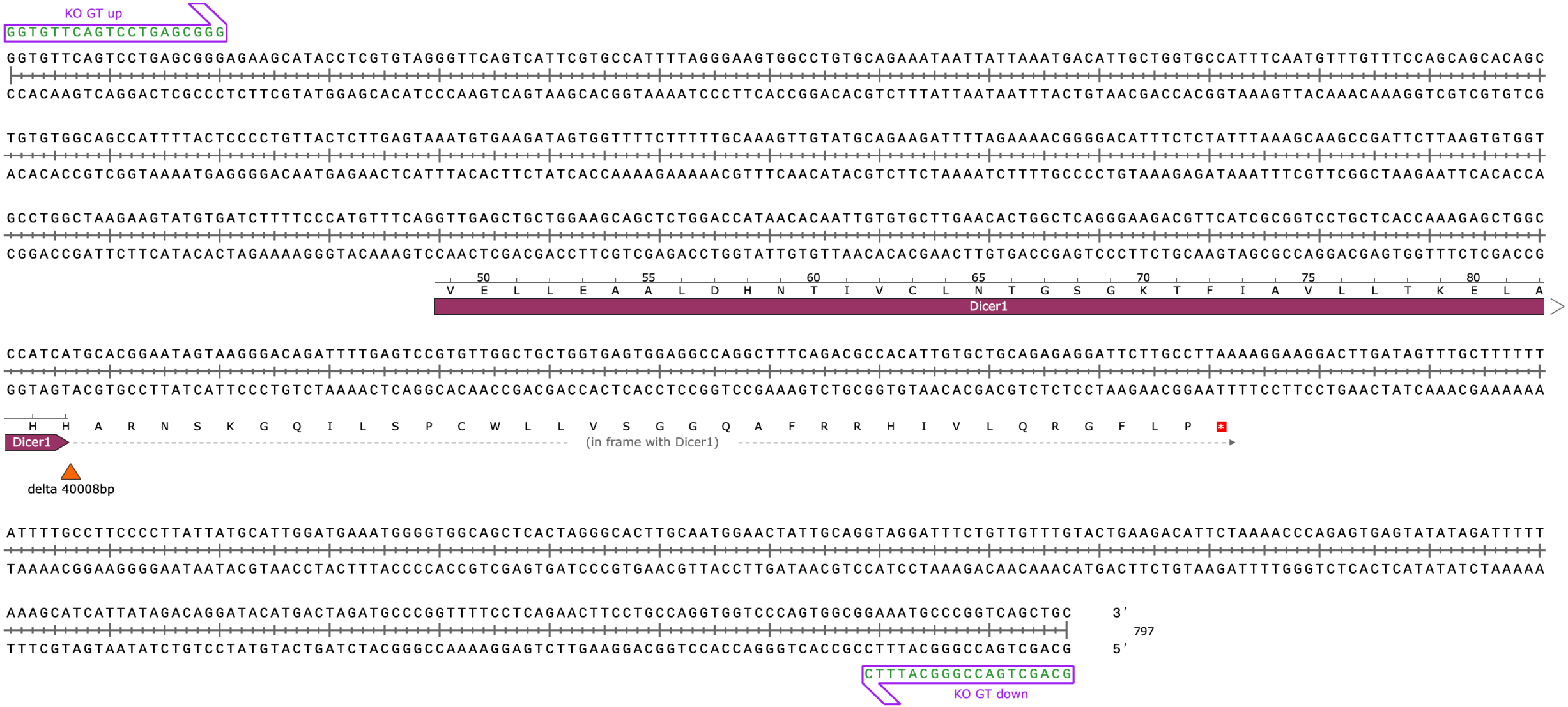
WT PCR band 564bp, the 1bp insertion results in nonsense amino acids 85-143 followed by premature stop codon.



Sequencing profile can be provided on request

Subclone 166-1 – allele 1

KO PCR band 797bp



Sequencing profile can be provided on request

Subclone 173-1 – allele 1

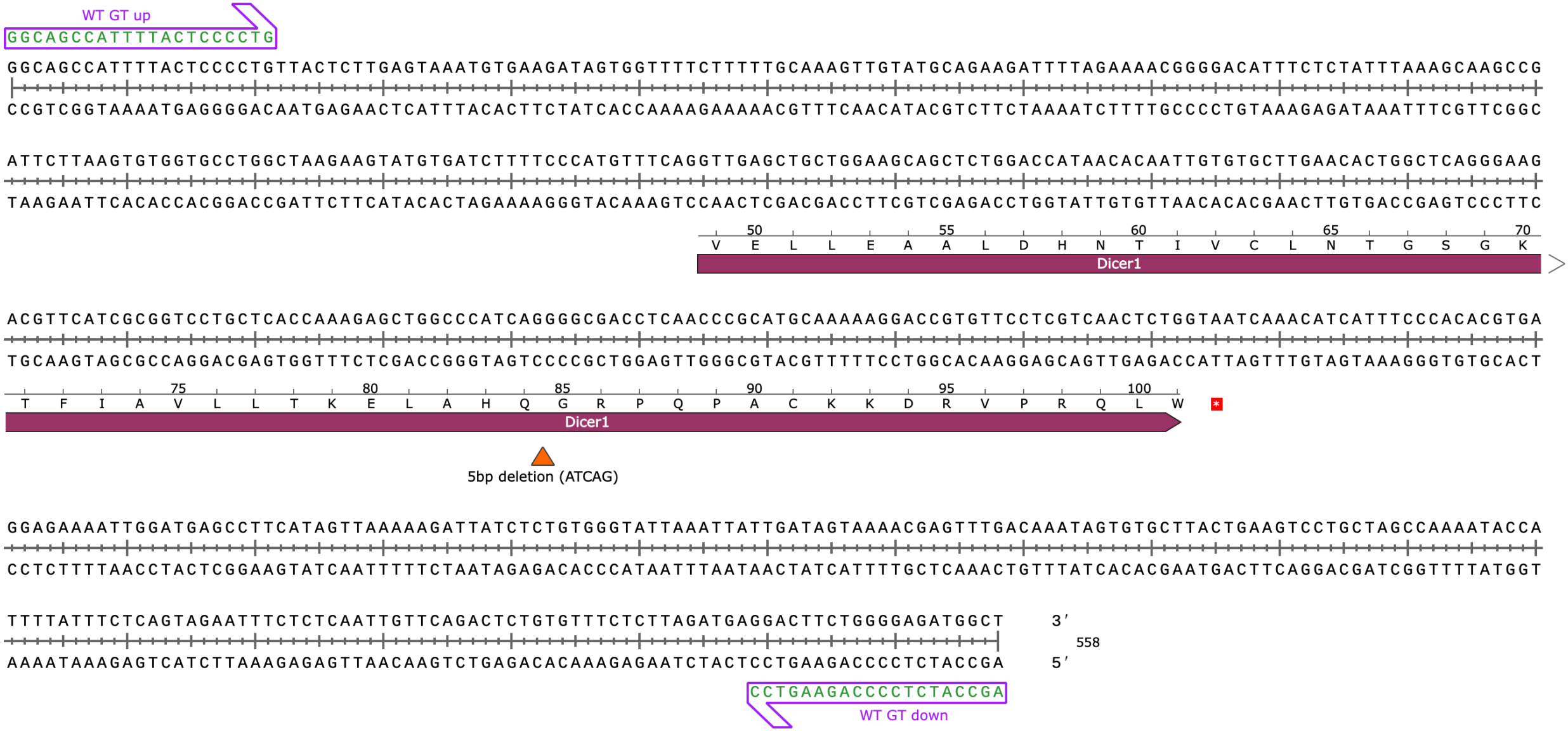
KO PCR band 582bp



Sequencing profile can be provided on request

Subclones 166-1 and 173-1 – allele 2

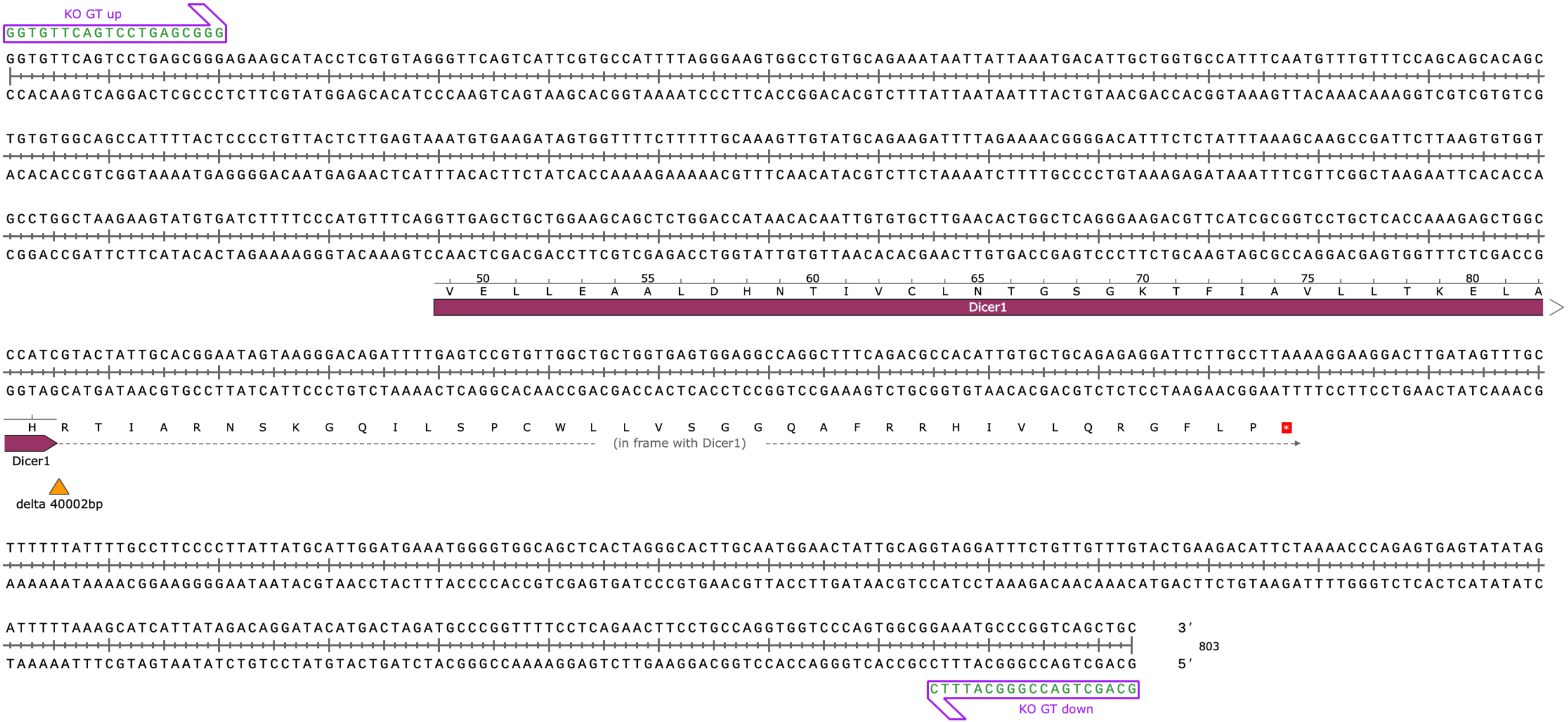
WT PCR band 558bp, the 5bp deletion results in nonsense amino acids 85-41 followed by premature stop codon.



Sequencing profile can be provided on request

Subclone 203-1 – allele 1

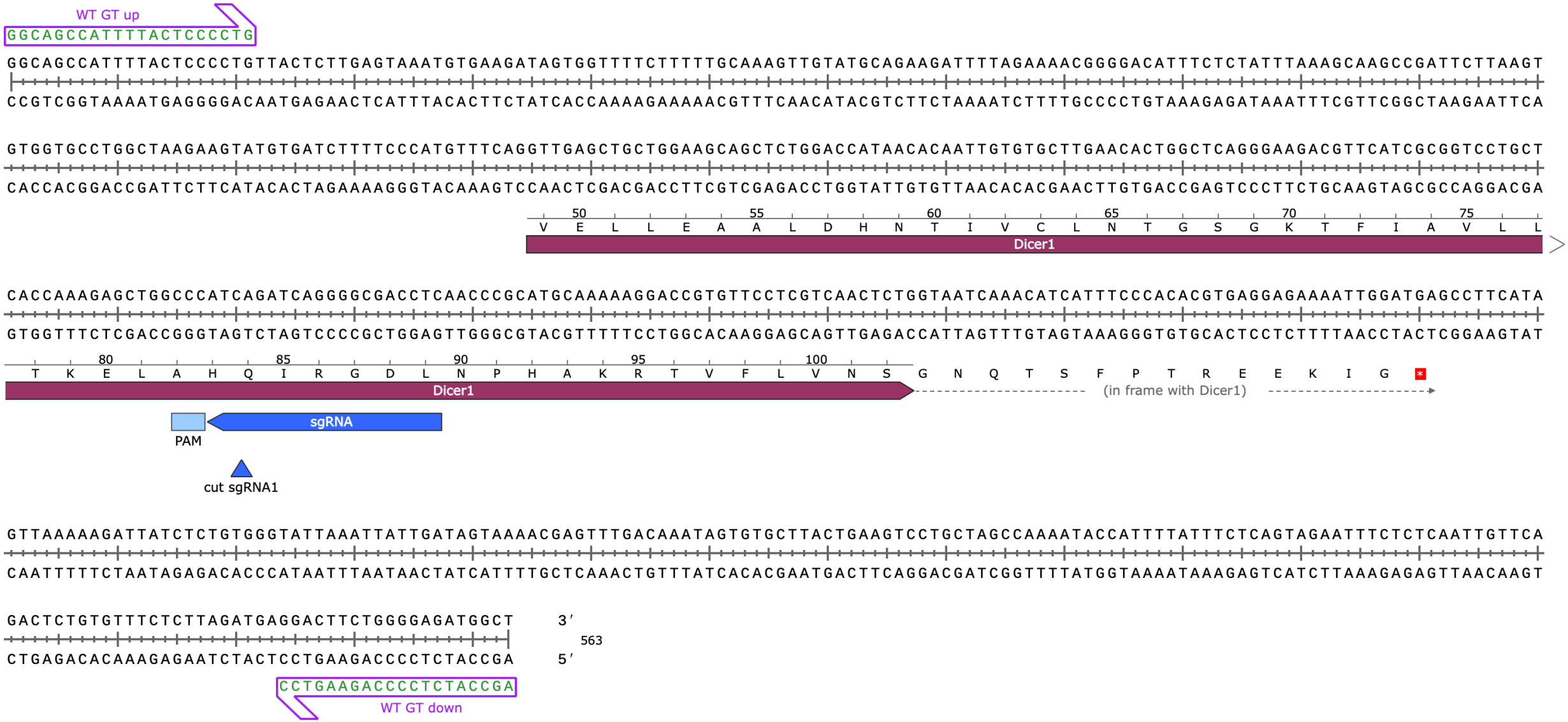
KO PCR band 803bp



Sequencing profile can be provided on request

Subclone 203-1 – allele 2 (WT)

sgRNA1 PCR band 563bp



Sequencing profile can be provided on request

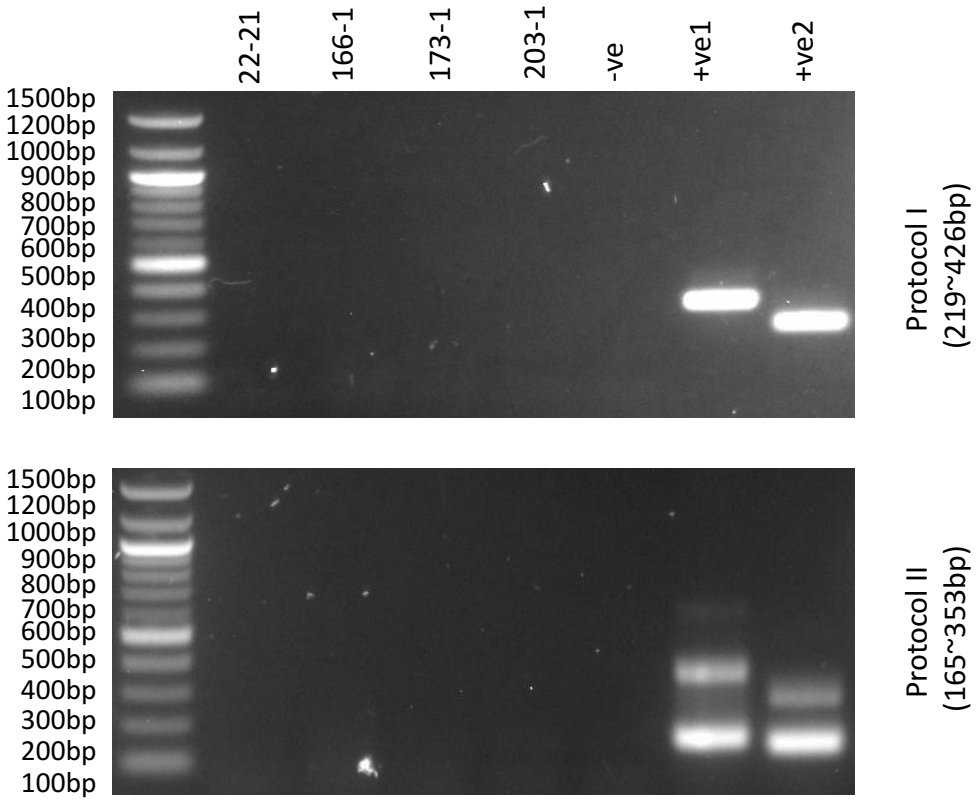
Subclones provided

Dicer1 KO (RAW264.7 cells)

Dicer1 KO subclones for handover

	Allele 1		Allele 2		Handover
	KO PCR	**KO deletion**	**WT PCR**	**Mutation at sgRNA1 site**	**Frozen vials**
Subclone 22-21 homozygous KO	707bp	40098bp	564bp	1bp insertion	2
Subclone 166-1 homozygous KO	797bp	40008bp	558bp	5bp deletion	2
Subclone 173-1 homozygous KO	582bp	40223bp (1bp change upstream of the mutation)	558bp	5bp deletion	2
Subclone 203-1 heterozygous KO	803bp	40002bp	563bp	WT	2

Mycoplasma screening



Protocol I and II are two independent PCR-based methods for detecting *Mycoplasma/Acholeplasma* species. +ve1 and +ve2 are two *Mycoplasma* positive samples, giving the expected products at 219-426bp (protocol I) and 165-355bp (protocol II).

None of the clones give a positive band, indicating they are mycoplasma-free.

Materials

Dicer1 KO (RAW264.7 cells)

MATERIALS

- DMEM (ThermoFisher, #10569044)
- Cas9-GFP (IDT Alt-R®S.p., #10008161)
- sgRNAs (IDT Alt-R® CRISPR-Cas9 sgRNA)
- Lipofectamine CRISPRMAX (ThermoFisher, #CMAX00015)

As per the Terms and Conditions of Phenomics Australia CRISPR Services, clause 16 (shown below), please include the relevant acknowledgement statement(s) in all publications.

In receiving the Material, you agree to include the following acknowledgement in any publication, presentation or press release concerning the Material: *"The [insert-e.g. mutant animals (including rats, mice and rabbits)] were produced via CRISPR genome editing by the Monash Genome Modification Platform (MGMP), Monash University as a node of Phenomics Australia. Phenomics Australia is supported by the Australian Government Department of Education through the National Collaborative Research Infrastructure Strategy, the Super Science Initiative and the Collaborative Research Infrastructure Scheme".*